DEVELOPMENTAL, MORPHOLOGICAL AND PHYSIOLOGICAL EFFECTS OF CHRONIC LOW DOSES OF IONISING RADIATION ON PLANTS ON EARTH AND IN SPACE

NICOL MIRIAM CAPLIN

A thesis submitted in partial fulfilment of the requirements of the University of the West of England, Bristol for the degree of Doctor of Philosophy

Faculty of Health and Applied Sciences, University of the West of England, Bristol

July 2019

Abstract

Conclusions in the current literature are essentially unanimous regarding what is known about the effects of ionising radiation on plants. It is agreed that acute high-dose effects (primarily from laboratory tests) are well-documented and understood but that the same cannot be said for lower doses. 'Low-dose' research is itself contentious until there is sufficient understanding to define what constitutes a 'low' dose. Studies using lower doses typically (but with some notable exceptions) feature dose-effect relationships at doses to plants orders of magnitude lower than high-dose studies (i.e. they examine doses measured in µGy-mGy as opposed to kGy-Gy). A compilation of data reported here emphasises not only the lack of studies that utilise low and environmentally-realistic doses of ionising radiation (µGy-mGy) but also the particular lack of such experiments that used a controlled environment. Additionally, the compilation revealed a lack of transgenerational studies.

In research reported here five generations of *Arabidopsis thaliana* were grown in soil contaminated with Cs-137 at low field-relevant dose rates (35 µGy/h). The developmental stages defined by a long-established phenotypic model (Boyes et al., 2001) were charted over entire life cycles. A detailed analysis of leaf morphology in generations of radioactively-exposed plants was undertaken with semi-autonomous image analysis software (LAMINA-Leaf shApe deterMINAtion). The same leaves were analysed for antioxidant changes via an assay for glutathione. No transgenerational trends were identified in any of the endpoints examined. Significant changes were detected in development and morphology in some treatments in some generations and are in line with stochastic effects expected to occur over generations under the same conditions. No significant differences were found in glutathione concentrations. DNA methylation was measured in the leaves of the first two generations exposed to Cs-137. It was reported that percentage of methylated DNA was significantly lower in radioactively exposed plants than control plants. No significant differences in root length were found between treatments or between generations. Lastly, seeds from two species of crop plants *Eruca sativa* and *Solanum lycopersicum* (rocket and tomato) that had flown aboard the International Space Station, and had received a cosmic radiation dose in low-Earth orbit of similar magnitude to *Arabidopsis thaliana*, were grown in Cs-137 contaminated soil. Previous exposure to cosmic radiation as seeds did not change radionuclide uptake characteristics of either species (measured via gamma counter) or total growth or root length.

In conclusion, while some effects have been observed, nothing was found to suggest that doses of ionising radiation at 'low' doses has a significant, negative impact on generations and populations of plants throughout these experiments. This contrasts with many reports from the field at similar dose rates and provides evidence that: a) current radioprotection limits are satisfactory at protecting plant populations, b) many effects on plants of low-dose radiation reported from the field are due to either past exposures to populations or other environmental factors and c) what constitutes a low dose of ionising radiation to plants could be redefined.

Acknowledgements

I offer deep appreciation to all the UWE academics, external field experts, fellow students, family and friends who have helped me complete this mission.

My wholehearted thanks go to my supervisor, Professor Neil Willey, for his unwavering support, expert guidance and constant encouragement throughout the entire PhD journey. This thanks is extended to my second supervisor, Professor John Hancock, for his helpful advice and warm spirit; Radiation Protection Supervisor, Alison Halliday, for all of the internalised stress, probably caused whilst handling radioisotopes in front of her; and to the whole of the CRIB and environmental technical teams who are undoubtedly some of the most hard-working people/magicians I have encountered.

Also, I want to express gratitude towards all members of the Transfer-Exposure-Effects consortium, the network has been an invaluable part of this project and fundamental to my professional development. Further appreciation extends to the Natural Environment Research Council for funding our collective research. Special thanks goes to the Interdisciplinary Biosciences Expert Group at the Belgian Nuclear Research Centre (SCK-CEN).

My grandfather, Henry Caplin, passed away just as I was embarking on my project, and I am certain that he would have enjoyed seeing me reach this stage.

✡

This work is dedicated to women scientists of the past, particularly those who never received recognition for achievements during their lifetimes; to women in the present who are relentlessly striving for research excellence in challenging times; to women in the future where I hope a scientific career is considered nothing out of the ordinary. Their discoveries, however, will be extraordinary.

Table of Contents

Table of figures

List of Tables

List of abbreviations

ANOVA	Analysis of variance
BLSS	Bio-regenerative Life Support Systems
Bq	Becquerel (Unit)
CEZ	Chernobyl Exclusion Zone
CPM	Counts per minute
DCRL	Derived Consideration Reference Level
DSB	Double Strand Break
DSLR	Digital Single Lens Reflex
EURT	East Urals Radioactive Trace
ERICA	Environmental Risk for Ionising Contaminants: Assessment and Management
FAO	Food and Agricultural Organisation (of the United Nations)
G	Generation
GR	Glutathione reductase
GSH	Glutathione
HR	Homologous recombination
HZE	Heavy ion particles
IAEA	International Atomic Energy Association
ICRP	International Commission on Radiological Protection
ISS	International Space Station
LAMINA	Leaf shApe deterMINAtion
LEO	Low Earth Orbit
NADPH	Nicotinamide adenine dinucleotide phosphate
NASA	National Aeronautics and Space Administration
NASC	National Arabidopsis Stock Centre
ND	No Data
NERC	Natural Environment Research Council
NPP	Nuclear Power Plant
RAP	Reference Animals and Plants
RATE	Radioactivity and the Terrestrial Environment
ROS	Reactive oxygen species
SAA	South Atlantic Anomaly
SCK-CEN	Belgian Nuclear Science Research Centre (English translation)
SOD	Superoxide dismutase
SSA	Sulfosalicylic acid
TAIR	The Arabidopsis Information Resource
UNSCEAR	United Nations Scientific Committee on the Effects of Atomic Radiation
UV	Ultraviolet
UWE	University of the West of England

Chapter 1: Introduction

1.1 Background

Ionising radiation (IR) is regarded as a plant stress by many biologists and environmental scientists. Indeed, if a plant has too much exposure to IR, a high enough total absorbed dose (measured in Grays (Gy) which is a measure of the total energy deposited in a unit mass of matter) delivered over a certain threshold rate can result in deleterious effects, and even death. The threshold for effects is much debated and some studies have reported hormetic responses to IR (Jan *et al*., 2012), i.e. that IR has positive effects at low doses and negative effects at high doses. It is, however, widely concluded in the literature that high doses of IR, particularly when delivered acutely, have pronounced negative effects on plants. Studies using this dose type, which are usually focused on mutagenesis, are heavily focused on DNA damage and other effects at the molecular level. Far less is known about the biological effects of IR at lower doses and/or the threshold for doses at which there might be 'no effect' because there are far fewer studies of them in both the field and the laboratory but particularly in the laboratory. Overall, it is clear that plants thrive in the presence of current ambient background IR, i.e. it does not cause them stress, and that they have higher 'radio-resistance' than humans and most other animals. The sources of IR plants are currently exposed to includes not only ambient background IR and naturally occurring radioactive materials (NORM), but also technologically enhanced NORM (including many wastes), radioactive accidents, weapons testing fallout and, potentially, stockpiles of nuclear waste.

1.1.1 Justifications for this project

Renewed interest in nuclear power production and the management of historical and future radioactive waste has increased attention on the ongoing debate around exposure thresholds for IR effects and subsequent consequences for humans, flora and fauna. Eight nuclear power plants are in current operation in the UK, with one more (Hinkley C) under construction. Although 'peak nuclear' production occurred in the UK around the year 2000 (Fig. 1.1), the new nuclear power station at Hinkley Point (Somerset) will have an energy capacity around three times as great as any of the UK plants currently in operation (Department for Business, Energy and Industrial Strategy, 2018). With no current geological disposal facility (GDF) in place for nuclear waste increasing concern surrounds the planned closure of eight nuclear power plants between 2023-2035, the waste legacy from these sites, the waste legacy from existing decommissioned sites e.g. Sellafield and the generation of waste from the new nuclear build(s).

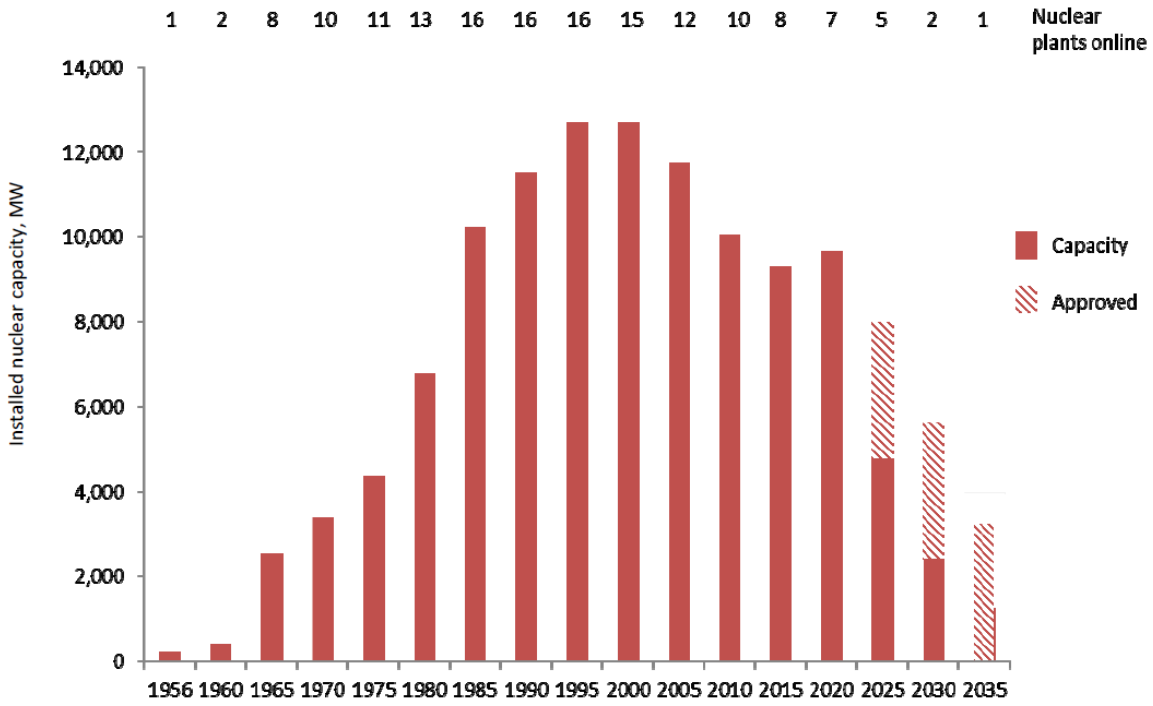

Fig. 1.1 UK installed nuclear power capacity and plants online 1956-2035 data reproduced with permission from BEIS (DUKES 5.10), www.gov.uk/government/statistics/electricity-chapter-5-digest-of-united-kingdom-energy-statistics-dukes

The research reported here was part of the TREE (Transfer-Exposure-Effects) project - a consortium funded by the Natural Environment Research Council (NERC), Environment Agency and Radioactive Waste Management Ltd as part of the £8mi Radioactivity and the Terrestrial Environment (RATE) programme. The TREE consortium was created with the aim of reducing uncertainty in assessments of the risks to humans and wildlife associated with exposure to radionuclides in the environment, in particular to decrease overly-conservative risk estimation. A primary context for this is the ongoing quest by government and private stakeholders to site and build a GDF for the storage of medium-high level radioactive waste in the UK (Department for Business, Energy and Industrial Strategy, 2018). To do this an environmental safety case is necessary, so potential impacts to wildlife through

various modes of transfer and exposure investigated by the TREE consortium are relevant. The £2.8mi TREE consortium included researchers from seven universities investigating a variety of exposure pathways and the effects of IR on a variety of organisms. At UWE, we focused on the transfer to plants and the effects on plants. Data from the consortium and from the project reported here is open-access and can be used to inform decision makers in both the private and public sectors relating to building safety case(s) for GDF construction.

The following sections (1.2 - 1.5.4) were the basis of a review published in Frontiers in Plant Science 26th June 2018 titled: *Ionising radiation, Higher Plants & Radioprotection: From Acute High Doses to Chronic Low Doses* in the section *Plant Abiotic Stress.*

1.2 Ionising radiation through geological time and the evolution of plants

Much research suggests that plants first colonised the land surface 420 million years ago. Evolutionary biologists have, however, recently presented claims that it may have been 100 million years earlier than this (Morris *et al*., 2018). Regardless of the exact date the land surface was colonised, the account of how plants evolved to withstand higher doses of IR than humans, and many other animals, remains essentially unchanged. IR was, in the context of evolutionary biology, a primordial stressor, i.e. present on the primordial Earth and the biology of plants reflects this plus exposure to the subsequent stresses of life on land.

Since the origin of life, activities of β and γ radiation from geological sources have decreased by about a factor of 8 (Karam & Leslie, 1999). Evidence suggests that eukaryotic life likely began >2.5 Ga ago (Archibald, 2015) under conditions that received five times current background levels of β and γ radiation. When plants first

colonised the land surface, background IR levels, despite only arising from primordial and cosmogenic sources (Shahbazi-Gahrouei *et al*., 2013) were significantly higher than at present. These figures are global averages – if background IR varied spatially as much in the past as it does now (Fig 1.2 gives an example of the variation in the year 2017 for annual dose derived from cosmic rays), many early life forms were exposed to much higher background IR than was average at the time. Life's early exposure to IR might help to explain the occurrence of radio-resistance, and sometimes even the ability to adapt to radiation, in some extant prokaryotes (Siasou *et al*., 2017).

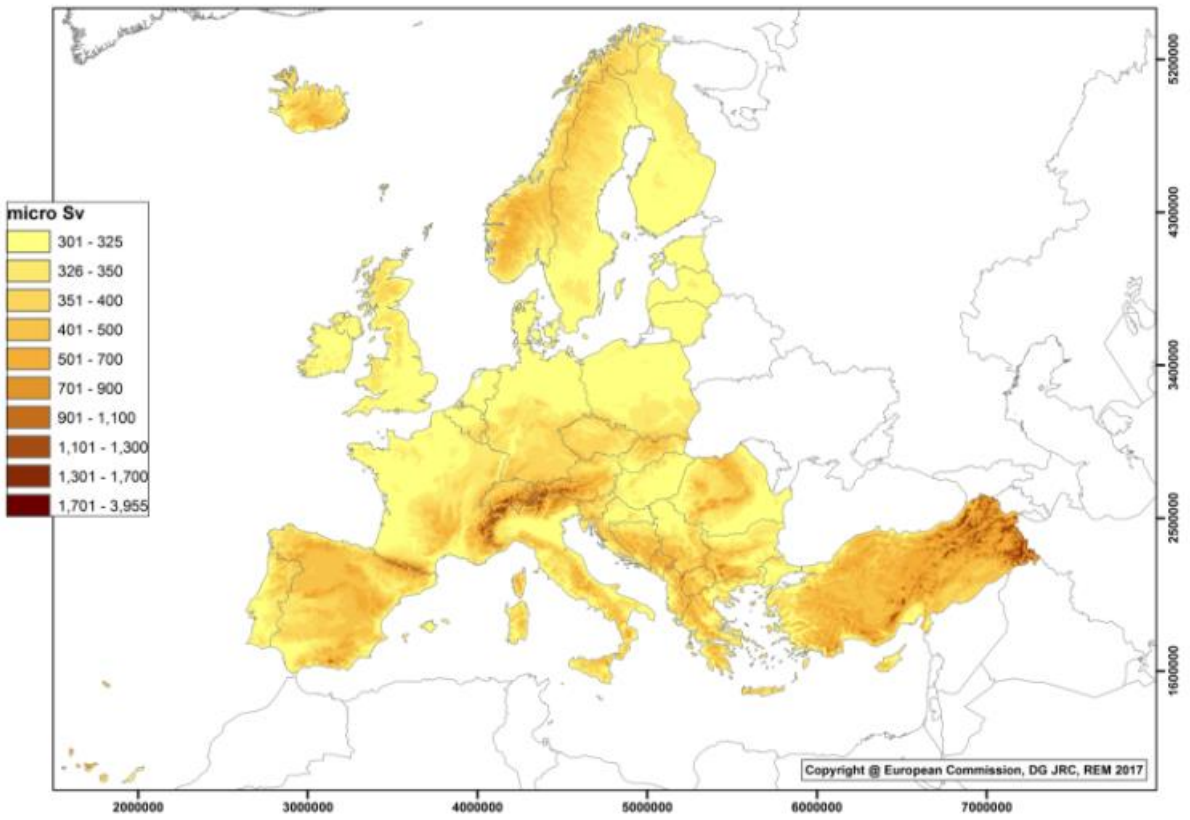

Fig. 1.2. The European Annual Cosmic-Ray Dose map reports the annual effective dose that a person may receive from photons, direct ionising and neutron components of cosmic radiation at ground level (European Union, 2019).

To estimate external doses of background radiation at the Earth's surface, geological events must first be understood. Total dose from background radiation is estimated using two key factors; dose rates derived from Rn-222 which is a significant geological source (currently averaging *c.* 1.2 mGy/y on Earth) that dominates external exposure and K-40, which dominates internal doses to organisms. The combination of these factors provides an estimate of total dose from background IR for an organism at the Earth's surface. This is why tectonic plate coalescence, which first occurred about 2.5.bi years ago, is a primary consideration for estimating total dose to organisms at the Earth's surface. Overall, there is a geological peak of exposure to background IR about 2.5 Ga (Fig. 1.3.) corresponding to the coalescing of protocontinents and the presence of eukaryotic life.

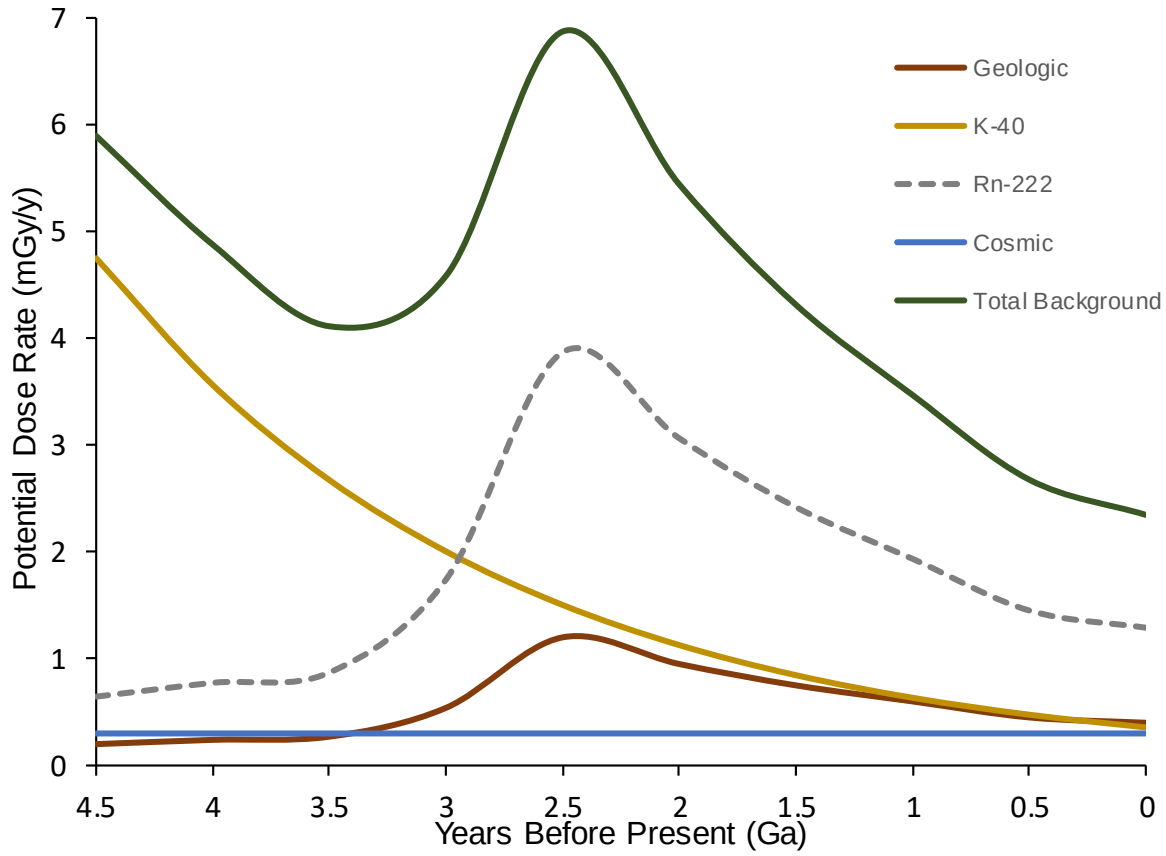

Fig. 1.3. Dose rate over geologic time (based on Caplin and Willey, 2018) Estimates established from doses taken from Karam and Leslie (1999).

When plants first emerged on land, they did not just colonise the land surface but also the atmosphere above it (Willey, 2016). This occurred through the evolution of morphological adaptations, such as increasing leaf area index that not only increased light capture but also allowed increased exchange of gases with the near-surface atmosphere. Rn-222 contributes very significantly (>60%) to current background doses to humans (HPS, 2015). During the evolution of higher plants Rn-222 may also have contributed to doses to some plants, especially those inhabiting canopies with low air flow. It is estimated that average background doses in the range up to 7 mGy/y (*c*. 20 µGy/d) occurred for a significant period of the evolution of plant life but high background areas may have had significantly higher dose rates. The success of higher plants is, in very significant part, attributable to the characteristics of prokaryotic life that was exposed to IR long before plants existed. Plants host plastids of prokaryotic origin (mitochondria and chloroplasts) and it is these plastids that had exposure to IR long before the plants that housed them did. To examine this chronologically, if plastids had already evolved in the presence of high background IR it is unsurprising that the plants that incorporated these demonstrate a level of radio-tolerance. Ultimately, the evolution of plants in background radiation significantly higher than present underpins the adaptation and success of plants on Earth. It should, therefore, be expected that plants continue to inhabit radioactively contaminated land, for example around Chernobyl (Ukraine, Belorussia (now Belarus), Russia) and Fukushima (Japan) following nuclear-fallout driven environmental contamination there in 1986 and 2011 respectively.

The extent to which primordial IR drove evolution is unclear because the thresholds, if they even exist, at which the effects of chronic exposure to relatively low doses of IR become significant are poorly described. The following sections will outline current

descriptions of the ‘no effect’ threshold and the current benchmarks recognised internationally for environmental protection purposes. There then follows a detailed literature review of research into the effects of IR on plants from the molecular level to whole ecosystem level.

1.3 Dose-effect data and implications for environmental protection

Estimating doses to non-human biota, including plants, can be challenging. A wide range of factors have to be taken into account when examining doses to plants, yet the very nature of the environment, a highly dynamic system with a multitude of environmental and temporal variables, can make it difficult to develop accurate dosimetric methods to inform environmental protection legislation and decision-making processes. There are now methods for dosimetry that are used by the radioecological community, largely set up by the International Atomic Energy Agency (IAEA) and improved upon by the International Commission on Radiological Protection (ICRP).

In general, data from accidents and controlled experiments suggest that, with some differences between species, acute high doses of IR in the range of 10-1000 Gy can be fatal to plants (UNSCEAR, 1996). Although fewer studies have examined chronic low dose effects of IR in plants, UNSCEAR (1996) suggested 10 mGy/d (417 µGy/h) as a threshold dose rate for radio-protection of plants (Nelson-Beyer & Meador, 2011). This confirmed a long-established IAEA threshold for radiation dose rates of <10 mGy d^{-1} having ‘no detrimental effects' for populations of terrestrial plants in the field (IAEA, 1992). To help account for differences in response between different organisms, including distinct types of plant, the ICRP developed the use of a set of reference

animals and plants (RAPs) (ICRP, 2008) that were later supplemented with Derived Consideration Reference Levels (DCRLs) for each RAP (ICRP, 2014). These took the form of a range of dose rates that could be useful in potential radiological impact estimates. Grass and pine RAPs are a well-developed international framework for protecting plants from the effects of IR. The ICRP's RAPs include plant DCRLs for grass of 1-10 mGy/d (41.7-417 µGy/h) and for pine trees of 0.1-1 mGy/d (4.17-41.7 µGy/h). The grass RAP provides a reference range for herbaceous higher plants and pine trees a reference range for the more IR-sensitive woody plants. The EU-funded ERICA project suggested, after including a safety factor of 5, a chronic exposure screening value of 10 µGy/h for ecosystems (Garnier-Laplace & Gilbin, 2006), however, ecosystems will include some organisms that are more sensitive than plants.

There are several reasons for probing the appropriateness of current DCRLs. The development of RAPs emphasised that the level of understanding about the effects of radiation on plants is much less than that for humans or other animals. This continues to be the case and can, in part, be attributed to the challenges of studying radiological impacts on plants. For example, when studying pine trees, it can be hard to establish either accurate external doses at different heights or accurate internal doses arising from accumulation in different local regions of a large organism (ICRP, 2008). Additional complications when studying plants, and about which relatively little is known, include the radio-sensitivity of different above- and below-ground organs (for example buds, roots and root hairs), significant differences in life-span of different species and seasonality in responses.

In radiobiology, IR-induced effects are generally divided into deterministic effects that occur when a dose-threshold is exceeded and can be estimated by endpoints such as mortality, morbidity or reproductive success, and stochastic effects that are

probabilistic and measured by endpoints whose incidence increases proportionately with dose (UNSCEAR, 2006). The importance of stochastic effects in plant radiological protection and for DCRLs, especially at chronic low doses (a contentious issue in itself), is unclear. In 2005, a European Commission report suggested that, despite observed impacts on some individuals, stochastic effects arising from chronic low doses of IR may be of little relevance to protecting populations of non-human biota, although the report did acknowledge that effects at a population level are not well known (Björk & Gilek, 2005). This is in part because stochastic effects can produce differences between not only individuals but also between different parts of a plant (Esnault *et al*., 2010). This presents some statistical challenges not least because in plants with a small biomass data is often pooled from several individuals and many responses can be hidden. Esnault *et al*. (2010) suggested that there is even a need for experiments to generate high definition intra-plant data. Such data are not yet available and the importance of stochastic effects to the protection of flora, although unlikely to be significant, are not clear.

Further, some areas on Earth have a naturally-enhanced background of IR and, for example, it has been suggested that the chronic exposure at Ramsar in Iran (Saghirzadeh *et al*., 2008) can have effects on plants at a dose rate (4 µGy/h) that is only about 10 times higher than the global average background (Ghiassi-Nejad *et al*., 2003) and, whilst DCRLs are meant to be conservative in terms of risk, is at the low end of the range of the DCRL for sensitive plants. Effects at similarly 'ultra-low' dose rates have been reported at Fukushima (Hayashi *et al*., 2015). In addition, many studies that have contributed to the development of DCRLs have used field locations with dose rate gradients as the basis for their research design. An association between existing environmental contamination and effects is only one indicator of cause,

because locations with different dose rates can vary in other ways, often to an unknown extent, in both systematic and specific respects, i.e. there can be significant confounding factors. For example, due to the short-half lives of most of the radioisotopes emitted from the Chernobyl nuclear power plant reactor most contaminated locations with elevated dose rates post-1987 had much higher, and short-lived, dose rates during 1986 in the immediate aftermath of the accident. At Chernobyl, when attempting to assess the effects of a particular dose rate it can be difficult to separate any lasting effects of 1986-1987 dose rates from any effects of the post-1987 dose rates. Clearly, although there are established transgenerational effects of IR, in studies conducted a significant time after the accident this may be less of a complication. Overall, an improved understanding of the effects of IR on plants and how they relate to currently used DCRLs is desirable.

1.4 Meta-analysis of studies involving IR and plants

In order to aid discussions of the effects of IR on plants, a meta-analysis of published studies of the effects of IR on plants was made and classified according to study type (controlled conditions vs field) (Fig. 1.4.).

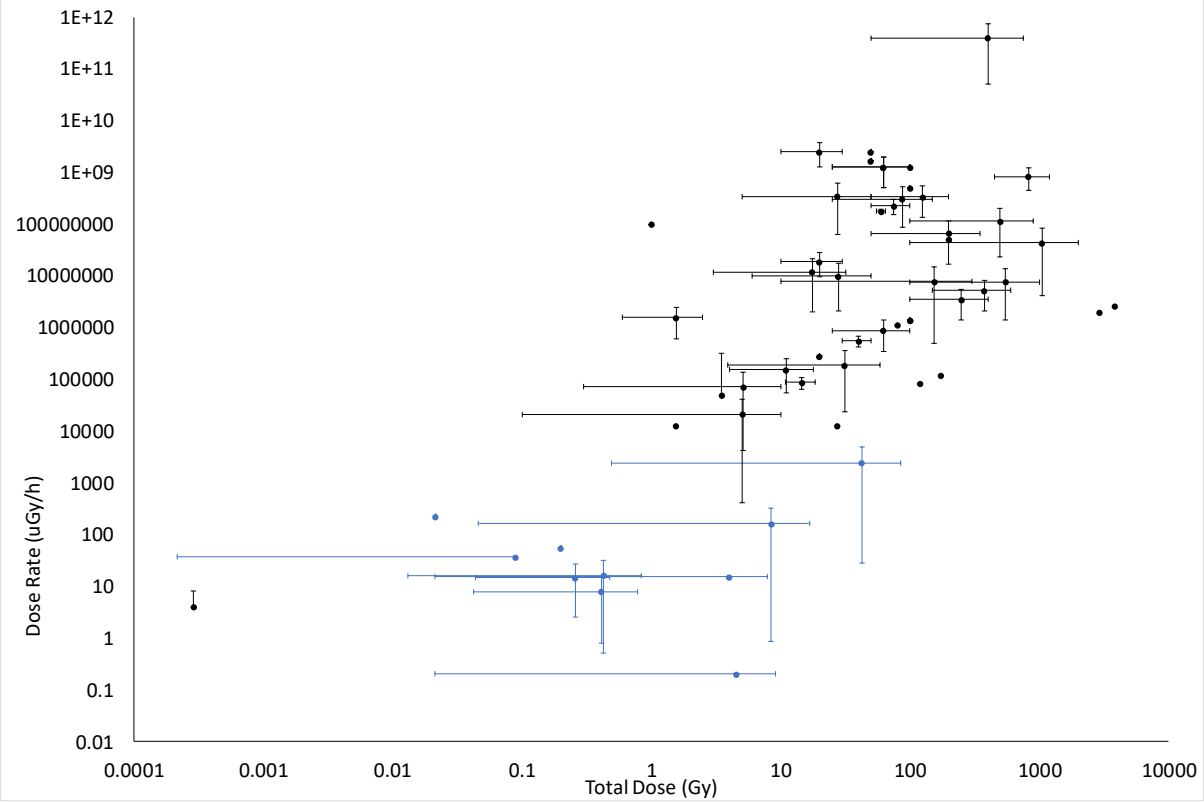

Fig. 1.4. The doses and dose rates used in studies of the effects of IR on plants (Caplin and Willey, 2018). Where possible, dose rates and total doses from published studies were determined from methods sections or by calculation of them from details provided. The bars on the points above represent the ranges of dose and/or dose rate used in the published works. Studies in the field are coded in blue, those from the laboratory in black. Although not all published studies could be included because doses or dose rates were not provided or could not be calculated, this significant selection of the published data shows that there are few laboratory studies at low doses, especially at chronic low dose rates (which would be located towards the right of the x axis). (Details of studies are in section 7.3 Supplementary Information).

It is clear from this analysis that there is a paucity of data on the effects of chronic low doses of IR on plants that was generated under controlled conditions, indicated by a gap around the area of low dose rates and total doses (and the combination of these). The studies that have investigated the effects of IR at contaminated sites clearly, and crucially for managing them, reveal what is happening at these sites under field conditions and provide primarily associative evidence that the cause of any effects is exposure to chronic low-level IR. The same data used in this analysis was also used

to ascertain the most likely endpoints for study in the range of doses already mentioned and this is further detailed in chapter 2.

1.5 Effects of ionising radiation on plants

The effects of IR in higher plants are of interest to agriculture, horticulture, ecology and space science. For the purpose of this thesis it is appropriate to have a multi-level analysis of effects (Fig. 1.5). This approach helps the interrogation of each level separately, as the foundation for later discussing the relevance of the levels and the relationships between them.

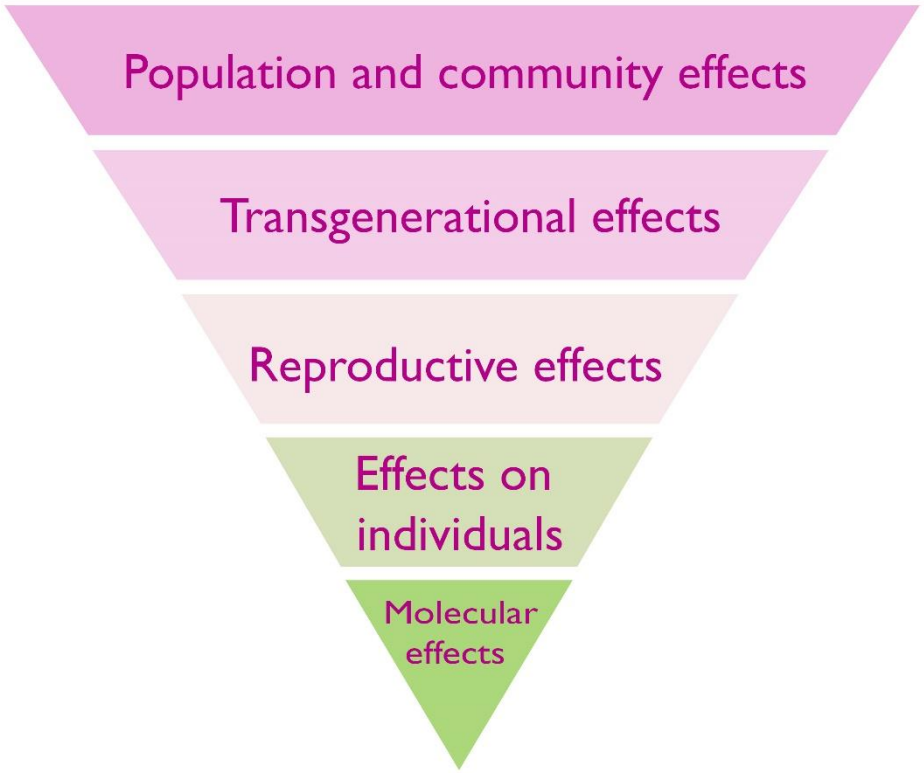

Fig. 1.5. A proposed hierarchy of effects levels for IR and plants from the molecular level to the population and community level.

Three important aspects of plant biology provide a vital context for understanding the effects of IR:

1) The **light reactions of photosynthesis** are initiated with photolysis of water - a process with the same products as the radiolysis of water and which, especially in plants under stress, can result in the formation of (compared to IR or UV) enormous amounts of oxidative radicals that plants are generally able to disarm because of their high production of anti-oxidants (Willey, 2016).
2) In multicellular plants the **dividing cells occur in meristematic tissues** that have quiescent centres with functional 'equivalence' to stem cells but that are not identical to them and do not have, for example, the same *p-53* mediated apoptotic capacity as animal stem cells, independent of glutathione (Coe *et al*. 2002). Meristems in plants are a biologically distinct product of an independent evolution of multicellularity (Fulcher & Sablowksy, 2009) and the effects of IR on them are not well known.
3) The meiotic divisions that produce the gametophyte generation in reproductive organs in plants are separated in each generation by many vegetative cell divisions in the sporophyte generation - i.e**. plants have no reserved germline**. Thus, current knowledge about the effects of IR on multicellular organisms is dominated by knowledge of effects on organisms with less anti-oxidant capacity than plants and that have stem cells and germ lines without exact plant equivalents.

1.5.1 Effects at the molecular level

It is widely accepted that IR damages DNA, both directly or indirectly. Numerous chemical and physical processes are routes for DNA damage and IR can induce this in a range of ways. One of the most notorious mechanisms through which IR can damage DNA directly is by inducing double stand breaks (DSBs) (Oladosu *et al*. 2016). Single strand damage is believed to have assisted the evolution of double-stranded molecules as genetic material, so that when a single strand was threatened with damage a second strand could act as a template for repair of damaged bases or nucleotides (Freidberg, 1997). Further, factors that caused DSBs, possibly including IR at high background locations, may have helped drive the evolution of chromosome pairs. A second DNA molecule can provide a template for repair of double stranded breaks. Homologous Recombination (HR) is an ancient process that in many eukaryotes helps produce variation in haploid gamete cells during meiosis, but the repair of DSBs, in which it has a key role (Jackson & Bartek, 2009), likely aided its evolution. Homologous pairing, an important DSB repair pathway, is promoted in archaea by *RadA*, in bacteria by *RecA* and in eukaryotes by *Rad51*, which are slightly different versions of the same gene in all organisms. Eukaryotic nuclear DNA probably acquired *Rad51* via transfer of *RecA* from prokaryotic endosymbionts (Lin *et al*., 2006). *Rad51* was identified through its radiation responsiveness although IR was not necessarily the DSB-causing agent that drove its evolution. Finally, the famed static image of the DNA double helix can detract from the reality of dynamic processes of DNA damage and repair that underpin life on Earth (Freidberg, 2003) and that evolved in response to primordial stressors, perhaps including IR. Direct effects of background IR on DNA are probably less significant now than they have ever been but, especially in ancient high background areas, they may have played a role in the evolution of both the genetic architecture and the DNA curation processes of life.

IR can also damage DNA indirectly via the products of radiolysis of water, which causes a cascade of reactive molecules (Fig. 1.6.). Many of these molecules play key roles in the processes of life, their reactivity making them useful in signalling and defence but also potentially damaging to biomolecules (Foyer & Noctor, 2016).

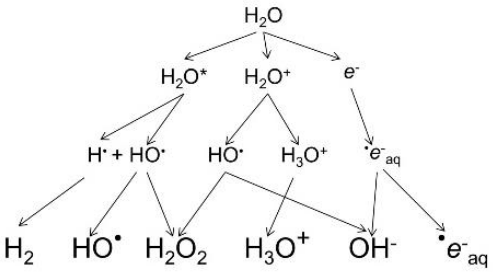

dose rate ($mGyd^{-1}$)	dose rate ($\mu Gy\ h^{-1}$)	H_2	$HO^{\bullet}$	H_2O_2	H_3O^+	OH^-	$^{\bullet}e^-_{aq}$	Σ_{ROS}
1	41.7	4.35	25.9	6.76	5.74	0.25	25.9	**69**
10	417	43.5	259	67.6	57.4	2.5	259	**690**
100	4170	435	2590	676	574	25	2590	**6900**

Fig. 1.6. The products of radioloysis of water (x10-16 mol/g). Smith et al. (2012)

The reactive oxygen species (ROS) resulting from radiolysis of water are important in producing its effects at high doses, including for example during radiotherapy or corrosion of pipes in nuclear reactors, and in an aqueous environment, e.g. cells and their concentrations can be calculated from dose rates (Smith *et al*., 2012). However, during the evolution of life, UV, which can also cause direct DNA damage, has been a much more significant source of ROS than IR. UV-C with a wavelength below 100 nm is ionising but is also absorbed by many atmospheric constituents, perhaps including some that occurred in the early atmosphere (Hessen, 2008), and has likely never been a particularly significant source of ROS in aqueous environments, including cells, at the Earth's surface.

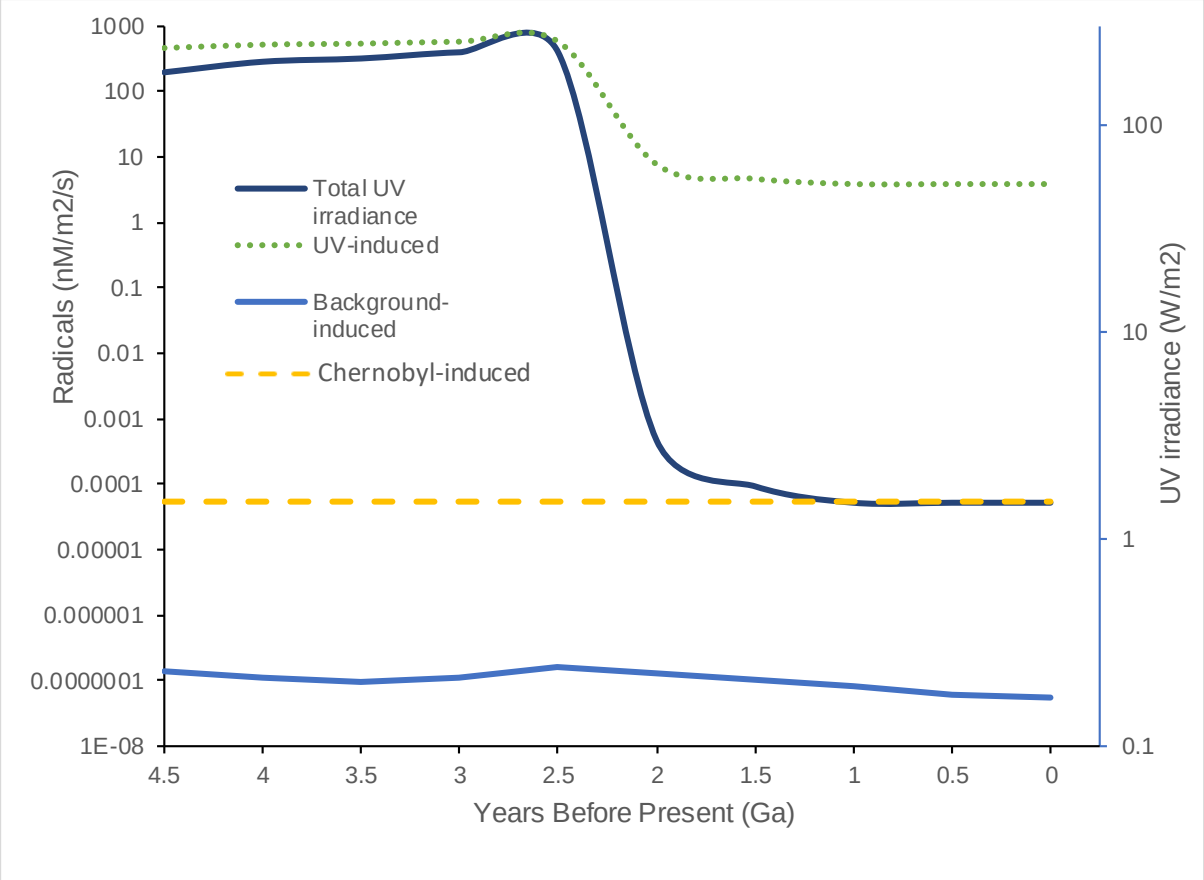

Fig. 1.7. Radical induction-potential from water by different radiation sources through Earth's history (adapted from Caplin and Willey, 2018).

UV with wavelengths longer than 100 nm does not generally ionise water but can ionise other organic molecules, including proteins. In an aqueous solution, these photo-ionised molecules can induce the production of ROS from H_2O (Pattison & Davies, 2006). The probability of this occurring is relatively low compared to the probability of radiolysis induced by IR but the amount of UV arriving at the Earth's surface is, even after the formation of the ozone layer, much more significant than the amount of background IR. Calculations of the production of ROS produced by UV over geological time compared to that from IR suggest that UV has, throughout evolution, been the most significant radiative source of ROS that organisms have had to contend with (Fig. 1.7). Overall, understanding the effects of IR must occur with recognition

that it was a feature of the primordial environment that is now less intense than it once was and that there are other radiative stressors that can damage DNA and promote the formation of ROS, often at much more significant rates, than IR does.

The concept of 'mutation' was first introduced in the beginning of the 20th century by Hugo de Vries, a botanist, early geneticist, and one of the rediscoverers of Mendel´s work. De Vries also suggested in 1904 that the recently discovered X-rays could be used to induce mutations (Blakeslee, 1936), so the initial attempts at mutagenesis used plants (and *Drosophila*) exposed to such radiation (Muller, 1927; Stadler 1928a, 1928b) and later to radium (Hanson & Heys 1928, Stadler, 1930). A significant proportion of all food consumed by humans now derives from plants improved by radiation-induced mutagenesis. More than 2500 of the crop cultivars used in current agriculture were developed with the aid of acute high-dose IR (10s of Gy or more) (Cheng *et al*., 2014) including the world's most important crops, e.g. rice and wheat (Cheng *et al*, 2014; Zhang *et al*. 2016). The FAO/IAEA Mutant Variety Database registers numerous new cultivars each year, including many produced using IR. Such mutagenesis also has an important role in the development of new horticultural varieties (e.g. Taheri *et al*., 2014). IR- induced mutagenesis can alter DNA in three different ways: 1) intragenic changes, also known as point mutations 2) intergenic changes (inversions, deletions, duplications, translocations of DNA) and 3) changes in chromosome number (Oladosu *et al*., 2016). In comparison to other mutagens (e.g. ROS), IR induces a high incidence of double stranded breaks (DSBs) in DNA, which has been verified in experiments with plants (e.g. Doná *et al*., 2013).

1.5.1.1 Oxidative stress in plants

Damage of DNA, RNA, protein and membranes via oxidation in biological systems is collectively known as oxidative stress. Here, some of the key drivers of oxidative stress, from the origins of it to the current mechanistic understanding of repair pathways through to redox signalling are described. Some contemporary concepts of oxidative stress are highlighted, including alternative perspectives on long-established scientific belief.

1.5.1.2 Reactive Oxygen Species

Reactive Oxygen Species (ROS) at their very basic level are excited or reduced forms of reactive atmospheric oxygen (Czarnocka and Karpiński, 2018). They are mostly formed in chloroplasts, mitochondria and peroxisomes but recent research has shown that ROS are also synthesised directly by NADPH oxidases and peroxidases (Demidchik, 2015).

It is generally agreed that ROS were being formed at least around 2.5 billion years ago (Mittler, 2017) which coincides with the time of rapid oxygenation of the atmosphere (Slesak *et al*., 2012) and subsequent total oxygenation of Earth's oceans (Fig. 1.8). Both prokaryotic and eukaryotic life had the potential to evolve in the presence of ROS (alongside enhanced levels of background radiation) prior to abundant atmospheric oxygen because evidence has shown many anaerobic organisms also generate ROS and have associated scavenging systems (Czarnocka and Karpiński, 2018). It has been suggested that the powerfully reducing environments in the primordial oceans may have converted the majority of freshly formed oxygen (by biological organisms) straight into ROS or similar intermediates (Mittler, 2017). This thought is based on evidence from the presence of a major ROS scavenging

enzyme, superoxide dismutase (SOD), throughout biological systems that evolved prior to eubacteria (from archaea) and fits the belief that all life must have evolved in the presence of ROS.

Interestingly, ROS are thought to have had a primary role during the oxygenation period on Earth, when organisms were utilising them as what can be thought of as "molecular biosensors" to detect unsafe oxygen levels on the planet. This later evolved into multi-factor sensing and ROS are now responsible for a number of regulatory mechanisms including stress signalling, development and programmed cell death (Mittler, 2017).

Recent opinion has challenged current ways of thinking about the role of ROS in plant biology. Rather than viewing ROS as purely damage-causing (either directly or through metabolic pathways) ROS have the potential to be not only beneficial to plants but essential for survival. Mittler (2017) states that while there is no denying that ROS are toxic by-products, key cellular processes are supported by ROS (cell proliferation and differentiation being two of the main processes) and that this phenomenon could not occur in the absence of ROS. By this logic, ROS signalling is an absolute requirement for life. It was further hypothesised that some form of hormesis could be occurring. This perspective thus proposes that ROS are a vital component of living systems.

Similar to ionising radiation (IR), ROS are not new phenomena for life to manage. Life evolved in both the presence of much higher levels of background radiation than currently persist (detailed in chapter 1) and as previously stated, life also evolved with ROS. The combination of these factors could be viewed as complementary - IR causes the radiolysis of water which generates ROS. What this results in is the need for a

constant system of DNA damage and repair, which is probably an absolute requirement for life. If IR and ROS (and associated antioxidant systems) are all in a balanced mode of redox homeostasis within organisms, then these are probably the ideal conditions to support life. Therefore, biological damage will occur when one of these factors has levels altered enough that the balance is upset and so negative effects occur (Fig. 1.9).

This is what happens when plants are exposed to high doses of radiation above a threshold, and although different species have been shown to vary in degrees of radiosensitivity, it is inevitable that high enough doses will cause mass oxidative stress and death. However, Mittler (2017) proposed that ROS are predominantly beneficial to plant cells, and that oxidative stress only occurs through deliberate activations of pathways involved in cell death, e.g. ferroptosis and regulated necrosis, as opposed to directly killing cells.

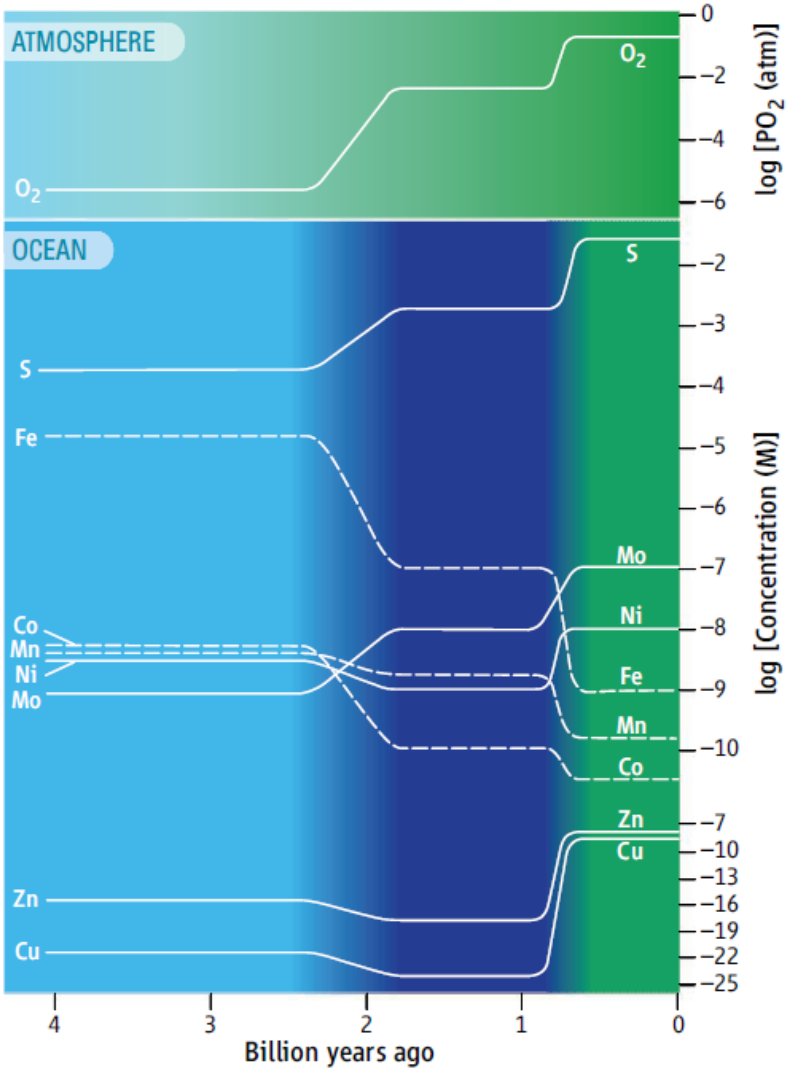

Fig. 1.8. The interaction of IR, ROS and antioxidants in biological systems (A) IR-induced ROS and antioxidant activity that lessens the potentially harmful effects of ROS (B) Overload of ROS that outweighs an antioxidant system eventually resulting in deleterious effects or death.

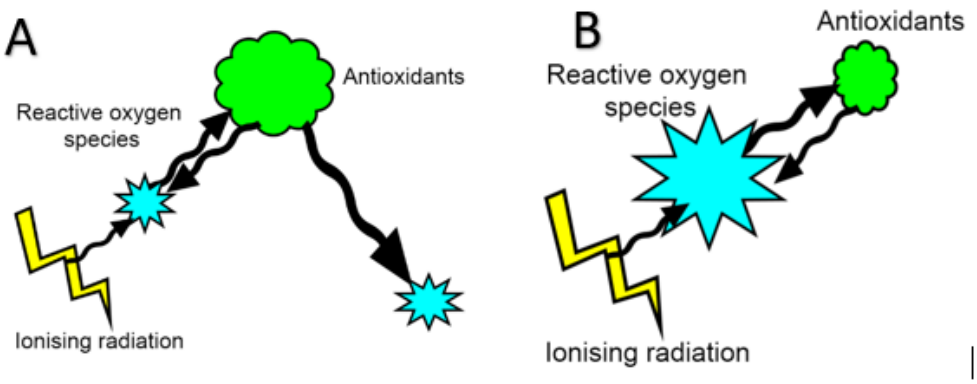

Fig. 1.9. Changes in element abundances through geologic time (Anbar, 2008) based on inferences from sediment extractions. Colour gradient indicates changes from anoxia (light blue), H2S rich oxygen (dark blue) and total oxygenation of the Earth's oceans (green). Dashed lines highlight falling concentrations of elements in the oceans. Reproduced with permission from Science.

1.5.1.3 Redox signalling

Redox signalling is a fundamental requirement for cellular homeostasis and if redox control is lost, cell components face a torrent of effects that excess ROS produces. If this loss of control is sustained, apoptosis and death can follow (Willey, 2016). Proteins associated with redox signalling play a vital role in responding to environmental stressors, such as triggering repair mechanisms (Pandey *et al*., 2015), and are also utilised in general growth and development regulatory activities (Foyer *et al*., 2017).

A traditional view of redox signalling is based on the concept of a state of equilibrium where ROS and antioxidants are balanced, even harmonious in relation to cellular processes. Oxidative signalling can alter this balance and in turn, ROS accumulate either from increased production or decreased antioxidant capacity. Depending on intensity, this has the power to trigger cell death pathways or those involved in stress

tolerance. Noctor *et al*. (2017) concluded that while this understanding is useful, it doesn't reveal the whole situation, mostly regarding how complex and specific antioxidant systems in plants are or how they operate during signalling.

Foyer *et al*. (2017) have worked to shift the focus around oxidative stress from the traditional damage-causing scenario to one of a redox signalling perspective as it is becoming increasingly recognised that directly labelling ROS as a lone agent of damage is an outdated viewpoint. They used photoinhibition and the loss of photosystem II as an example in which management of light interception and energy conversion are regulated by numerous "stabilising mechanisms" that ensure normal regulatory function during dynamic situations of irradiance flux in the natural environment. Some of these mechanisms include the production of ROS which are highly important in regulating photosynthesis. Foyer also placed emphasis on the dubious use of the expression "photoinhibition" because of two different activities that are often bundled together underneath the same term. These are the down-regulation of photosystem II and photodamage, yet even though the latter is said to be the term traditionally associated with photoinhibition, mounting evidence suggests that it doesn't have as much of a central role as previously thought.

1.5.1.4 Antioxidant systems in plants

The classical explanation of the role antioxidants have is that they function by chemically quenching ROS and in turn, protecting against damage that would otherwise likely occur (Larson, 1988). As previously mentioned in the last section, a traditional view for ROS is of the catalyst- the activator of antioxidant systems in

plants, battling the threat and onslaught of cellular damage to maintain ROS at manageable levels for healthy cellular functions. Noctor *et al*, (2017) described this interpretation as the dominant view, but suggested to a changed perspective on the entire situation. This suggestion was to banish the term "antioxidant systems" altogether and replace it with "ROS processing systems" when describing cellular components likely to encounter ROS and transmit associated oxidative signals. This is agreed upon by Foyer *et al*. (2017) where the idea of ROS versus antioxidants is described as a "*Manichean notion that sets evil ROS on one side and benevolent antioxidants on the other"* or put simply, tagging each side as functional polar opposites when current science understanding shows that this is no longer likely.

1.5.1.5 The role of glutathione in plants

Essential for plant growth and development, glutathione, L-ɣ-glutamyl-L-cysteinylglycine, (GSH) a thiol central to cellular antioxidant systems of the highest importance (Couto *et al*., 2016). If an organism lacks glutathione reductase (GR), the enzyme that catalyses the NADPH-driven reduction of glutathione in the oxidised state (GSSG) into GSH, then it is common to discover that this is substituted with thiols of similar functions (Couto *et al*., 2016).

GSH and GR are two physiologically linked components of the ascorbate-glutathione pathway (Fig. 1.10) and are found alongside ascorbate in cellular components including mitochondria, peroxisomes, chloroplasts and cytoplasm (Fig. 1.11) in varying concentrations (but the reduced form is normally present at around 2-3 mM (Cheung *et al*., 2015). Ascorbate is also found in the apoplast (Anjum *et al*., 2010).

The characterisation of ascorbate and GSH took place in the 1930's and since then the discovery of the close relationship between the molecules has been built upon by researchers to give our present day understanding of the molecules themselves and their interactions, roles and implications. There has been a change in focus of GSH-ascorbate interactions, from their use as photosynthetic regulators (prominent in the 1970s), to oxidative stress and oxidative signalling (both of which have gained momentum since the late 1980's) (Foyer and Noctor, 2011).

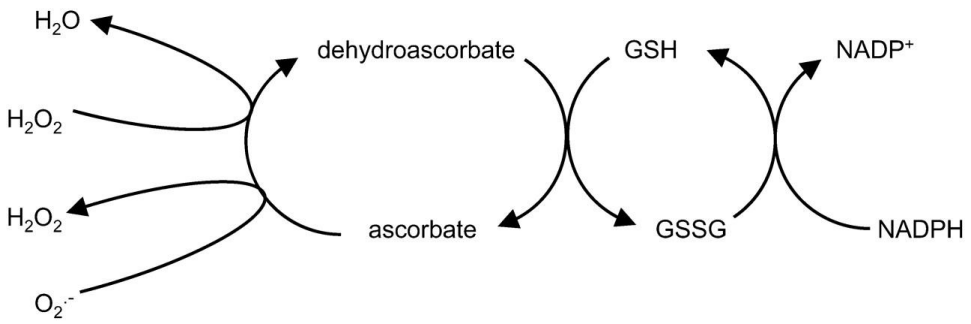

Fig. 1.10 The chloroplast ascorbate-glutathione cycle as a simple metabolic scheme (Foyer and Noctor, 2011) Permission granted for reproduction from Plant Physiology.

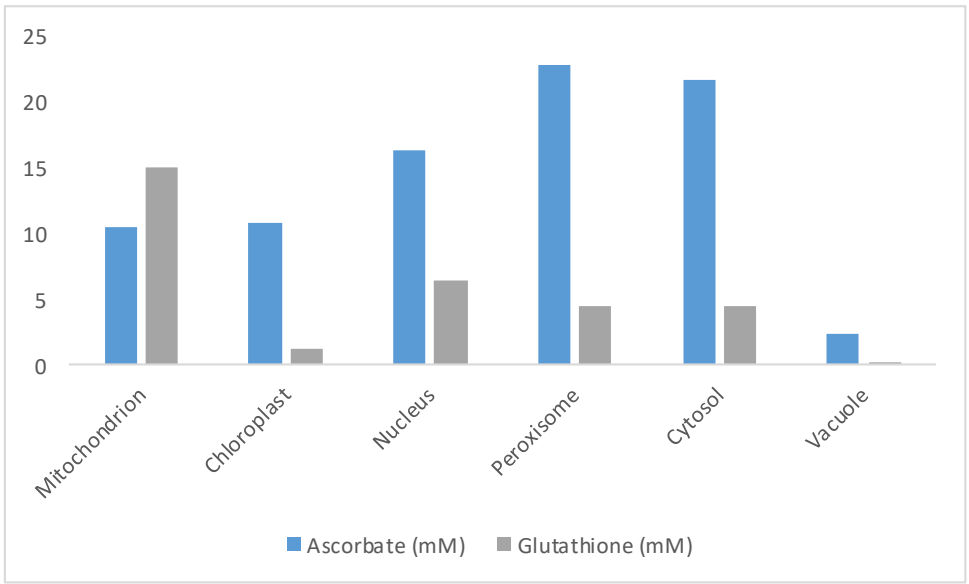

Fig. 1.11. Concentrations of Ascorbate and Glutathione in cells of early rosette leaves of A. thaliana determined using immunogold labelling. Concentrations in mM. Adapted from data in Pandey et al. (2015).

Both GSH and ascorbate are of low molecular weight and work in a system of detoxification (Fig. 1.12) towards ROS and toxic by-products of ROS. The ratio of GSH and ascorbate as well as the ratio of oxidised forms of these molecules are fundamental to the activation of repair mechanisms.

Environmental stressors can produce an additional ROS load to plants and if not kept at a basal level, will cause damage. This is where the role of the antioxidant is most crucial, as this basal level can only be maintained by ROS scavenging mechanisms such as GSH. Not only does GSH control ROS but it has a secondary function where it transmits oxidative signals (Foyer, 2017). GSH also has a role in scavenging reactive nitrogen species (Couto *et al*. 2016). It is also a strong regulator of ROS accumulation, meaning that proteins and associated components of cells can continue to function normally and ultimately provide an indirect method of biomonitoring for environmental stress perception (Latowski *et al*., 2010). This regulatory-monitoring system allows for the signalling of prescribed action, in other words the defence system is truly an in-house operation.

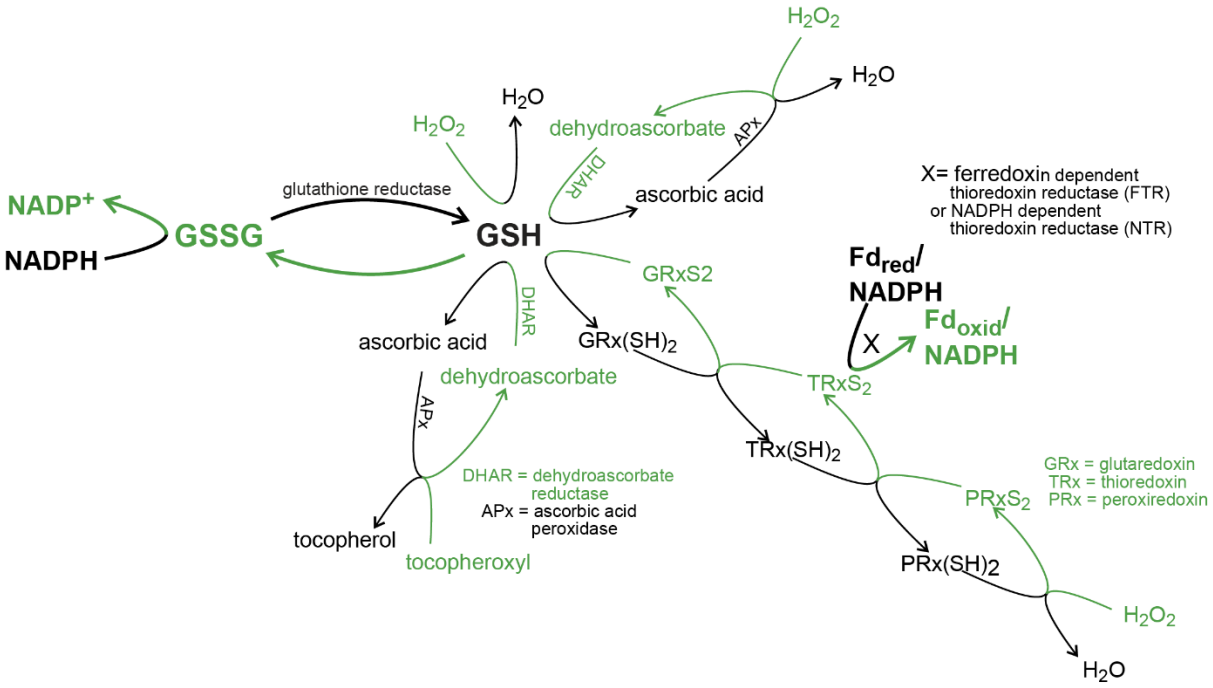

Fig. 1.12. The primary antioxidant system in plant cells reproduced from Willey (2016): Reducing power from NADPH derived from photosynthesis passed on via GSH- central to plant cell antioxidant capacity. Reduced species are shown in black and oxidized species shown in green. GSSG is the oxidised form of GSH. Other interactions are shown to illustrate the interconnectedness of the antioxidant system and how dependant plant cells are on GSH activity.

A long-known indicator of oxidative damage, GSH concentrations undergo perturbation of levels when such damage occurs. For example, when a plant is severely dehydrated, concentrations of GSH are much changed (Cheung *et al*., 2015). Further, Cheung *et al*. (2015) describes the role of GSH as "conditionally important" in response to excess heavy metal load, as GSH is the precursor of phytochelatins - the compounds synthesised in response to metal exposure such as cadmium.

Phytochelatins are of extreme importance to plants, where the action of these compounds sequester metals, transporting them to the safety of vacuoles in plant cells, preventing them from disturbing other cellular processes. This is achieved through multiple stages involving the ascorbate-GSH cycle and two key enzymes (S-transferase and phytochelatin synthase) which aid the sequestration of metal ions into

the vacuole (Yadav, 2010). Therefore, GSH is fundamentally important for phytochelatin function.

1.5.1.6 Glutathione in plants exposed to IR

As IR causes the radiolysis of water and creates ROS which oxidises antioxidants, measuring GSH in plants that have been exposed to IR is a logical endpoint to investigate. For if the dose of IR is high enough to overload the system by flooding it with ROS, then measuring GSH may be a good indicator of assessing how the plant system is coping with such a dose. What is equally interesting is if doses of IR show little or no effect on GSH concentrations then the antioxidant system could be perceived to have the capacity to function fully. Therefore, it is possible to ask whether certain doses (e.g. low doses, even low doses that have an effect on endpoints such as DNA methylation rates) impact the antioxidant system at all.

1.5.1.7 Epigenetic mechanism of DNA methylation and IR in plants

DNA methylation is an epigenetic mechanism used to control gene expression via the addition of a methyl group to DNA (Simmons, 2008) at the carbon 5 position of the cytosine ring. Methylation is defined as epigenetic because changes in expression can occur without mutating DNA and can be transmitted through generations. In plants, this is factor-specific over a multitude of organisational levels depending on species, age, tissue and organelle (Vanyushin, 2006). DNA methylation can also be described as an epigenetic signalling tool (Phillips, 2008) whereby genes can be deactivated, (also known as gene silencing). DNA methylation is the most common epigenetic modification in plants used for genomic stabilisation (Kovalchuk *et al*., 2003). In the halophyte *Mesembryanthemum crystallinum* hypermethylation of DNA is involved in the expression of a new metabolic programme under conditions of salt stress. It

occurs alongside a switch-over to crassulacean acid metabolism (CAM) from C_3 photosynthesis (Dyachenko, 2006). This suggests that DNA methylation and alterations in plant function could be a response to stress alongside other processes. One of the most notable differences between DNA methylation and other forms of epigenetic change is the heritability factor, where methylation is an epigenetic mark with a higher degree of permanency in generations of plants (Vanyushin and Ashapkin, 2011). This is exemplified in processes such as vernalisation (Vanyushin and Ashapkin, 2011), where plants can be selective for favourable conditions for life-cycle timing events such as flowering.

Kovalchuk *et al*. (2003) discovered the first epigenetic change in response to chronic IR exposure in *Pinus sylvestris* in the field at Chernobyl, observing that exposed pine trees had undergone considerable hypermethylation. This was investigated using DNA extracted from pine needles obtained from various sites of tree crowns and a cytosine extension assay that detected methylation via a methylation-sensitive endonuclease. Pine trees from the site had been studied in previous years and morphological disturbances were reported including absence of needles, growth depression and differences in shoot orientation. The trees later recovered from some of the effects and so potential adaptation was hypothesised. Ten-year-old progeny of the same morphologically altered trees were examined and dose-dependent hypermethylation of DNA was recorded. Parental pine generations (exposed to about 20 – 40 Gy) exhibited a higher rate of methylation than control trees, and interestingly, a second generation which received a lower dose were also less methylated. Also notable was that young trees planted in radioactively contaminated sites exhibited a much higher methylation rate than trees planted from previously radioactively-exposed seeds and grown in uncontaminated soil- indicating that methylation occurs at a later

developmental stage and not at seed. Even though mutation rates are increased by IR, the speed of the adaptation and widespread mutation in an entire tree population suggests epigenetic change rather than that of mutation.

1.5.2 Effects at organism level

While the impacts of IR at the molecular level are fundamental to our understanding of effects (directly or indirectly) on the core components of plants, it is appropriate to question whether, at particular doses, molecular effects are having an overall impact on the fitness of an organism as a whole. Acute high external doses of IR (10s of Gy) have long been known to affect most aspects of shoot growth, with recent reports suggesting effects on developmental timings (Nishigughu *et al*., 2012; Sidler *et al*., 2015), morphology (Celik *et al*., 2014; Sever-Mutlu *et al*., 2015), anatomy (De Micco *et al*, 2014) and the development of bulbs (Mostafa *et al*., 2015). As there have been for many years, there are recent reports that acute high doses sometimes have positive (hormetic) as well as negative effects on subsequent growth. For example, at 10 Gy given over 10 secs Hamideldin and Hussien (2014), using different potato varieties, noted some positive as well as negative effects on subsequent height, leaf area, stem diameter and tuber diameter. Several studies carried out in the immediate aftermath of the Chernobyl accident not only confirmed the sensitivity of the shoots of some species to IR and but also detailed a variety of effects that supplemented very significantly knowledge about acute effects of IR in the field. These studies have now been complemented by some research to elucidate the effects of chronic low doses.

Mousseau *et al*. (2013) used tree cores of *Pinus sylvestris* at Chernobyl to observe that trees in locations near the reactor had different, and more variable, growth rates of above ground parts after irradiation from the accident. Although these effects were correlated with dose rates in 2009, it was not possible to disentangle the effects of high acute post-accident doses from any due to subsequent lower doses. The extensive studies carried out on *P. sylvestris* in the Bryansk region of Russia since 2003 by the Russian Institute of Radiology and Agroecology, coupled with detailed dose calculations, can more clearly distinguish effects caused by chronic low doses of IR in the period remote from the accident. In general, these studies are in good agreement with the ERICA (2003) recommendation for exposure of 100 mGy/a [*c*. 10 µGy/h] to be used as a safety margin for non-human biota (Makarenko *et al*., 2016). It is notable that of the many endpoints measured in these studies, there are some in which significant effects of IR are reported, especially cytogenetic ones, but that these are not, overall, adverse enough at the level of the individual or above to merit a reconsideration of the 100 mGy/a dose-rate limit. At the Semipalatinsk nuclear test site in Kazakhstan, studies of *Koeleria gracilis* (crested hair grass) that had inhabited for 50 years soils contaminated with radioactivity and with a current dose rate of 4 to 285 mGy/a, also showed cytogenetic effects at the highest doses but no morphological effects (Geras'kin *et al*., 2011), strengthening the opening point regarding the significance of effects at higher biological levels. Further to this, seeds collected from the most exposed plants did not differ in their response to irradiation suggesting that IR has not exerted any selection pressure over 50 years and that recommended dose limits were appropriate.

Studies carried out at Chernobyl by the Ukrainian Institute of Agricultural Radiology have provided evidence of effects on whole plants at lower chronic low doses. In

studies on *P. sylvestris* planted after the accident at Chernobyl and investigated 25 years later, normalised dose rates for the period, based on the sum of both internal and external doses, of 10 µGy/h and less were related to significant cytogenetic and morphological effects (Yoshenko *et al*. 2011). At 40 µGy/h there were significant effects on apical dominance, with cytogenetic effects being related to incidence of morphoses. In experiments with *Lemna minor*, which enables detailed developmental analysis under controlled conditions, doses of 80 µGy/h to 4.95 mGy/h had no effect on physiological, morphological or developmental parameters (Van Hoeck *et al*., 2017). Overall, therefore, some effects of chronic low dose IR on individual plants shoots have been reported at the low end of DCRL ranges although it has not been suggested that they are significant at the population or community level.

Plants are well known to respond to soil stresses via changes in their roots (e.g. Bochicchio *et al*., 2015), which can then affect overall plant function. Gunckel (1956) noted that roots are shielded from much α and some β IR by the soil which, together with practical difficulties of experimenting with roots, may have contributed to relatively few studies of the effects of IR on roots having been reported. However, the fact that the long-term fate of much contamination following accidents at Khyshtym, Chernobyl and Fukushima has been in soil root zones highlights how important the effects of IR on roots might be. This is particularly relevant in the earliest stages in the plant life-cycle that have particular proximity to the soil and that are generally the most susceptible to the effects of stress. Further, even for the biologically mobile Cs, accumulation from root uptake is almost always higher in roots than shoots (Danchenko *et al*., 2016) - a distribution that is generally more pronounced the less mobile a radioisotope is.

Acute high doses of IR have long been known to quickly affect roots, primarily via the root meristem. Gray and Scholes (1951) found that irradiated *Vicia faba* roots (1.2 Gy) had inhibited growth and that exposing only root meristems had the same effect as exposing the entire root system. In pea and maize, survival of root apical meristems post-irradiation event (3 – 32 Gy) showed that resistance to radiation at different points in the cell cycle varied slightly between species, and that there were overall differences in resistance depending on phases of early growth (Gudkov and Grodzinsky, 1982). Duration of individual phases of the cell cycle and overall cell cycle period was also changed depending on species. Exposing *Arabidopsis thaliana* roots to 3 kGy inhibited elongation from the root tip and induced root hair elongation and cell expansion (Nagata *et al*., 2004). Some studies report either root elongation or growth inhibition depending on dose (Maity *et al*., 2005; Yadav, 2016). Acute doses from ion beams on root meristems indicate that they are a key exposure site (Zhang *et al*., 2016) and several studies note the role of changes in ROS in roots after acute high exposures (e.g. Nagata *et al*., 2004).

Biermans *et al*. (2015) using solution cultures reported that, over 7 days, doses of 11 mGy/h from Am-241 reduced the root growth of *A. thaliana* and affected its dry matter but that lower doses did not have the same effect. Sahr *et al*. (2005) reported that dose rates of 100 µGy/h (from 60 kBq/L Cs-134 in a solution culture) affected *A. thaliana* root growth but that doses of 50 µGy/h did not. Below these dose rates there are no reports of morphological changes, although several studies have reported genetic and cytogenetic changes which yet again, lends strength to the argument that effects at one level are not necessarily detected at another, and more importantly, have any deleterious effects on organisms or at any other organisation level.

That being recognised, there may be some discrepancies in genetic and cytogenetic effects between root and shoot portions of a plant. A standard *Allium* root tip test revealed a linear relationship between dose and chromosome aberrations up to a dose of about 80 µGy/h in Chernobyl contaminated soil (Kovalchuk *et al*., 1998 a+b). Similar studies with Sr-90 contaminated sites have also shown similar effects at even lower dose rates. In naturally enhanced background areas at Ramsar (with up to 12,500 Bq Ra-226/kg soil and doses of up to 100 µGy/h) Saghirzadeh, *et al*. (2008) also described chromosomal aberrations in *Allium* root tips. However, in neither of these studies were threshold relationships tested.

There is, therefore, much to be learned about the effects of IR on roots - the 'hidden half' of plants. It seems likely that there are detectable effects of chronic low doses at the genetic and cytogenetic levels at the low end of DRCLs, and perhaps below. There is some evidence of morphological, or other whole root effects, close to DCRLs. Downie *et al*. (2005) emphasised how often roots are examined artificially flat and that there is still a lack of focus on root-environment interactions. Methods for examining roots *in situ* have been developed for a variety of media including soil (Yuan *et al*., 2016), paper wick (Adu *et al*., 2014) and gels (Bochiccino *et al*., 2015), which would be very useful for examining the effects of chronic low dose IR on root systems.

Overall, plant morphology has long been known to alter when exposed to high doses of radiation. In recent years, advances in image-based analysis has enabled the study of phenomics. Phenomics is concerned with phenotypic variation and its causes, effects and implications. Houle *et al*. (2010) explained that the understanding of phenomics is far less comprehensive than that of genomics. If this is the case then it might be possible to say that the same can be said to an even larger extent within the field of radioecology. Morphometrics, the quantitative analysis of shape and/or form of

a subject is fast-becoming a key method of producing high-throughput data for phenomics. Ultimately, root and shoot studies in radioecology should employ high throughput image analysis to complement the increasing plant stress biology phenomic data as it is a fast and powerful way of analysing subtle environmentally-induced changes in plants using large datasets and semi or fully automated systems.

1.5.3 Effects on reproduction and viability

Reproductive capability in plants is often used as an indicator of IR stress response, just as it is used as an endpoint in general environmental stress-response analyses. Depending on mechanisms, reproductive effects on organisms can be stochastic or deterministic (Copplestone *et al*., 2004) and confounding factors, as observed in a variety of plant stress-related endpoints in the field, potentially contribute to this.

IR has a long-standing history of recognition as a threat to reproductive organs, and this is exemplified by the conservativism in specialist radioprotection measures in human biology e.g. Ionising Radiation Regulations (Crown copyright, 2017) concerning restriction of exposure during pregnancy (part 2:9). It is therefore unsurprising that detrimental reproductive effects have also been discovered in non-human biota and are cause for further investigation. For example. with *Caenorhabditis elegans* investigations of the impact of IR often use reproductive endpoints (Buisset-Goussen, *et al*., 2014). In general, propagules in plants almost always have very high, often extremely high, levels of redundancy, i.e. the toll of adverse environmental effects (which essentially always exist in the wild) on success is overcome by the high numbers of propagules produced. There are many reports that acute exposure of seeds to high dose rates of IR produce hormetic effects on subsequent growth (recently, e.g., Ahuja *et al*., 2014; Maity *et al*, 2005; Marcu *et al*., 2013a+b; Yadav *et*

al., 2016). Acute high dose rates have also been shown to affect a variety of seed constituents (e.g. Jan *et al*., 2012; Tilkai *et al*., 2015; Vaizogullar & Kara, 2016), which might affect subsequent germination and growth. In the field, soon after the Chernobyl NPP accident, dose rates around 2 mGy/h produced lethal embryo mutations in *A. thaliana* (Abramov *et al*, 1992) and extensive studies of *P. sylvestris* near the Chernobyl NPP have shown that plants that received total doses of >2 Gy in areas of high short-term contamination had decreased reproductive ability and that this effect lasted for more than a decade (Fedetov *et al*., 2006). Boubriak *et al*. (2008) reported that in pollen collected from control and contaminated sites near the Chernobyl NPP different IR exposure affected the rate of DNA synthesis. In general, seeds and pollen have high resistance to environmental stressors but, perhaps because IR can penetrate their protective coats, it seems that relatively low total doses delivered at high dose rates can have effects, including hormetic effects, whilst large doses received at high dose rates can produce significant adverse effects.

Based on studies with 94 species (Kordium & Sidorenko, 1997) and 111 species (Møller *et al*., 2016), it has been suggested that, at time periods remote from the high post-accident doses, in the area around the Chernobyl NPP about 10% of species have slightly decreased pollen viability associated with enhanced doses of IR. Møller *et al*.'s study was carried out in 2008-2011 and included maximum dose rates of about 150 µGy/h. In long-term studies of *P. sylvestris* in the Chernobyl-contaminated Bryansk Oblast of Russia, germinating seeds have rates of cytogenetic damage of up to 1.3% that correlate with dose rate (Geraskin *et al*., 2011), and that is repeated elsewhere at even lower dose rates (Evseeva *et al*., 2009). Several detailed studies of plants growing in the East Urals Radioactive Trace (EURT), which has the longest history (1957 onwards) of any widely studied radioactively contaminated site and has

dose rates of up to 240 mGy/y (*c*. 28 µGy/h), have shown dose-dependent effects on germination or viability of seeds of *Taraxicum officinale* (Pozolotina *et al*., 2012), *Meliandrum album* (Antonova *et al*., 2013) and *Leonurus quinquelobatus* (Karimullina *et al*., 2015). Several authors have noted that chronic low dose rates of IR can make germination more variable, particularly in response to weather conditions (Antonova *et al*., 2013; Geraskin *et al*., 2016) and other soil contaminants (Evseeva *et al*., 2009; Karimullina *et al*., 2015). There is, however, evidence from studies in Bryansk, Russia, that such effects do not alter the overall reproductive capacity of *P. sylvestris* (Geras'kin *et al*., 2017).

Studies in areas contaminated from the Chernobyl NPP accident (in particular with the relatively sensitive *P. sylvestris*), and especially in the EURT, have shown that chronic low dose effects on plant propagules can be sustained for many generations. Boratyński *et al*. (2016) hypothesised that effects of IR on life history responses might be sustained for generations in the absence of irradiation. Wild carrot plants, sampled from around Chernobyl (0.08 to 30.2 µGy/h) and then grown in uncontaminated soils in a greenhouse showed correlations between previous radiation dose and the timing of developmental events. The presence of trans-generational effects has perhaps helped prompt some discussion about 'adaptation' of plants to chronic low-level doses of IR. For example, studies of flax and soya seeds grown over several generations near the Chernobyl NPP have shown differences in seed constituents and prompted suggestions of adaptation to chronic low dose IR (Gabrisova *et al*., 2016 and refs therein), as have effects of high doses on pollen (Boubriak *et al*., 2008), the ability of plants from Chernobyl to resist the effects of mutagens (Kovalchuk *et al*., 2004) and studies at a number of other contaminated sites (e.g. Boubriak *et al*., 2016; Geras'kin *et al*., 2013; Møller & Mousseau, 2015). These references, and references therein,

provide evidence that at chronic low doses in the range of a few 10s of µGy/h, some plants can have increased heterozygosity, increased rates of DNA repair and increased variability of key seed properties and constituents. There is also evidence of some increase in radioresistance, at the DNA and cytogenetic level, in some species at these dose rates.

1.5.4 Effects on plant communities and populations

This section deals with the final level of investigation (or the first, depending on which perspective one takes) into plant responses to IR at environmentally relevant doses. As previously discussed, effects observed at one level focused further down the scale of biological organisation may not always be reflected in effects further up the scale, and that is why it is important to examine communities and populations of plants and to determine how appropriate drawing conclusions and basing recommendations from those derived from another level (for the purpose of providing environmental protection measures) at the communities and populations level is. It may be the case that basing legislation on high-resolution findings at lower levels are causing overly conservative limits to be in place. More will be discussed in chapter 6, but first, the literature to date regarding population and community effects will be examined. It is worth mentioning, however, that studies at this level, particularly field studies with a whole-ecosystem approach are, much rarer than detailed laboratory studies and so this imbalance has the potential to skew results, potentially creating unnecessary inferences made in legislation, or the inverse.

Key insights into plant population biology and community ecology have been derived from studies of stress and disturbance. From early on in the nuclear age, high-dose

IR of 10s to 100s of Gy was used not just to understand its effects but also to gain fundamental ecological insights using its unique properties as a stressor where high activity point sources produced predictable, continuous gradients of stress and could be switched on and off using shielding. For example, the US Atomic Energy Commission's experiments, primarily in the 1960s, with high activity point sources in a variety of ecosystems (Jordan, 1986) informed early thinking about tropical forests in particular (Lugo *et al*., 2004) and the results of studies at US nuclear weapons test sites in Micronesia probably influenced important conceptions of ecosystem ecology (Deloughrey, 2013). Aside from ecological insights, from these studies, and from those in the USSR, it became clear that populations of plants were most sensitive in the order trees>shrubs>herbs, and that coniferous trees were more sensitive than hardwood trees. It was originally suggested that sensitivity of plant populations correlated with chromosome size and number (Woodwell, 1962) but later syntheses of these experiments suggested a better correlation with proportion of non-photosynthetic to photosynthetic material (Jordan, 1986). Plant populations that underwent fatal doses close to point sources had, when studied, not recovered decades later (Stalter & Kincaid, 2009) but plants more distant from sources helped inform the IAEA suggestion that a dose rate of 100 µGy/h or less did not affect plant populations.

Numerous studies post-Chernobyl in locations proximal to the reactor that received high acute doses added an impressive range of details to the understanding of high-dose effects and, overall, supported previous suggestions about the adverse effects of high doses and of the sensitivity of plant populations. In particular, *P. sylvestris* was found to be particularly sensitive and *Picea abies* to an even greater extent (Geras'kin *et al*., 2008). At sites contaminated from the Chernobyl accident together with other

studies in Russia in the EURT and at uranium mine tailings, lower dose rates (even at around previously suggested dose limits) have shown cytogenetic effects (Geras'kin *et al*., 2013), decreasing significantly the dose rates at which effects have been demonstrated. The significance of these effects for plant population health is unclear. Discoveries at U-mine tailing sites infer that there is the possibility of chemical toxicity (that explain some of the effects that might change populations) and at Chernobyl-contaminated sites the possibility of persistence of effects from previous high-dose exposure to populations might have occurred and continue to occur. At the Semipalatinsk test site, there is good evidence of cytogenetic changes at doses of 10 µGy/h but also supporting evidence that it does not affect plant populations (Geras'kin *et al*., 2013).

Climate, soil type, species of plant, and the topographical and geological features of a region can all affect the behaviour and effects of IR in natural ecosystems. Mechanisms of forest contamination in the long-term still has many unanswered questions as, even though more than 30 years have passed since the Chernobyl accident, that entire timescale is only half of an average forest cropping cycle in many contaminated areas (Takahashi *et al*, 2016). Overall, evidence suggests that the cytogenetic changes found in the DCRL range probably do not affect population characteristics or that if they do the effects are subtle. Subtle effects may be of some ecological significance, with the magnitude of stress and disturbance from other sources perhaps playing a key associative role.

1.6 Cosmic radiation effects on plants

Space exploration is a growing industry in both government and private sectors. No longer are space programmes exclusively led by governments and national space agencies. The possibility of commercial space flight is fast becoming reality. On 6th February 2018 a significant step was made when the private company, SpaceX, launched the Falcon Heavy rocket in its maiden test flight, complete with a payload heading for Mars orbit. Historically, SpaceX rockets have been routinely used to resupply the International Space Station (ISS), alongside government shuttle missions. This introduction of lower-cost launches (Falcon Heavy cost *c*.90 million USD, compared to the average space shuttle launch by NASA at *c*.450 million USD) signalled a turning point in the possibilities of sending more missions to space. With increased space exploration, more interest is now being shown in astrobiology and exobiology- the fate of biological organisms in the extra-terrestrial environment relative to Earth, and of other planetary bodies respectively.

In order to support life for a prolonged period of time, without the need for continuous (and costly) resupply missions, a sustainable method of growing plants in space, known as Bioregenerative Life Support Systems (BLSS) (Arena, De Micco and De Santo, 2012) is currently being sought. A significant challenge to growing plants for food (and other beneficial reasons such as air regeneration and overall wellbeing) in space is cosmic radiation. Understanding the impact of this radiation on general crew performance and health is already recognised as crucial to performing successful missions in space (Reitz, 2008).

To successfully grow plants in lunar and Martian environments, consideration must be given to the lack of atmospheric layers that traditionally protect planet Earth and allow plants to grow with shielding from cosmic rays and other high-energy particles. Heavy ion particles (HZE) have historically been the key area of focus for radiation effects during spaceflight for radiobiologists as they are the most damaging (induce the highest incidence of genetic mutation) (Arena, De Micco and De Santo, 2012), but recently attention has been given to the "softer" particles, i.e. belt electrons and low-energy protons. These soft space rays are responsible for 99.9% of total dose absorbed in Low Earth Orbit (LEO), the region in which the ISS resides.

Plants have successfully been grown in LEO on the ISS by various space agencies in several different programmes. A key line of enquiry is that of the effect of weightlessness on plant growth but also cosmic radiation effects. Facilities on board the ISS now include a stable orbital environment, growth chambers with modification capabilities, laboratory benches, dedicated crew support and a reliable method of storing and returning samples for analysis (Paul *et al*. 2013).

Studying the effects of cosmic radiation on seeds that have been flown in LEO and had chronic exposure (6 months) aboard the ISS (shielded) is interesting because the radiation doses received on the ISS are in the range of but do not exceed the average doses to plants outlined in chapter 2, which were designed to be comparable to the radiation doses currently received in most areas of the Chernobyl exclusion zone. An ongoing project with the designated operative nomenclature label "DOSIS-3D" is a unique attempt at mapping radiation dose across the entire ISS. The study has previously used and continues to monitor different segments of the station with a combination of active and passive dosimeters (Berger, 2017). In combination with solar cycle data it has been possible to examine radiation dose correlation. 11 passive

dosimeters comprised of thermoluminescent detectors and nuclear track etch detectors were positioned at various locations within the European laboratory module, Columbus (Fig. 1.13). The most recent findings have shown that absorbed dose values correlate with shielding configurations local to each detector package. Between the years 2010-2012, the minimum recorded value for absorbed dose was 195 µGy/d and maximum dose was 360 µGy/d (Berger *et al*. 2016). Such dose is reported to be modulated by a combination of solar activity and ISS altitude variation.

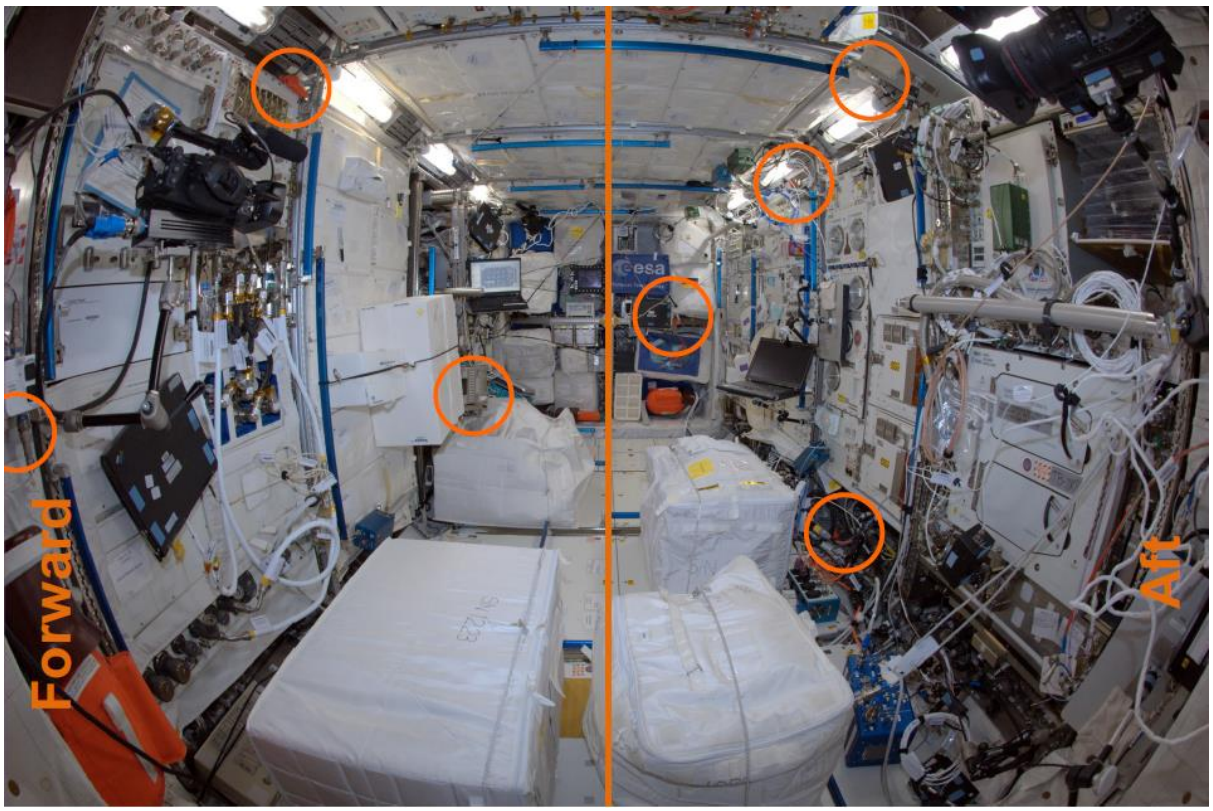

Fig. 1.13 Positions of radiation detectors aboard the European laboratory module on the International Space Station (Columbus Module) (Berger, 2017).

Observations have shown that plants can thrive in the elevated radiation environment aboard the ISS. However, it is crucial to point out that the ISS not only has enhanced shielding from cosmic radiation (built into the spacecraft) but that it is also within the magnetosphere, the region of near-Earth space where the geomagnetic field is confined by solar wind surrounding planet Earth (Consolini, 2018) which deflects the

most harmful high-energy particles. Without this layer, plus the additional physical shielding of the ISS, the radiation dose would be much higher, and this is a key concern for exploration to Mars (Dartnell, 2011). That said, it is still a valid line of enquiry to investigate effects within the shielded ISS as efforts for sustaining life aboard it are ongoing. Further, although it is energy deposited into water or DNA that is key to producing the effects of ionising radiation, the type of particles that deposit it, which are different in cosmic radiation as compared to, for example, the Cs-137 that now dominates the Chernobyl exclusion zone, may produce different effects.

There is a marked variance in the average absorbed dose that astronauts on the ISS have registered using dosimeters depending on the stage of the solar cycle (ranging from 80 mGy over 6 months at solar maximum to 160 mGy at solar minimum) (NASA Facts, 2002). The solar maximum is the period when there is the maximum number of sunspots and the maximum solar magnetic field for particle deflection. This variance should be taken into consideration when calculating cosmic radiation doses in space.

1.6.1 Experiments using plants on board and external to the International Space Station (ISS)

Sugimoto *et al*. (2014) examined oxidative stress-induced transcriptome effects on *Mizuna* plants grown from seed aboard the ISS for 27 days. *Mizuna* was selected due to crop cultivation potential as a food source for astronauts as well as for aesthetic/wellbeing purposes. It was found that a range of genes relating to general abiotic and biotic stresses were up-regulated in the plants as well as some genes specific to the spaceflight environment. Whether the latter were cosmic radiation stress-induced or activated by another factor such as weightlessness is unclear, but

the plants grew just as well, if not better in the space environment (fresh weight (g) 82.9g, water content (%) 92.5% in ISS flown Mizuna compared to 58.0g and 92.0% in ground-based controls). This led to a suggestion that spaceflight prompts the up-regulation of stress-related genes but plants appear to utilise these to cope with or adapt to stress, akin to how plants can react on Earth to stressful environments. This "reprogramming" of the plant's ROS-related gene network in particular enabled plants to successfully grow in LEO. The question remains, however, of how plants would be able to grow and adapt in the absence of radiation shielding on the ISS.

The Expose-E multi-user facility was an experimental protocol physically attached to the ISS's EuTEF platform that ran for 18 months. The system comprised several component trays on the outside on the ISS attached to the Columbus laboratory module that allowed for the unshielded study of various exobiological experiments in electromagnetic radiation, space vacuum, cosmic radiation effects and a Martian surface simulator (Rabbow *et al*. 2012). It is vital to test biological samples located externally to the ISS because spacecraft interiors not only often have some shielding but also host reactions between primary particles and the structural materials (of the craft) which produce secondary radiation. Passive thermoluminescence detectors (TLDs) were applied to different sites on the EXPOSE-E to provide reference doses for experiments during missions (Berger *et al*., 2012). The EXPOSE-E tests were carried out to investigate the ability of plants (amongst other organisms such as tardigrades and lichens) to withstand space travel. The aim of this type of investigation is to ascertain if theories of panspermia, the idea that carbon-based life has been transported to Earth from the extra-terrestrial environment, are plausible. Two thousand one hundred seeds from *A. thaliana* and *Nicotiana tabacum* were placed in Expose-E for the entire duration of the project and returned to Earth where they were

germinated (Tepfer *et al*. 2012). Only 23% of seeds produced viable plants, of which survival was higher in *N. tabacum* (44%) (Fig. 1.14). The total dose that the seeds were exposed to was 295.6 mGy, derived from three sources: galactic cosmic rays (53.1 mGy), South Atlantic Anomaly (SAA) protons (237.7 mGy) and outer radiation belt electrons (4.8 mGy). The total dose was the sum of each of these sources. SAA protons occur when the displacement of the magnetic dipole axes causes the radiation belt to move closer to the surface of Earth (Reitz, 2008).

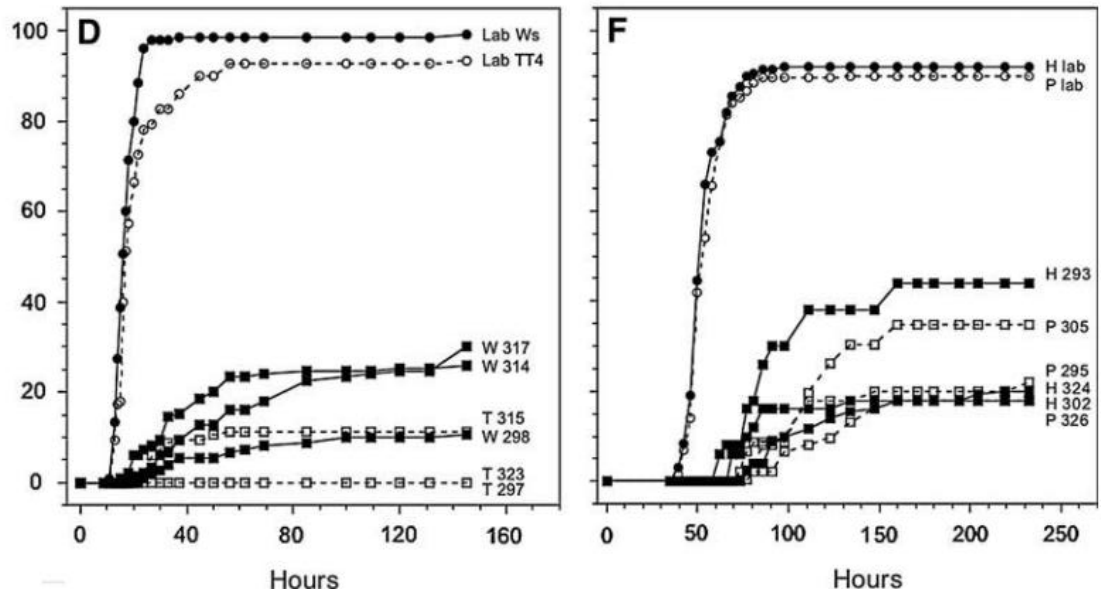

Fig. 1.14. Percentage germination over time of (D) wild type A. thaliana (F) N. tabacum exposed on the ISS to complete space conditions. For A. thaliana (D) Each curve represents 150 seeds summarised as the mean of a 50-seed sample (n = 50 x 3) and this is the same for control samples. For N. tabacum each curve represents 50 seeds (n = 50) and controls represent the mean of 4 samples (n = 50 x 4). Samples denoted Lab x or x Lab are control (Earth-based) samples in both species and ISS-flown sample group tags are denoted by a letter followed by three digits (X nnn). The y axis represents germination rate as a percentage (100% meaning all samples had successfully germinated.) (Reproduced with permission from Tepfer et al., 2012).

Effects delivered from the (accumulated) three types of space radiation previously mentioned were considered 'minor, but measurable' after the 18-month exposure and was attributed to species-specific delays in germination, 7h in *A. thaliana* and 14h in

N. tabacum (Fig. 1.15). These were reported to be the most significant effects of radiation from space in the study. Changes in DNA repair mechanisms were not expected due to the dry state of the seeds and thus the production of very few free radicals from photolysis or photoionisation of water.

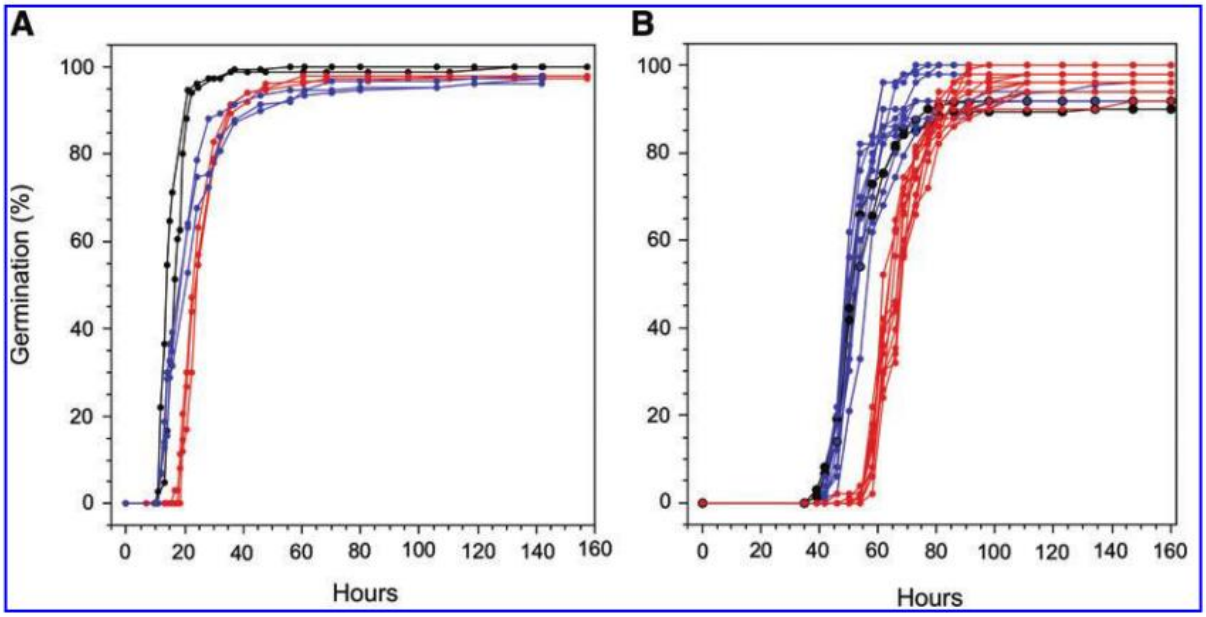

Fig. 1.15. Delay in germination (shown along y axis as percentage germination and x axis in hours) in (A) A. thaliana and (B) N. tabacum Legend: lab controls (black), ground based analogue for space radiation (blue) and ISS (red). Each curve represents accumulated germination as the means of three samples where a single sample contains 50 seeds (n =1 x 50 seeds). (Reproduced with permission from Tepfer et al., 2012).

In a later experiment by the same group, the EXPOSE-R research included a protocol with *A. thaliana* attached to the exterior of the Columbus laboratory of the ISS (note, R indicates that the EXPOSE hardware was used on the Russian segment of the space station, and E, the European segment). In this experiment, the exposure time was 124 days longer than in EXPOSE-E, and cosmic radiation dose was greater by a factor of 1.6. *A. thaliana* seeds on EXPOSE-E were almost completely sterilised upon

return to Earth for germination tests (0-3% in all varieties including wild type) but this was attributed to the UV dose received during spaceflight, confirmed in ground-based analogues (Tepfer and Leach, 2017). Interestingly, space relevant UV doses were tested on seeds of *C. arvensis* and these were found to be resistant to doses previously lethal to *A. thaliana* and *N. tabacum*. This supports the assertion that a more robust seed coat (as in *C. arvensis*) may hold the key to germinating plants outside of a shielded environment in space.

1.6.2. Radiation data from NASA missions on board the ISS

NASA Genelab made radiation data from each of the eight space shuttle missions to the ISS publicly available (Fig. 1.16). These doses were measured inside the ISS.

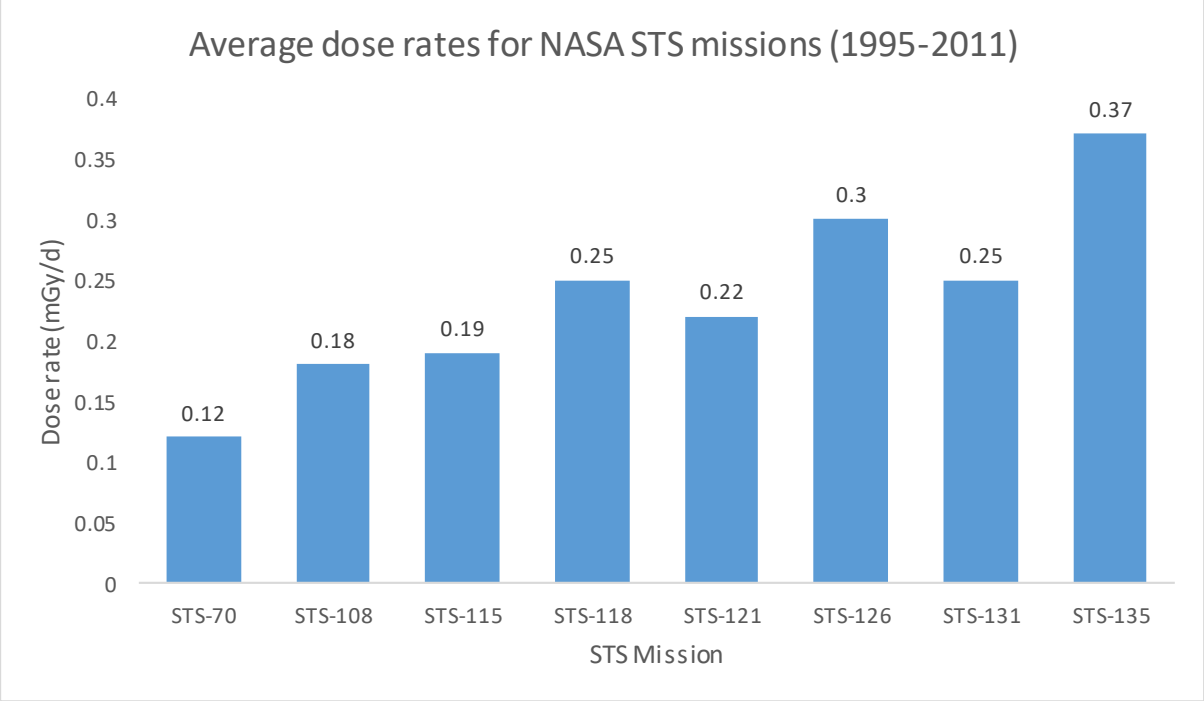

Fig. 1.16. Average dose rates in mGy/d for each of the eight NASA STS missions between the years 1995 and 2011 using publicly available data from NASA Genelab: https://genelab-data.ndc.nasa.gov/genelab/environmental/radiation.

1.7 Morphometrics

Leaves are the most diversified organs among terrestrial plants ahead of flowers, stems and roots (Tsukaya, 2017). This diversity arose partly from the need for plants to carry out photosynthesis in their leaves and thus, due to the variation in environmental conditions, leaf shape has been, and continues, to be a key evolutionary response.

There are only two mentions of the term “morphometrics”/” morphometrical” in the Proceedings of the Third International Symposium on the Protection of the Environment from Ionising Radiation (2002) and they are for fish and *Daphnia* respectively. But the field of morphometrics is currently gathering momentum internationally for plant stress studies for stressors other than IR. The word morphometrics itself comes from the merging of two classical Greek words; morphé which means “form” and metron or “that by which anything is measured”. First mentioned in the scientific literature in the 1960s, this measuring of form was primarily utilised as a method of identifying plant species (Remagnino *et al*., 2017) and wasn’t widely employed until ‘Multivariate Morphometrics’ was published (Blackith and Reyment 1971). This book took the concept of multivariate statistics and applied it to measurement data (consisting of linear dimensions) from which it made inferences based on statistical reasoning. Rohlf and Marcus (1993) described the methodology as revolutionary, praising the effectiveness of morphometrics in information capture with regards to object shape, prompting its application in various fields of research such as taxonomy and evolution.

Allometry is the study of biological scaling, i.e. the relationship between geometric measurements and biological levels of organisation such as anatomy or physiology.

For example, allometry could be used to investigate the relationship between IR and impediment or promotion of leaf area in exposed plants. Niklas (2004) alludes to the method as useful not just at the individual level, but for populations of plants too. Fluctuating asymmetry, the deviation from ideal bilateral symmetry in leaves, is a popular plant morphometrical endpoint in stress studies, useful in its own right and in the study of allometry. Wadhwa *et al*. (2017) proposed the measurement as a bio-indicator of abiotic stress in plants and animals and used measurements of leaf symmetry as an ecotoxicological indicator for heavy metal stress in tree populations. More recently, Alves-Silva *et al*. (2018) provided a new perspective on fluctuating asymmetry, and identified that there was a lack of standardisation for sample size. When tested, evidence showed that histograms are more useful than P-values when assessing this endpoint and that there is still no 'rule of thumb' value for sample size.

1.8 Summary of relevant knowledge gaps

Overall, there has been particularly limited research into plant responses to IR at low doses, especially under controlled conditions. Using a variety of research outputs that have reported data from controlled conditions to the field, it is evident that there is still much debate about the effects of IR on plants at low doses. This debate appears to exist regardless of the biological level at which effects are studied. Further, there is little attempt in the literature to reconcile effects described in the field with those generated under laboratory conditions. Assumptions are made about the cause of effects in the field without follow up experiments under controlled conditions, especially at lower doses. Even more markedly, there is a lack of data regarding transgenerational effects at low doses, with an almost total absence of studies of this kind which combine investigations at different levels of biological organisation. There

is, therefore, great scope for conducting research into transgenerational effects of chronic IR at low doses under controlled conditions. Most notable throughout the literature is a shortage of morphological studies on individual plants, especially the effects of IR on roots of individual plants. This is important because it is the individual, primarily through its phenotype, that is the primary unit of natural selection and, therefore, the basis of long-term environmentally significant effects.

1.9 Project outline and scope

1.9.1. Aims and objectives

The experiment that formed backbone of this project was a transgenerational study with the aim of growing *A. thaliana* plants under chronic low level IR and tracking them through the entire life cycle (seed to seed) by using image analysis to understand developmental timings and morphometric characteristics, and biochemical analyses to measure antioxidant status. A second aim was to create a novel protocol for studying plants roots *in situ* that could be used to study internal and external radiation doses under similar conditions. A later opportunity arose to study two different types of horticulturally important crops (tomato and lettuce) that had received a cosmic radiation dose on board the International Space Station.

Objectives were as follows:

1. Grow several generations of *A. thaliana* under identical controlled conditions using a cadmium positive control and low-dose Caesium-137 radioactive treatment and measure uptake to examine whether there are any differences between treatment groups.

2. Use a high-resolution digital single lens reflex camera (DSLR) to take pictures of plants over the course of the growth cycle using a specialist bracket for birds-eye-view images to examine whether there are any differences between treatment groups.
3. Construct time-lapse videos of plant growth using images from objective 2.
4. Harvest mature *A. thaliana* leaves and scan them using a wireless high-resolution scanner and analyse using morphometric software to examine whether there are any differences between treatment groups.
5. Design and construct a hydroponic tank to allow for non-invasive image analysis of plant roots that can also be used in experiments with radioisotopes in solution to provide a novel and useful protocol for this and future research.
6. Perform germination tests on each generation of *A. thaliana* seeds after several generations had been harvested, using specialist germination paper in controlled conditions to examine whether there are any differences between treatment groups.
7. Measure total glutathione (GSH+GSSG) in transgenerational *A. thaliana* samples to examine whether there are any differences between treatment groups.
8. Grow seeds of rocket lettuce and tomato that have been flown on the International Space Station and exposed to a near-identical dose to the *A. thaliana* experiment by growing in soil treated with Caesium-137, analysing uptake of Caesium-137 and performing morphometric analyses with scanned leaves to examine whether there are any differences between space flown and control sample groups.
9. Grow seeds harvested from transgenerational *A. thaliana* experiment in agar plates for root image analysis to examine whether there are any differences between treatment groups.
10. Grow seeds from space exposed rocket lettuce and tomato in agar plates for root image analysis to examine whether there are any differences between space flown and control sample groups.

1.9.2. Hypothesis

The aims and objectives set out in the previous section were used to test the following hypothesis:

Chronic ionising radiation, at environmentally realistic low doses, has **a significant effect** on populations of higher plants over multiple generations.

Chapter 2: Effects of Chronic Low-Dose Ionising Radiation on the Stages of Development of *Arabidopsis thaliana*

2.1 Introduction

The most common endpoint for studying the effects of IR on plants, in any dose range and at any biological level has been DNA damage and repair. From 55 studies in both the field and laboratory, 53% of studies were found to have DNA damage and repair as the primary area of focus (Fig. 2.1). This was followed by analysis of cytogenetic changes (22%). Morphology accounted for a much smaller proportion of studies as an endpoint alongside seed viability (both 9%). Oxidative stress (as a standalone area of focus) was the least common endpoint (7%) but is linked to DNA damage and repair.

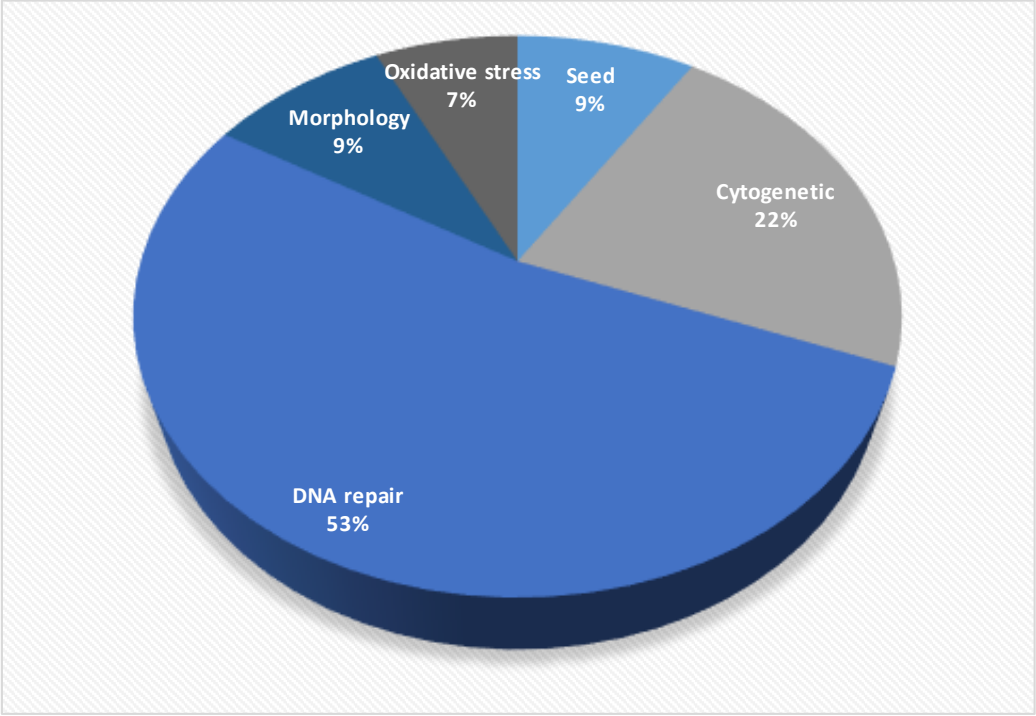

Fig. 2.1. Popularity of different endpoints in the study of effects of ionising radiation on higher plants from 55 published studies displayed as percentages. Data available in supplementary information.

Arguably, field experiments at sites with naturally-occurring enhanced background radiation together with radioactively contaminated legacy sites (e.g. active debris from disaster fallout) can, with respect to effects on non-human biota, be considered chronic exposure experiments. The general limitation to this claim is confounding factors and a particular limitation in the case of contamination events, a lack of knowledge about whether the effects discovered were caused before or after contamination event.

Recently, an increase in interest has emerged in the research community on the topic of transgenerational effects. Studying effects in multiple generations of non-human biota is helpful in establishing trends but may also indicate epigenetic influences. This may be useful if there is no evidence of change at the genome level of an organism but there are detected hereditary effects. Conversely, absence of trends but evidence of effects may suggest probabilistic effects related to a potential stressor.

The following experiment aimed to examine plant development over several generations, with each generation exposed to IR, at a level that was environmentally realistic (relatable to average dose found in the Chernobyl Exclusion Zone) and rarely studied in the laboratory. The dose assigned in this experiment was slightly below the ICRP Derived Consideration Reference Level (DCRL - *c*.40 μGy/h) for plants and which several field studies have called into question. This experiment was designed to shrink the data gap as described in the meta-analysis (detailed in chapter 1 and accessible in supplementary information).

2.2 Materials and methods

2.2.1 *A. thaliana* as a model plant

A. thaliana (thale cress) is a member of the Brassicaceae family. It is a popular plant for scientific study owing to several characteristics. It was the first plant to undergo entire genome sequencing. The sequence is small and transformation can be achieved through the use of *Agrobacterium tumefaciens*. It has a short life-cycle of around sixty days from germination to seed production making it ideal for whole life-span studies in a relatively short timeframe. Cultivation is straightforward in terms of care, and harvesting is simple but can be made easier by specially adapted growth systems (e.g. the Aracon system). Each silique produces between 30-60 seeds. Once a silique matures and dries it bursts open. Each plant can produce *c*.50 siliques producing a total seed production into the thousands. Seed handling is generally straightforward, however, due to small seed size (0.5mm) mechanical handling can be a slow process and great care must be taken to avoid sample loss and cross-contamination (The Arabidopsis Information Resource, 2002).

2.2.2 Growth-stage based phenotypes of *A. thaliana*

Plant morphology was an area identified as having a data gap in the literature for effects of IR. A highly cited method of measuring plant developmental stages was selected as the primary method of analysis for a long-term transgenerational experiment for *A. thaliana*. Growth-stage based phenotypic analysis (and a subsequent model for functional genomics) was developed by Boyes *et al*. (2001) as a reaction to the outcome of the *A. thaliana* genome sequencing success. This process was based on defined growth stages that acted as developmental milestones and benchmark points for morphological data collection. The stages are numerical with a descriptive tag and corresponding illustration for validation purposes. Stages cover

the entire cycle from imbibition to senescence (Table 2.1). Average timing for wild type (var Columbia – 'Col-0') plants are shown in Fig. 2.2.

Table 2.1 Growth stages and phenotypic descriptions with average day from date of sowing for the soil-based A. thaliana platform. (Reproduced with permission from The Plant Cell from (Boyes et al. 2001)).

		Col-0 Data		
Stage	Description	Days[a]	SD	CV[b]
Principal growth stage 1	Leaf development			
1.02	2 rosette leaves >1 mm in length	12.5	1.3	10.7
1.03	3 rosette leaves >1 mm in length	15.9	1.5	9.5
1.04	4 rosette leaves >1 mm in length	16.5	1.6	9.8
1.05	5 rosette leaves >1 mm in length	17.7	1.8	10.2
1.06	6 rosette leaves >1 mm in length	18.4	1.8	9.8
1.07	7 rosette leaves >1 mm in length	19.4	2.2	11.1
1.08	8 rosette leaves >1 mm in length	20.0	2.2	11.2
1.09	9 rosette leaves >1 mm in length	21.1	2.3	10.8
1.10	10 rosette leaves >1 mm in length	21.6	2.3	10.9
1.11	11 rosette leaves >1 mm in length	22.2	2.5	11.2
1.12	12 rosette leaves >1 mm in length	23.3	2.6	11.3
1.13	13 rosette leaves >1 mm in length	24.8	3.2	12.8
1.14	14 rosette leaves >1 mm in length	25.5	2.6	10.2
Principal growth stage 3	Rosette growth			
3.20	Rosette is 20% of final size	18.9	3.0	16.0
3.50	Rosette is 50% of final size	24.0	4.1	17.0
3.70	Rosette is 70% of final size	27.4	4.1	15.0
3.90	Rosette growth complete	29.3	3.5	12.0
Principal growth stage 5	Inflorescence emergence			
5.10	First flower buds visible	26.0	3.5	13.3
Principal growth stage 6	Flower production			
6.00	First flower open	31.8	3.6	13.3
6.10	10% of flowers to be produced have opened	35.9	4.9	13.6
6.30	30% of flowers to be produced have opened	40.1	4.9	12.3
6.50	50% of flowers to be produced have opened	43.5	4.9	11.2
6.90	Flowering complete	49.4	5.8	11.7
Principal growth stage 8	Silique ripening			
8.00	First silique shattered	48.0	4.5	9.3
Principal growth stage 9	Senescence			
9.70	Senescence complete; ready for seed harvest	ND[c]	ND	ND

[a] Average day from date of sowing, including a 3-day stratification at 4°C to synchronize germination.
[b] CV, coefficient of variation, calculated as (SD/days) × 100.
[c] ND, not determined (see text for details).

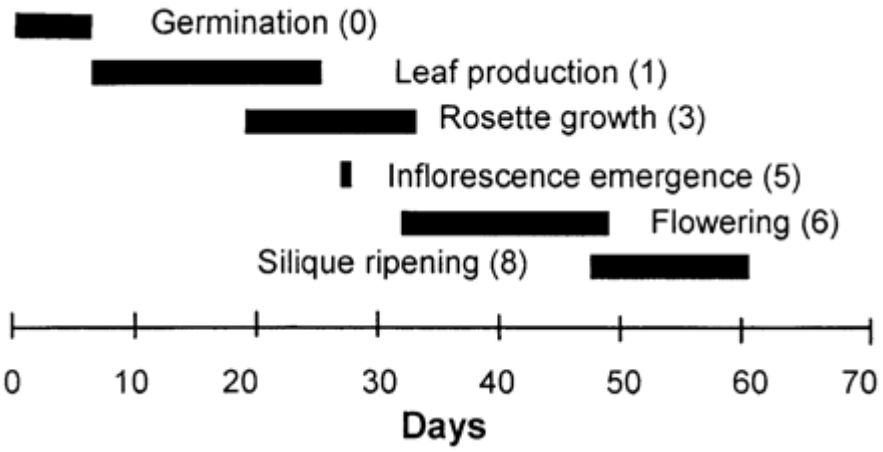

Fig. 2.2. Timeline for growth stages and phenotypic descriptions along a timescale measured in days with average day from date of sowing of wild type A. thaliana plants (Col-0). Reproduced with permission from The Plant Cell from (Boyes et al. 2001).

The Boyes *et al*. (2001) phenotypic tags and associated growth stages were considered appropriate for this experiment because the same methods have been successfully used in single generation IR stress studies (Ricaud *et al*. 2007), and many other plant stress studies such as those of salinity (Renault *et al*. 2010) and drought stress responses (Harb *et al*. 2010). The Boyes *et al*. (2001) method has been cited in over 1000 studies to date (Google Scholar, 2018).

2.2.3 Exposure of *A. thaliana* over multiple generations to chronic ionising radiation

Plants were grown from seed in a controlled laboratory environment within a growth chamber (for the entirety of the growth cycle) for a total of seven generations in environmental conditions aimed to be identical throughout the generations. In the initial phases of protocol development some methods were trialled and continued while other methods discarded. This section details the entire process from idea conception, prototype testing and optimisation.

2.2.4 Experimental design overview and optimisation

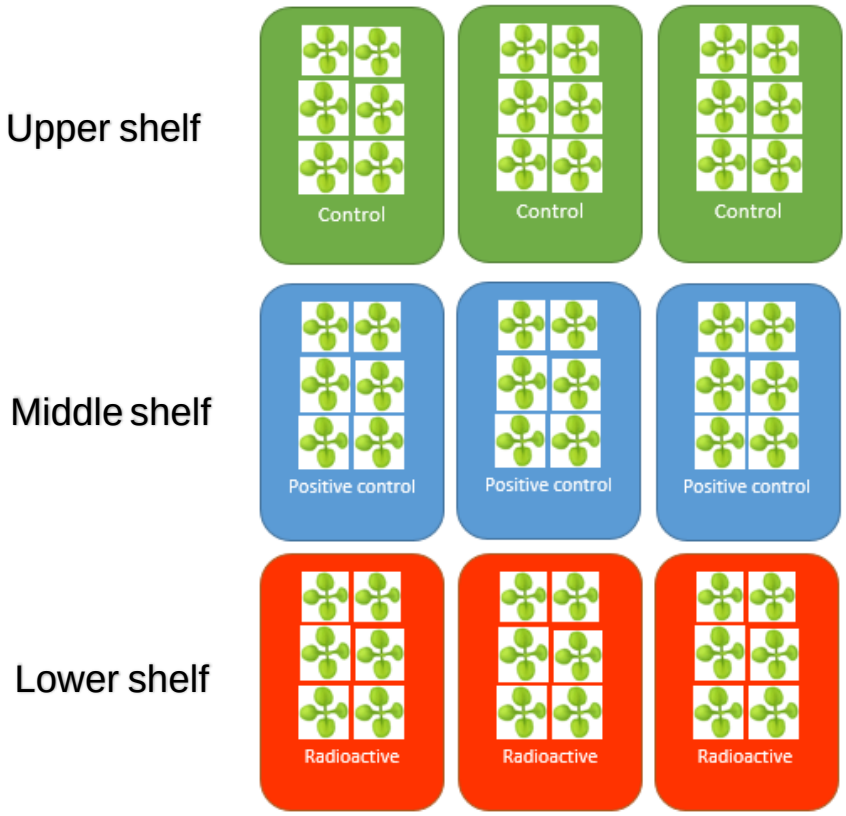

Fig. 2.3. Plan of multi-generational experiment in a single growth chamber with number of individuals in treatment groups visible (6 per container). There were 54 plants in total across three treatment groups with an equal number of individuals in each treatment group (18) and container (6). The configuration of containers was changed regularly after commencement of experiment to avoid spatial bias within the growth cabinet, and this illustrated configuration demonstrates just one possible layout.

Nine containers each with six plants throughout the entire life cycle* were arranged on shelves within a controlled growth environment cabinet (Fig. 2.3). Each plant was coded corresponding to treatment group, container and location. The code was as follows:

T= treatment, R = replicate group, I = individual. For example, the first plant in the first replicate group of the first treatment was given the code T1R1I1. Individual positioning

of plants (I 1-6) began in the same marked place in all containers and travelled clockwise from that point (Fig. 2.4).

*Data for developmental stages was recorded from first observable growth stage above soil until senescence.

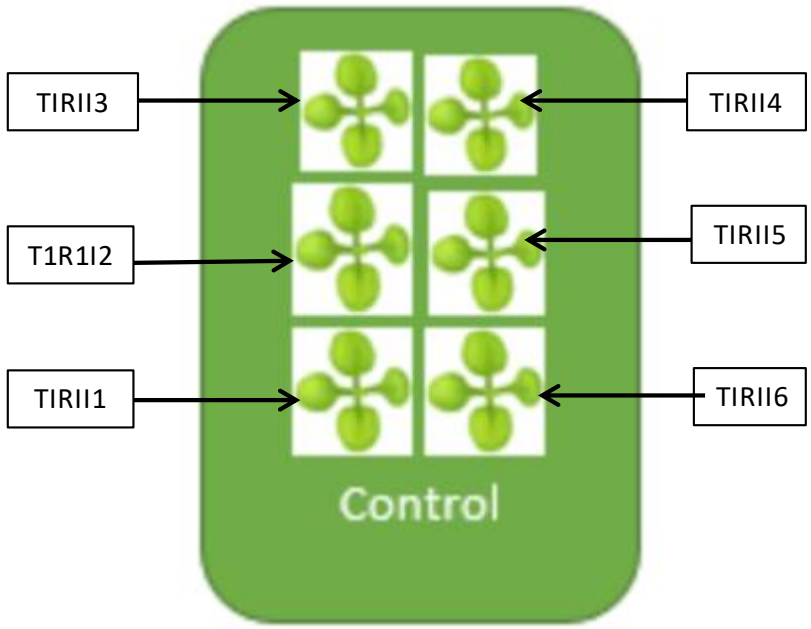

Fig. 2.4. Codes for individual plants in multi-generational experiment with A. thaliana. The example shown is for a control container of plants.

The experimental treatments were provided via growth medium as shown below (Table 2.2).

Table 2.2 Treatment groups and compositions for multi-generational experiment with A. thaliana.

Treatment	**Composition**
Treatment group 1	Control (Levington F2+S compost)
Treatment group 2	Positive control (Levington F2+S compost and 10µM $CdCl_2$)
Treatment group 3	Radioactive (Levington F2+S compost and 90 kBq/L Cs-137)

The experiment ran under controlled conditions inside a growth cabinet (Panasonic MLR-352/352H) set at a day length of 16 hours of light at 22 ºC and 70% humidity, and reduced to 50% humidity once siliques had been formed. This was to aid drying and accelerate the harvesting process as only dry seeds were harvested.

The complete life cycle from seed-to-seed took approximately 65 days under the growth conditions used in this study. The growth cabinet was split into three levels with shelving to support three containers per level. Containers were rotated around different levels in the cabinet approximately every 10 days of the growth cycle post-germination (representative example in Table 2.5), whilst remaining together in the same treatment groups to ensure there was no conditional or spatial bias throughout the growth cycles. Lead blocks (1.5 inches deep) were installed between each shelf to shield beta particles and gamma rays between treatment groups. This shielding was tested with a handheld monitor and was satisfactory as no more than ambient background radiation was detected on the side of the lead shielding where unexposed plants were growing.

Table 2.5 Rotation schedule for generation 5 (G5) from 11/10/16 – 16/11/16.

G5 CONFIGURATION	**CABINET LEVEL**	**LEFT**	**RIGHT BACK**	**RIGHT FRONT**
DATE				
11/10/2016	UPPER	T1R1	T1R2	T1R3
	MIDDLE	T2R1	T2R2	T2R3
	LOWER	T3R1	T3R2	T3R3
21/10/2016	UPPER	T2R3	T2R1	T2R2
	MIDDLE	T3R3	T3R1	T3R2

	LOWER	T1R3	T1R1	T1R2
29/10/2016	UPPER	T3R2	T3R3	T3R1
	MIDDLE	T1R2	T1R3	T1R1
	LOWER	T2R2	T2R3	T2R1
06/11/2016	UPPER	T1R1	T1R2	T1R3
	MIDDLE	T2R1	T2R2	T2R3
	LOWER	T3R1	T3R2	T3R3
16/11/2016	UPPER	T3R3	T3R1	T3R2
	MIDDLE	T1R3	T1R1	T1R2
	LOWER	T2R3	T2R1	T2R2

Before the experiment followed the above-described format, seed numbers were bulked up and different growth configurations were trialled (generations 1 and 2). The seed ecotype used was Columbia (Col-0) of traceable origin obtained from Nottingham Arabidopsis Stock Centre. One hundred seeds were originally supplied. Each *A. thaliana* plant can produce several thousand seeds. After two generations had been grown and harvested under negative control conditions, radioactive and positive control treatments were introduced to the growth protocol (Table 2.2). The third generation of the transgenic plants was, therefore, the first exposed to ionising radiation. Initially three containers were used for generations 1 to 4. These containers were divided into two halves, one side densely seeded and the other side with six individual seeds spaced out (Fig. 2.5 & 2.6) and Cs-137 was supplied with a 10 mM stable CsCl carrier rather than carrier free.

Fig. 2.5. Preliminary experiment (generation 4) with Cs-137 treatment (left), CdCl2 (centre) and negative control (right) in a trial configuration in small plastic containers with sparsely sown and densely sown plants in the same container, separated with a plastic divider. High-density lead blocks (located between the Cs-137 container and the CdCl2 container were used at all times to shield control group plants from ionising radiation.

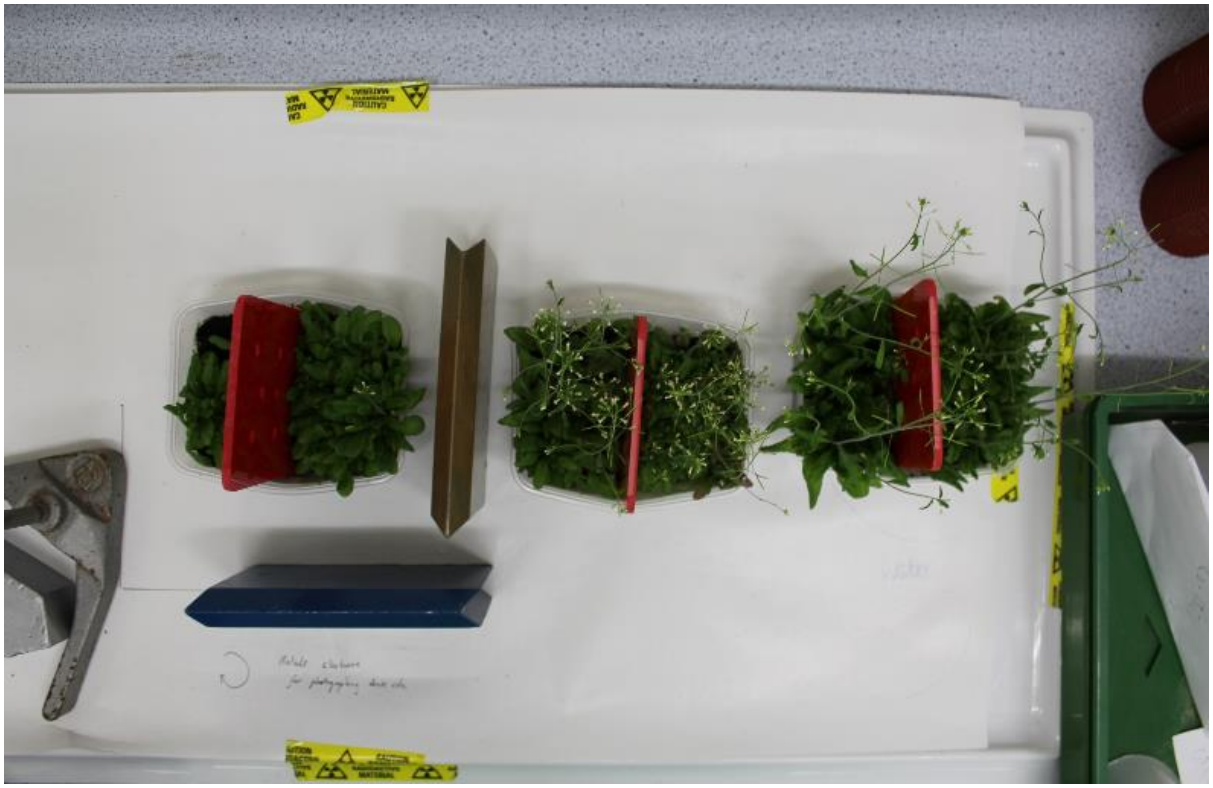

Fig. 2.6. Top-down view of preliminary experiment with Cs-137 treatment (left), CdCl2 (centre) and negative control (right). A visible difference is seen in the number of flowering plants but when the same seeds were re-tested in the experiment with larger containers this difference was not apparent.

In the first iteration of generation 4 it became apparent that there might be significant effects of the Cs-137 and $CdCl_2$ treatments (Fig. 2.5 & 2.6) and that these might be due to chemical toxicity. Generation 4 was, therefore, repeated with replicate containers and Cs-137 was supplied carrier-free, meaning that it did not contain stable Cs because it is possible that the stable Cs carrier was causing chemical toxicity. To isolate heavy metal as a stress factor, $CdCl_2$ was still used as a positive control. Thus a full experimental design was used for generations 4 to 7 so that any effects observed in the Cs-137 treatment groups could be attributed to IR-induced stress, and not heavy metal stress. After trials with the preliminary configuration of generations 1 to 4, experimental generations 4 (repeat) to 7 had only six individuals per container to

ensure plants were spaced out sufficiently as to not impede growth of neighbouring plants and to enable appropriate image analysis to be performed. Thus, the red plastic central divides (visible in Fig. 2.5 & 2.6) were not used after the preliminary generations and the densely seeded versus sparsely seeded configurations were terminated.

Additional replicates were introduced to increase data resolution. Samples increased from six plants in a single container per treatment group to 18 plants across three containers per treatment group amounting to a total of 52 plants per experiment. Containers were also changed to be slightly larger and more robust. Original containers were made of clear thin polyethylene measuring 12x17x4cm and optimised containers were white opaque polyethylene measuring 18x26x8 cm (Fig. 2.7).

Fig. 2.7. Final layout of containers in growth cabinet (Panasonic MLR-352/352H) set at a day length of 16 hours of light at 22 ºC/14ºC and 70% humidity. Note the bulge in the second shelf from the top that held the lead shielding. This is due to the weight of the shielding. A plastic beaker containing plastic tweezers is also pictured on the fourth shelf from the top (which also had a layer of lead shielding) and this was for removal of any unwanted plants (i.e. germinated plants hidden beneath the leaves of the deliberately placed replicates).

2.2.5 Cultivating *A. thaliana*

Dry *A. thaliana* seeds are 0.5 mm in length and weigh approximately 20 µg. For this experiment, vernalised seeds kept for a minimum of 48 hours in a refrigerator at 4ºC were added to water in an Eppendorf tube. Using a 1ml pipette, seeds in suspension were taken up and deposited onto the growth media evenly distanced at 6 sites in

each container and placed into a growth cabinet (Panasonic MLR-352/352H) set at a day length of 16 hours of light at 22 ºC (day) and 14 ºC (night) and 70% humidity. Water was added to the growth medium every 1-3 days with a water bottle (if compost appeared dry and light in colour) which therefore remained damp until seed harvest. Excess seedlings were removed at the first sign of development (emergence of cotyledons) as carefully as possible taking care not to disturb the roots of the single seed that remained in place. Where possible, seedlings in clumps were removed around a single seedling that had no contact with neighbouring seedlings to minimise mechanical disturbance. Plant leaves were routinely misted using a spray bottle on a weekly basis. Care was taken not to overwater.

2.2.6 Harvesting *A. thaliana* leaves

Leaves were harvested at plant maturity ahead of analysis. One week prior to the seed harvest, leaves were harvested by removing them at the petiole with scissors. This was to ensure the petioles do not interfere with image analysis. After image analysis was carried out fresh leaf samples were weighed and inserted into 1.5ml Eppendorf tubes and snap frozen in liquid nitrogen (a process whereby samples are submerged until frozen, typically in a short space of time). The samples were kept in storage at -80°C until required for physiological analysis. Refer to chapter 4 for further details on these processes.

2.2.7 Harvesting *A. thaliana* seeds

Seed harvest was carried out over the course of seven days, after leaves had been harvested for analysis. During harvest, the growth chamber settings were modified to the minimum humidity settings that were possible (50% humidity) and watering activities ceased. Once the plants had dried out and the siliques turned yellow-brown, they were removed, threshed on paper and transferred to 1.5ml Eppendorf tubes.

Equipment was cleaned and/or changed to minimise cross-contamination between harvesting of treatment groups. Following harvesting, each generation's seeds were kept refrigerated at 4°C until they were ready for sowing or germination testing (the refrigeration aided the plant process known as vernalisation). The seeds were kept in 1.5ml Eppendorf tubes and carefully handled so as not to induce cross-contamination. This was a crucial element as the seeds are extremely small and therefore the risk of cross-contamination was high. Seeds were stored in a refrigerator for a minimum of 48 hours prior to use in further experiments.

2.2.8 Positive control

Positive control plants were grown in compost medium containing 10μM cadmium chloride ($CdCl_2$ 99.9% trace metals basis). 500 ml of 10 μM $CdCl_2$ solution was added to each container. This was mixed well into the medium to ensure distribution was as uniform as possible.

Cadmium was selected as a positive control for multiple reasons. First, it is known to have effects on plant morphology and development at high soil concentrations (Yadav, 2010). Second, any similarities of effects between Cs-137-exposed plants and cadmium-exposed plants may be attributed to metal toxicity as both are metallic. Further, if significant differences were detected between the two groups then results could have been attributed to radiation effects and not (explicitly) the effects of metal toxicity. Throughout the analyses, mention of positive control strictly pertains to the cadmium treatment and no other positive control was used.

2.2.9 Irradiation

Caesium-137 (Cs-137) is a radioisotope of caesium and is a beta-gamma emitter. It has a half-life of 30.17 years and is highly soluble in water. It is one of the more

common radioisotopes created as a fission product (most abundantly via fission of uranium-235) in nuclear reactors and weapons.

Selecting this radioisotope at the doses detailed in this section made for a comparable radiation source to field conditions upon accidental and deliberate release of radionuclides to the environment.

Plants were irradiated with Cs-137 in solution mixed well into growth media by adding a beaker containing the solution into dry soil and mixed until a visually uniform distribution (dampness throughout) was visible. Cs-137 activities were calculated based on small volumes of solution taken from a Cs-137 stock solution. The stock was originally purchased from isotope centre Polatom (05-400 Otwock Weirk, Poland) product code RCs-3 and came in the form of CsCl in 0.1M HCL solution. The concentration of the isotope was 337.00 MBq/cm^3 and the stock activity was 74MBq on 03/05/2006.

The Cs-137 stock available to this experiment had had numerous aliquots taken from it and been subject to multiple dilutions (which maintain the remaining Cs-137 in solution) and due to this, the exact activity of Cs-137 per L was subject to change. Each experiment used stock with recorded activities and was measured on a gamma counter. Every effort had been made during dosing of the growth medium to achieve a soil with an activity that represented an environmentally realistic dose rate in the field. However, when soil was spiked with Cs-137 over different generations, the activities varied slightly between generations due to differences in the stock solution. Total radioisotope activities used ranged from 221.55 kBq – 323.4 kBq (Table 2.4). These activities were verified retrospectively by gamma counting (Compugamma).

Table 2.4 The activities of soils spiked with Cs-137 for the Cs-137 treatment groups in the transgenerational experiment. The table includes non-active generations used in the "bulking up" phase to increase seed production and the variation in activities due to protocol change and source differences.

Generation	Activity container 1	Activity container 2	Activity container 3	Total Activity
Generation 1	Not active	Not active	Not active	-
Generation 2	Not active	Not active	Not active	-
Generation 3	250ml 90 kBq	-	-	90 kBq (250ml)
Generation 4	250ml 90 kBq	250ml 90 kBq	250ml 90 kBq	270 kBq (750ml)
Generation 4 (repeat and protocol change)	500ml 73.85 kBq	500ml 73.85 kBq	500ml 73.85 kBq	221.55 kBq (1.5L)
Generation 5	500ml 73.85 kBq	500ml 73.85 kBq	500ml 73.85 kBq	221.55 kBq (1.5L)
Generation 6	500ml 107.8 kBq	500ml 107.8 kBq	500ml 107.8 kBq	323.4 kBq (1.5L)
Generation 7	500ml 107.8 kBq	500ml 107.8 kBq	500ml 107.8 kBq	323.4 kBq (1.5L)

As radioactivity wasn't introduced to the experiment until the third generation of *A. thaliana* from the NASC seed stock, it is important to note that the generation tags relate to the generation of seeds from the stock and not generations of exposed plants. In this series of experiments, generation 4 was the second generation of exposed

plants, 5 was considered the third generation of exposed plants and so on. When results are given in later sections, this generational code applies. Data from the initial experiment for generation 4 was omitted from transgenerational analysis due to the change of protocol. To clarify, generations 4 (repeat) to 7 were grown using the same protocol. Details of the preliminary protocol used for generations 3 and 4 (prior to the repeat) are detailed in 2.4. The focus of this experiment was the developmental stage analysis but, given that seeds were collected from each generation some preliminary seed germination and root growth tests were also carried out.

2.2.10 Developmental stage analysis

A digital SLR camera (Canon 1200D) was set up on a bracket (Manfrotto 035C Universal Super Clamp) and pointed downwards against a plain white background (Fig. 2.8). Approximately every 2-5 days of growth was photographed from a bird's eye view (Fig. 2.9 & 2.10) for each of the nine containers to produce a high-resolution image of 5,184 x 3,456 pixels and 72dpi at a focal length of 24mm. The image data was then used to plot growth stages of individuals against the Boyes *et al*. (2001) descriptive chart of development (Table 2.1). The developmental benchmarks were used to identify and interpret phenotypic differences (if any) in plants potentially attributed to radiation stress.

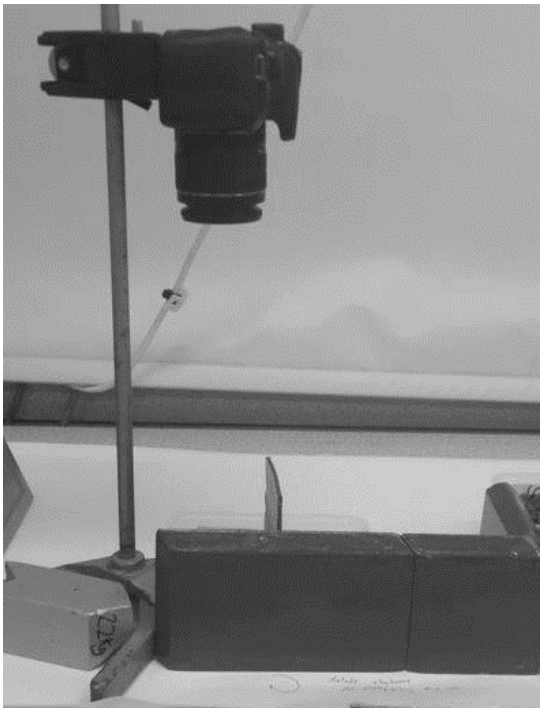

Fig. 2.8. Camera and bracket setup. Lead shielding surrounded the photography area to comply with radioprotection guidelines regarding minimisation of exposure time for close work with any of the containers that contained Cs-137.

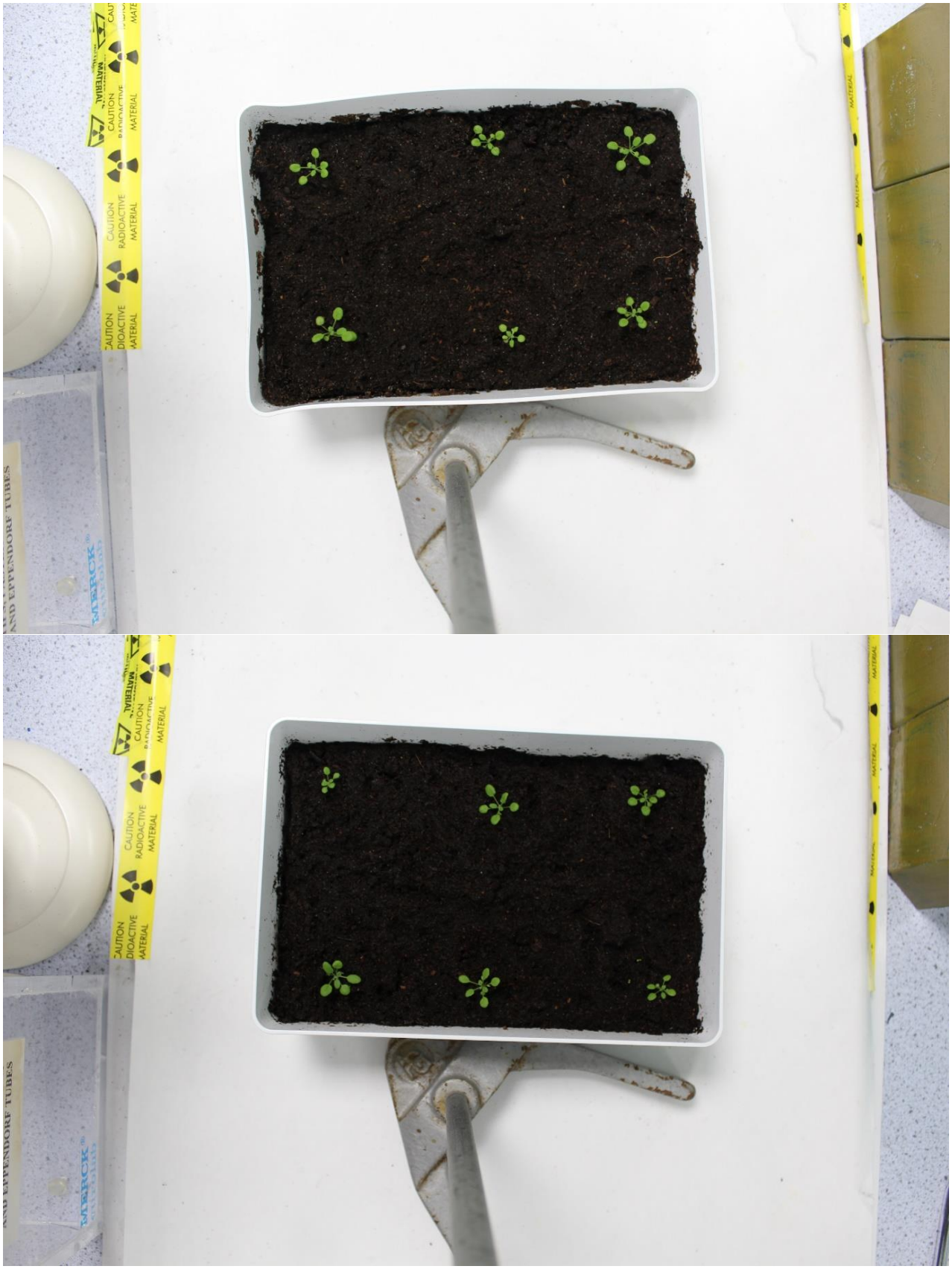

Fig. 2.9. Image used for developmental stage analysis. Six individual A. thaliana photographed at 19 days post-germination Control group (top) and Cs-137 treatment group (bottom).

Fig. 2.10. Image used for developmental stage analysis. Six individual A. thaliana photographed at 34 days post-germination Control group (top) and Cs-137 treatment group (bottom).

Using free time-lapse video software (Time Lapse Tool available from: *https://timelapsetool.com*) a time-lapse video was made for the 2nd generation of plants in radioactivity. The transitions were not very smooth due to slight movement of the image recording hardware and this was thought to be down to other laboratory users disturbing the set-up, either deliberately or accidentally. Overall, it was easy to see clear progression in plant development for all treatment groups. However, this was not deemed useful data and was not repeated after the first video was made. However, it was useful for science communication and outreach purposes as a conceptualising tool for the dynamics of plant growth and development in the different soil conditions.

2.2.11 Germination tests

A simple test was performed to assess germination rates in *A. thaliana* seeds exposed to IR over the generations. Each generation of seeds were harvested and stored in 1.5ml Eppendorf tubes and transferred immediately to a refrigerator and kept at 4°C. Sterilisation method (see 2.2.12) was omitted from seeds used in the germination test. A small amount of seeds was placed onto strips of damp germination paper (Anchor Paper Co) in round petri dishes (Fig. 2.11) and moved into a growth cabinet with identical settings to those reported in 2.2.5.

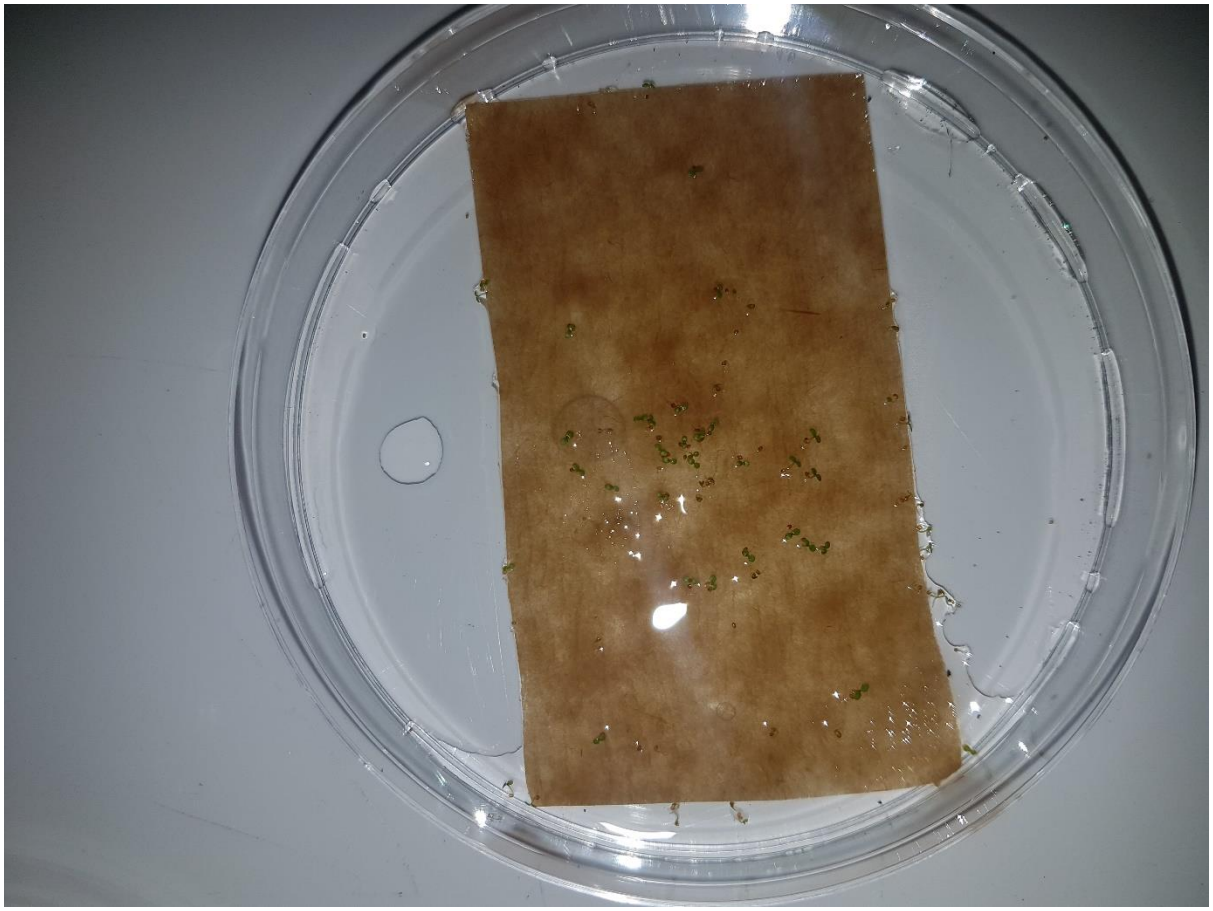

Fig. 2.11. Germination test. A wet strip of germination paper was placed in a round petri dish and seeds were added on top. Petri dishes were covered and incubated for 36 hours in a growth cabinet (under the same conditions as the A. thaliana were grown under in the transgenerational experiment). This top-down image shows the first cotyledons produced post-germination.

Each germination test was recorded via a digital camera and uploaded to a computer where quantification of germinated seedlings was recorded using image analysis software (ImageJ) (Fig. 2.12). ImageJ was used to perform analysis using the count function with a grid overlaid onto each image. For each germinated seedling, a mouse click over the location of that seedling in the image tagged the seedling with a number: either 1 for germinated or 2 for dormant/sterile. Each result was recorded in Excel and percentages calculated.

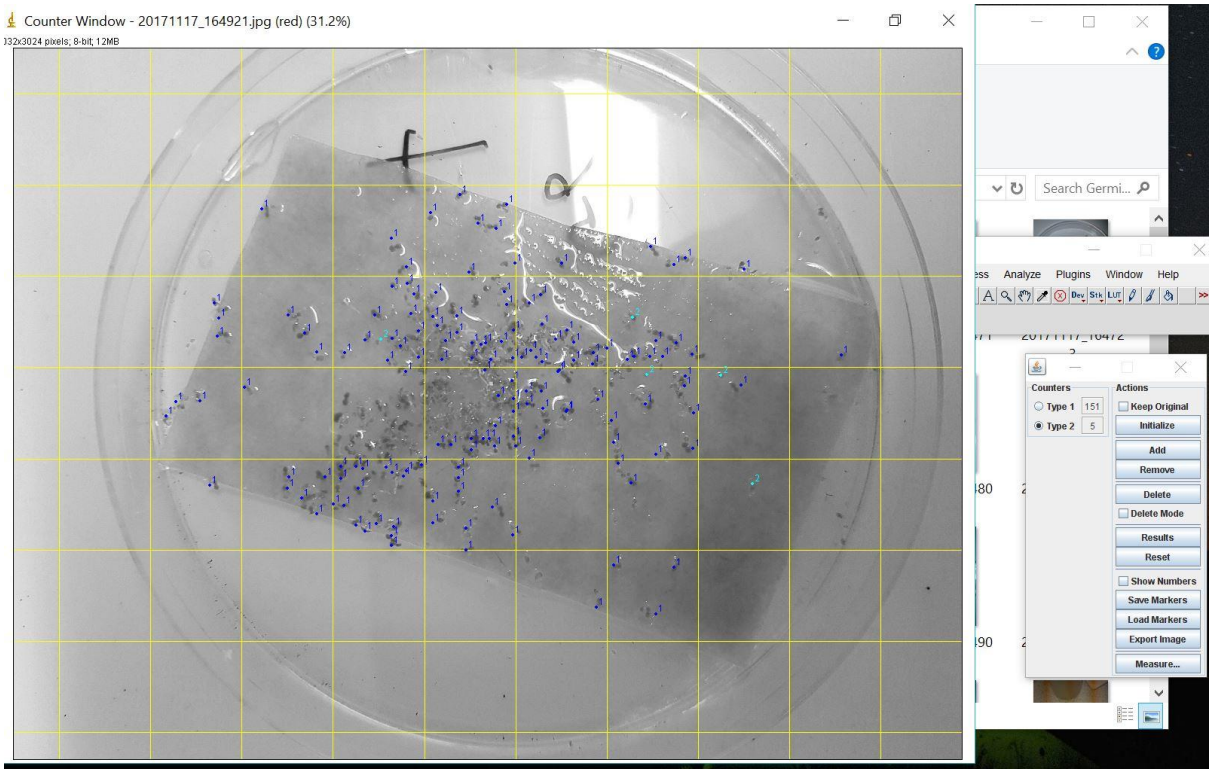

Fig. 2.12. Quantifying germinated seeds using ImageJ. This is a screenshot of the programme ImageJ with an image present in the left-hand window for analysis. The dark blue markers (or markers annotated as "1") are markers for germinated seedlings, and light blue markers (or "2") pinpoint dormant or sterile seeds. Each mouse click serves as a count and when all counts are completed a tally is displayed. From this tally it is possible to calculate percentage germination rate.

2.2.12 Root development analysis

Early on in the literature review stage, it was found that, a paucity of data on root morphological studies was evident. Further, there was an even greater absence in this type of data relating to IR effects. Over the course of six months, a specialist hydroponic tank with capabilities for analysing IR effects in roots was designed (Fig. 2.13), built (Fig. 2.14) (by Amalgam Modelmakers, Bristol) and tested as a technology demonstration only (Fig. 2.15) as too few samples were grown to analyse in an experimental context.

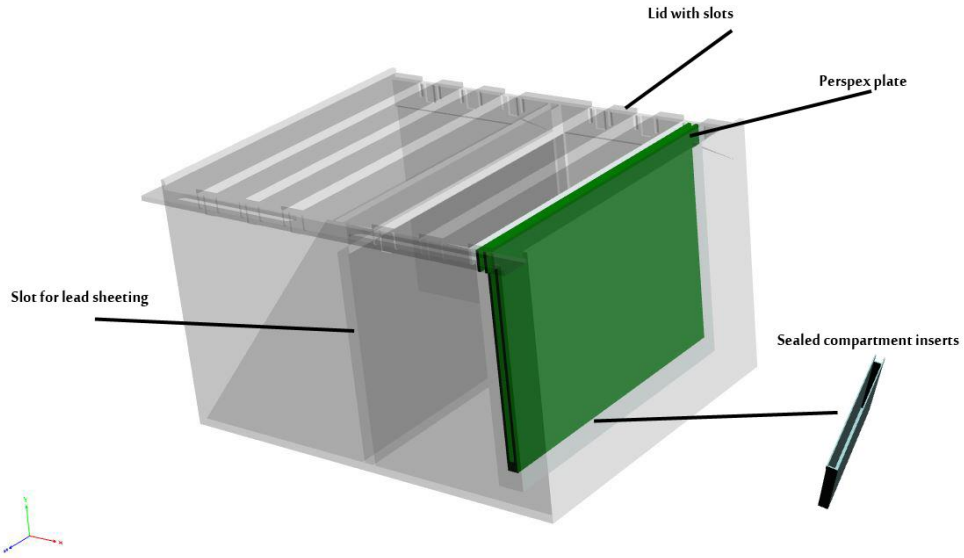

Fig. 2.13. Hydroponic tank 3D drawing showing slot for lead shielding, removable lid with holes for slots, perspex plate (green) which were later discarded in favour of the sealed compartment inserts and bracket arrangement (Fig. 15) instead.

Fig. 2.14. Hydroponic tank exterior with removable cover shown in place with handles shown closest to the camera. Six inserts are visible from the top with inner slides and outer tanks. Inner slides were discarded in favour of a metal bracket with sample housing drilled at five intervals (visible in Fig. 2.15).

Fig. 2.15. Hydroponic tank with aeration system setup. Spaces for six inserts (housing 5 samples) built into the design with a large diameter space between three inserts capable of housing a lead sheet for sample shielding against gamma rays.

Seeds from each generation of *A. thaliana* exposed to IR from Cs-137, alongside positive and negative controls were grown for 10 days in half-strength MS agar in square petri dishes. After germination, containers were placed vertically and wrapped in foil so that only the tops of the petri dishes received light, and that the roots could grow downwards with gravity and away from the light. Seeds were sterilised in 70% ethanol for two minutes and commerical thin household bleach (NaClO, 50%) for two minutes. They were rinsed four times with sterile deionised water and placed in agar. The plates were sealed with Parafilm® to ensure the growth media remained free of contamination while not jeopardising gas exchange. One seed from each generation of a treatment group was placed in a row (Fig. 2.16 & 2.17). Each row was scored horizontally across the agar with a sterile blade to ensure accurate placement of seeds. After 10 days petri dishes were removed from the growth cabinet. Lids were removed and the petri dishes were photographed top-down using the camera and

bracket described in the previous section, against a dark coloured background to offset the light colour of the roots. A scale was included in each image in preparation for the analysis stage.

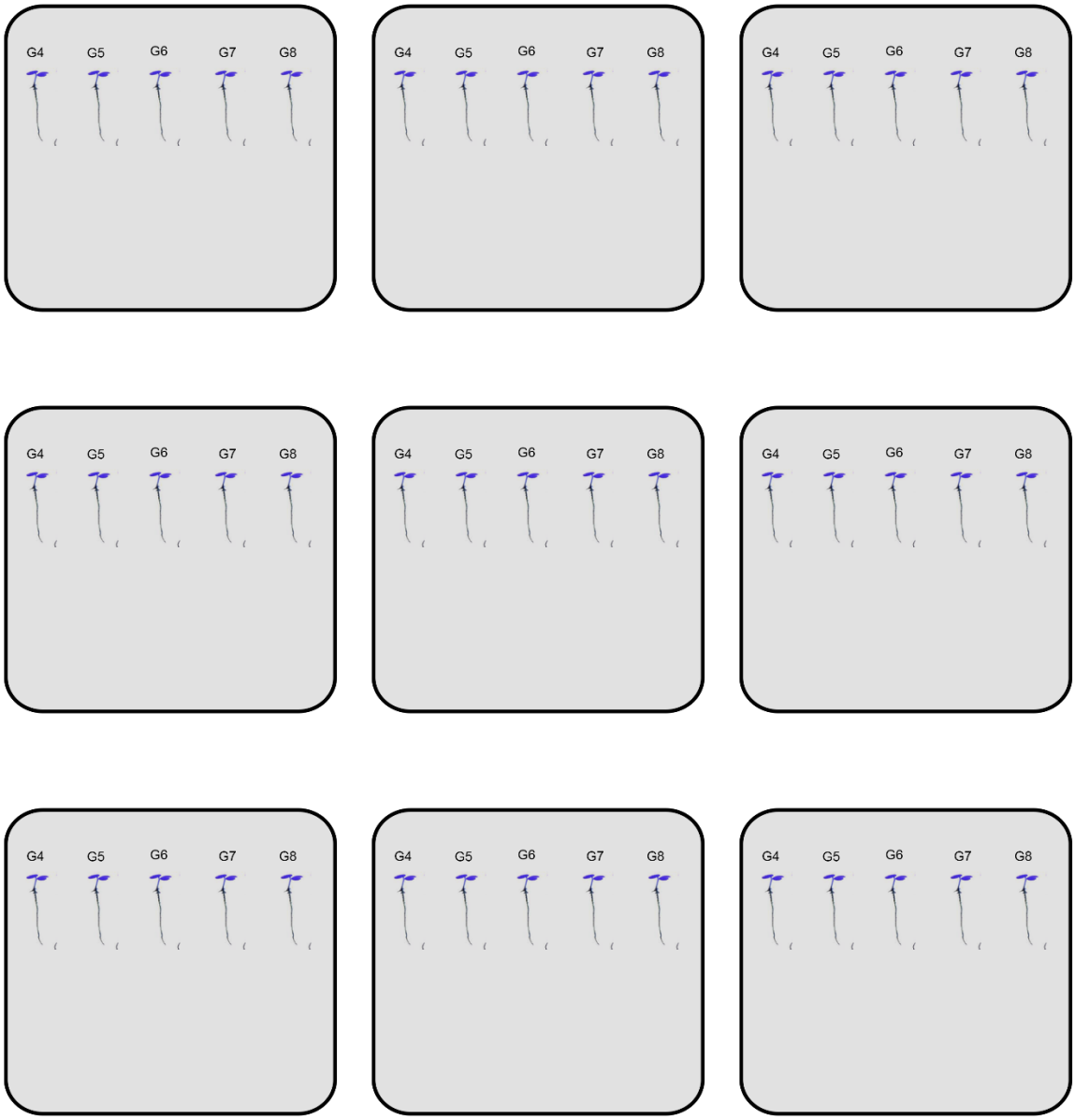

Fig. 2.16. Schematic of experimental design for root analysis. The numbers correspond to the generation tags. Three containers per treatment group housed five seeds, one from each generation of plants exposed to radioactivity.

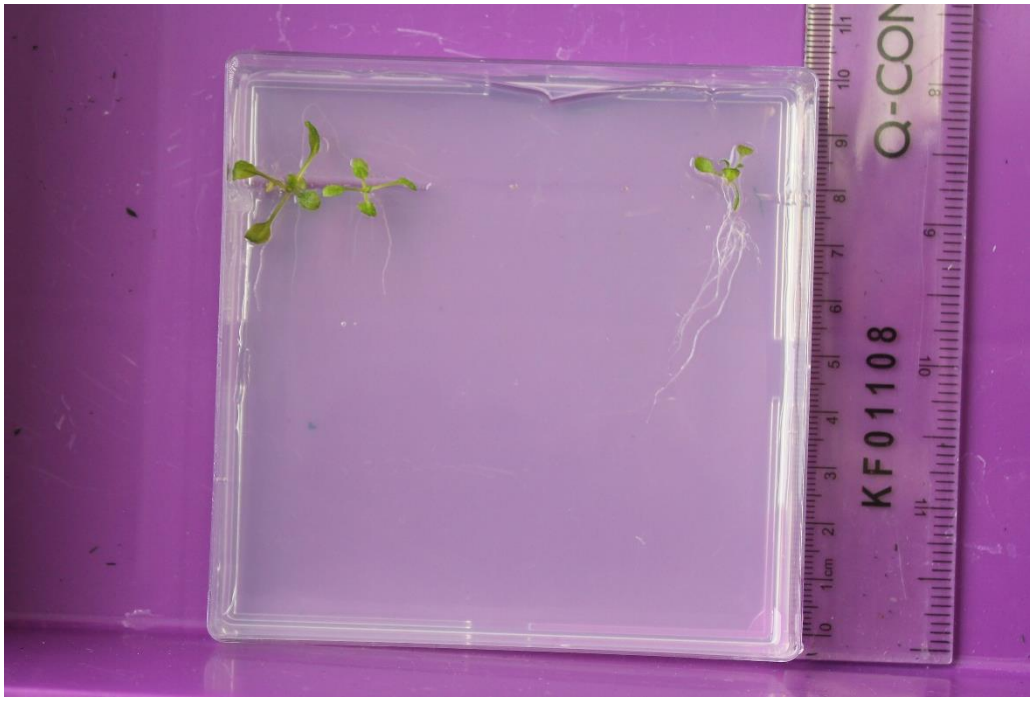

Fig. 2.17. A. thaliana seedlings in agar photographed against a dark background to enable easy recognition of roots. A scale is placed to the right of the petri dish to assist with image analysis in the software phase. In this example, negative control plants in positions G4, G5 and G8 had germinated successfully with roots growing across the surface and into the agar. The absence of generations G6 and G7 was consistent across other replicate dishes and suggest an error in the sterilisation process, as the same batch of seeds had previously germinated successfully (during germination tests).

Root analysis was carried out using the Java freeware, ImageJ (Fig. 2.18). ImageJ allows for the manual tracing of roots and calculates length along a specified scale. A ruler was included in each image and this enabled the software to calculate length. Lengths were pooled for treatment groups but divided into generations. Only one generation group had successfully grown plants in each treatment group, and that was generation 4 (G4)- the second generation of plants exposed to IR after the bulking up phase. The lack of germination in the other groups/generations meant results were omitted from the final data set, and data from G4 was the only useful numerical data available.

Fig. 2.18. A screenshot from ImageJ displaying the overlaid root trace method corresponding to a calibrated scale. Measurements were taken for each individual root that was traced.

2.2.13. Statistical Analyses

For the analysis of developmental stages an arithmetic mean of day number of the six biological replicates in each of the three growth containers was used. For overall means, an arithmetic mean for all the plants in the three growth containers was used. When necessary a Shapiro-Wilks test of normality was used and for non-parametric testing of differences between treatments a Kruskal-Wallis test was used. Further details of this approach are outlined in Appendix 1 and detailed statistical outputs are in Appendix 2.

2.3 Results

2.3.1 The effects of low-dose ionising radiation on transgenerational plant development using a phenotypic model

The developmental stage data from photographs was plotted onto line graphs in Excel for individual generations and treatment groups (Figs. 2.19-2.30). Treatment groups in the same generations were compared and then compared across the generations to see if there were visible differences after multiple generations of exposure to Cs-137.

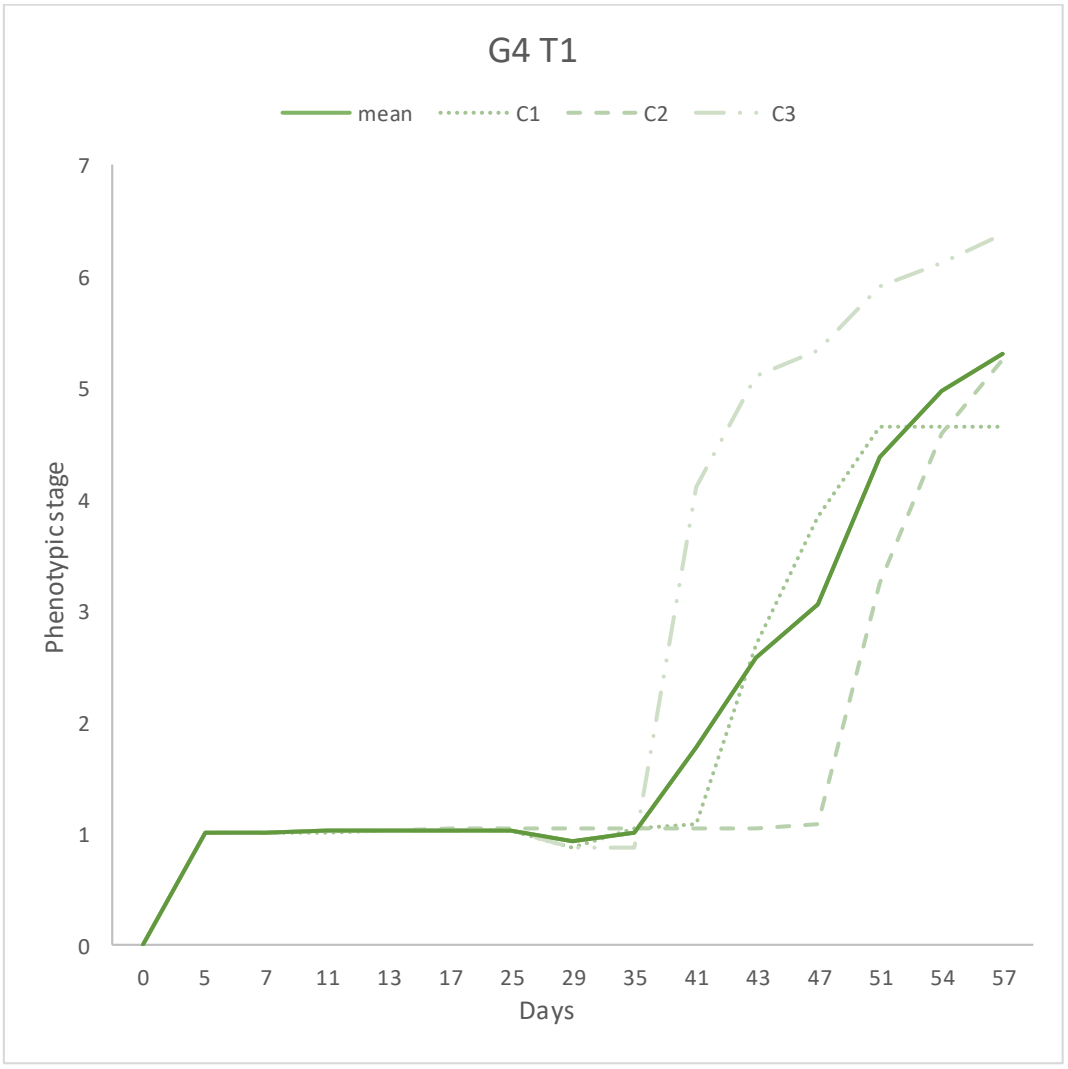

Fig. 2.19. Negative control phenotypic stage data full experimental protocol G4 (Generation 4). Phenotypic stages seen in photographs were plotted against time (days). Solid line shows the mean development of the negative control treatment group (n= approx 18). Dashed lines represent means of each of the three containers (denoted C1-3, n = approx 6). On average, stages began to differ in terms of timing after 25 days of growth. The dip in mean growth stage after 25 days is due to death of some replicates.

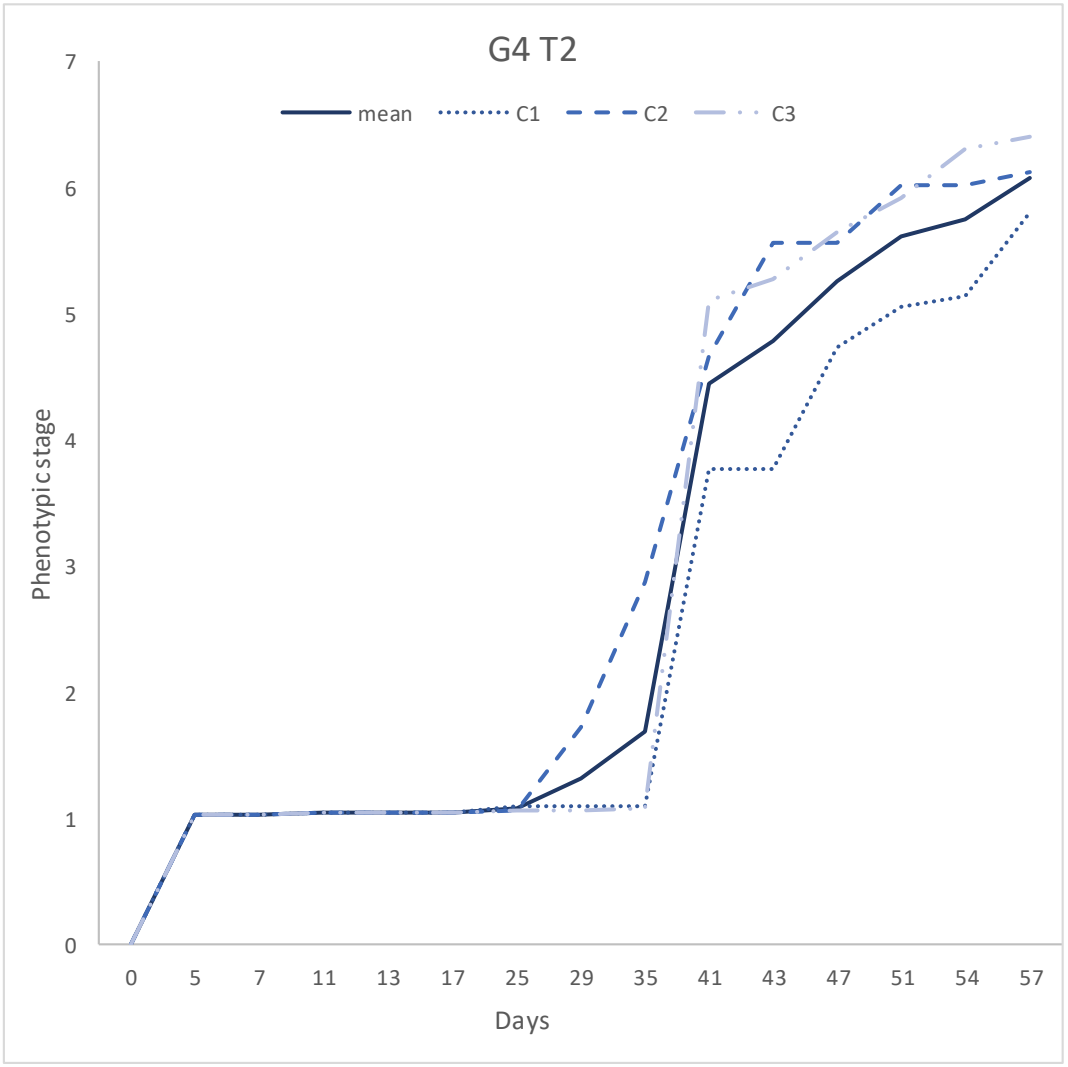

Fig. 2.20. Positive control group phenotypic stage data from full experimental protocol G4 (generation 4). Phenotypic stages were plotted against time (days). Solid lines indicate the mean of the positive control treatment group (n= approx. 18). Dashed lines represent means of each of the three containers (denoted C1-3, n= approx. 6). On average, stages began to differ in terms of timing after 25 days of growth.

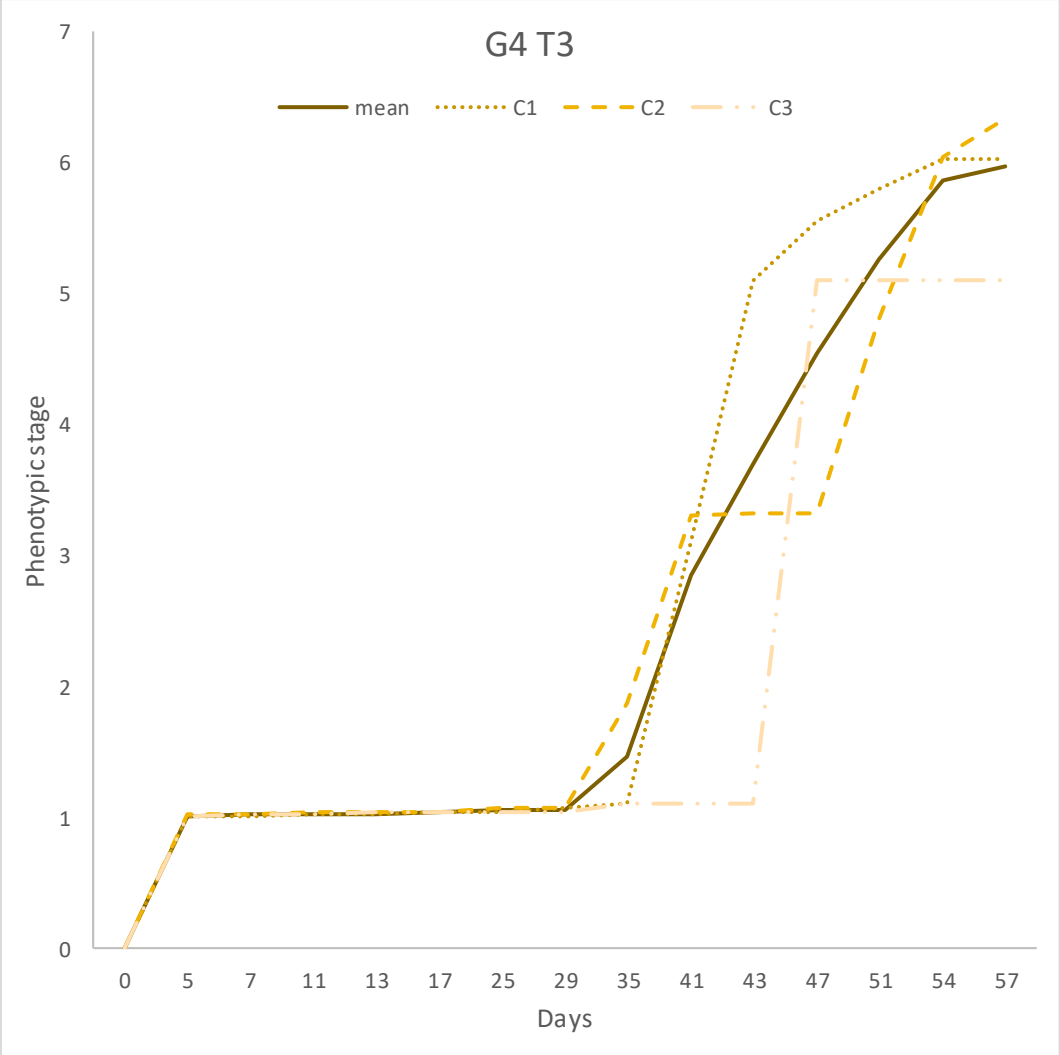

Fig. 2.21. Cs-137 treatment group phenotypic stage data for full experimental protocol G4 (Generation 4). Phenotypic stages were plotted against time (days). Solid line indicates the mean of the Cs-137 treatment group (n= approx 18). Dashed lines represent means of each of the three containers (denoted C1-3, n= approx 6). On average stages began to differ in terms of timing after 29 days of growth.

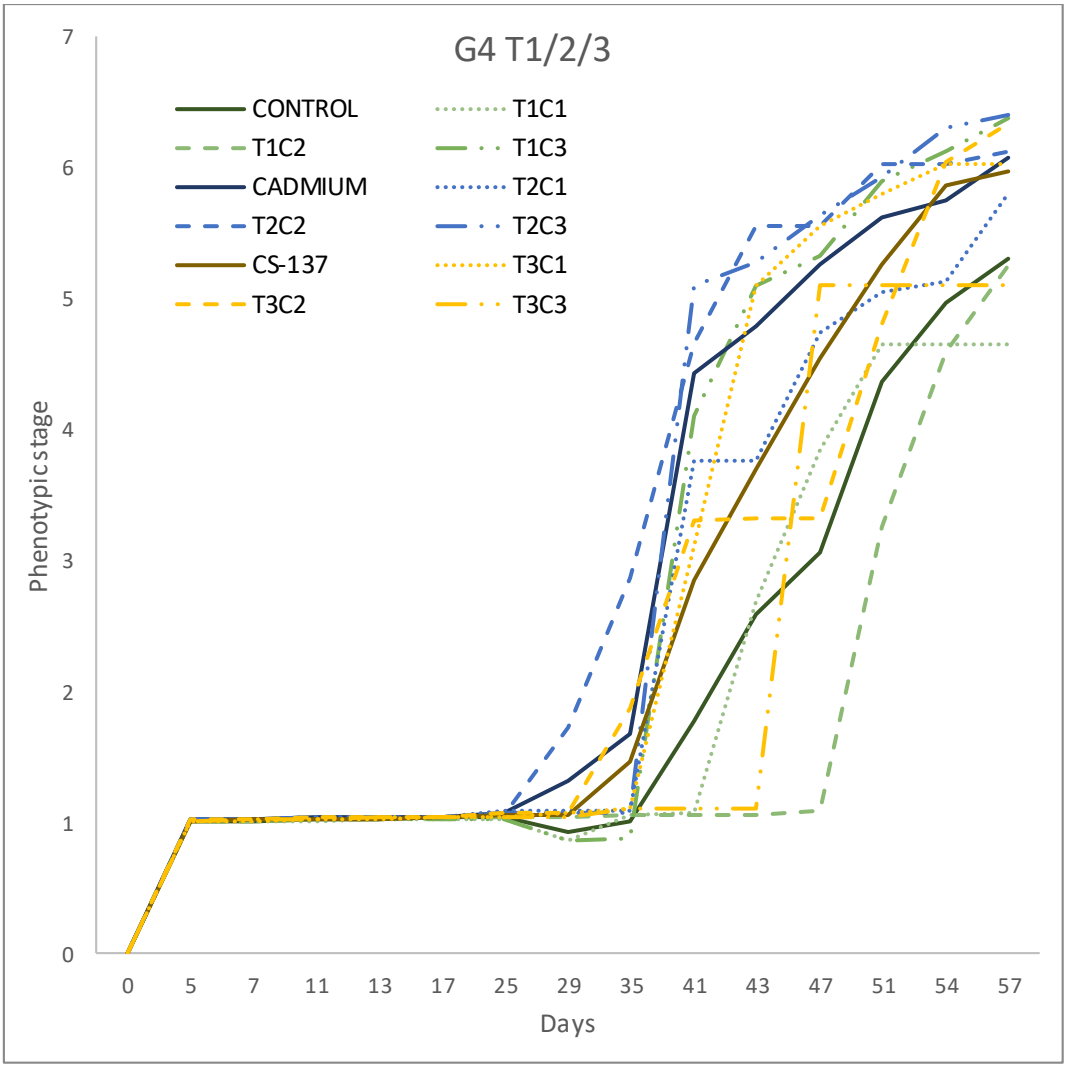

Fig. 2.22. All treatment groups G4 (generation 4). All of the data from the fourth generation was merged into one graph for comparative purposes. Variation in the timing of phenotypic stages was evident through position of the lines representing each group. Average values were highlighted with solid lines.

In G4, all groups follow a similar trend until the 25th day of growth. The Boyes *et al*. (2001) phenotypic description indicates that by 26 days, the first flower bud will be visible (known as phenotypic growth stage 5.1). In this experimental generation the first flower bud appeared later than this, with, on average, the positive control reaching this stage first, followed by Cs-137 treatment and then the negative control. This trend continued until the first flower bud was observed to open first in the Cs-137 treatment,

and then in the positive control. The mean negative control continued to lag behind, although open flowers were present in one of the control group replicate containers at an early stage.

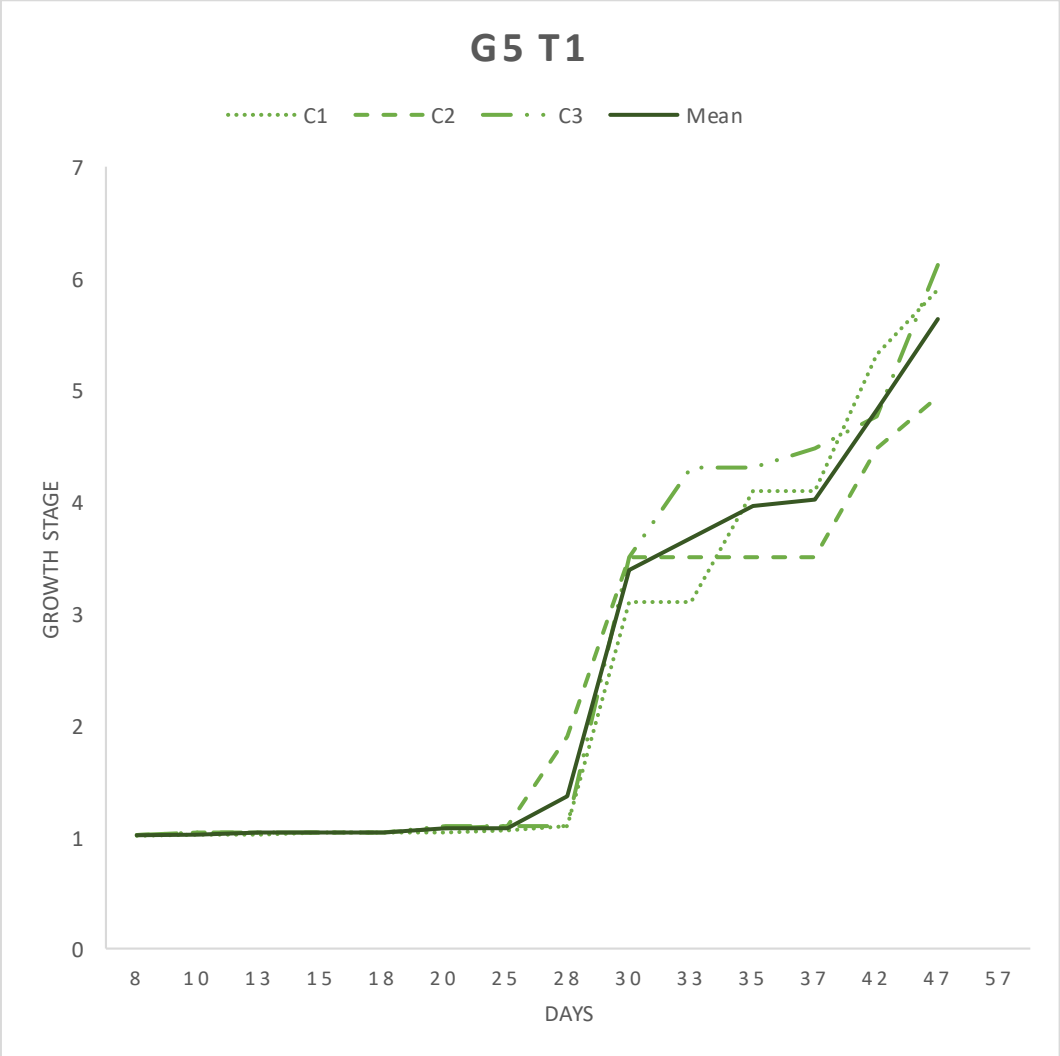

Fig. 2.23. Negative control phenotypic stage data G5 (Generation 5). Phenotypic stages were plotted against time (days). Solid lines indicate the mean of the negative control treatment group. Dashed lines represent each of the three containers (denoted C). On average stages began to differ in terms of timing after 25 days of growth.

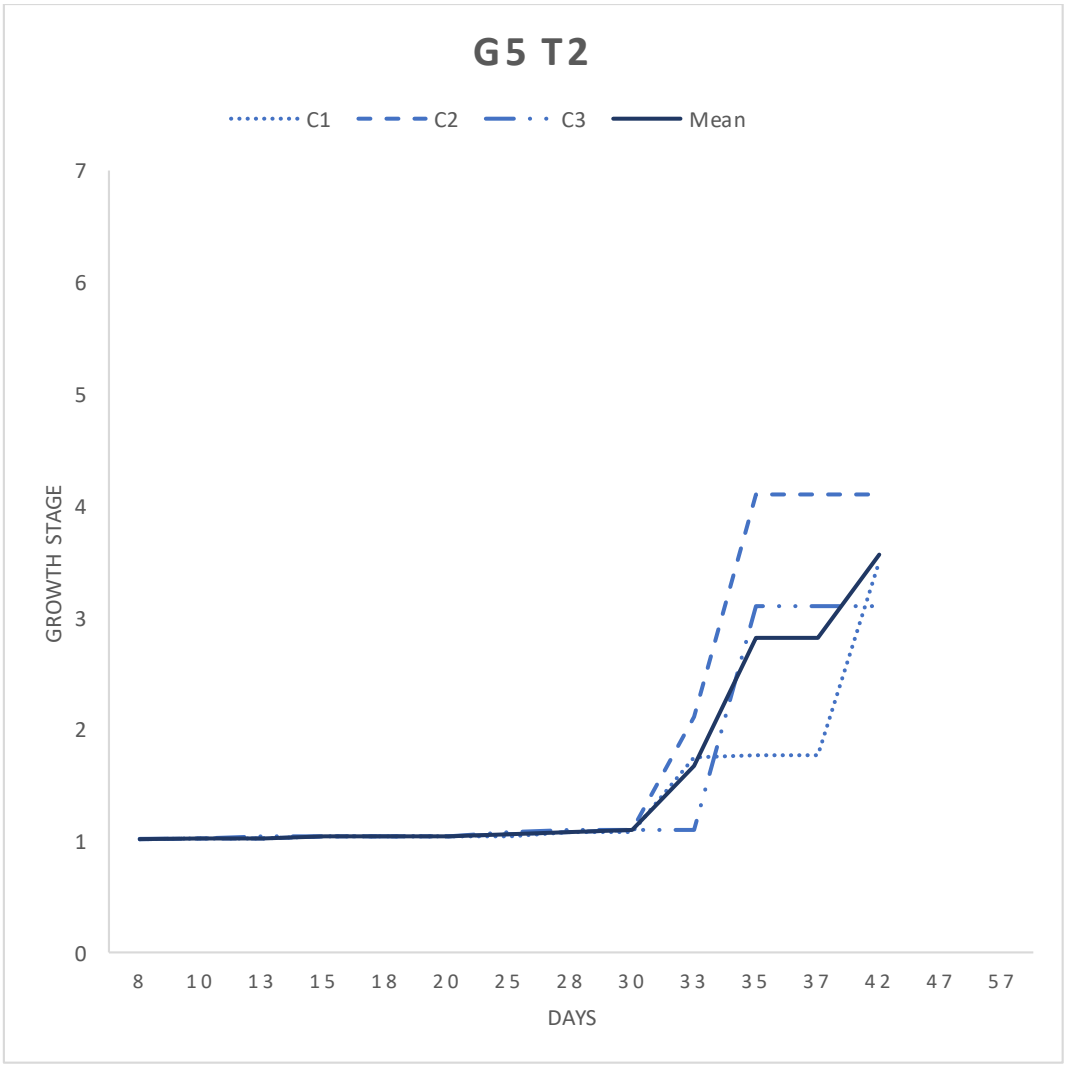

Fig. 2.24. Positive control phenotypic stage data G5 (Generation 5). Phenotypic stages were plotted against time (days). Solid lines indicate the mean of the negative control treatment group. Dashed lines represent each of the three containers (denoted C). On average stages began to differ in terms of timing after 30 days of growth.

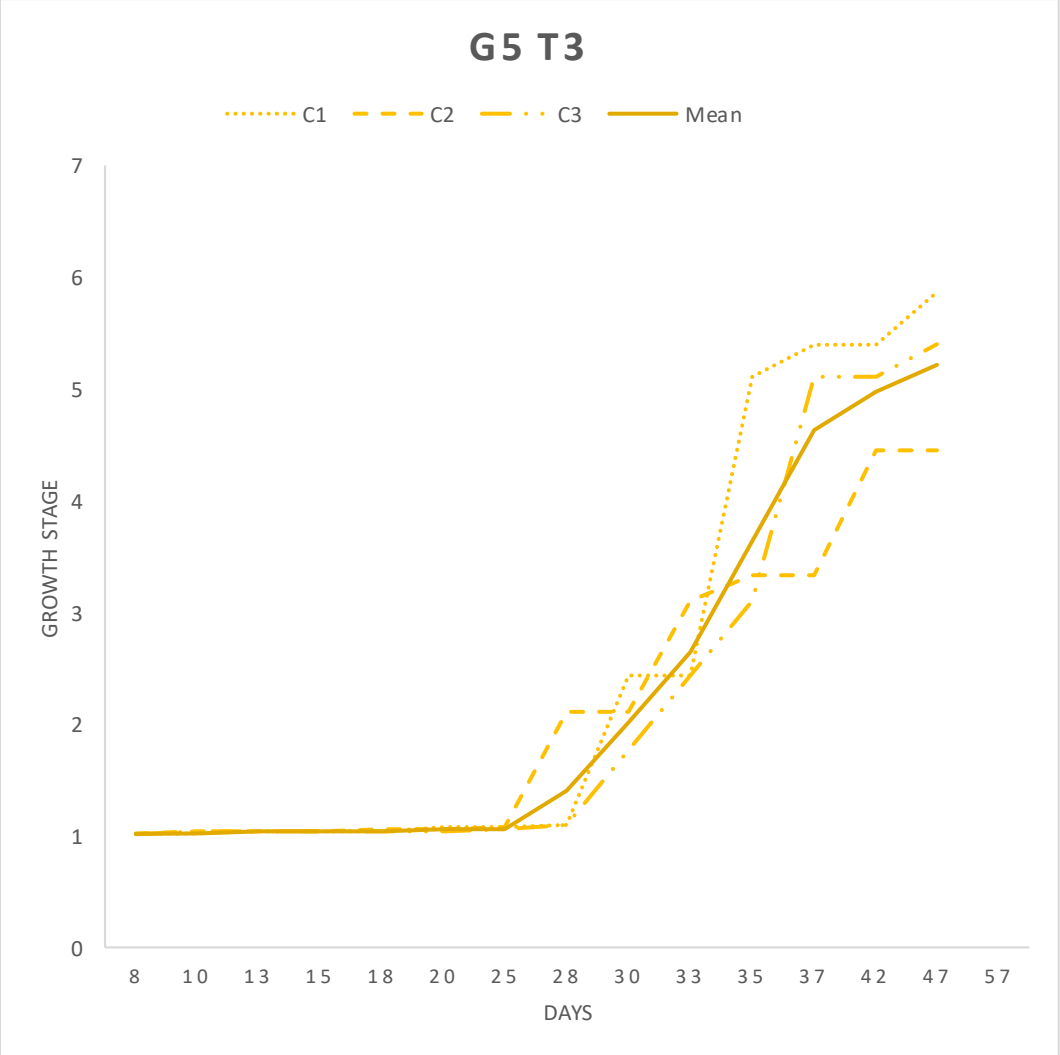

Fig. 2.25. Cs-137 treatment group phenotypic stage data G5 (Generation 5). Phenotypic stages were plotted against time (days). Solid lines indicate the mean of the Cs-137 treatment groups. Dashed lines represent each of the three containers (denoted C). On average stages began to differ in terms of timing after 25 days of growth.

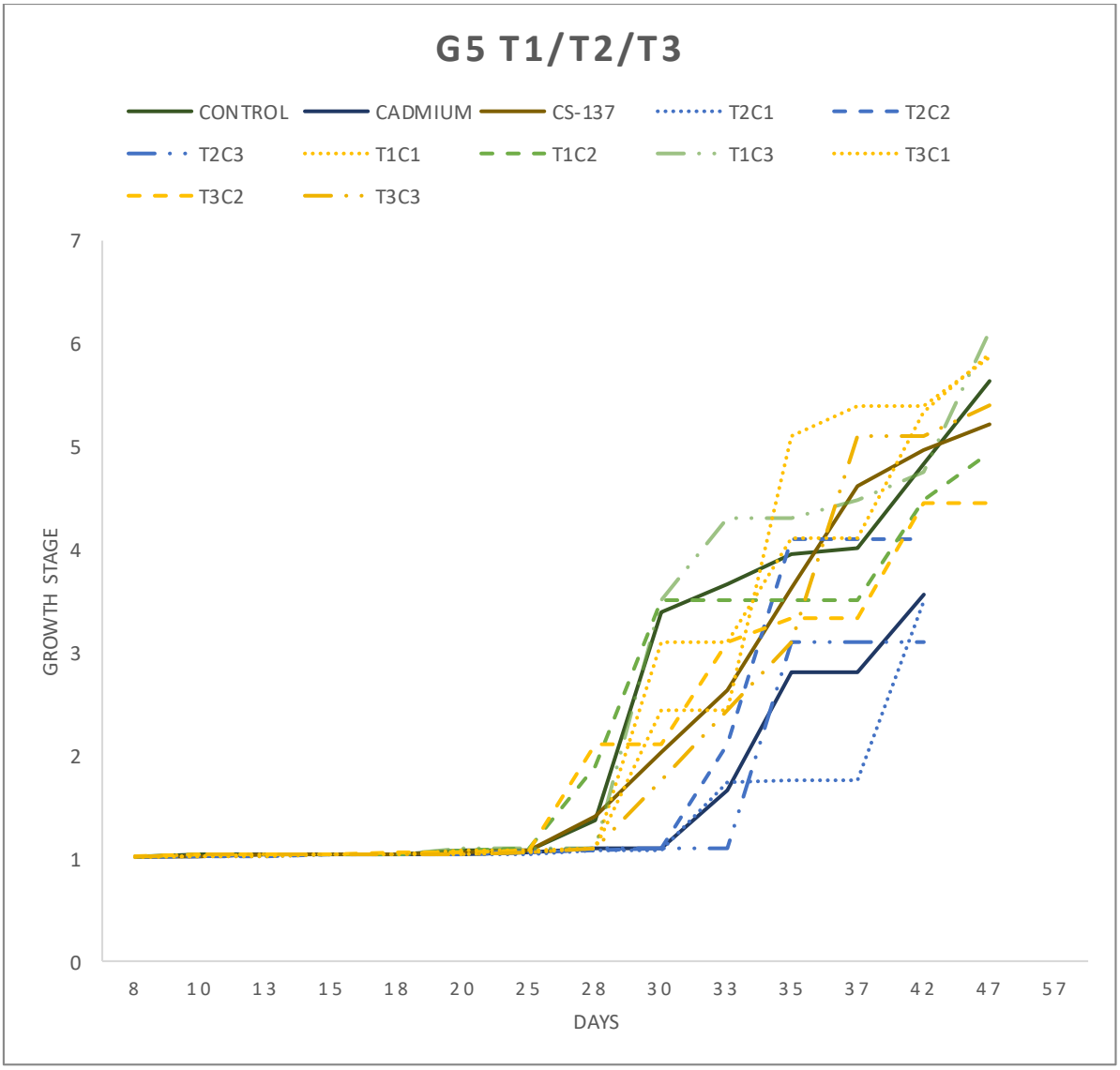

Fig. 2.26. All treatment groups G5 (generation 5). All of the data from the fifth generation was merged into one graph for comparative purposes. Variation in the timing of phenotypic stages was evident through position of the lines representing each group. Average values were highlighted with solid lines.

In G5, with the exception of one negative control group which grew at a faster rate than all of the other groups, generally the growth was similar amongst all of the treatments. Positive controls showed some supression of growth in this generation.

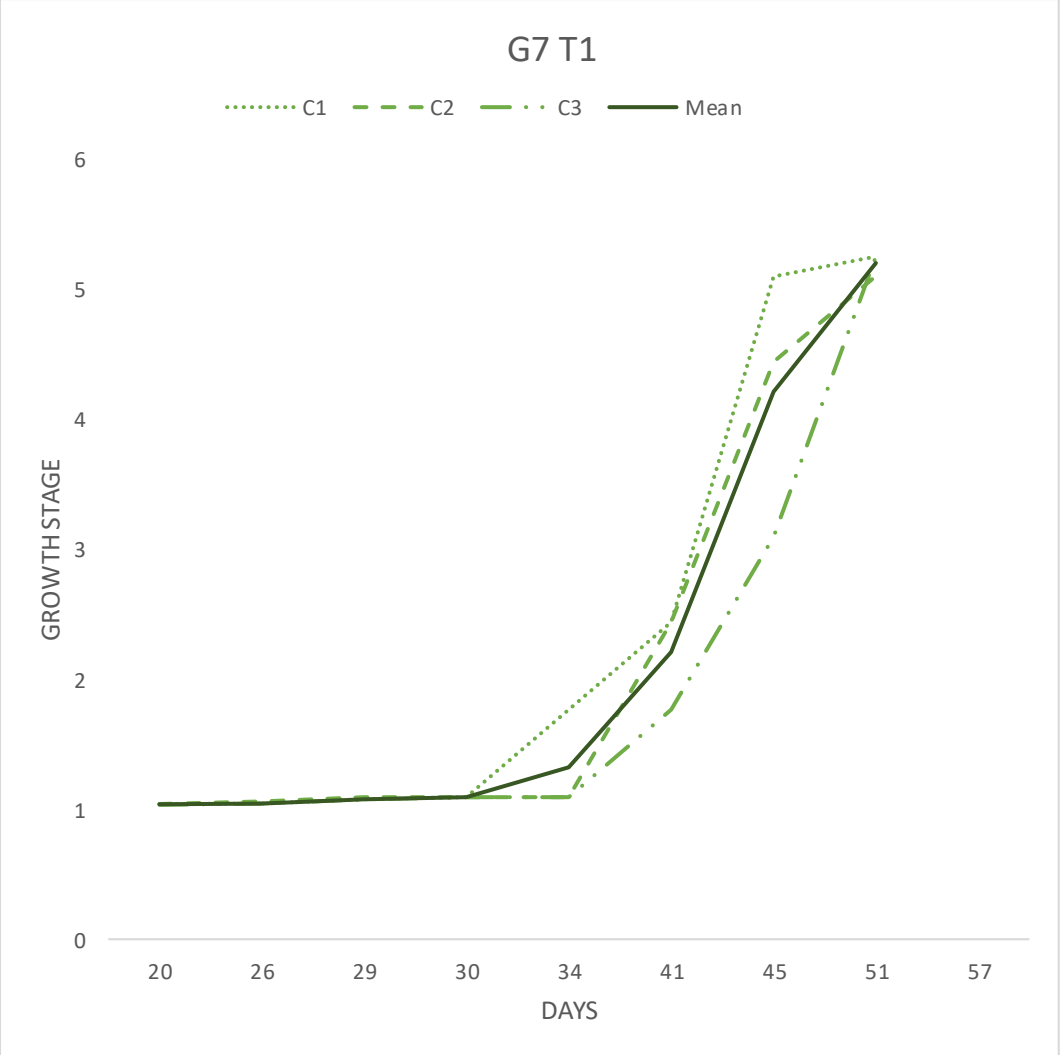

Fig. 2.27. Negative control phenotypic stage data G7 (Generation 7). Phenotypic stages were plotted against time (days). Solid lines indicate the mean of the negative control treatment group. Dashed lines represent each of the three containers (denoted C). On average stages began to differ in terms of timing after 30 days of growth.

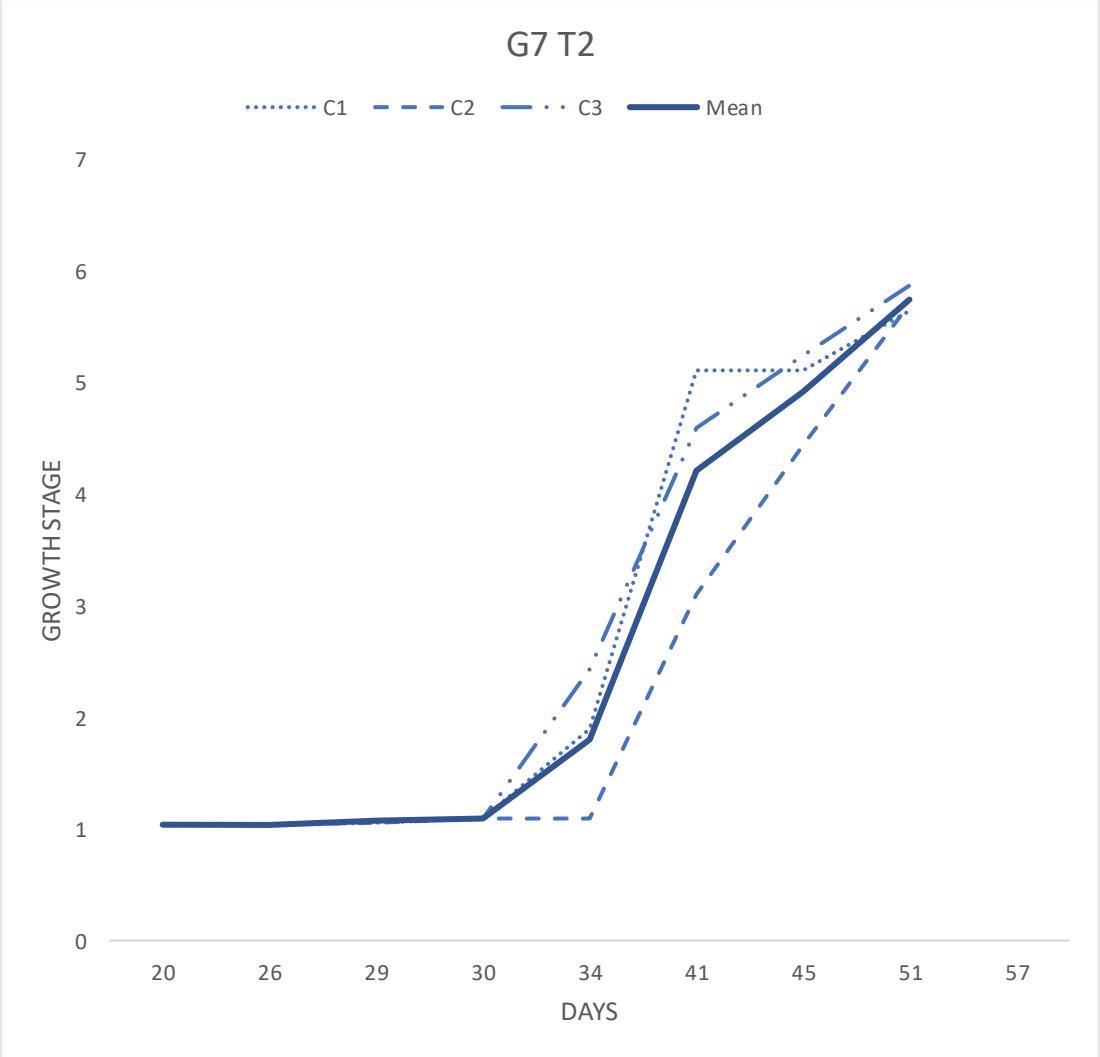

Fig. 2.28. Positive control phenotypic stage data G7 (Generation 7). Phenotypic stages were plotted against time (days). Solid lines indicate the mean of the positive control treatment group. Dashed lines represent each of the three containers (denoted C). On average stages began to differ in terms of timing after 30 days of growth.

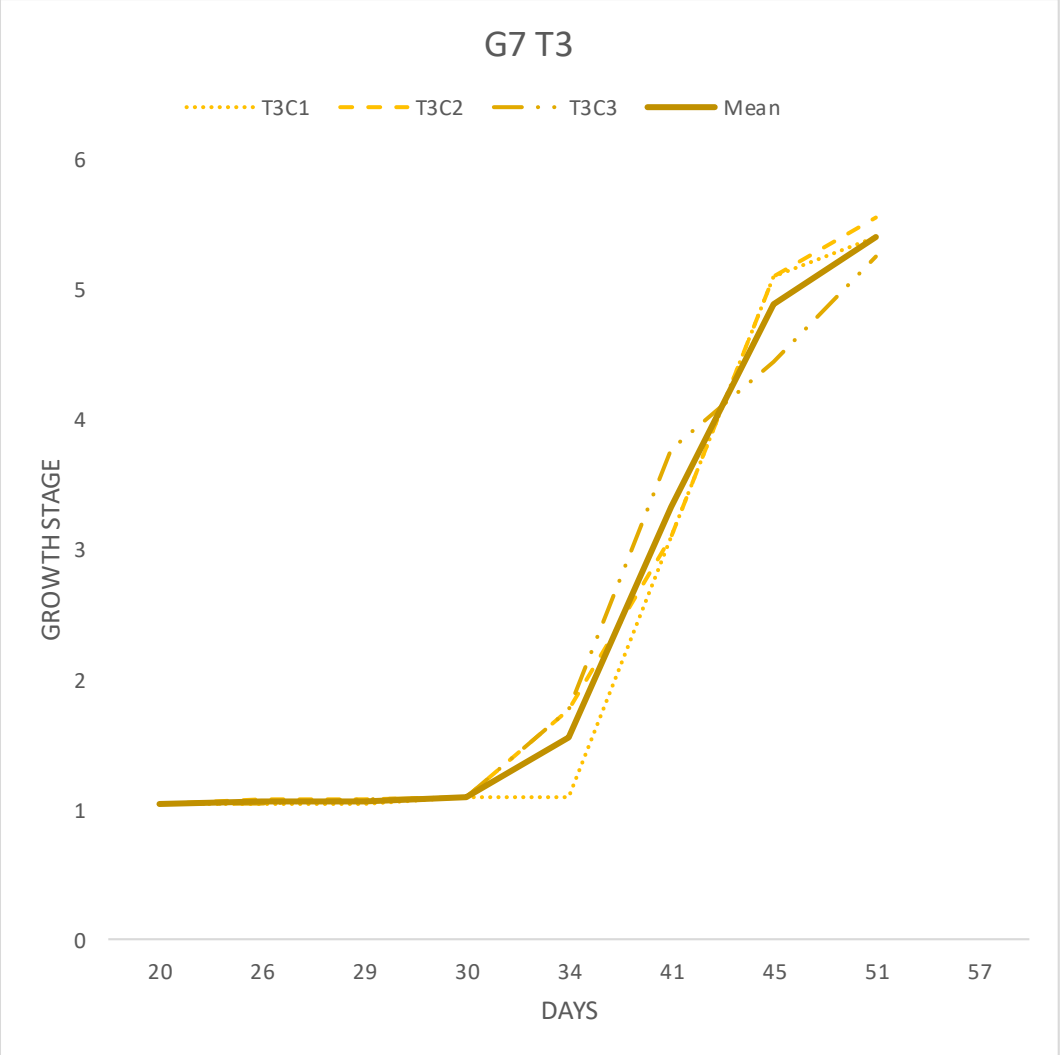

Fig. 2.29. Cs-137 treatment group phenotypic stage data G7 (Generation 7). Phenotypic stages were plotted against time (days). Solid lines indicate the mean of the Cs-137 treatment group. Dashed lines represent each of the three containers (denoted C). On average stages began to differ in terms of timing after 30 days of growth.

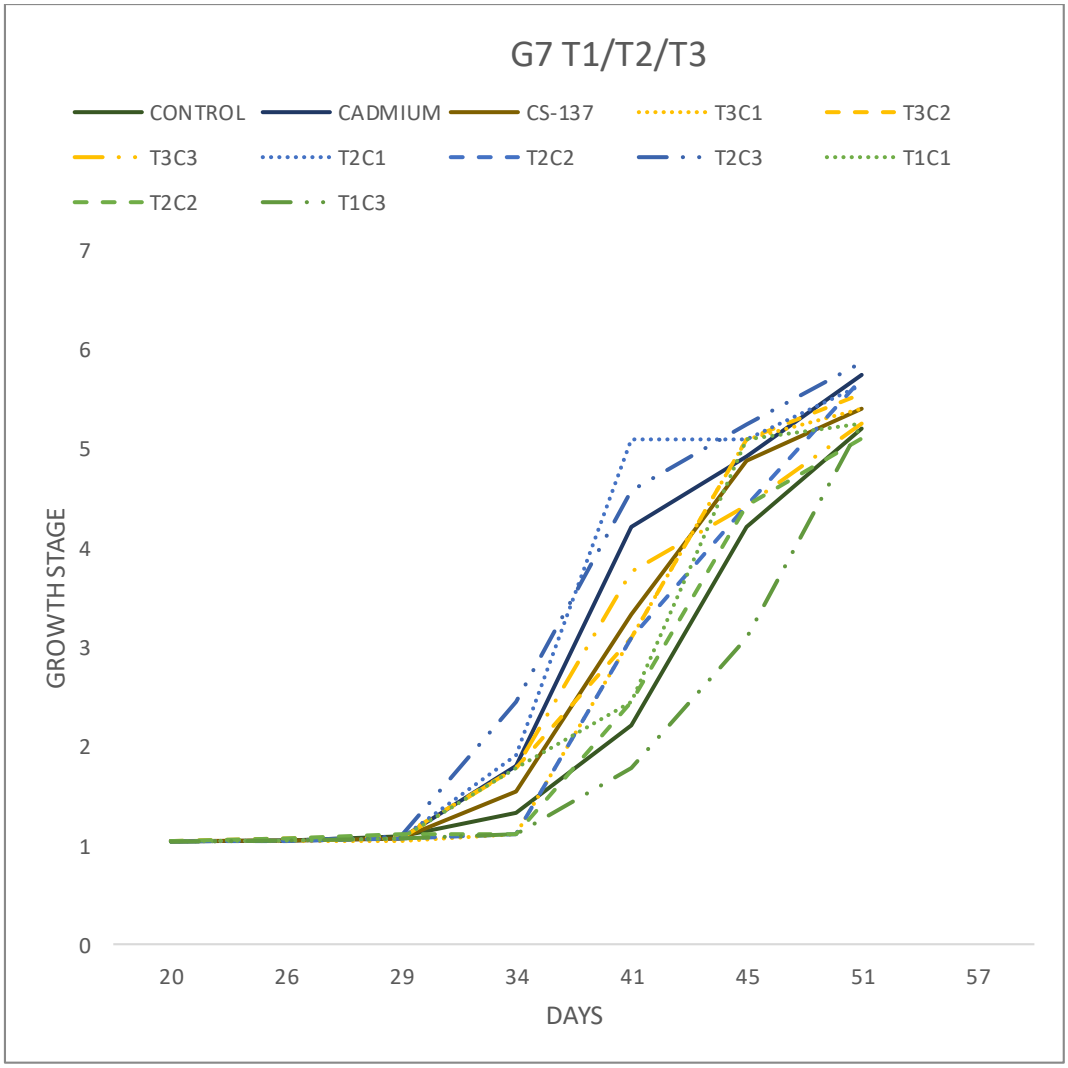

Fig. 2.30. All treatment groups G7 (generation 7). All of the data from the seventh generation was merged into one graph for comparative purposes. Variation in the timing of phenotypic stages was evident through position of the lines representing each group. Average values were highlighted with solid lines.

Positive controls in G7 were observed to have earlier growth success compared to the other groups which is the opposite of what occurred in G5 and similar to the earlier stages in G4. Cs-137 treated plants had slightly enhanced growth compared to the negative controls, which is also similar to phenomenon in G4. All of these observations are in terms of means, however some fluctuations and crossing-over of growth stages occurs throughout all of the treatment groups across all generations.

2.3.2 The effects of low dose IR on seed viability from multiple generations of plants exposed to Cs-137

Seed germination rate percentages were calculated in Excel. G = generation. (Refer to section 2.2.9 for more information on generation codes).

Generation 4 was the second generation exposed to Cs-137 in this experiment. All three treatment groups had germination success and varied slightly between treatment groups. Generation 5 had no positive control data due to lack of seeds but had germination success in the groups that remained. Conversely, generation 6 had a similar issue whereby there was no negative control, but success in both of the other groups.

Generation 7 seeds were omitted from analysis due to complete lack of germination in the negative control and hardly any germination in the positive control (5.8% success rate) believed to be caused by loose petri dish lids which resulted in excessive drying of the germination paper and therefore produced little to no seedlings. Although some germination success was observed in the Cs-137 treatment (85% success), with no suitable controls to compare to it was decided that generation 7 wasn't included in further analysis.

Generation 8 seeds (a generation which were never sown but still received doses of IR through development during generation 7) had germination success across all groups and had the highest success rate for germination of the Cs-137 treatment group from all of the other generations (Table 2.5, Fig. 2.31). A trend was observed where the more recent generations had a higher germination success percentage with the exception of generation 6 (Fig 2.32).

Table 2.5 Number of germinated seeds vs dormant/sterile seeds across multiple generations of A. thaliana with calculated percentages. ND= no data available.

Generation	Germinated	Not germinated	total	Percentage germinated
G4 - control	234	34	268	87%
G4 + control	9	30	39	23%
G4 IR	57	36	93	61%
G5 - control	12	3	15	80%
G5 + control	ND	ND	0	ND
G5 IR	16	5	21	76%
G6 - control	ND	ND	0	ND
G6 + control	151	5	156	97%
G6 IR	17	12	29	58%
G7 - control	0	160	160	0
G7 + control	10	162	172	6%
G7 IR	46	8	54	85%
G8 - control	201	11	212	95%
G8 + control	98	13	111	88%
G8 IR	36	4	40	90%

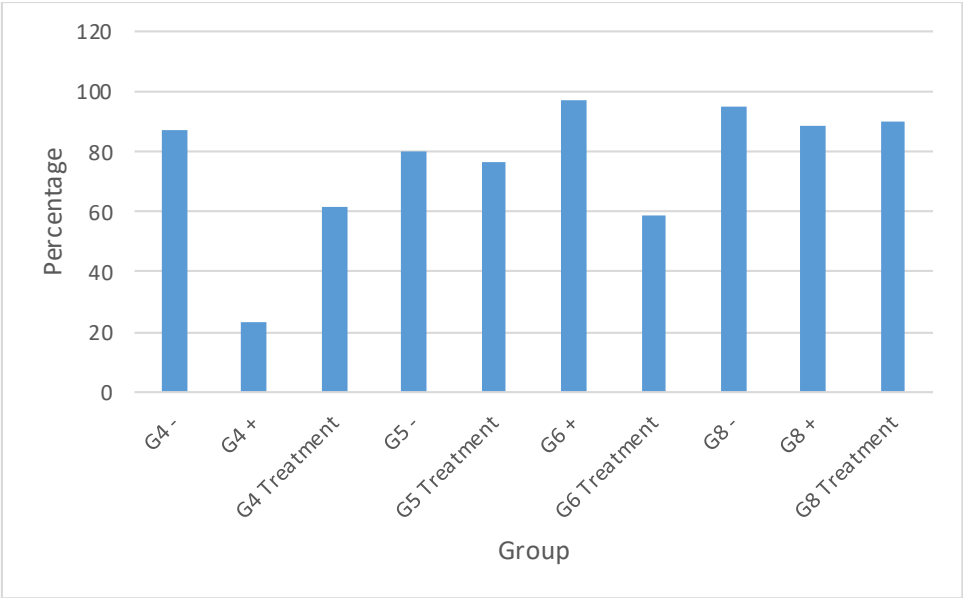

Fig. 2.31. Percentage of germinated seeds vs dormant/sterile seeds across multiple generations of A. thaliana for all treatment groups. Some groups omitted as highlighted in Fig. 2.30. Group labels: - = negative control, + = positive control (cadmium treatment) and Treatment = Cs-137 treatment.

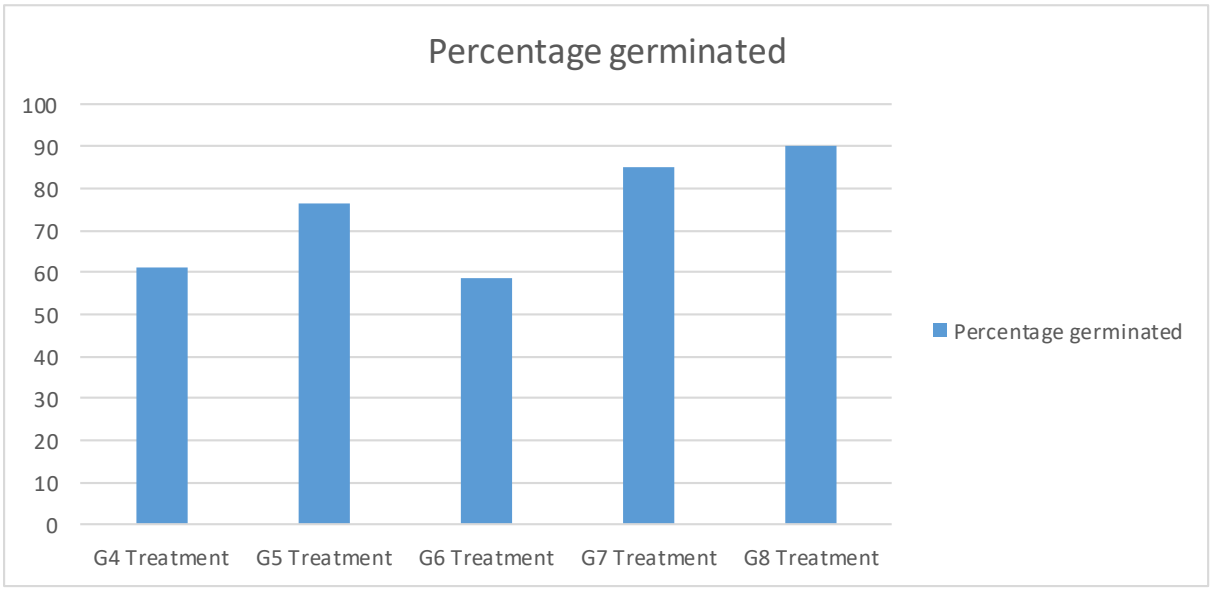

Fig. 2.32. Percentage of germinated seeds vs dormant/sterile seeds across multiple generations of A. thaliana Cs-137 only.

2.3.3 The effects of IR on root development after two generations of exposure to Cs-137 *in A. thaliana*

Root data was only available for G4 (generation 4), the second generation of *A. thaliana* exposed to radioactivity in the transgenerational experiment. Upon testing for normality, the data appeared non-normal in histograms and a disproportionate number of outliers was evident from the box plot (Fig. 2.33). This was probably due to too few samples (evident from the sparseness of Fig. 2.34). Nevertheless, a nonparametric test was selected (Kruskal-Wallis test for significance) and delivered a P value of 0.07, failing to find a significant difference between the treatment groups due to the small data set.

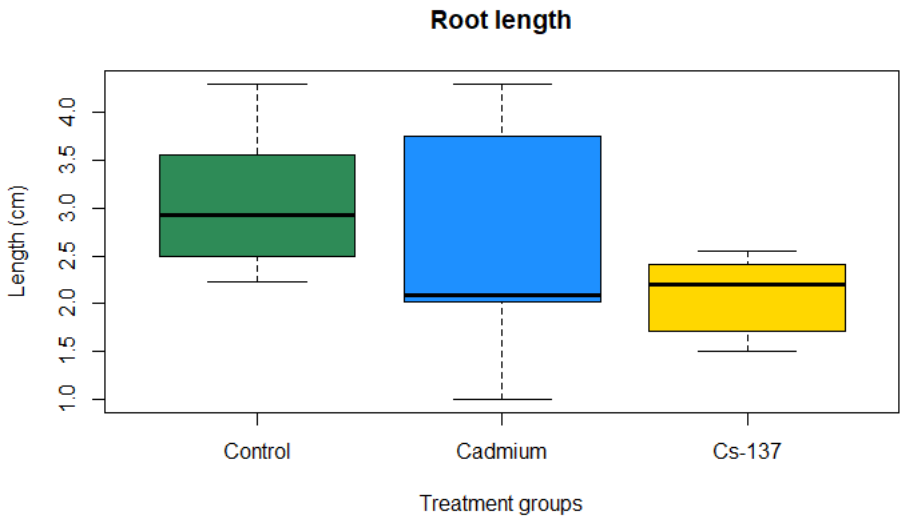

Fig. 2.33. Boxplot displaying root length in cm across all treatment group in generation 4 (G4). The cadmium positive control appeared to have the largest spread of root lengths and the Cs-137 treatment group appeared smaller. However no significant differences were detected using a Kruskal-Wallace nonparametric test for significance

at the 95% confidence level. NB: n= x+1 to avoid negative values for measurements <1 cm.

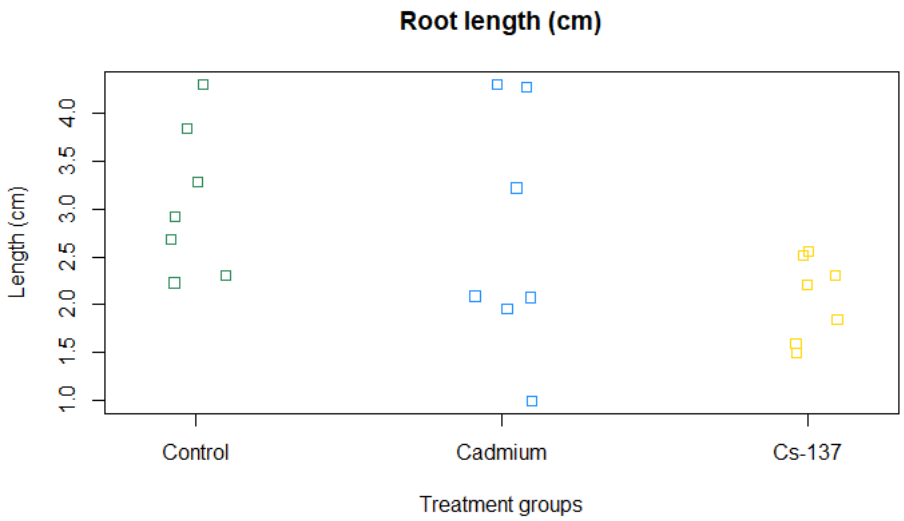

Fig. 2.34. Scatter plot showing each individual data point for generation 4 (G4). NB: n= x+1 to avoid negative values for measurements < 1 cm.

Chapter 3: Morphological Analysis of Leaves of *Arabidopsis thaliana* Exposed to Low-Dose Ionising Radiation Over Multiple Generations.

3.1 Introduction

As a general observation, the 30km Chernobyl Exclusion Zone (CEZ) 30 years post-accident has plants growing wherever there are soils to host them. Even in dense urban areas trees are found growing in and around abandoned buildings, including the most contaminated areas. The 'Red Forest' was, and still is a dense pine forest situated in the closest emissions trajectory to the disaster at the Chernobyl Nuclear Power Plant. For the first two years from the date of the accident, vast populations of pine trees, known to be amongst the most radiosensitive of plant species, were destroyed due to biologically injurious fallout from the reactor explosion. After this time, radiation levels had significantly fallen and the area began to recover (Volkova *et al*., 2017). The oldest trees in the region are still characteristically shades of red and orange from the damage (which gives the forest its name), but new growth has since occurred, and this is a testament to how plants can withstand higher doses of radiation than some other species of non-human biota.

Even though an obvious point, is also important to mention that unlike other types of wildlife that are found in the exclusion zone, plants are sessile. While other types of wildlife can be found in highly contaminated areas, because of mobile capability and large home ranges (in many species) they are generally not receiving a constant dose. Larger animals can, and do, move into and out of the CEZ. For plants this is not the case and their ability to inhabit areas with a relatively high constant dose helps to confirm that they are more radio-resistant than many animals. Populations of organisms in environments may appear to be growing normally but it has been

reported that physiological processes have been altered. It may be the case, therefore, that morphological changes have been overlooked as these can be harder to detect. Recent advances in the field of morphometrics, the study of morphology of living organisms, coupled with fast data analysis methods mean that it is now be easier than ever before to screen many different plant organs and produce high-resolution morphological data. This might provide complementary datasets to findings from physiology and aid the building of an integrated picture surrounding the effects of IR on plants, and indeed other stressors.

3.2 Materials and methods

3.2.1 Scanning equipment

The Doxie Flip (Fig. 3.1) is a wireless high-resolution scanner. Doxie donated one wireless scanner to this project to be used as a prototype after proposing to the company that their product may have wider applications. No contract was made and the product was donated in good faith. A wireless scanner in particular was sought because of its portability. This meant leaf scans could be performed *in situ* immediately after harvest on fresh samples. It also meant that is the method was successful it might be suitable for field use, particularly as the scanner relies on 2 x AA batteries for power, a widely available and rechargeable power source.

Fig 3.1. The Doxie Flip scanner (Apparent Corporation, 2017). The small size of the scanner (26.0 x 16.4 x 3.4 cm) and weight (560g) makes it extremely easy to use in the laboratory and potentially practical for field use.

For this project, depending on availability 10-20 leaves from an individual *A. thaliana* plants (from the same samples as reported in Chapter 2) were positioned on the scanner surface. Very small leaves (<0.5 cm diameter) were not scanned as there was a risk they could appear as artefacts and the software could automatically omit these (as it occasionally did with soil clumps or dirt). Further, small leaves were difficult to scan because closing the scanner lid created disturbances for very lightweight objects. The scanner could also be used without the plastic lid (Fig. 3.2) but this feature was not desirable for leaf scanning in this project due to the requirement for consistent light levels across all sample images. Leaves were spaced far enough apart so that they did not come into contact with other leaves, which was crucial for the data analysis stage described later. The results were positive, and the scanner could host, on average, 10 leaves of mixed sizes from a representative *A. thaliana* plant. The scanner surface also coped well with the addition of a thin sheet of polyethylene stretched over the glass to avoid radioactive contamination from samples. The scanner recorded colour and detail with high accuracy, making it ideal for leaf morphometric analyses as well as colour analyses (e.g. studies of chlorosis etc.). Some limitations occurred with respect to the leaf scans. For example, torn and or folded leaves were not used in the data set. Torn leaves occurred when folded leaves were unfurled and spread onto the scanner surface, with the introduction of the lid (and its consequent weight) introducing pressure onto leaves and causing mechanical splitting. It would have been desirable to study leaves that had folded naturally as these were typically the earlier leaves from initial growth stages. As radiation is said to have more of an effect on plants during early development (Esnault, 2010), it would have made an ideal scenario if it were possible to study early development in the leaves prior to them folding, and then run a comparative study with the turgid, mature leaves at the end of the growth cycle. Due

to the transgenerational nature of the project and corresponding time constraints, this was not performed on this occasion.

Fig 3.2. Doxie Flip scanner shown during a scan with the lid removed. The live view screen displays scans in real time for accuracy purposes. The control panel allows the user to review images prior to storage and upload.

Each scan of leaves produced a high resolution digital image file (JPEG) which was uploaded to a computer and stored for analysis.

Scans included labels alongside leaves displaying sample codes (Figures 3.4 & 3.5). The information assigned to each code is explained in Fig. 3.3.

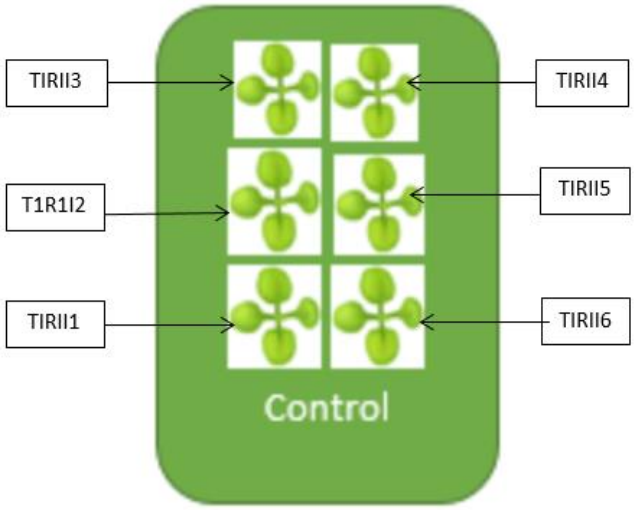

Fig. 3.3. Codes for individual plants in multi-generational experiment with A. thaliana. The example shown is for a control container of plants.

3.2.2 Choice of endpoints and use of LAMINA

Scanned images as described in the previous section were used to analyse leaf morphology using computer software. The software chosen for this section of the project was LAMINA (Leaf shApe deterMINAtion) and was developed by Bylesjö *et al*. (2008). The Java-based programme is available as freeware from www.plant-image-analysis.org for Windows, Mac and Linux. The version downloaded in this project was for Windows 10 Education Edition. LAMINA is a semi-autonomous tool for providing classical measurements of leaves. The software is capable of measuring shape (blade dimensions), area, serrations, holes, circularity and symmetry and can perform measurements for these multiple endpoints simultaneously. For the purpose of this project, two key endpoints were chosen as most suitable for analysis of *A. thaliana* leaves: area and symmetry.

Communication with one of the developers (Nathaniel Street, Umea University) was sought to consult the use of the software for the selected endpoints. After consultation with the developer, it was noted that petioles must be removed for symmetry measurements otherwise the software would not recognise true fluctuations in asymmetry. For the first batch of scans (Fig. 3.4.) each image was digitally altered in Adobe Photoshop CC 2017 via deletion of the petioles. For all subsequent scan batches the petioles were removed by cutting straight across them, therefore removing the need to digitally alter the images (such in Fig. 3.5.).

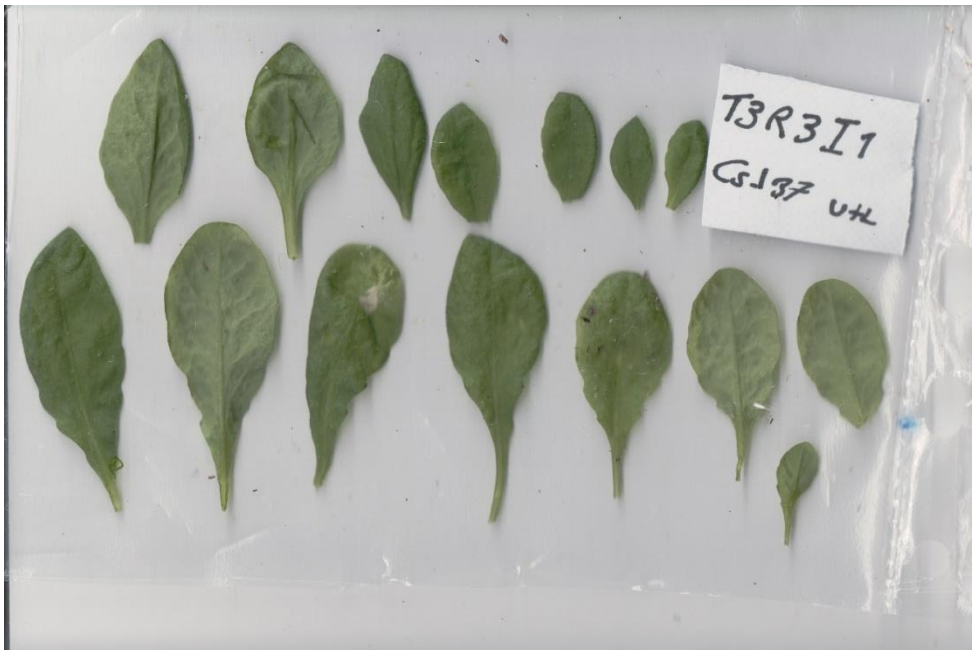

Fig. 3.4. An example scan of mature A. thaliana leaves from generation 4 (G4) with petioles attached to leaves. Code in top right-hand corner of scan corresponds to treatment type, container number and individual. Codes are detailed in Fig. 3.3. Code identifies this sample as a Cs-137 treatment plant.

Fig. 3.5. An example scan of mature A. thaliana leaves from generation 4 (G4) with petioles attached to leaves. Code in top left-hand corner of scan corresponds to treatment type, container number and individual. Codes are detailed in Fig. 3.3. Code identifies this sample as a negative control treatment plant.

LAMINA relies on the end-user to feed in images, to which it responds by overlaying digital grids and performs calculations for each endpoint. This is achieved through eight sequenced steps:

1) Thresholding – In this step the software identifies candidate pixels that represent leaves. It works by making automatic calculations relating to leaf colour and identifying colours typically found in leaves i.e. non-blue objects as blue is very rarely found as a leaf colour.

2) Segmentation – Once the previous step has been established, the software then groups together the pixels it has identified during the thresholding stage, therefore identifying patterns of pixels that represent leaves and recognising similar groups of pixels as other leaves from the same image.

3) Filtering – This step involves locating objects deemed as surplus to analytical requirements and ensures that, based on density of object, artefacts are removed. This stage can be, and was, manually checked in the visual output to make sure that no small leaves are considered artefacts in error.

4) Object boundaries – This step calculates distances within objects.

5) Cavities – This step identifies holes in leaves, calculated by an absence of pixels unconnected to the outer boundary of an object, the object being the leaf.

6) Serrations and indents – This step involves the calculation of the distances between two points on the boundary surface.

7) Indent depth – This step locates the deepest coordinate between two points identified in the previous step.

8) Boundary coordinates – Equally-spaced points around the surface of the object are identified in this step to ensure that measurements are independent of object positioning in an image.

Once the above steps have been completed, LAMINA creates three files ready to be saved to a user-specified output directory. These three files consist of two image-based screen grabs (Fig. 3.6.), (Fig. 3.7.) and a Microsoft Excel file with numerical data. The screen grabs show two features; first the overlaid grids used to calculate numerical data in the output file, and, second, an image displaying number ID tags over each leaf. This makes for rapid identification of leaves in the numerical data and should errors occur in leaf scans it is simply a case of deleting unwanted leaf scans that may be unsatisfactory due to torn leaves or leaves that had folded over (e.g. as visible in leaves #1, #4 and #5 in Fig. 3.6 & 3.7). Torn leaves typically occurred during the scanning process, as every effort was made to ensure leaves were complete upon incision. This occurred through the introduction of the scanner lid that caused splitting when it was positioned too heavily on the leaves. Folded leaves occurred naturally, towards the base of plants but were not suitable for scanning as they would have to be unfurled and this caused them to split.

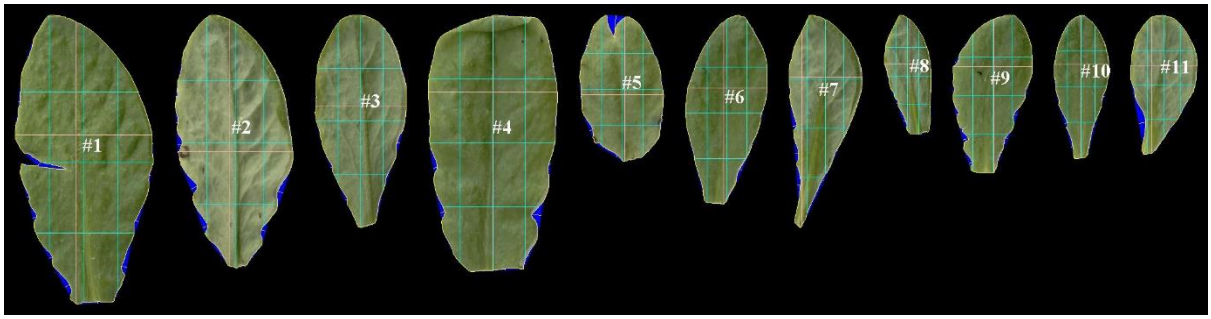

Fig. 3.6. Image output with numerical LAMINA ID tags and overlaid grids used for numerical data outputs. The blue false colouring is generated by the software and identifies indents. The three light-blue vertical lines show the vertical midline in terms of area (middle vertical light-blue line) and 25% of the total area measured from the left (left-hand vertical line) and 75% of the area measured from the left (right-hand line). The three light-blue horizontal lines show the horizontal midline in terms of area (middle horizontal light-blue line) and 25% of the total area measured from the bottom of the leaf (lower horizontal light-blue vertical line) and 75% of the area measured from the bottom of the leaf (upper horizontal light-blue line). The yellow lines show the widest and longest leaf line (which in some instances coincide with the blue are division lines).

Fig. 3.7. Image data output from LAMINA displaying numerical LAMINA ID tag associations for individual leaves.

3.2.3. Statistical Analysis

All statistical tests on vertical symmetry and leaf area were coded in R using the RStudio graphical user interface. Normality tests involved generating histograms and using Bartlett's test to gauge variance in samples between groups. Analyses of variance (ANOVA) tests were used to determine significant differences between treatment groups. If a significant difference was detected then Welch two sample t-tests were employed to narrow down the areas of significance and identify which exact groups reported differences. A significance level of 0.05 was used for each test. Statistical outputs from R studio are available in supplementary information.

In the analysis reported here vertical leaf symmetry was chosen as the endpoint. This is calculated by dividing the length of the 25% vertical area line and the 75% vertical area line (from the left-hand side) of a single leaf. This measure of leaf symmetry has established use in toxicology studies (Alves-Silvia *et al*., 2018), in which an increase in asymmetry (which reflects developmental instability) is a commonly agreed upon indicator of stress (Kozlov and Zvereva, 2015).

3.3 Results

3.3.1 Vertical symmetry measurements in *A. thaliana* leaves

For each generation of *A. thaliana* analysed for leaf vertical symmetry the number of individual leaves differed between generation and treatment group. Table 3.1 shows the exact number of individual leaf scans included in the data.

Table 3.1 Number of individual leaf samples used in LAMINA image analysis software. In each generation, there were three replicate containers each with up to six plants, i.e. up to 18 plants in total. In some instances, individual plants failed to grow so n= <18.

Generation tag	Number of leaves: Negative control	Number of leaves: Positive control ($CdCl_2$)	Number of leaves: Treatment (Cs-137)
Generation 4(G4)	127	83	62
Generation 5(G5)	211	187	226
Generation 6(G6)	184	181	190
Generation 7(G7)	206	193	180

3.3.1.1 Generation 4 (G4)

Figure 3.8 shows histograms of the leaf symmetry in generation 4 (two generations of exposure to IR) while figures 3.9 & 3.10 show the spread of the data across all treatment groups (outliers are more obvious in a boxplot while individual samples are easier identified in a scatter plot, hence the decision to use both to represent the data for these endpoints in all generations). A value of 0.0 is indicative of a perfectly symmetrical leaf, negative and positive values indicate leaf asymmetry.

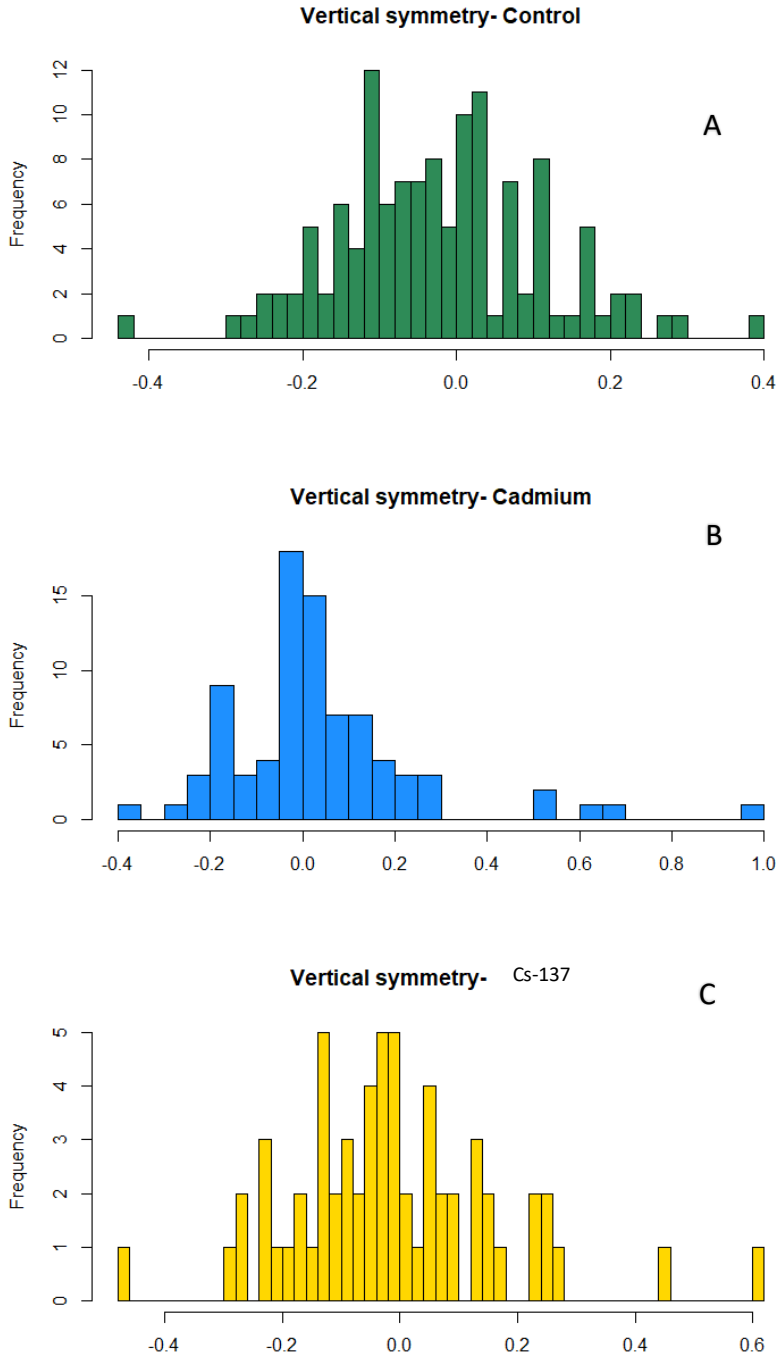

Fig. 3.8. Histogram of leaf vertical symmetry measurements in generation 4 (G4) for individual leaves in each treatment group (A = negative control, B = positive control and C = Cs-137 treatment).. The x axis indicates the value FOR symmetry measurement (0.0 = perfect symmetry) while the y axis displays the number of leaves with each vertical symmetry value. Control (n=127), positive control (CdCl2) (n=83), Cs-137 at 90 kBq/l growth medium (n=62). From the shape of the histograms it is apparent that in each treatment most leaves fall around perfect symmetry, with departures from perfect symmetry evident in both directions (negative values indicate a higher incidence of asymmetry to the left of a leaf when observed as a 2-dimensional

scan while positive values indicate the same phenomenon to the right). There is some indication of leaf asymmetry in the positive control and Cs-137 treatments.

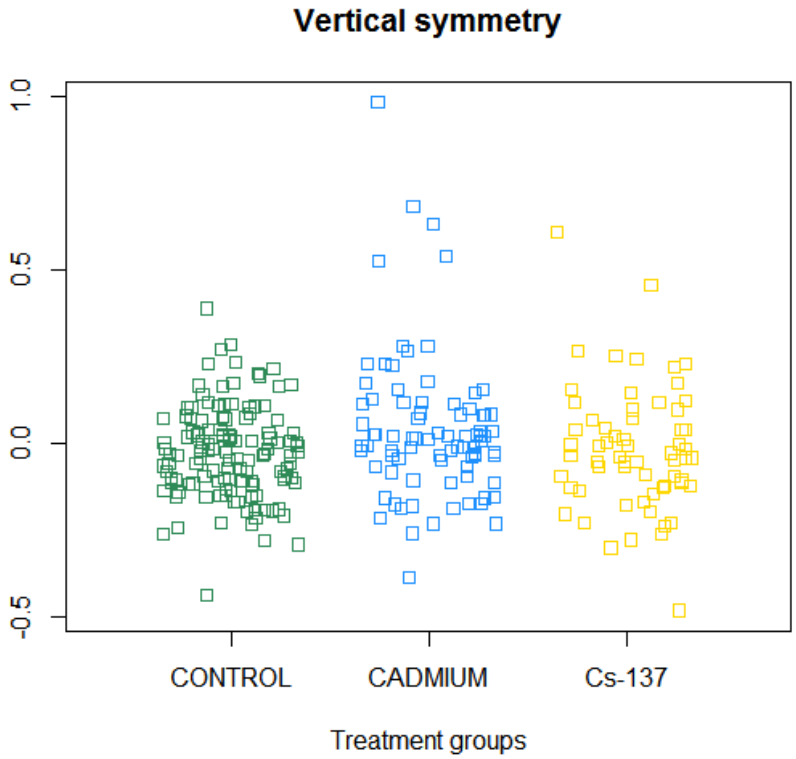

Fig. 3.9. Scatter plot of generation 4 mature A. thaliana leaves (G4) showing all individual leaf data points across all treatment groups. Symmetry is measured on a relative scale where 0.0 denotes perfect symmetry and negative and positive values show dominant skewness of symmetry to the left and to the right respectively. The higher or lower the value departs from 0.0 the more pronounced asymmetry is. (For control n= 127, for cadmium n=83, for Cs-137 n= 62. Data points have been spread in the x axis direction in order to aid visualisation).

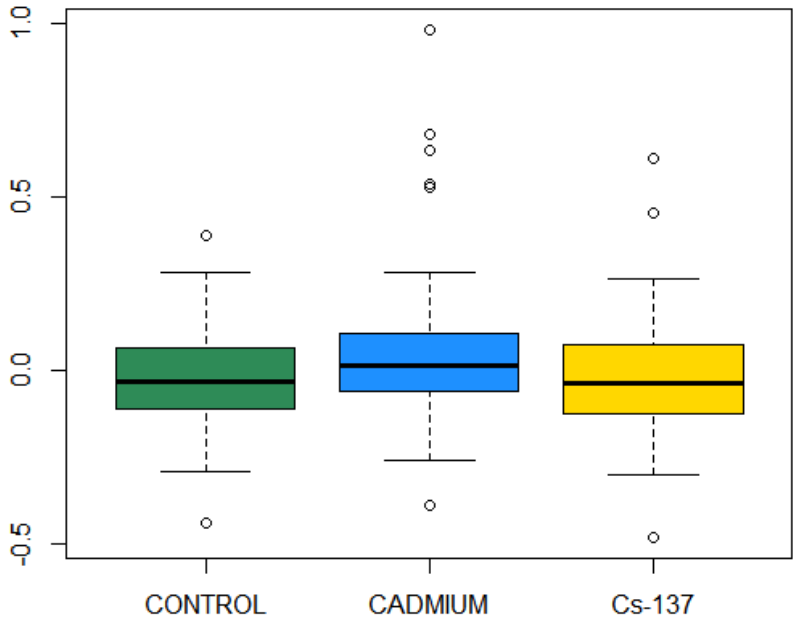

Fig. 3.10. Boxplot of generation 4 mature A. thaliana leaf vertical symmetry data (G4). The axes are identical to the scatter plot but the boxplot identifies outlier data points that represent leaves with particularly unusual leaf symmetries. (for control n= 127, for cadmium n= 83, for Cs-137 n= 62).

In generation 4 (G4), all histograms had a normal distribution in each treatment group. Bartlett's test for homogeneity of variance provided a significant result which indicated statistically significant differences in the variance of data between treatment groups. The data was still analysed using ANOVA and Welch's test, due to the large number of samples present and the normality of each histogram. Both analysis of variance (ANOVA) and Welch two sample t-tests were used, as appropriate, on this generation 4 data and subsequent generations of leaf symmetry data.

The ANOVA for G4 vertical symmetry showed that there were, overall, some significant differences in the means between treatment groups. To pinpoint differences in the groups the Welsh two sample t-tests was used to compare negative with positive control, negative control with Cs-137 treatment and positive control with Cs-137 treatment. A significant difference was found between positive and negative control. No significant differences were detected between any other group pairing.

3.3.1.2 Generation 5 (G5)

Figures 3.11 to 3.13 show vertical symmetry data for generation 5 of *A. thaliana* plants grown under controlled experiment conditions. Overall, the number of leaves harvested was significantly greater in generation 5 than generation 4 although the development of growth stages was quite similar (Fig. 2.19, chapter 2).

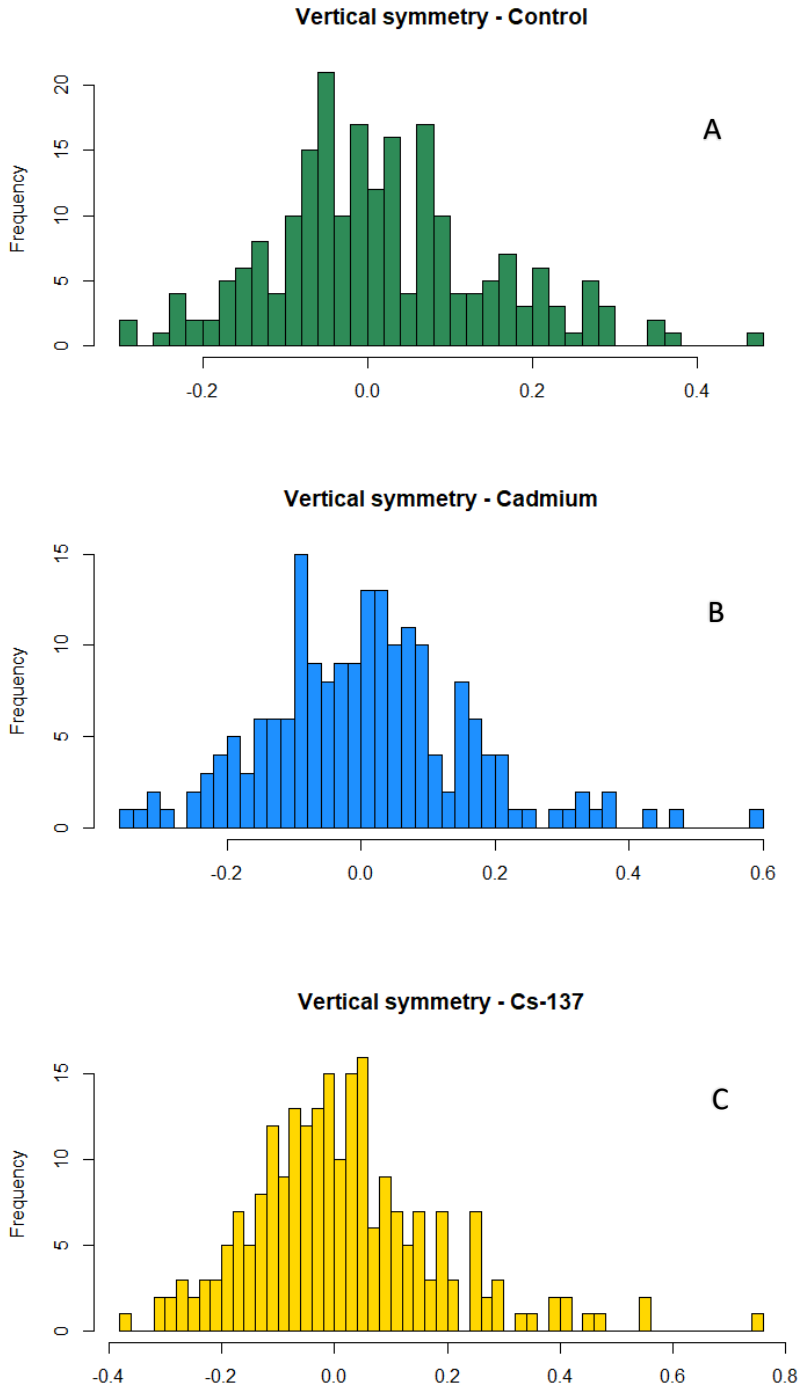

Fig. 3.11. Histogram of mature A. thaliana leaf vertical symmetry measurements in generation 5 (G5) individual leaves for each treatment group (A = negative control, B = positive control and C = Cs-137 treatment. The x axis indicates symmetry measurements (0.0 = perfect symmetry) while the y axis displays the number of leaves that fall into each symmetry category. Control (n= 221), positive control (n= 187), Cs-137 (n=226). From the shape of the histograms it is apparent that most leaves fall around perfect symmetry, with departures from perfect symmetry evident in both

directions (negative values indicate a higher incidence of asymmetry to the left of a leaf when observed as a 2-dimensional scan while positive values indicate the same phenomenon to the right).

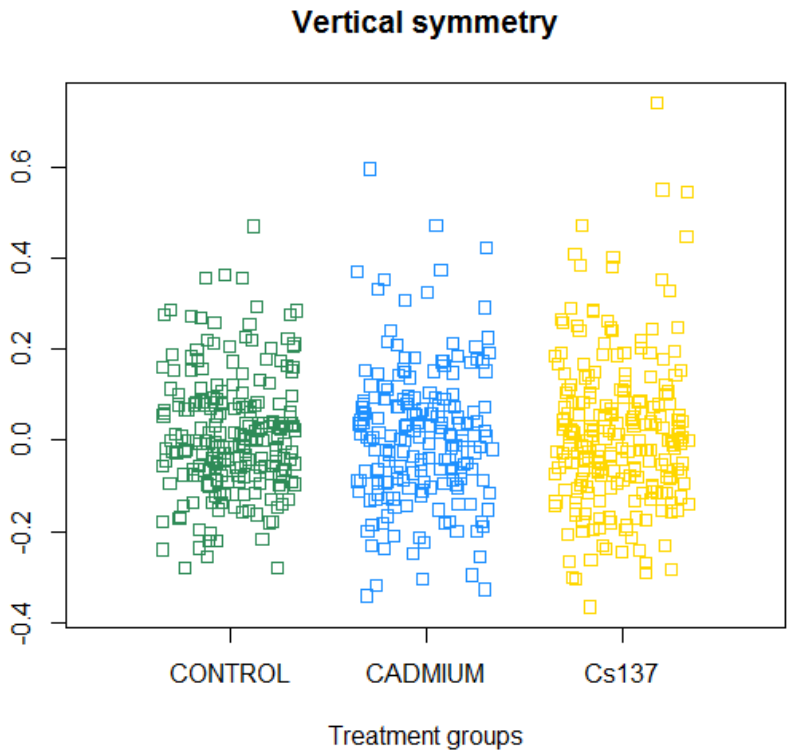

Fig. 3.12. Scatter plot of generation 5 mature A. thaliana leaves (G5) showing all individual data points across all treatment groups. Symmetry is measured on a relative scale where 0.0 denotes perfect symmetry and negative and positive values show dominant skewness of symmetry to the left and to the right respectively. The higher or lower the value departs from 0.0 the more pronounced asymmetry is. (Control n= 221, cadmium n= 187, Cs-137 n=226. Data points have been spread in the x axis direction in order to aid visualisation).

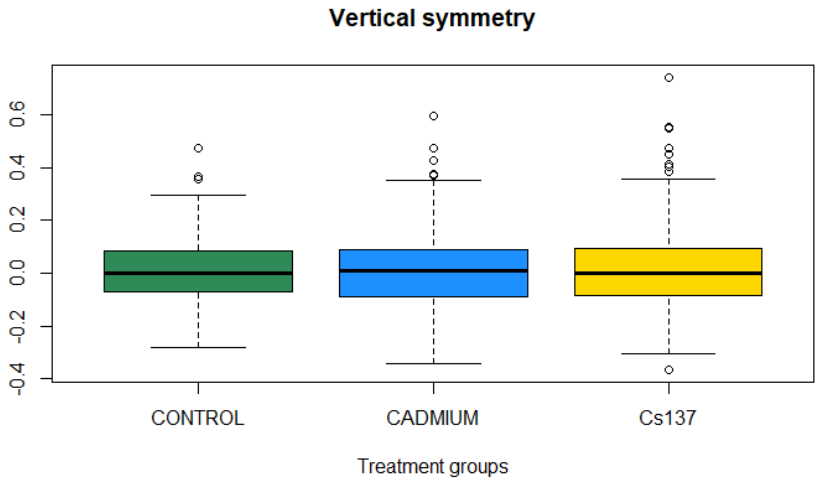

Fig. 3.13. Boxplot of generation 5 (G5) mature A. thaliana leaf vertical symmetry data. The axes are identical to the scatter plot but the boxplot identifies outlier data points that represent leaves with particularly unusual leaf symmetries. (For control n= 221, for cadmium n= 187, for Cs-137 n= 226).

In generation 5 (G5), all data groups had a normal distribution. Bartlett's test was applied and shown to be significant which indicated significant differences in variances between treatments. This pattern was the same for G4, however, by contrast in generation 5 there were no significant differences in mean symmetry between treatment groups.

3.3.1.3 Generation 6 (G6)

In generation 6 plants in all treatments again grew well and a large number of leaves were harvested and analysed. The analysis of vertical symmetry for leaves of generation 6 (three generations of exposure to radioactivity) is shown in figures 3.14 to 13.6.

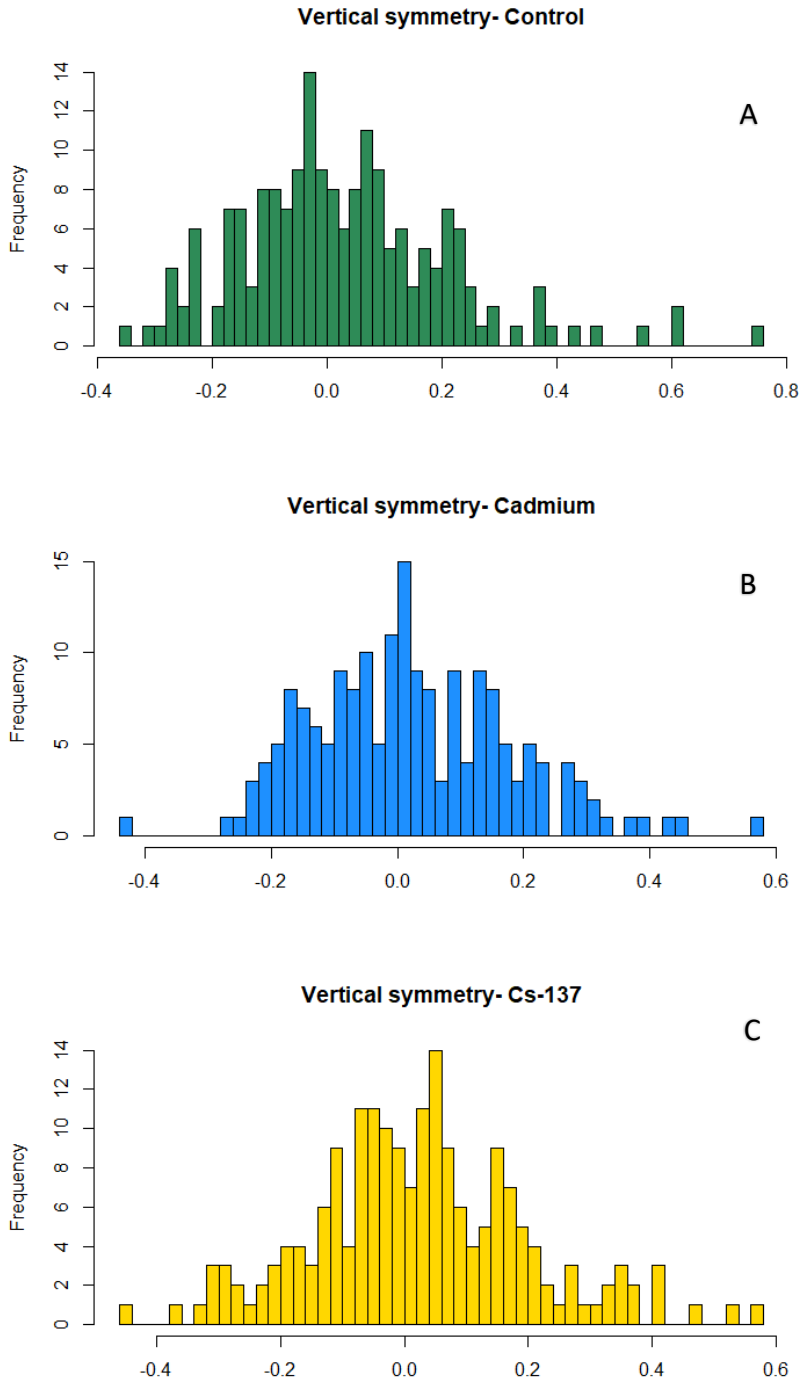

Fig. 3.14. Histograms of mature A. thaliana leaf vertical symmetry measurements in generation 6 (G6) for individual leaves for each treatment group. (A = negative control, B = positive control and C = Cs-137 treatment. The x axis indicates leaf symmetry measurements (0.0 = perfect symmetry) while the y axis displays the number of leaves that fall into each symmetry category. Control (n= 184), positive control (n= 181), Cs-137 (n=190). From the shape of the histograms it is apparent that most leaves fall around perfect symmetry, with departures from perfect symmetry evident in both directions (negative values indicate a higher incidence of asymmetry to the left of a

leaf when observed as a 2-dimensional scan while positive values indicate the same phenomenon to the right).

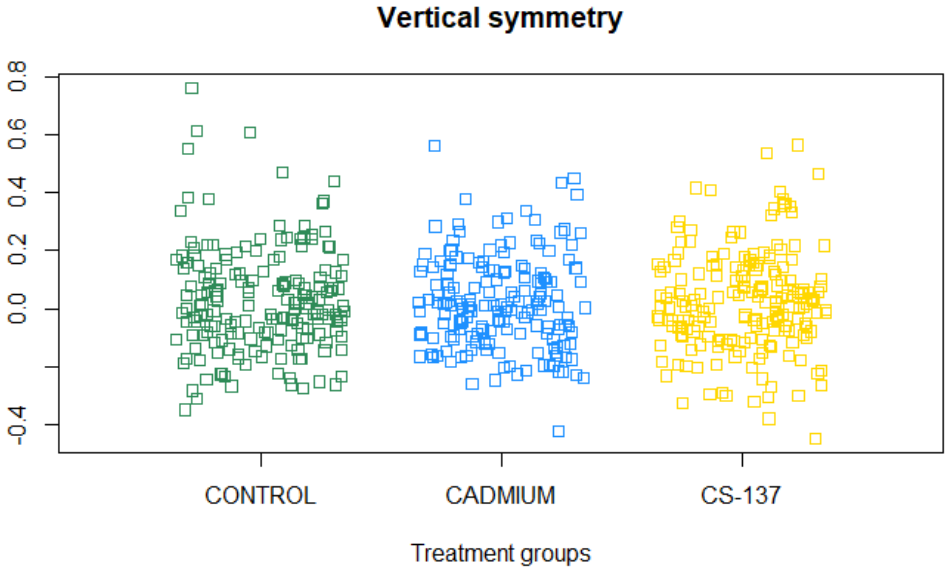

Fig. 3.15. Scatter plot of mature A. thaliana leaf symmetry measurements for generation 6 (G6) showing all individual data points across all treatment groups. Symmetry is measured on a relative scale where 0.0 denotes perfect symmetry and negative and positive values show dominant skewness of symmetry to the left and to the right respectively. The higher or lower the value departs from 0.0 the more pronounced asymmetry is. . (Control n= 184, positive control n= 181, Cs-137 n=190. Data points have been spread in the x axis direction in order to aid visualisation).

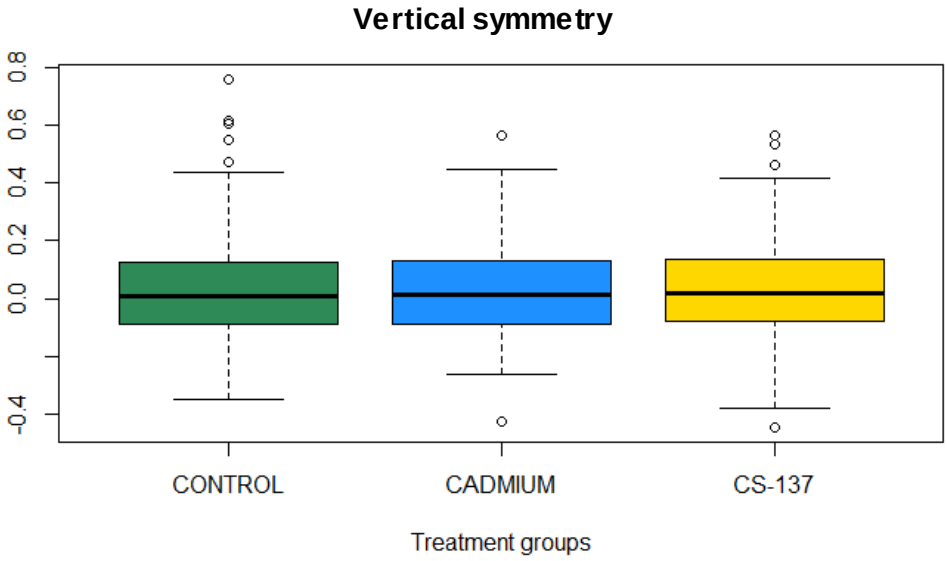

Fig. 3.16. Boxplot of generation 6 (G6) mature A. thaliana leaf vertical symmetry data. The axes are identical to the scatter plot but the boxplot identifies outlier data points

that represent leaves with particularly unusual leaf symmetries. (Control n= 184, for cadmium n= 181, for Cs-137 n= 190).

In generation 6 (G6) leaf symmetry data was normally distributed and no significant differences were detected between the mean values in both ANOVA tests and t-tests between treatment groups.

3.3.1.4 Generation 7 (G7)

In generation 7 (four generations of exposure to IR) plants in all treatments again grew well. The progression of developmental stages were similar to previous generations (chapter 2, Figures 2.16 to 2.27).

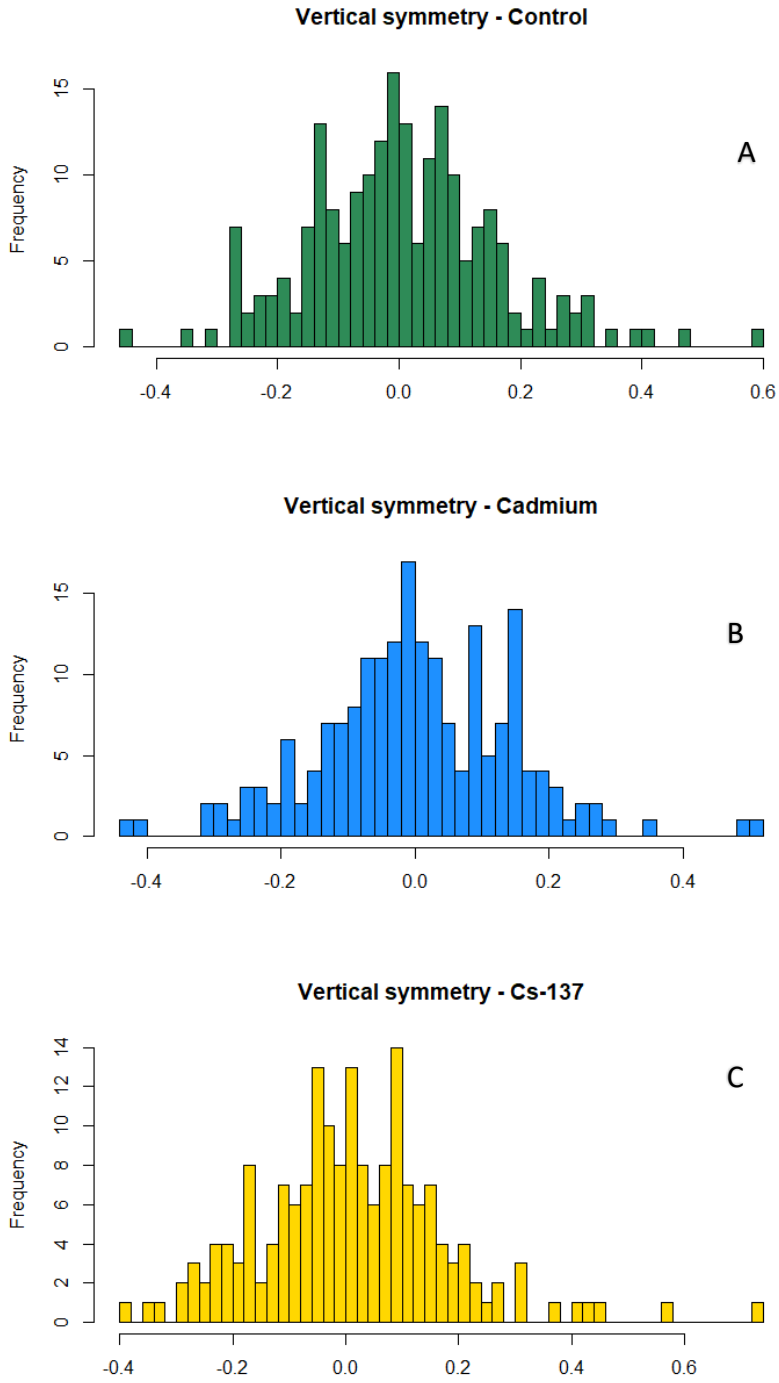

Fig. 3.17. Histograms of mature A. thaliana leaf vertical symmetry measurements in generation 7 (G7) for individual leaves for each treatment group (A = negative control, B = positive control and C = Cs-137 treatment.) The x axis indicates leaf symmetry measurements (0.0 = perfect symmetry) while the y axis displays the number of leaves that fall into each symmetry category. Control (n= 206), positive control (n= 193), Cs-137 (n=180). From the shape of the histograms it is apparent that most leaves fall around perfect symmetry, with departures from perfect symmetry evident in both directions (negative values indicate a higher incidence of asymmetry to the left of a leaf when observed as a 2-dimensional scan while positive values indicate the same phenomenon to the right).

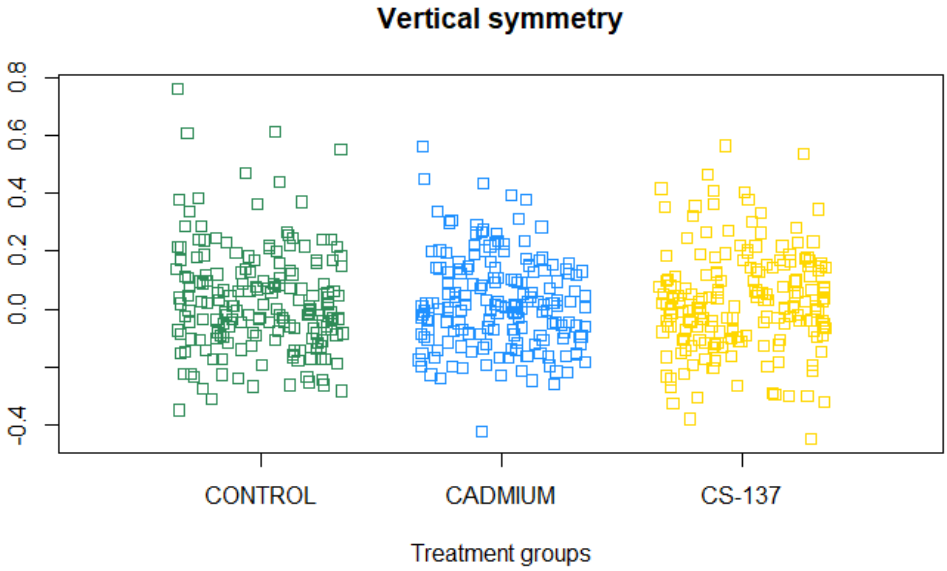

Fig. 3.18. Scatter plot of mature A. thaliana leaf symmetry measurements for generation 7 (G7) showing all individual data points across all treatment groups. Symmetry is measured on a relative scale where 0.0 denotes perfect symmetry and negative and positive values show dominant skewness of symmetry to the left and to the right respectively. The higher or lower the value departs from 0.0 the more pronounced asymmetry is. . (Control n= 206, positive control n= 193, Cs-137 n=180. Data points have been spread in the x axis direction in order to aid visualisation).

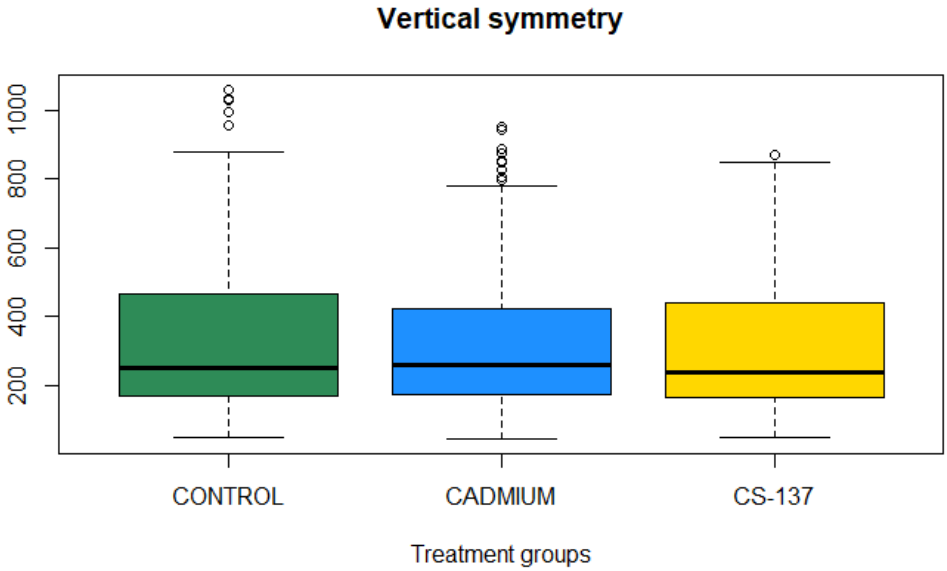

Fig. 3.19. Boxplot of generation 6 (G6) mature A. thaliana leaf vertical symmetry data. The axes are identical to the scatter plot but the boxplot identifies outlier data points that represent leaves with particularly unusual leaf symmetries. (Control n= 206, for cadmium n= 193, for Cs-137 n= 180).

In generation 7 (G7) data was normal and no significant differences were detected in both ANOVA tests and t-tests between treatment groups.

3.3.2 Total leaf area measurements in *A. thaliana*

The same leaves analysed for vertical symmetry measurements were used for area and so the number of leaves are identical to the individual samples listed in Table 3.1.

3.3.2.1 Generation 4 (G4)

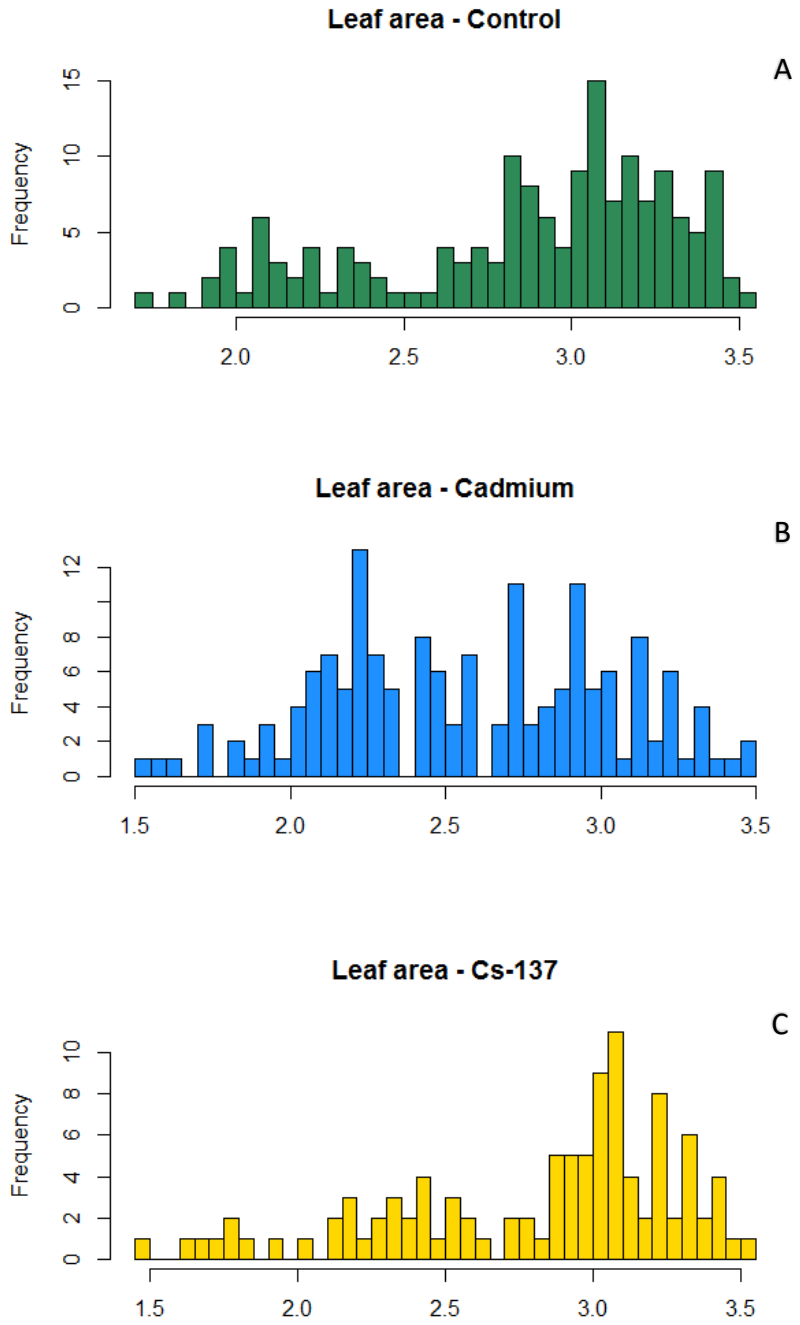

Fig. 3.20. Distribution of leaf area measurements in generation 4 (G4) individual samples for each treatment group. (A = negative control, B = positive control and C = Cs-137 treatment. The x axis indicates leaf area measurements in mm2 while the y axis displays the frequency of samples that fall into each measurement. From the shape of the histograms it is apparent that there is a spread of measurements ranging from 1.5 mm2 to just over 3.5 mm2. (Control n= 206, positive control n= 193, Cs-137 n=180).

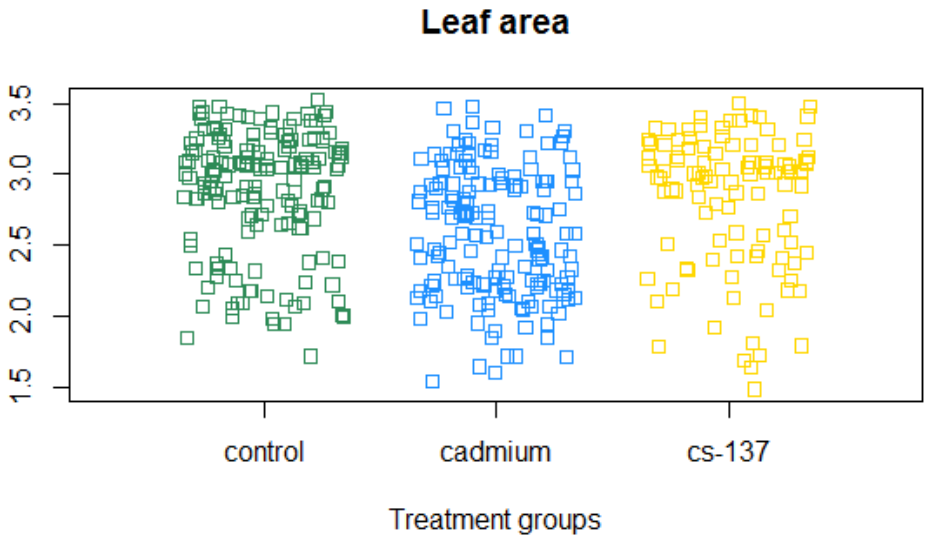

Fig. 3.21. Scatter plot of generation 4 (G4) leaf area data displaying all individual data points across all treatment groups. The y axis displays leaf area in mm2. The denser the cluster of points the higher the frequency of samples pertain to a particular size or range of sizes. (Control n= 206, positive control n= 193, Cs-137 n=180).

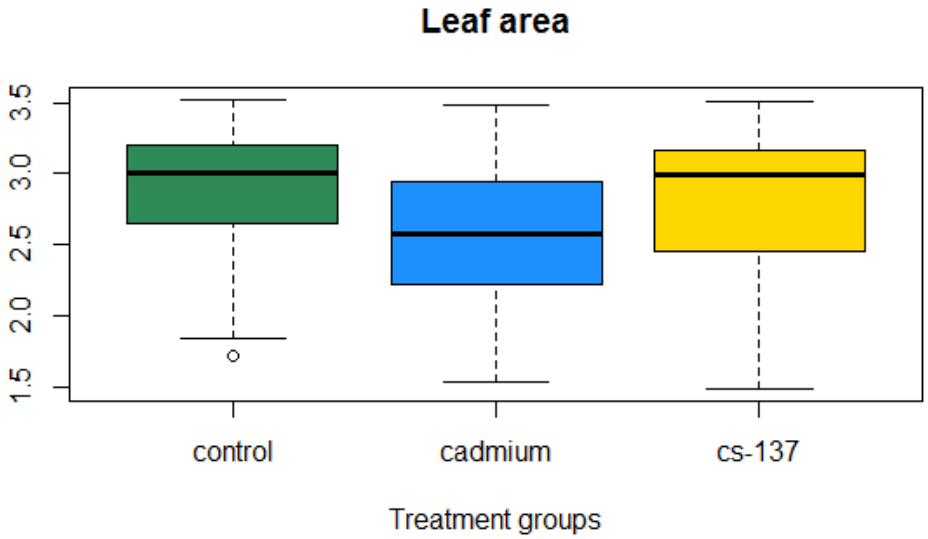

Fig. 3.22. Boxplot of generation 4 (G4) showing data overlaps and outliers across all sample groups for leaf area. The scale is identical to the scatter plot but displays outliers and data overlaps more clearly. The range of leaf area is displayed on the y axis in mm2. (Control n= 206, positive control n= 193, Cs-137 n=180).

Following normality tests, leaf area data (Figures 3.20-3.22) from generation 4 (G4) was observed to be normal data. An ANOVA test was employed and yielded a result where there was a significant difference in the variance between groups. To pinpoint the source of variance, Welch two sample t-tests were used. There were significant differences between the positive control and negative control, and between the negative control and cs-137 treatment group. This data implies that the positive control had more of an effect on leaf area than the cs-137 treatment.

3.3.2.2 Generation 5 (G5)

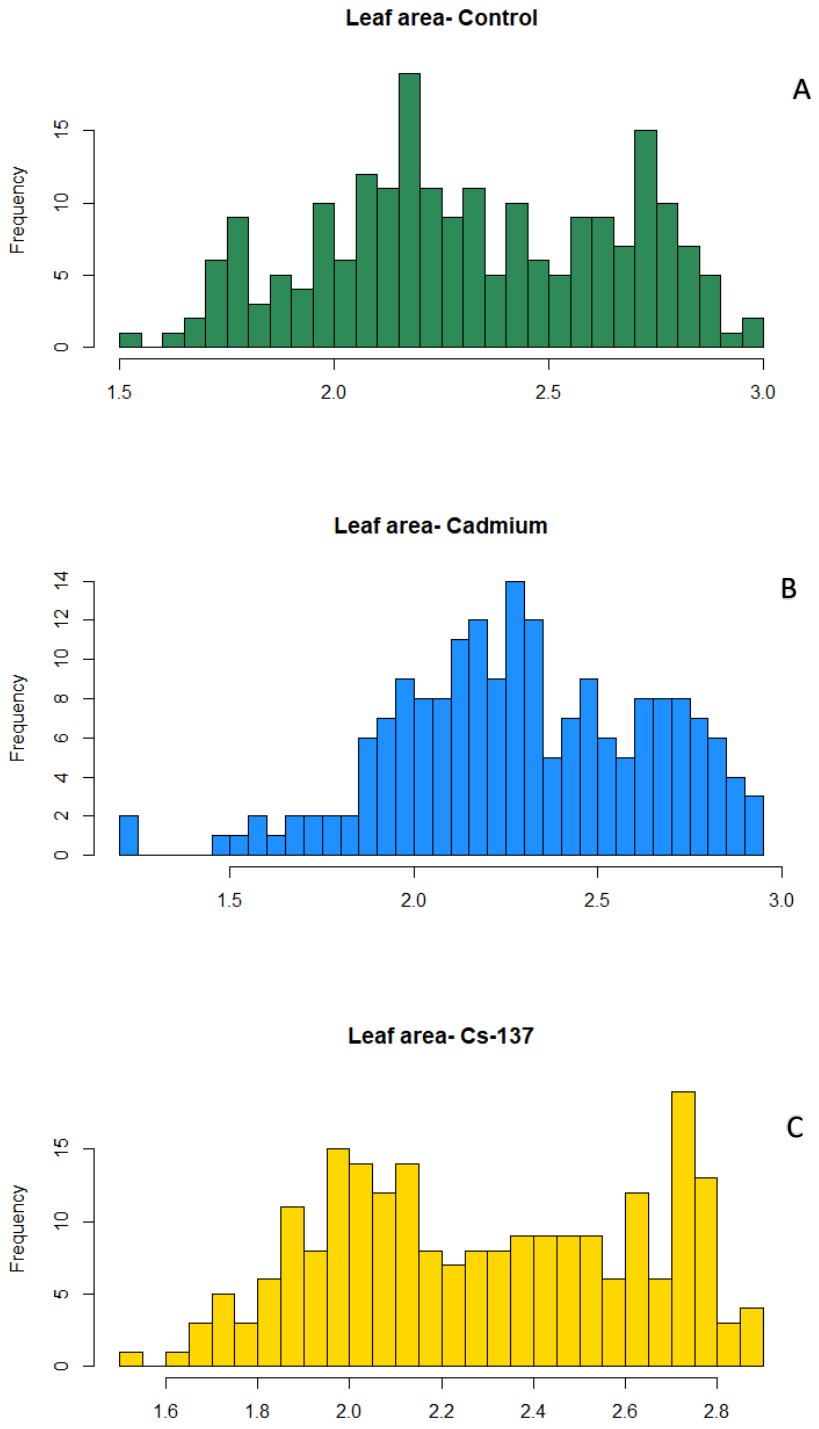

Fig. 3.23. Distribution of leaf area measurements in generation 5 (G5) individual samples for each s each treatment group. (A = negative control, B = positive control and C = Cs-137 treatment. The x axis indicates leaf area measurements in mm2 while the y axis displays the frequency of samples that fall into each measurement. From the shape of the histograms it is apparent that there is a spread of measurements

ranging from 1.4 mm2 to 3.0 mm2. (Control n= 206, positive control n= 193, Cs-137 n=180).

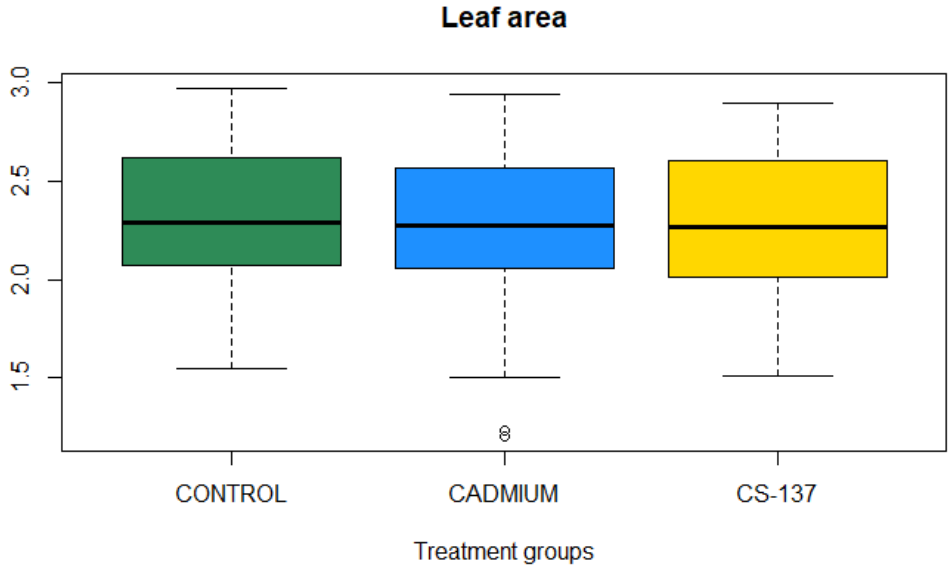

Fig. 3.24. Boxplot of generation 5 (G5) showing data overlaps and outliers across all sample groups for leaf area. The scale is identical to the scatter plot but displays outliers and data overlaps more clearly. The range of leaf area is displayed on the y axis in mm2. (Control n= 206, positive control n= 193, Cs-137 n=180).

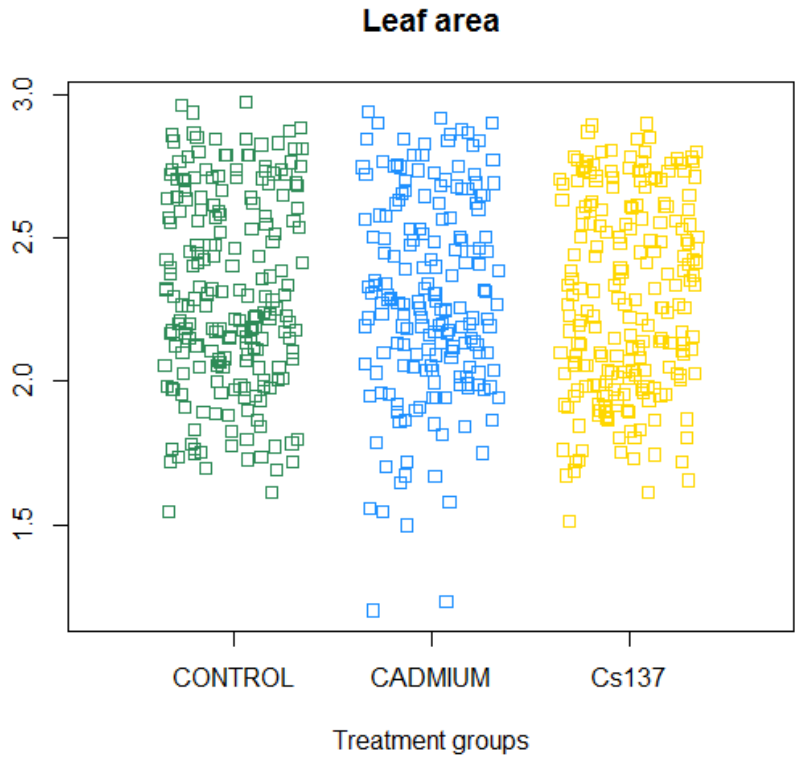

Fig. 3.25. *Scatter plot of generation 5 (G5) leaf area data displaying all individual data points across all treatment groups. The y axis displays leaf area in mm^2. The denser the cluster of points the higher the frequency of samples pertain to a particular size or range of sizes. (Control n= 206, positive control n= 193, Cs-137 n=180).*

Logged data was used in generation 5 for data handling purposes and to achieve fewer skewed results. Bartlett's test was used to examine the data for homogeneity of variance. Data was then used in an ANOVA and no significant differences were detected in the variance between groups.

3.3.2.3 Generation 6 (G6)

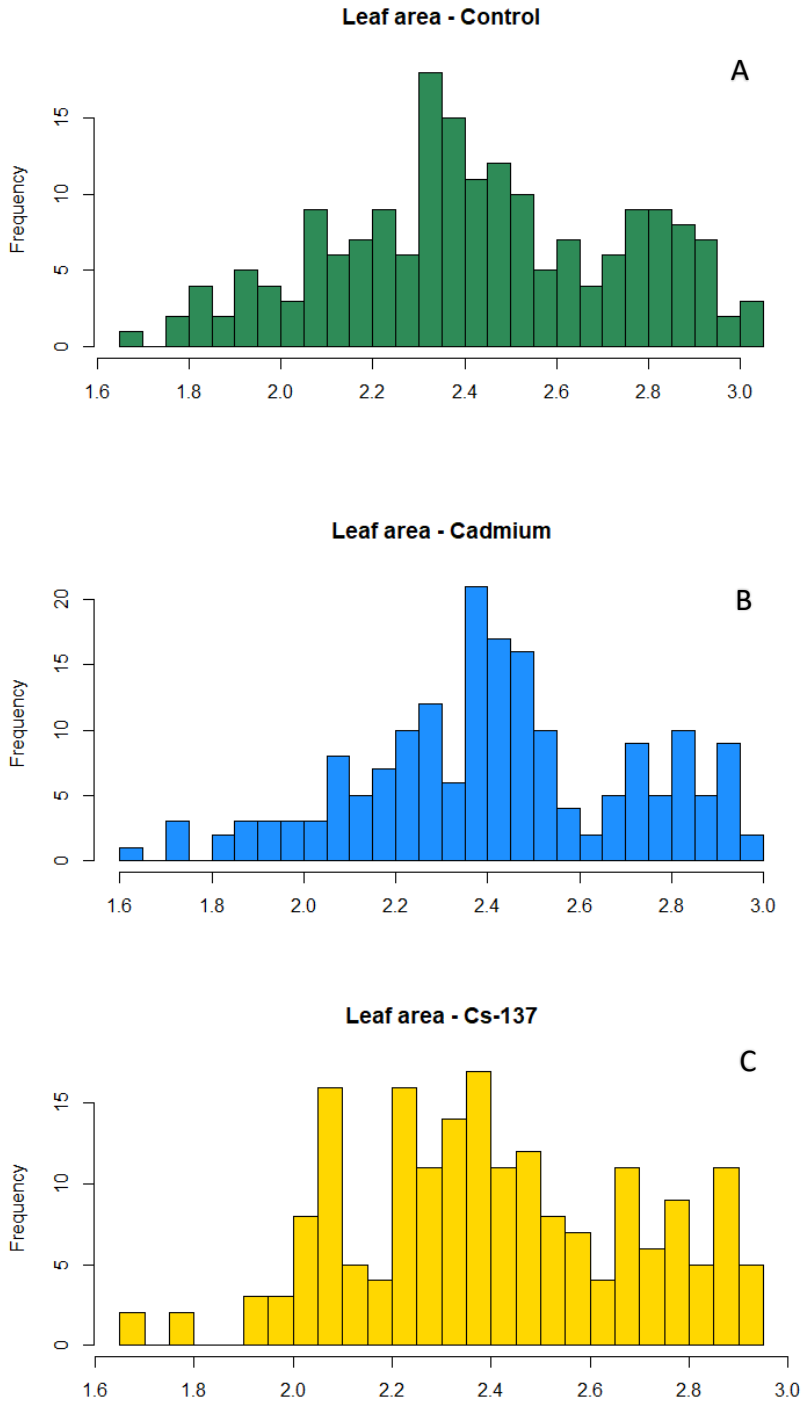

Fig. 3.26. Distribution of leaf area measurements in generation 6 (G6) individual samples for each treatment group. (A = negative control, B = positive control and C = Cs-137 treatment. The x axis indicates leaf area measurements in mm2 while the y axis displays the frequency of samples that fall into each measurement. From the

shape of the histograms it is apparent that there is a spread of measurements ranging from 1.6 mm2 to 3.0 mm2. (Control n= 206, positive control n= 193, Cs-137 n=180).

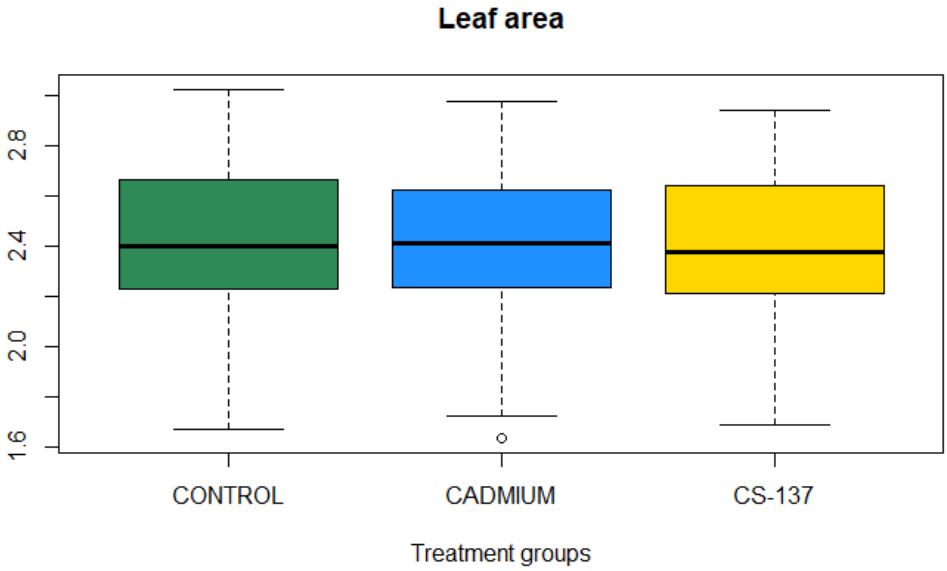

Fig. 3.27. Boxplot of generation 6 (G6) showing data overlaps and outliers across all sample groups for leaf area. The scale is identical to the scatter plot but displays outliers and data overlaps more clearly. The range of leaf area is displayed on the y axis in mm2. (Control n= 206, positive control n= 193, Cs-137 n=180).

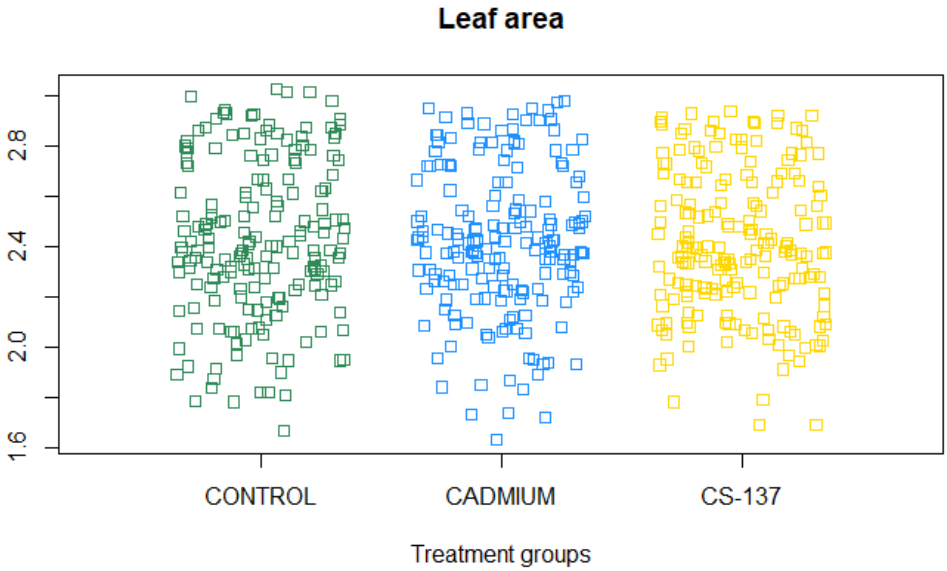

Fig. 3.28. Scatter plot of generation 6 (G6) leaf area data displaying all individual data points across all treatment groups. The y axis displays leaf area in mm2. The denser

the cluster of points the higher the frequency of samples pertain to a particular size or range of sizes. (Control n= 206, positive control n= 193, Cs-137 n=180).

Like the previous generation, logged data was used in generation 6 for data handling purposes and to achieve fewer skewed results. Bartlett's test was used to examine the data for homogeneity of variance. This test is sensitive towards departures from normality. Data was then used in an ANOVA and no significant differences were detected in the variance between groups.

3.3.2.4 Generation 7 (G7)

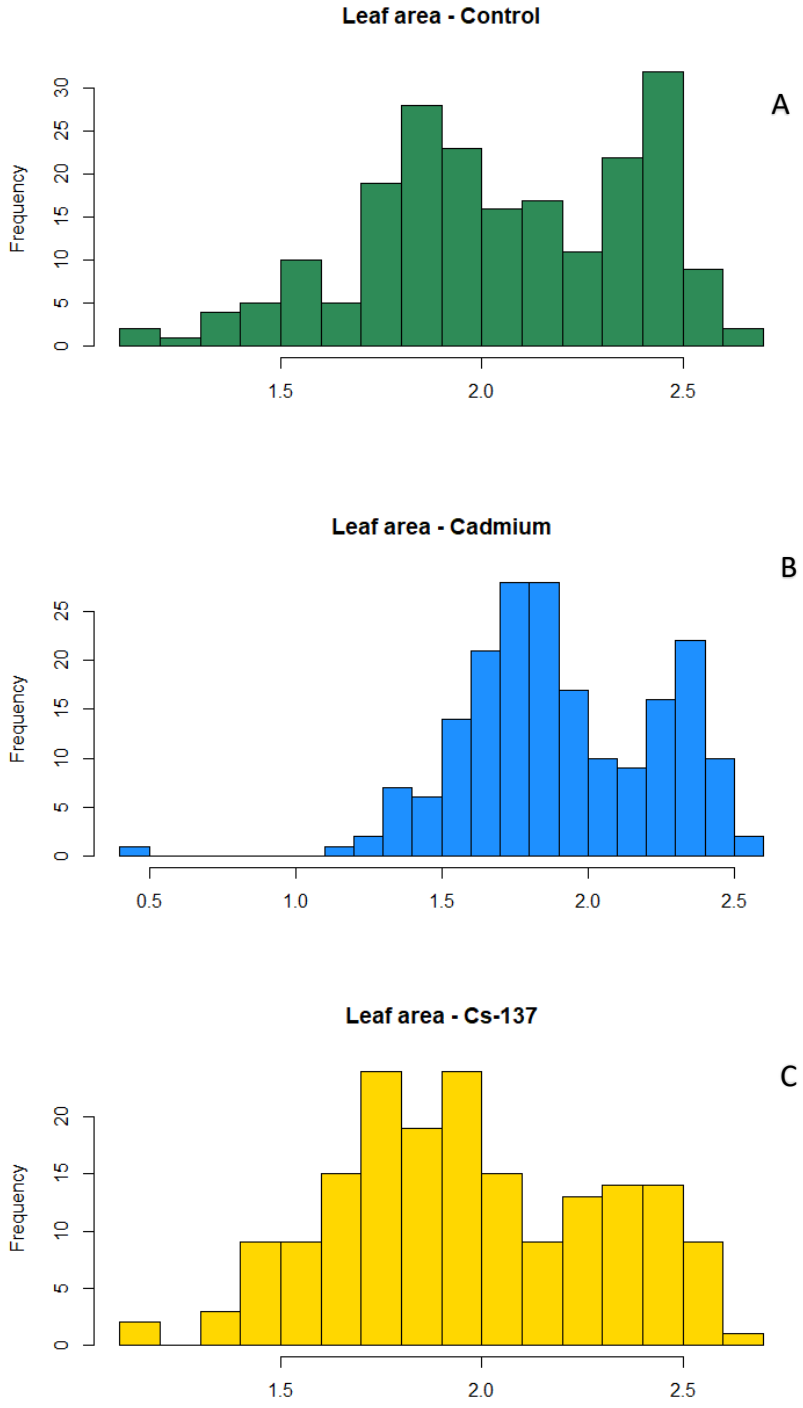

Fig. 3.29. Distribution of leaf area measurements in generation 7 (G7) individual samples for each treatment group. (A = negative control, B = positive control and C = Cs-137 treatment. The x axis indicates leaf area measurements in mm2 while the y axis displays the frequency of samples that fall into each measurement. From the shape of the histograms it is apparent that there is a spread of measurements ranging from 0.5 mm2 to 3.0 mm2. (Control n= 206, positive control n= 193, Cs-137 n=180).

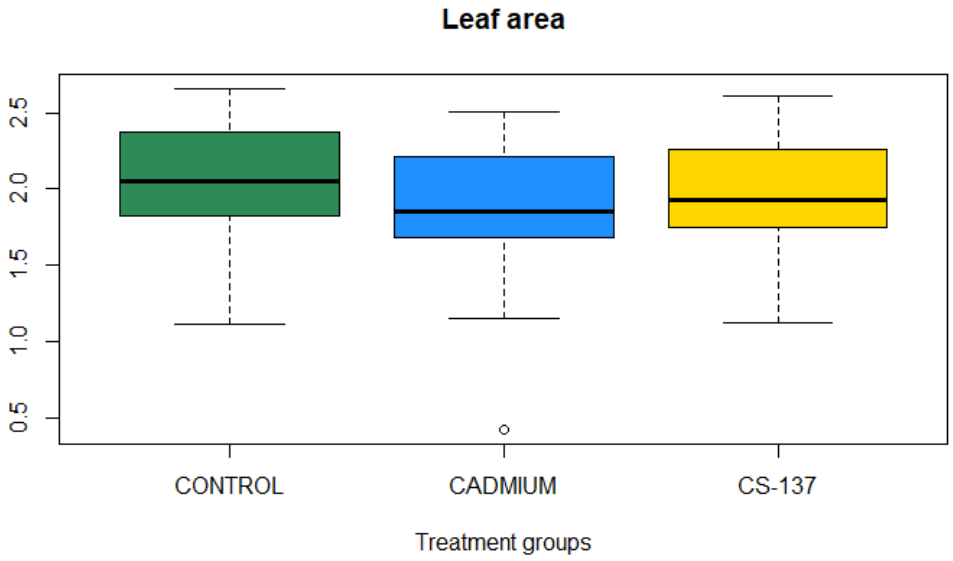

Fig. 3.30. Boxplot of generation 7 (G7) showing data overlaps and outliers across all sample groups for leaf area. The scale is identical to the scatter plot but displays outliers and data overlaps more clearly. The range of leaf area is displayed on the y axis in mm2. (Control n= 206, positive control n= 193, Cs-137 n=180).

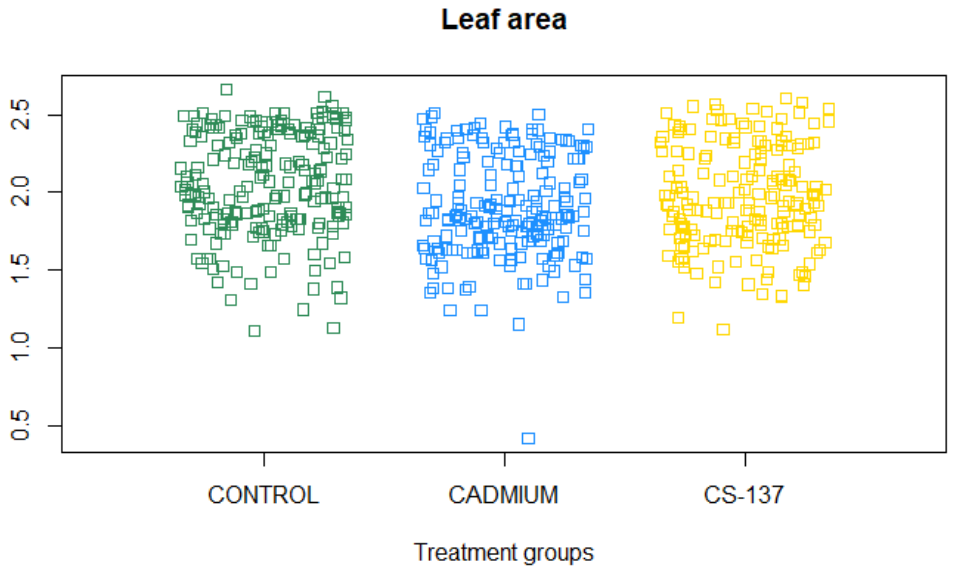

Fig. 3.31. Scatter plot of generation 7 (G7) leaf area data displaying all individual data points across all treatment groups. The y axis displays leaf area in mm2. The denser the cluster of points the higher the frequency of samples pertain to a particular size or range of sizes. (Control n= 206, positive control n= 193, Cs-137 n=180).

Logged data was used in generation 7 and a Bartlett's test was use to assess homogeneity of variance. The test is sensitive to departures from normality. Data was used in an ANOVA for generation 7 which yielded a significant result for differences in the variance between groups. This significance was pinpointed as being between the negative control and treatment, and the negative control and positive control through Welch two sample t-tests. No differences were detected between the positive control and Cs-137 treatment.

Table 3.1 The instances of statistical significance for leaf morphometric endpoints in A. thaliana plants grown for 7 generations with the last four generations including exposure to Cs-137.

Generation	Vertical symmetry	Leaf area
2nd (G4)	Pos control sig dif. from other groups	Pos control and Cs-137 sig dif from other groups
3rd (G5)	Pos control and Cs-137 sig dif from other groups	No differences between treatment groups
4th (G6)	No differences between treatment groups	No differences between treatment groups
5th (G7)	No differences between treatment groups	Pos control and Cs-137 sig dif from other groups

Chapter 4: Physiological and Epigenetic Traits of Arabidopsis thaliana Chronically Exposed to Low Dose Ionising Radiation

4.1 Introduction

As visited in Chapter 1, IR through the radiolysis of water ROS are generated which impact the antioxidant system of a plant, and a high enough dose of IR can overload the system by flooding it with ROS. Measuring glutathione is one of the antioxidant parameters that can provide an outlook on how a plant's antioxidant system is coping with (or failing to manage) an influx of ROS generated by exposure to IR. It is important to reiterate here that if exposure to IR at the given dose rates in this experiment showed little or no effect on GSH concentrations then the antioxidant system could be perceived to have the capacity to function normally with no detrimental impact. Therefore, it is possible to ask whether certain doses impact the antioxidant system at all.

4.2 Materials and methods

4.2.1 Glutathione assay

Total glutathione was measured first in *Trifolium* treated with H_2O_2 using a glutathione assay kit (Sigma Aldrich CS0260). The protocol had to be optimised for use in plant leaf samples by modifying the dilution factor (of sample) to stay within a detectable range by omitting the dilution step in the protocol. Once successful measurements were taken, the protocol was then used on *A. thaliana* samples from each generation exposed to radioactivity, cadmium positive controls and negative controls. The concentrations were measured via a kinetic read on a plate reader at 412 nm. The results yielded low concentrations of glutathione, however, when compared to other literature (Cheng *et al*. 2015) concentrations were slightly below control samples in an

experiment with drought stressed plants. The drought stressed plants exhibited higher concentrations of glutathione but upon examining the images provided they were highly stressed/shocked almost to the point of death. The data was input into a well-established model by Smith *et al*. (2012) and showed good agreement in that at doses examined in this experiment, hardly any effect on redox poise was to be expected.

To determine GSH concentration in leaf samples, frozen leaves were harvested from *A. thaliana* grown in soil spiked with Cs-137 (see 2.2.3 Exposure of *A. thaliana* over multiple generations to chronic ionising radiation). Four plants from each generation and treatment group were analysed. The leaves were snap frozen in liquid nitrogen immediately after excision and stored at -80 °C. Leaf samples were prepared using sample preparation instructions in Sigma Aldrich (CS0260) assay technical bulletin and further optimised for use in plants as the assay was not explicitly designed for plant use (e-mail contact with a Sigma Aldrich technical representative was established for confirmation of this). Frozen leaves were ground to as fine a powder as achievable using a pestle and mortar chilled in liquid nitrogen. Liquid nitrogen was added to the sample frequently to avoid thawing from heat generated through the grinding process. One hundred mg of powder was used for each sample, deproteinised using 0.3 ml 5% 5-sulfosalicylic acid (SSA), centrifuged at 18,000 RPM for 10 minutes in a temperature-controlled centrifuge. Remaining supernatant measured 0.5 ml and was used in the final analyses. Treatment groups were analysed independent of generational differences.

Ten µL of each sample was used in a 96-well plate kinetic read assay (Sigma-Aldrich CS0260 technical bulletin). The procedure summary was as follows:

The biological sample was first deproteinised with the 5% 5-Sulfosalicylic Acid Solution, centrifuged to remove the precipitated protein, and then assayed for glutathione (see Appendix, Sample Preparation). The measurement of GSH used a kinetic assay in which catalytic amounts (nmoles) of GSH cause a continuous reduction of 5,5'-dithiobis(2-nitrobenzoic acid) (DTNB) to TNB and the GSSG formed is recycled by glutathione reductase and NADPH. The GSSG present also reacts to give a positive value in this reaction:

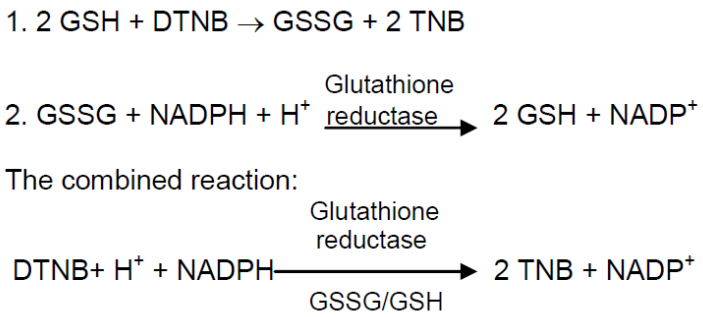

The reaction rate is proportional to the concentration of glutathione up to 2 µM. The yellow product, 5-thio-2-nitrobenzoic acid (TNB) is measured spectro-photometrically at 412 nm. The assay uses a standard curve of reduced glutathione to determine the amount of glutathione in the biological sample..

A dilution step was originally recommended for the sample preparation, in order for the samples to stay within a detection range of GSH standards but as the concentrations of the plant samples was low to very low, this step was not necessary. This was checked with Sigma-Aldrich (now Merck) who admitted that the protocol was not specifically geared towards plant tissue extract and there was no issue with optimising the detection range/dilution factor. The GSH standards were therefore also modified for a more fitting detection range for samples- The most concentrated

standard was halved from the recommended 50 µM concentration to 25 µM which complemented the sample results.

4.2.2 DNA methylation

Seeds from the first two generations of *A. thaliana* exposed to IR in this project were sent to the Belgian nuclear research centre SCK-CEN in Mol, Belgium for analysis. Nineteen samples were grown using a protocol from Vanhoudt *et al*. (2014) under control conditions for three weeks and DNA methylation rates were analysed using methods described in Volkova *et al*. (2018).

4.2.3. Statistical Analyses

When appropriate the Shapiro-Wilkes test of normality was applied to data. A oneway ANOVA was used to test for differences between the three treatments. Details of the overall statistical approach and of particular protocols are provided in Annex A and Annex B respectively.

4.3 Results

4.3.1 Glutathione assay

The glutathione assay results show individual data points across all treatment groups (Fig. 4.1) and the boxplot (Fig. 4.2) visualises the minimum, lower quartile, median, upper quartile and maximum values with outliers. Both figures used the same data and all samples fell within a similar range. The data represents all generations and all

treatment groups. It was not necessary to compare generations as the data across all treatment groups fell within a similar range.

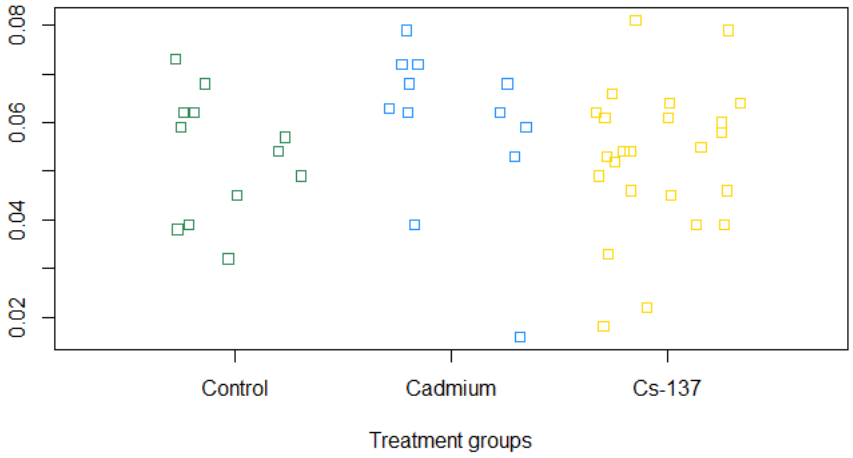

Fig. 4.1. Individual data points for absorbance measured from kinetic read assay at 412nm across all treatment groups for A. thaliana. Measurements along the y axis are absorbance values (ΔA/412nm) and treatment groups are differentiated across the x axis.

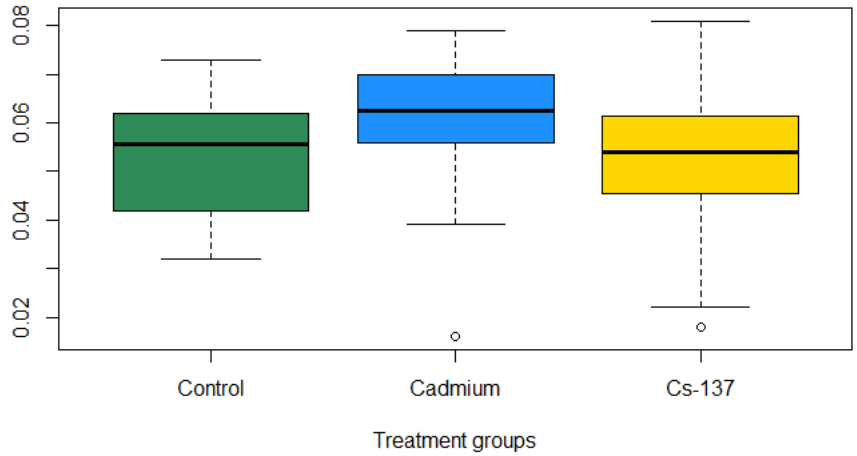

Fig. 4.2. Boxplot to demonstrate clear data overlaps and subtle differences in absorbance measurements for the positive control group compared to the negative control and Cs-137 treatment group. Measurements along the y axis are absorbance values (ΔA/412nm) and treatment groups are differentiated across the x axis.

From the boxplot a substantial amount of overlap in values is evident. Average values were plotted against a standard curve to determine GSH concentration in all treatment groups (Fig. 4.3) with data overlaps shown clearer in Fig. 4.4. Both sets of data (individual and pooled average) were examined using student's t-tests in R Studio. No significant differences between treatment groups was detected.

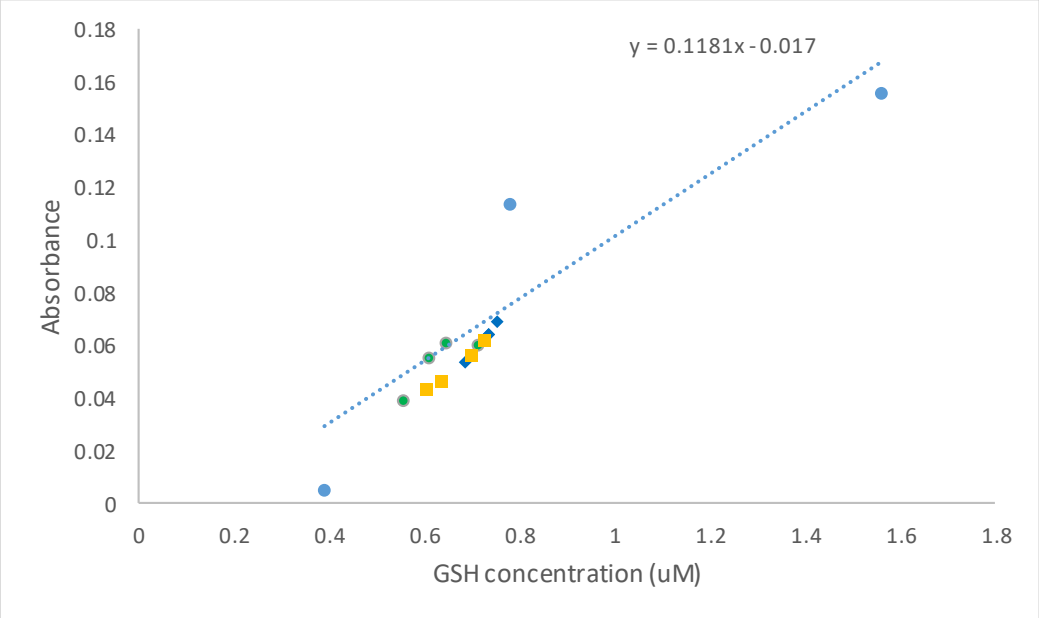

Fig. 4.3. Average concentrations of samples across all treatment groups. All of the groups appeared in a similar range of GSH concentrations (denoted on x axis in µM) when plotted against a GSH standard. Measurements on the y axis are absorbances (ΔA/412nm).

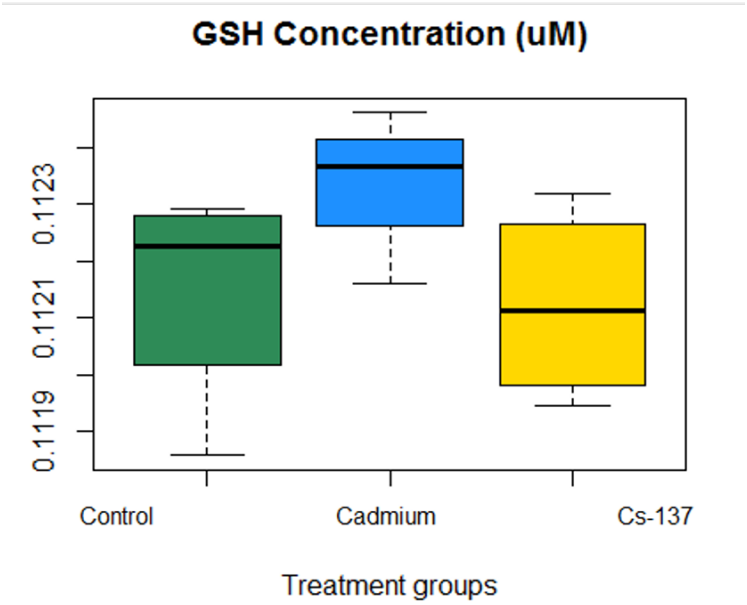

Fig. 4.4. Boxplot to demonstrate clear data overlaps and subtle differences in the average GSH concentrations (positive control group compared to the negative control and Cs-137 treatment groups). Measurements along the y axis indicate GSH concentrations (µM) and treatment groups are displayed across the x axis.

4.3.2. Redox model

Redox potential, Eh (volts) will change when ROS saturate a cell and trigger an antioxidant response: The amount of glutathione (GSH) decreases due to its transition from the reduced state to an oxidised state (GSSG). This potential can be quantified by considering the concentration of GSH present and used to calculate the effects of environmental stressors such as IR. A model developed by Smith *et al*. (2012) uses a series of calculations to predict the effect that dose rate has on redox potential. Figure 4.4 shows a scenario where a low dose rate (0.01 mGy/d) (with a GSH concentration of 0.1 uM as per the experiment results in 4.4.1) has virtually no effect on redox potential. Even at three orders of magnitude (up to 1 mGy/d) the model predicts little change in redox due to oxidants produced by radiolysis of water.

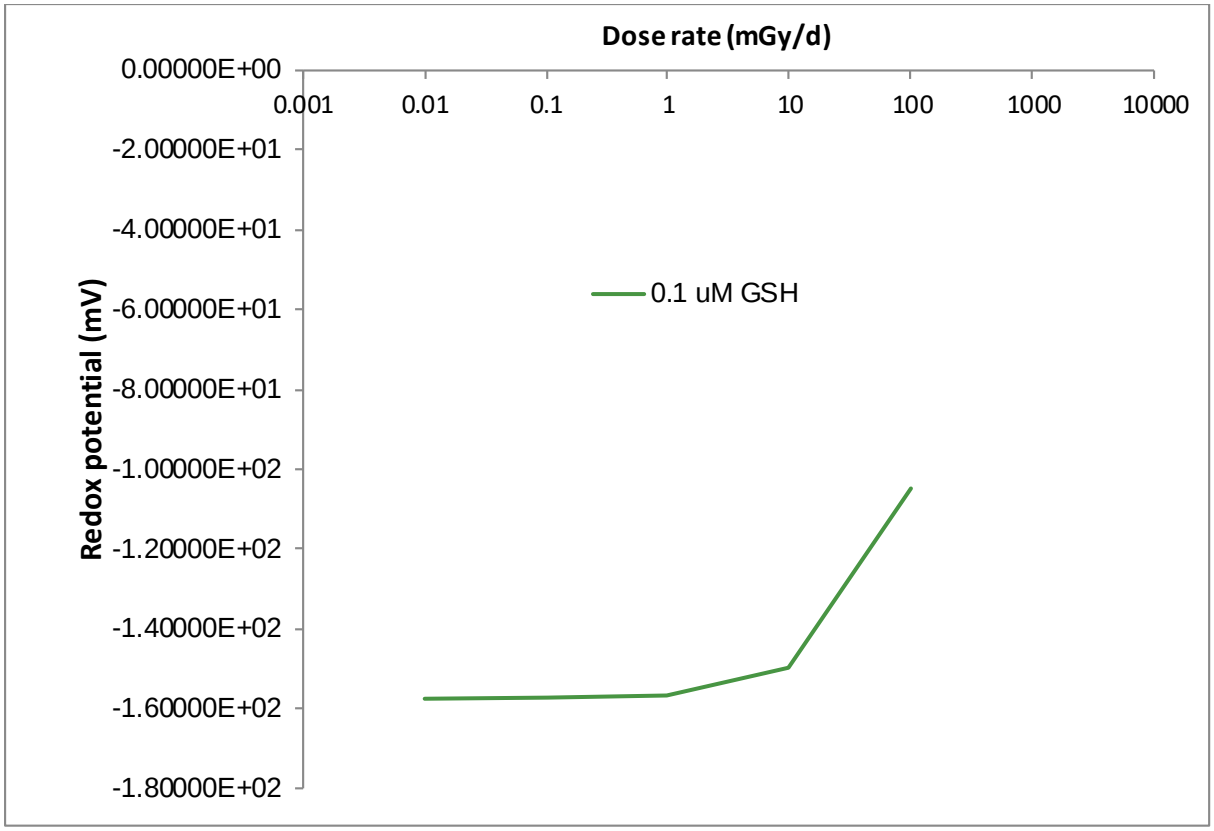

Fig. 4.4. Data from section 4.3.1 was plotted from values estimated using a model constructed by Smith et al. (2012) and shows the effect that doses of ionising radiation is predicted to have on GSH concentration has on overall redox potential (Eh) assuming that radiolysis products direct oxidise GSH and that GSH concentrations set redox potential (as per the Nernst equation). The calculations showed that there was virtually no change in redox potential up to three orders of magnitude greater than the dose rate that the experiments reported here were exposed to (0.01 mGy/d).

4.3.3 DNA methylation

An ANOVA test was used on the DNA methylation data, despite the small sample size (n = 19). A significant difference was found (F ratio = 8.664, P value = 0.0047 at 95% confidence interval) between the groups and this was in good agreement with the box plot in Figure 4.5. The results show that there was a decreased rate of DNA methylation in samples exposed to Cs-137 when compared to negative control plants, and the same trend occurred in the positive control (cadmium exposed plants) when compared to negative control plants.

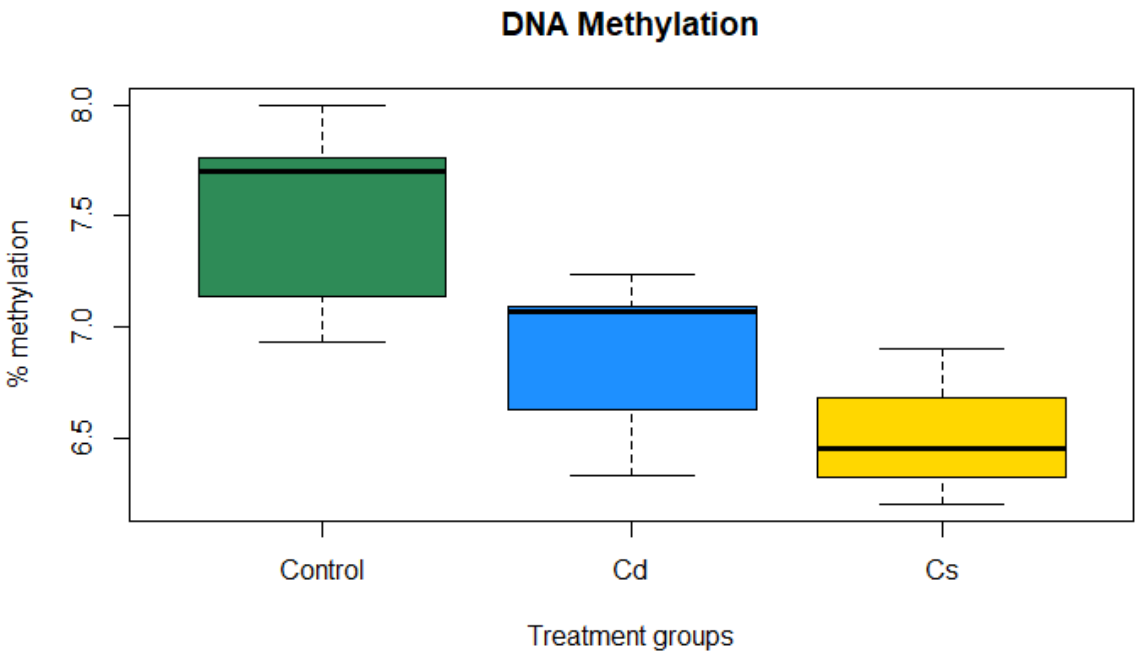

Fig. 4.5. Box plot of percentage methylation between treatment groups displaying data differences and overlaps. NB: Cs = Cs-137.

Chapter 5: Cosmic Radiation and its Effects on Plants

5.1 Re-exposure of plants to doses of radiation comparable to doses on the ISS

NASA hypothesised that exposing seeds to radiation on the ISS could help to identify those with radioresistant traits. Re-exposure of plants grown from ISS seeds might identify those with an epigenetic memory of exposure to radiation, and upon germination this might lead to altered gene expression to give radioresistant traits, perhaps based on adaptation mechanisms such as reduction of DNA damage to plant cells. This epigenetic (without DNA mutation) altering of gene expression is described by Boyko and Kovulchuk (2008) as a short-term strategy for plant stress response. To test the hypothesis that plants previously exposed to radiation on the ISS can have altered responses to IR, experiments reported here re-exposed seeds flown on the ISS to doses of radiation comparable to doses detailed in section 1.5.7. Uptake of radioisotopes, morphology and general growth were examined in these plants.

5.2 Materials and Methods

5.2.1 Exposure of *Eruca sativa* and *Solanum lycopersicum* to cosmic radiation aboard the ISS

Seeds from *Eruca sativa* (rocket) were launched on 2rd September 2015 from Baikonur, Kazakhstan on the Soyuz TMA-18M which reached the ISS on the 4th September 2015 and returned to Earth on the 2nd March 2016 (Kazakh steppe landing). During the 6-month stay aboard the ISS, the seeds remained dry in packaging. Control seeds from the same experimental batch also remained dry and in packaging on Earth. These seeds were received in the laboratory at UWE directly from

the Royal Horticultural Society's Schools Gardening project coordinators on 16th April 2016. *Solanum lycopersicum* (tomato) seeds that had been aboard the ISS for 39 days during July-August were also received in dry packaging in November 2017. These were obtained from the Tomatosphere project, run by the Canadian Space Agency in November 2017. Upon receiving the seeds at the laboratory they were immediately placed in a refrigerator at 4°C.

5.2.2 Seed viability

Simple germination tests were carried out on *Eruca sativa* seeds by placing 11 (maximally due to small number of samples available for test) dry seeds on a single disc of specialist textured paper (one per experiment group) (Anchor Paper Company) moistened with tap water (Fig. 5.1). Germination was measured after three days by counting. Any sign of radicle emergence was reported as a successful germination. An increased number of replicates would have been desirable for more statistically robust data and in hindsight the paper-germinated seedlings could have been transplanted. However, as early growth in response to radiation exposure was a key line of inquiry this could have potentially interfered with data. Tomato seeds were therefore not subjected to germination tests to avoid this issue and maximise sample number.

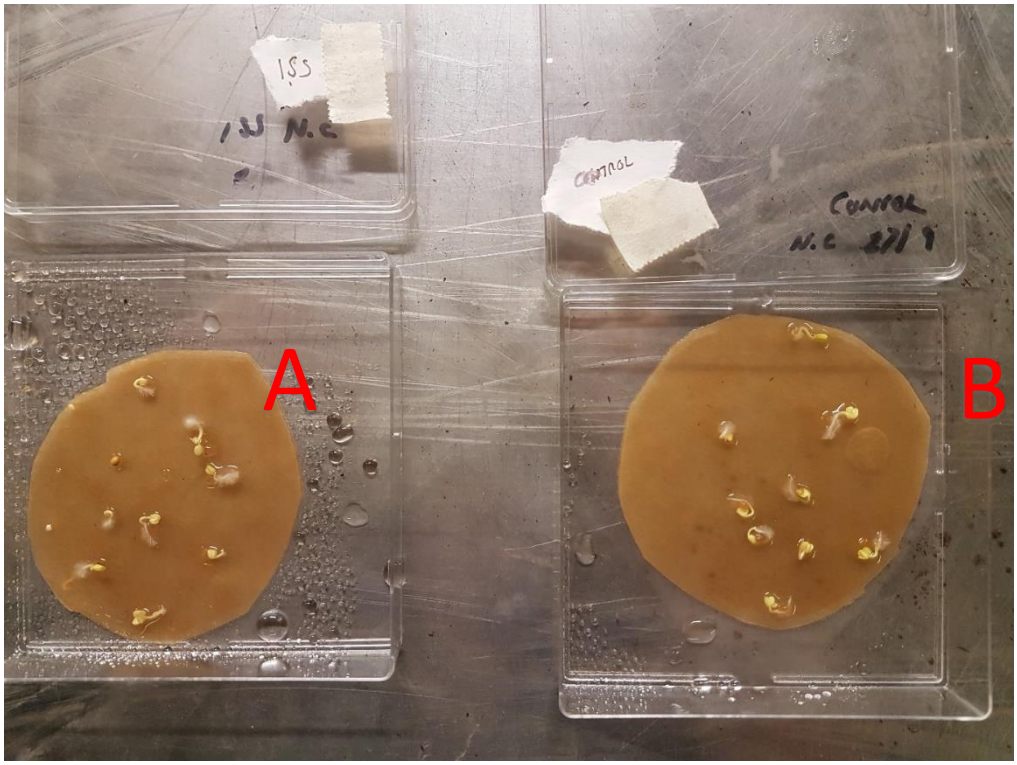

Fig. 5.1. An example of germinated seeds of rocket on wetted specialist germination paper. (A) Rocket seeds from the ISS (B) Control seeds that remained on Earth.

5.2.3 The re-exposure experiment

The primary aim of the re-exposure experiment was to test if exposure to cosmic radiation aboard the ISS (as seeds) influenced general growth and uptake of radionuclides in adult plants grown from the seeds of *E. sativa* in the presence of elevated radiation (at a similar dose) from Cs-137. Eight containers were arranged in a growth cabinet at identical settings as outlined in chapter 2. Half of the containers were filled with Levington's F2+S compost spiked with 90 kBq/kg Cs-137 (which provided a dose of *c*.35 µGy/h) (as detailed in chapter 2) while the remaining containers only contained compost (Levington's F2+S). *Solanum lycopersicum* (tomato) seeds that had been aboard the ISS for 39 days during July-August were grown in identical conditions.

5.2.4 Experiment configuration

Configuration was as follows:

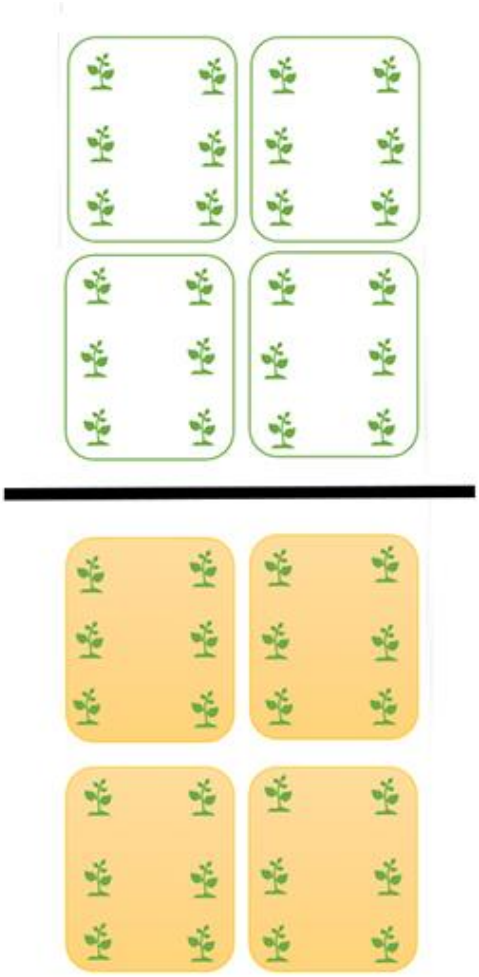

- Container with soil spiked with 90 kBq/kg Cs-137 (dose rate *c.*35 µGy/h)

- Container with control soil

- *Eruca sativa*

- Lead shielding (50mm thickness)

Container contents:

6 x *Eruca sativa* plants (control) in control compost	6 x *Eruca sativa* plants (ISS) in control compost
6 x *Eruca sativa* plants (control) in control compost	6 x *Eruca sativa* plants (ISS) in control compost
6 x *Eruca sativa* plants (control) in compost spiked with *c.*35 µGy/h Cs-137	6 x *Eruca sativa* plants (ISS) in compost spiked with *c.*35 µGy/h Cs-137
6 x *Eruca sativa* (control) plants in compost spiked with *c.*35 µGy/h Cs-137	6 x *Eruca sativa* plants (ISS) in compost spiked with *c.*35 µGy/h Cs-137

Containers were rotated around the cabinet to minimise risk of spatial bias due to potential differences in the microenvironment.

An identical experiment was run in parallel with tomato seeds:

6 x *Solanum lycopersicum* plants (control) in control compost	6 x *Solanum lycopersicum* plants (ISS) in control compost
6 x *Solanum lycopersicum* plants (control) in control compost	6 x *Solanum lycopersicum* plants (ISS) in control compost
6 x *Solanum lycopersicum* plants (control) in compost spiked with *c.*35 µGy/h Cs-137	6 x *Solanum lycopersicum* plants (ISS) in compost spiked with *c.*35 µGy/h Cs-137
6 x *Solanum lycopersicum* (control) plants in compost spiked with *c.*35 µGy/h Cs-137	6 x *Solanum lycopersicum* plants (ISS) in compost spiked with *c.*35 µGy/h Cs-137

5.2.5 Morphometric analysis of leaves

The Doxie flip scanner (detailed in chapter 3) was used to scan rocket leaves for morphometric analyses which measures prescribed morphological characteristics of in-tact excised leaf matter. Parameters examined were leaf vertical symmetry (and any deviations from perfect symmetry) and total leaf area. Morphometric analyses were discarded after too few leaves were successfully scanned and the data pool not large enough for robust analysis. This was due to an elevated level of curl (typical of mature rocket leaves) against the scanner surface. This curling was not considered a measurable effect due to the fact that it occurred throughout every sample regardless of control group, it was a naturally occurring characteristic unfavourable for scanning (unlike *A. thaliana* leaves).

5.2.6 Leaf gamma count

A gamma counter (1282 CompuGamma by LKB-Wallac) was used to measure gamma radiation emitted by Cs-137 in leaf samples. Samples were prepared for gamma counting by first drying for 24 hours in an oven. They were then transferred to boiling tubes and ground to a powder using a homogeniser. Sample weights were recorded after the powdered leaves were transferred to glass gamma counter tubes. Tubes were sealed with a plastic lid and counted immediately following preparation. Gamma count windows were checked for accuracy with the radiation protection supervisor.

Counts were calculated from standard “USN 53” received by the department at UWE Bristol in August 1977 and checked on 11/10/2016. The initial activity of the source

was 4.51 kBq (270,600 CPM) using a decay factor of 0.4062. Counts per minute (CPM) from the standard on 11/10/2016 was 83278 CPM.

Thus,

83278/4.51 = 18465 CPM/kBq

Then, to calculate kBq in samples against the standard:

CPM/18465 = kBq

5.2.7 Root development

A straightforward test was carried out to examine if spaceflight and consequent radiation exposure during a stay on the ISS influenced root length. Tomato and rocket seeds from each group (ISS flown vs control that remained on Earth) were first sterilised in 70% ethanol for two minutes followed by commercial thin household bleach (NaClO, 50%) for another two minutes. Seeds were rinsed a total of five times. Half-strength MS media was poured into square petri dishes, set and scored with a sterile blade a quarter of the way from one edge. This was to mark a point for the placement of seeds for comparison of length. A mark was drawn on the petri dish lid to separate two sides of the petri dish, so that treatment groups could be studied side-by-side (Fig. 5.2). Seeds were sown on the agar surface, petri dish lids applied and wrapped in parafilm® to prevent contamination but allow for gas permeability. Petri dishes were kept in a growth cabinet under identical conditions as in all the previous experiments in the growth cabinet, except for humidity which was decreased to the cabinet minimum (50%) as watering was not needed. Petri dishes were laid equally

spaced apart and flat. Once germination had occurred, the root zone was covered in high-density silver foil to minimise light penetration and to simulate a light gradient as in the field with soil root zones. The containers were also rotated so that they stood upright and roots could navigate downwards with gravity while the cotyledons remained in the light. This was the same technique as employed for the *A. thaliana* root development study detailed in chapter 2. Foil root shielding was removed from petri dishes and plants were photographed *in situ* 11 days post-germination (Fig. 5.3).

Fig. 5.2. Top-down view of petri dish with seedlings growing in half strength MS agar. A bold line was drawn across the petri dish lid to aid seed placement and comparison when growing two treatment groups side-by-side. This example shows control (left) and ISS (right) seedlings against a centimetre scale. The dark background assisted with root identification during image analysis.

ImageJ was used to quantify root length and statistical analysis was carried out in RStudio.

Fig. 5.3. View of 12-day old rocket seedlings growing in half-strength MS agar against a centimetre scale, with control seedlings to the left and ISS seedlings to the right. Roots to the right formed before containers were rotated vertically, hence the growth towards the "top" of the container. Once rotated, the roots grew downwards with gravity and into darkness where the root zone was covered with high-density silver foil.

5.2.8. Statistical Analyses

Shapiro-Wilkes test for normality was applied as appropriate and t-tests were used for testing for differences between the two treatments – those plants grown from seeds that had gone into space and those that had not. Details of the statistical approach and of protocols are provided in Annex A and Annex B respectively.

5.3 Results

5.3.1 Seed viability through germination tests

Rocket seeds that had flown on the ISS did not germinate at the same rate as control seeds (81.8% germination in space flown seeds compared to 100% germination in control seeds). However, due to the limited sample size, available germination tests were only carried out on a small number of seeds (n = <11).

5.3.2 Morphometric analysis of mature tomato leaves grown from seed flown on the ISS

Tomato plants that had been grown from seed and completed their life cycle in Cs-137 spiked soils were harvested for leaves, and scanned in an identical protocol to *A. thaliana* as detailed in chapter 3. Vertical symmetry was assessed in leaves excised from plants grown from seeds exposed to space conditions and control (Earth) conditions (Figure 5.4).

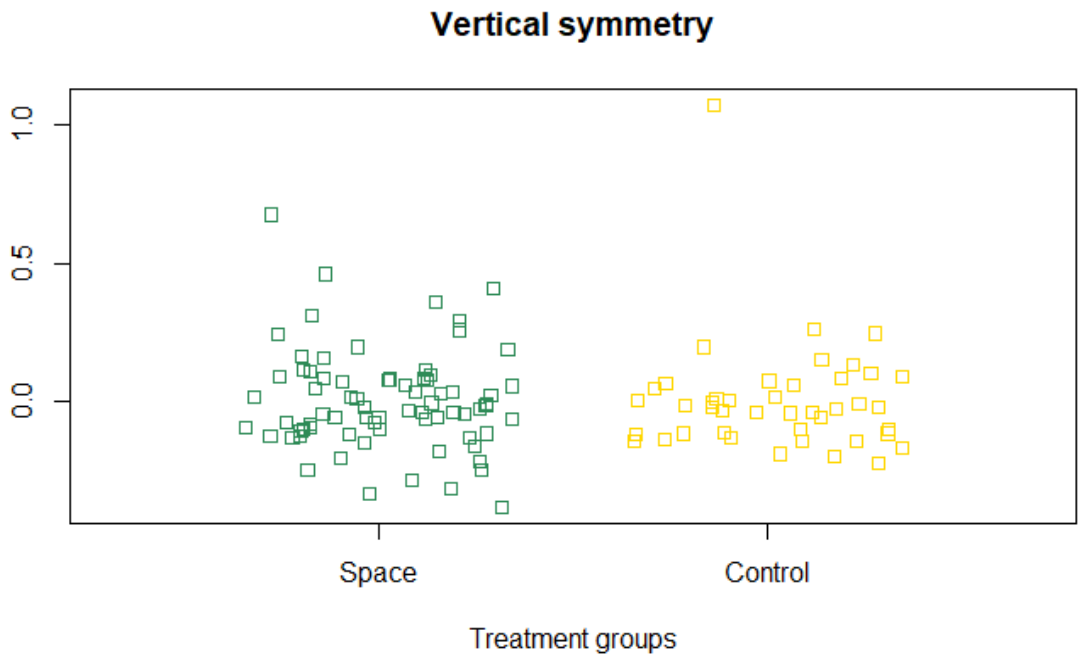

Fig. 5.4. Scatter plot of individual leaves from tomato plants across two treatment groups, space (for plants grown from seeds flown on the ISS) and control (for plants grown from control seeds that remained on Earth) and grown in Cs-137 spiked soils. The y axis indicates the treatment group and the x axis denotes measurement of vertical symmetry, where 0.0 is perfect symmetry and negative values indicate dominant asymmetry to the left of a leaf (when viewed as a 2-dimensional scan) and

positive values indicate the same phenomena to the right. The denser the cluster of data points the higher the frequency of leaves that share similar symmetrical properties. Outliers are also visible in the data.

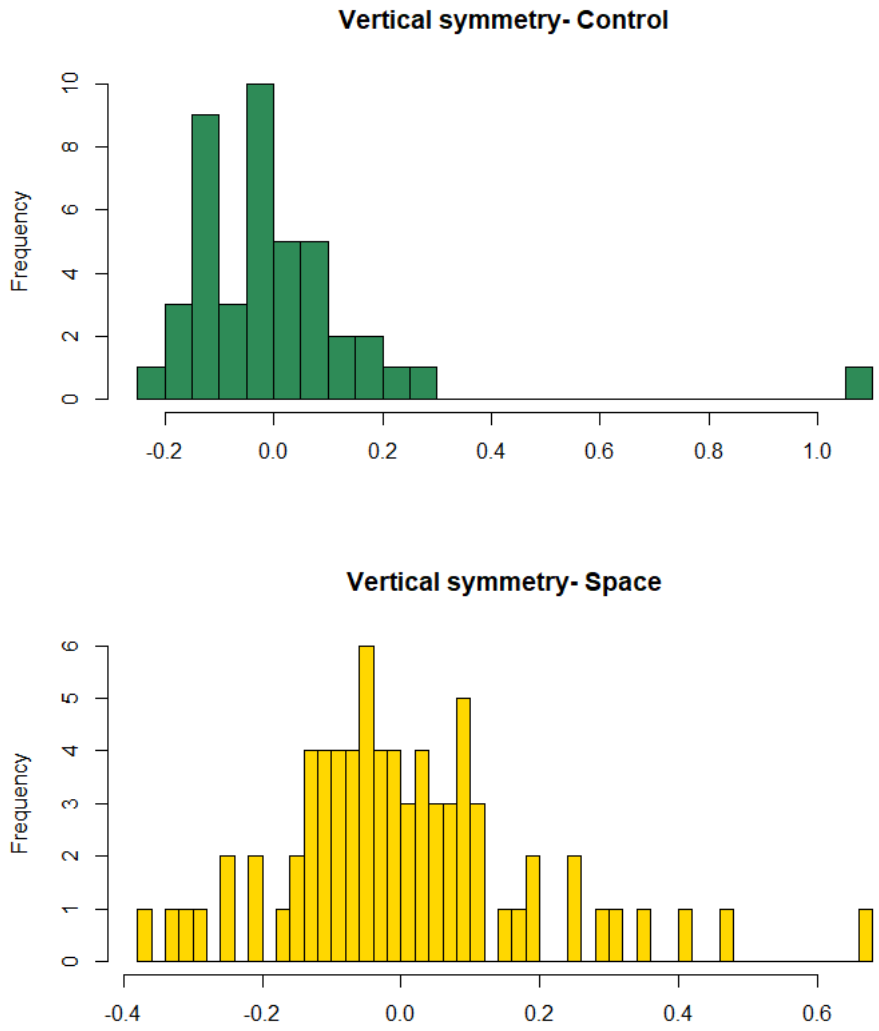

Fig. 5.5. Vertical symmetry measurements in leaf samples from mature tomato plants grown from seeds flown on the ISS. Distribution of data were essentially normal with few outliers in both treatment groups. The x axis indicates symmetry measurements (0.0 = perfect vertical symmetry) and departures from perfect symmetry to the left and to the right of a 2-dimensional scan. The y axis denotes frequency of sample occurrences in relation to symmetry measurements. The total number of control samples re-exposed to Cs-137 was lower than the samples that had flown in space and re-exposed to Cs-137 spiked soil.

Distribution of samples was normal with the exception for an outlier in each of the treatment groups (Figure. 5.5). T-tests found no significant difference between treatment groups (P value = 0.9711 at 95% level of significance).

5.3.3 Gamma counts as a measure of Cs-137 accumulation from soil in mature leaves of rocket and tomato plants

Dry, powdered samples of rocket and tomato leaves from each treatment group, including controls, were analysed using a gamma counter (Compugamma LKB-Wallac 1282). Results were given in counts per minute (available in supplementary data section) and activity concentrations in becquerels per gram (Bq/g) were calculated using the formula:

KBq Cs-137 = CPM/18465

Ans*1000 = Bq Cs-137 /wt

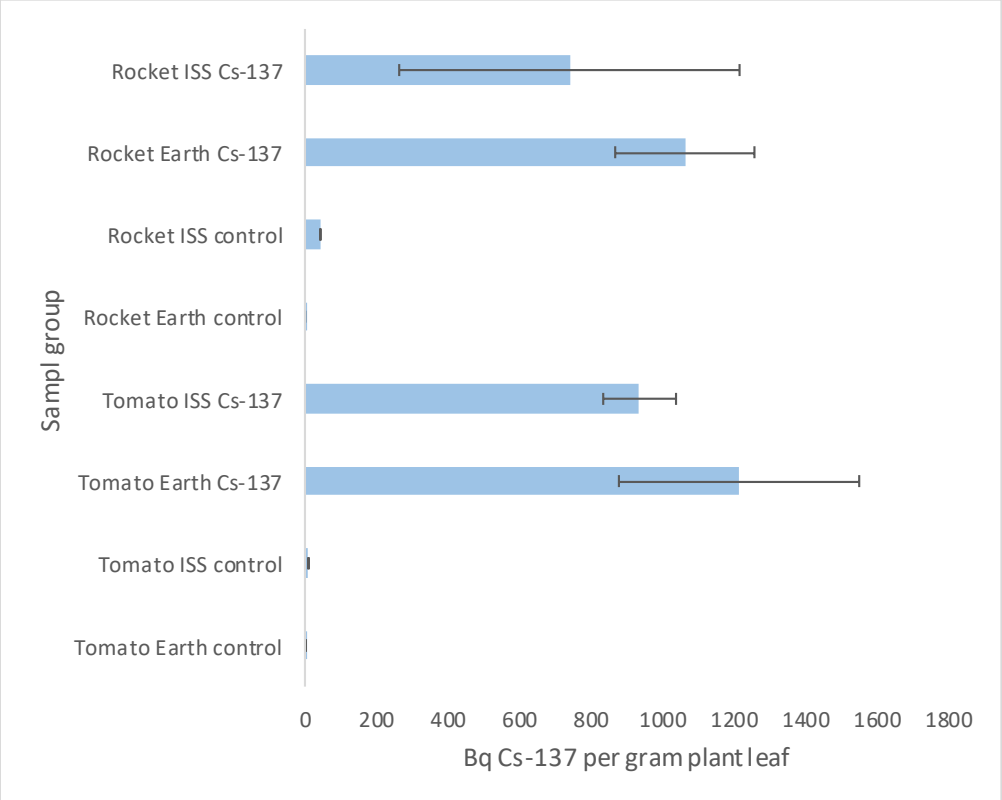

Fig. 5.6. Mean Cs-137 activity concentration across all treatment groups. The y axis displays sample groups and the x axis denotes Bq Cs-137 per gram plant leaf. Standard error bars are also shown. Raw data available in supplementary information.

The preliminary results (expressed with standard error bars in Figure 5.6) from the gamma counting showed that plants grown from seeds flown on the ISS and re-exposed to a similar dose of radiation accumulated less Cs-137 in leaves than plants grown from control seeds that remained on Earth. However, statistical tests (Welch two sample t-test) showed that there were no significant differences between the groups (P = 0.2 – 1 across all paired combinations at 95% confidence interval). A large variance in activity concentration occurred most likely due to sample size.

5.3.4 Root image analysis

The relatively small number of samples (around 20 roots per analysis group) resulted in a data distribution that was not precisely normally distributed, yet not overly skewed. The distributions of both treatment groups were compared using a quantile-quantile plot (Fig. 5.8) and showed that both distributions were similar. Based on these observations t-tests were applied.

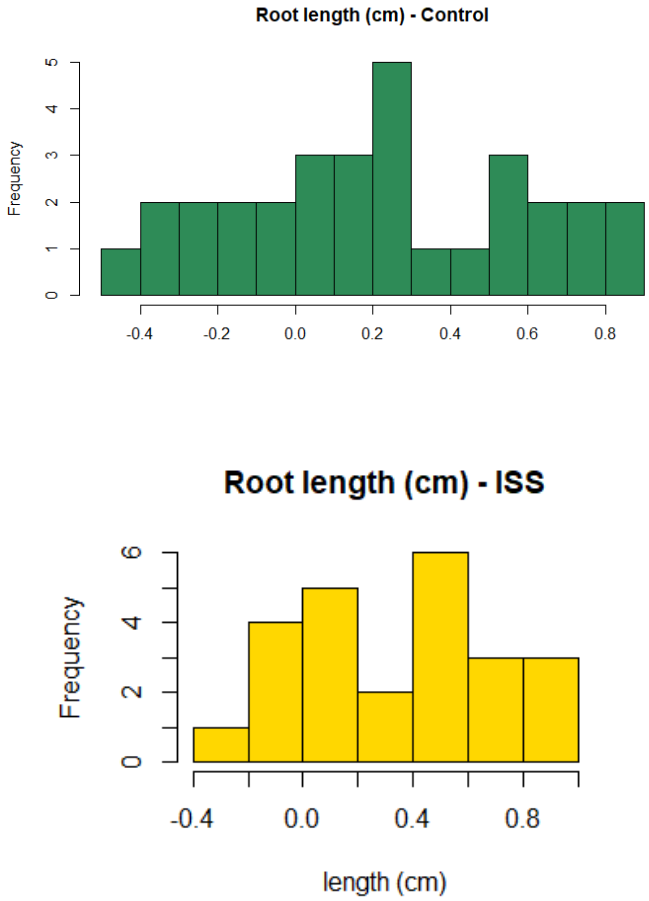

Fig. 5.7. Histograms of root length data for control rocket plants (green) and rocket plants grown from seeds flown on the ISS (yellow). The values on the x axis denote length in cm transformed to log base 10.

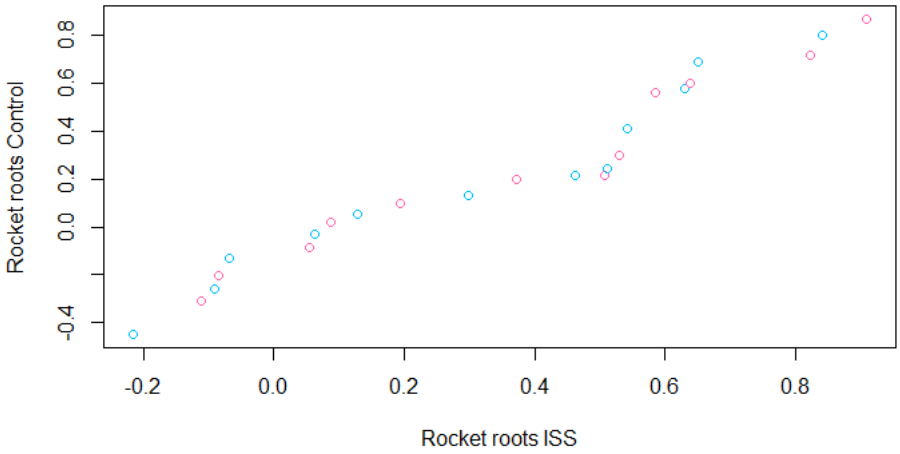

Fig. 5.8. Quantile-quantile plot (Q-Q plot) to show the similarities in distribution of space flown rocket roots and control rocket roots. The plot draws the correlation between a given sample and the normal distribution.

The data for rocket roots was assumed normal based on descriptive tests shown in Fig. 5.7 & 5.9 and further tests for normality using Shapiro-Wilk tests confirmed this assumption (data available in supplementary information). A t-test showed that there were no significant differences between rocket roots that had been flown on the ISS compared to controls that remained on Earth (P value = 0.19 at 95% confidence interval).

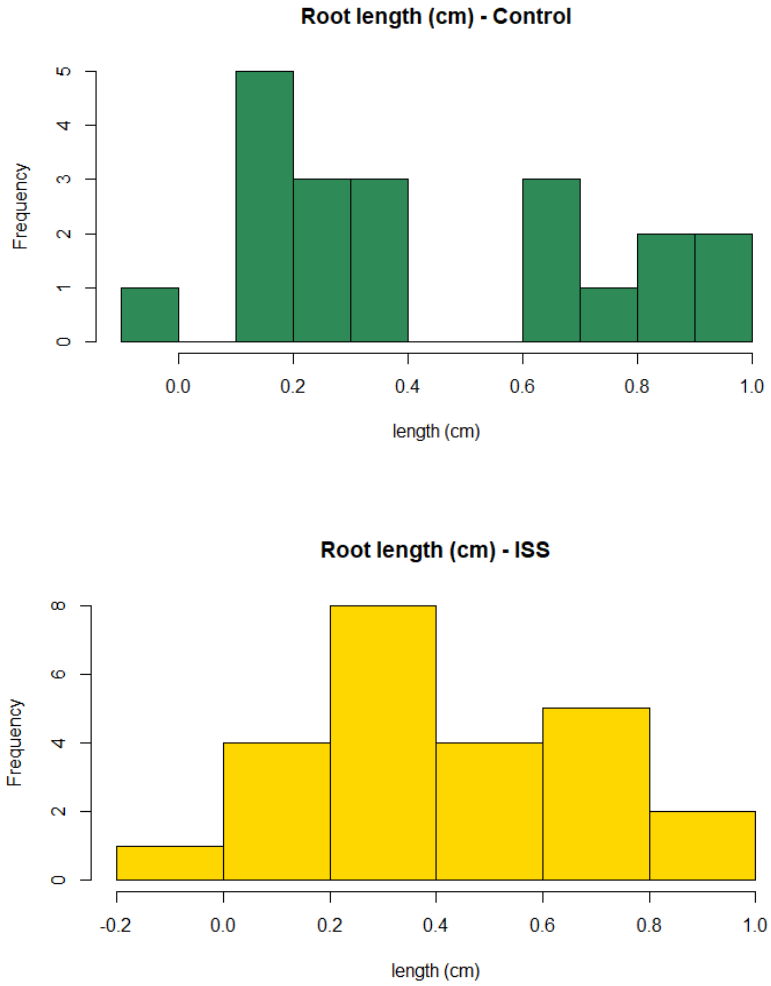

Fig. 5.9. Histogram displays of root length data distribution for control tomato plants (green) and plants grown from seeds flown on the ISS (yellow). The values on the x axis denote length in cm transformed through log base 10 function. The distribution of data is normal (fewer departures from normality in ISS data due to a larger number of samples available).

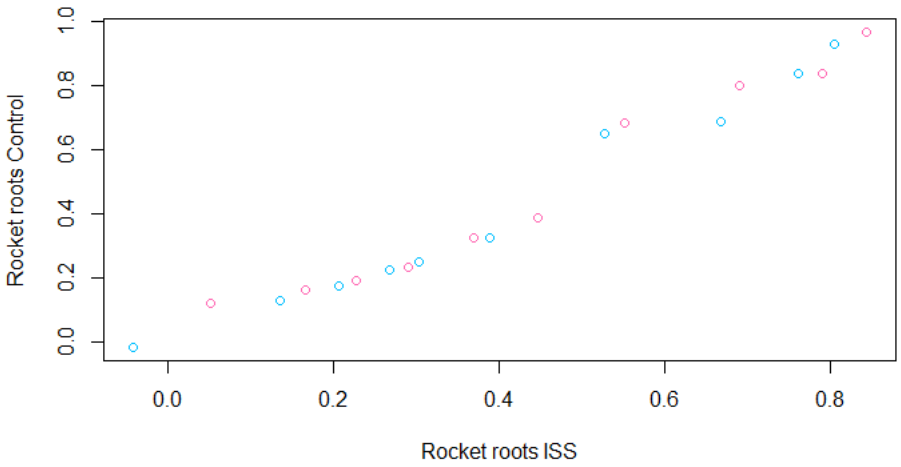

Fig. 5.10. Quantile-quantile plot (Q-Q plot) to show the similarities in distribution of space flown tomato roots and control tomato roots- The plot draws the correlation between a given sample and the normal distribution.

Like the rocket data, the tomato data was tested for normality using the same method in R (Fig. 5.9 & 5.10). However, the control group data appeared non-normal (P = 0.03) but the ISS data was normal (P = 0.22). The data was further assessed for significant differences between treatment groups with a Kruskal-Wallis rank sum test, a non-parametric test to assess the data set inclusive of the non-normal data. No significant difference was detected.

Chapter 6: Discussion & Conclusion

In this chapter a detailed, systematic discussion of the project is presented. Achievements and limitations are highlighted and discussed. Particular attention is drawn to persistent data gaps and suggestions are made for strategies that have the potential to both strengthen existing knowledge and create new research. Opinion on suitability of present legislation for radioprotection is a feature. Finally, a new perspective on effect definitions of low-dose ionising radiation (IR) on higher plants is given and future research areas are recommended.

6.1 The Developmental, Morphological and Physiological Data

The first objective was to grow several generations of *A. thaliana* under identical conditions using a cadmium positive control (selected for its known toxicity to plants) and environmentally relevant low-dose Caesium-137 radioactive treatment. Overall, objective 1 was successfully met because five generations of *A. thaliana* were successfully grown from seed to seed under treatment conditions to provide plants comparable to those widely used elsewhere in the literature for other experimental purposes. There are no previous reports of a comparable multi-generational exposure of a plant species to chronic low-dose ionising radiation.

All controllable parameters for growth were used according to recommendation from The Arabidopsis Information Resource (TAIR) (namely light regime, humidity, temperature and water regime) and this worked well. It was established that spiking soil with the radioisotope Cs-137 was appropriate for attempting to get as close to field conditions in the laboratory as possible owing to the environmental distribution of radioactive fallout in well-characterised places (e.g. Chernobyl and Fukushima).

Originally, plans were made in the prototype experimental design to run a "two-halves" experiment in parallel within the same growth container. The initial design was to have two sides of a container (measuring 12x17x4cm) housing *A. thaliana* plants; one half of the container was to have a densely seeded population and the other between 4-6 individuals spaced evenly apart.

Fig. 6.1. Initial layout of plants in a "two-halves" configuration with one side of a container densely seeded and another side with individuals spaced apart. The problem that is clear from the image is that in the densely seeded side it is very difficult to count leaves and ascertain growth stages and the sparely seeded side shows some clear growth stages but the plants are still too close together to obtain accurate data.

This was an effort to investigate plants as close as possible to how they would grow in the natural environment (upon maturity *A. thaliana* siliques burst open and, as a result, dense populations of plants often occur in close proximity to one another) while simultaneously being able to track developmental stages using a few individuals spaced apart. This design, while conceptually intriguing was not favourable for the

types of endpoints that were later examined. One endpoint that would have been measured should this design have been properly implemented was the effects of plant population and competition (on the densely seeded side). It would have been interesting to see if competition influenced growth and survival of plants exposed to radioisotopes in soil, as there may have been increased pressure to mine for nutrients in a potentially stressful condition. Unfortunately, the containers were too small and the quantity of plants growing in one half of the container had roots that interfered with the other half of the container (visible from below) and made contact with the sparsely populated individuals but despite the effort to space individuals apart, overlap above soil was still occurring (Fig. 6.1) and it was not logical to reposition plants as any disturbance could jeopardise growth, introducing a mechanical damage factor. The only way to have avoided this would be to increase the container size but this would have been beyond the limits of the experiment for two reasons: The dimensions of the growth cabinet would not permit such a container and the amount of Cs-137 required to give the same dose to plants would have had to be dramatically increased, meaning an increased risk for safe use and a potential contravention of the laboratory rules concerning safe limits for human exposure. As well as these aspects, there was also the potential for skewness in results where bias in competing plants, in terms of light and nutrients, may have been present where plants were subjected to other processes separate from radiation exposure. In addition, there were not enough individuals successfully growing to present statistically robust results. The original protocol was trialled twice in radioactivity, by this point the seed stock contained seeds that had been exposed for two generations but no useable data.

After the cessation of the two-halves design, a second protocol was created. In the second design, steps were taken to increase the number of isolated individuals over

more containers, giving rise to more pseudo-replicates and more true replicates. The larger size of the container 18x26x8 cm was a much better way of handling the plants from both a health and safety perspective (deeper containers reduced the risk of contact with contaminated soil when moving containers during routine rotations within the growth cabinet and also during data capture detailed in objective 2) as well as providing better conditions for plant growth as there was more space for each individual to root into the soil, spread a rosette onto the soil surface and produce inflorescences without coming into contact with neighbouring individuals (above ground). The new protocol had seeds sown that had already been exposed to radiation for one generation (the second generation in the previous experiment was discarded).

Objectives 2, 3, and 4 were to capture and analyse still and video images of growing plants. Video capture proved not to be useful for capturing the endpoints of interest to this project but the still images provided developmental data comparable to previous reports and the LAMINA software worked well to provide data in accord with results and reviews in published literature (Fiorani and Schurr, 2013; Frei et al., 2014). The software proved ideal for analysing *A. thaliana* in terms of leaf area and asymmetry. Other parameters were available and considered (such as leaf circularity) but due to the excision of leaves at the petiole, circularity was shown to be a less accurate endpoint. Objective 5 was achieved through the design and building of a bespoke hydroponic tank. Potential uses for the tank include radiation effects studies, where radionuclides could be hosted in various compartments where shielding would isolate the area to be studied, thus producing concentrated results. This could also be applied to nutrient deficiency studies, or any study where isolation of a property in solution was required. Amalgam Models (a model making studio in Bristol) were commissioned for the manufacture the tank. The tank was constructed of solid opaque thick polyethylene

which housed six inserts of clear polyethylene with an extra layer of sealant. Six metal brackets were designed to fit over the clear inserts with spaces drilled into them to house five adequately spaced apart holes for Eppendorf tube insertion. Inserts filled with hydroponic solution were lifted from the tank and placed against a plain background. Photographs were taken of roots growing downwards in solution (Fig. 6.2).

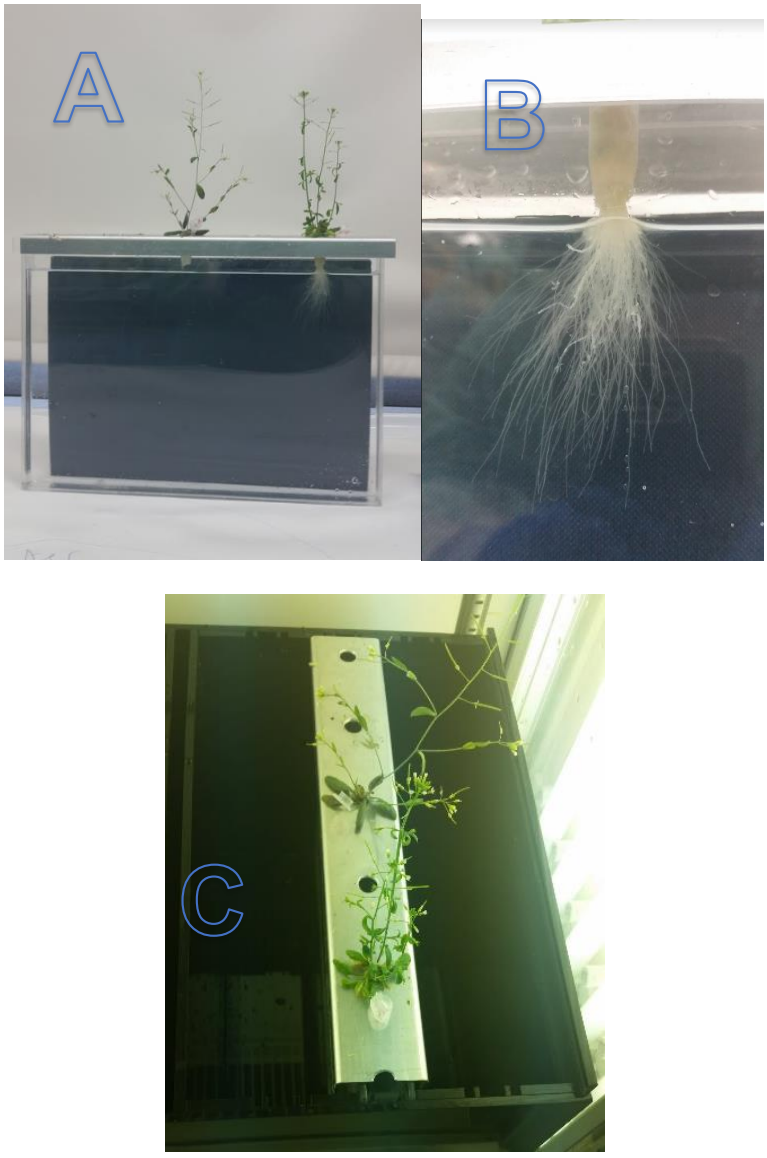

Fig. 6.2. Hydroponic tank insert in functional/biocompatibility test (A) Perspex insert filled with Hoagland's solution for hydroponic growth of A. thaliana showing two mature plants. (B) Close-up image of root system emerging downwards from an agar-filled Eppendorf plug. (C) Placement of insert into hydroponic tank (aeration not shown).

The tank build was largely a success in terms of testing but a few issues with contamination arose, wholly from the exposure of the agar plug in the Eppendorf tubes to the air (discolouration probably from contamination visible in Fig. 6.2 (B)). While some plants grew successfully, others did not (In the example in Fig 6.2 (A and C), five seedlings were placed in the tank initially but only two survived), and it was heavily suspected that contamination was the cause. Therefore, the decision was made to implement more traditional methods (sealed agar plates) for the purpose of root studies for this project. Further testing of the tank, perhaps with different growth media is suggested.

Objective 6 was met through GSG measurements but comet assays and DNA methylation endpoints were also investigated. A comet assay as described by Navarette *et al*. (1997) was carried out on *Trifolium* treated with H_2O_2 – this was to trial the protocol on an experiment with a documented stress outcome. The assay worked successfully in one sense that the staining appeared correctly under a microscope, however all that was visible was cellular debris (cell wall etc.) and no nuclei were detected. This method was repeated using *A. thaliana* but no nuclei appeared under the microscope. Leaves were both sliced and scored with a razor blade to encourage release of nuclei but the method continued to be unsuccessful. The method was ultimately discarded and alternative physiological endpoints were sought. The Interdisciplinary Biosciences Expert Group at the Belgian Nuclear Research Centre (SCK-CEN) offered to examine some of the samples for DNA methylation and provided results as percentage DNA methylation per group. After extensive literature review, it was decided that samples would also be assayed for glutathione.

Objectives 7, 8, 9 and 10 were all successfully achieved and thus the results reported here provide a significant body of data on the developmental, morphological and

biochemical responses of plants to chronic exposure to low dose ionising radiation. In particular they provide data on responses, for the first time, over 5 generations of exposure in *Arabidopsis thaliana* and from plants grown from seeds exposed on the International Space Station to cosmic radiation. Due to the changes in growth protocol for Arabidopsis, in discussion of results it must be noted that individual plants grew in the absence of competition from other individuals. In addition, although the experiments did provide some data from roots and a new hydroponic tank for root experiments was constructed, the data is primarily from shoots.

6.2 Discussion of Results

6.2.1 Plant development

Data from the plant development experiment showed some subtle effects but overall there was no clear trend linked to radiation, as previously suggested in the literature (Geras'kin *et al*., 2011; (Van Hoeck *et al*., 2015 in Chapter 1). In some generations (G4 and G7) development was accelerated in radioactively-exposed *A. thaliana* when compared to controls (G4, where flowering was observed at an earlier date and G7 had slightly enhanced growth) while in other generations development was similar in radioactive treatment and the negative control. In some generations (G4 and G7) the negative control exhibited a faster progression through development. Effects on timing, earmarked by developmental stages, may well be caused by IR stress as claimed in Nishigughu et al., 2012 and Sidler et al., 2015. However, the frequency of significant differences between treatment is low and based on these findings it would be logical to acknowledge possible effects but also that such effects had no overall

negative impact on the ability for plants to carry out normal growth function, as all of the stages in the complete life cycle were fulfilled.

The results of the germination test indicated that seed viability was not affected by treatment with Cs-137 or cadmium (details of dose/concentration shown in Chapter 2). However, due to the small harvest size from each treatment group throughout some of the experiment generations (including controls), germination tests were performed using seeds in a range of 15-268 seeds per treatment group. The poor harvest of some groups was probably due to handling errors during the harvest period and not a reflection of treatment group, although this cannot be completely ruled out without replication of the entire set of experiments. Handling errors included seed spillage which resulted in the discarding of seeds to avoid cross-contamination. Missing the point at which seed siliques burst open upon drying also impacted overall seed yield as this took place within hours or overnight and some seeds could be lost to the growth medium below. One attempt at avoiding this problem was the purchase of Aracon units. Aracons (obtained from the University of Bristol) are specially-designed plastic units that serve to catch seeds in a tray built over the base of plants. Unfortunately, the placement of the Aracon trays over the rosette base caused excessive dying of rosette leaves. When tested, this resulted in leaves that were unfit for morphometric analysis. A suggestion would be that Aracons could be used in the same experiment design permitting that the growth containers were larger and that extra replicates could be placed in parallel to plants used for morphometric analysis without the threat of the Aracons interfering with other replicates. This would, however, take significant growth cabinet space in a radiologically controlled laboratory and involve thorough planning to reflect requirements.

In the second generation *of A. thaliana* exposed to Cs-137, positive control (cadmium) reached the flowering stage (stage 5.1 as described in Boyes *et al*. (2001)) prior to Cs-137 treatment, followed by the control. There was some crossing over between cadmium and Cs-137 in later stages (mid-flowering) but the development of these two treatments was accelerated when compared to negative control. In the third generation exposed to Cs-137, negative control plants reached the flowering stage around the same time that the Cs-137 treatment plants did, and the positive controls lagged behind both of the other groups. The data for the fourth generation exposed to Cs-137 was of a low resolution, missing some key data points for developmental stages and a decision was made to omit this generation from the overall results. In the fifth generation exposed to Cs-137 it was observed that positive controls developed at an overall faster rate than other treatment groups, at every fundamental stage past true leaf development (the primary leaves of the rosette that arrive after cotyledon production). This was followed by Cs-137 treatments and then negative controls which mirrored the Cs-137 treatment group in terms of timing between developmental events but was overall slower when compared. Due to measurements taken at different intervals to the average growth stage and day relationships detailed in Boyes *et al*. (2001), it was not possible to have a direct comparison between this series of experiments and the average growth stage data from the literature. However, the developmental stages were useful when making comparisons between each generation of plants.

The lack of clear trend in the data indicated that, just as controls varied slightly in their development between generations, so did the other treatments and it was discovered that there was as much variation in results for control groups than there were for Cs-137 exposed plants. Over five generations of exposure in the Cs-137 treatment the

dose rate is below a threshold where development is impacted. The radiation exposure was at a dose rate below the DCRLs for grass but at the lower end of the range for a sensitive species (*Pinus sylvestris*) (Geras'kin *et al*., 2005). These findings do not necessarily imply that radiation at these doses has no effect, but that effects may be subtle and no more significant that those ordinarily found in non-exposed populations over generations and that can be regarded as non-threatening to communities and populations. Therefore, based on findings for the developmental stages of plants exposed to low-doses of ionising radiation at environmentally relevant doses, no cause for concern is raised. Further, these results come from a combination of internal and external doses. Internal and external doses were never discriminated from each other for the simple reason that no clear trend for effects was observed. If a pattern emerged in the data then it would be logical to determine if the effects were a result of internal or external dose, or perhaps a combination of both. The data also emphasise that measurements taken on a single generation can be misleading for ascertaining overall long-term trends - the variation across generations is quite significant and results in instances in which differences between treatments occur. This might help explain reports in the field in which IR exposed populations are sometimes found to have different characteristics to non-exposed populations.

6.2.2 Morphometric analysis of leaves

The main purpose of this strand of project was to investigate differences, if any, in the shape and size of leaves of *A. thaliana* exposed to Cs-137 for several generations.

Asymmetry is a common endpoint in research from other members of the RATE TREE programme examining effects of IR in other non-human biota such as *Daphnia* and freshwater crustaceans (Fuller *et al*., 2017). Having a comparable endpoint was

important because it enabled wider discussion about the current ways of thinking about radiation doses to multiple categories of wildlife.

For the morphometric analysis of leaves, a simple data compilation was made in Chapter 3 but repeated here for convenience (Table 6.1) which showed where significant differences between treatment groups in experiments detailed in Chapter 3 occurred. From these data it was observed that there were significant differences in both endpoints in some generations of the experiment but this data appeared sporadic with no clear trend.

Table 6.1 Summary of results for vertical symmetry and leaf area morphometric data displaying 50% of overall results for A. thaliana leaves having no significant differences detected through ANOVA testing at 95% confidence intervals. Repeated here from Chapter 2.

Generation	Vertical symmetry	Leaf area
2nd	Positive control significantly different from other groups	Positive control and Cs-137 treatment group significantly different from other groups
3rd	Positive control and Cs-137 significantly different from other groups	No differences between treatment groups
4th	No differences between treatment groups	No differences between treatment groups
5th	No differences between treatment groups	Positive control and Cs-137 treatment group significantly different from other groups

Overall, in 50% of all generationally-examined morphometric endpoints no significant differences were detected. Evidence suggests a similar story to the developmental stage analysis in Chapter 2; in some generations significant differences are shown in plant morphology that have been exposed to IR through Cs-137. However, attributing

those differences to radiation may not be an appropriate conclusion as previously claimed in Celik et al., 2014 and Sever-Mutlu et al., 2015. As detailed in Chapter 1, other environmental stressors exhibit a wide range of negative impacts. The hypothesis that hormetic effects can be observed in plants exposed to low-dose IR are not out of the question, but in this study the only evidence of hormesis occurred in the third generation of plants exposed to IR where the first flowering date was accelerated compared to dates in the control groups. However, that is only a hormetic effect from one perspective, as it could be that the early onset of flowering is triggered by, for example, a stress response leading to the need to accelerate the reproductive process. The latter seems to be the most likely given the early onset of flowering in the positive (Cd) controls in two-thirds of the developmental stages experiment.

It is also important to highlight the potential limitations of morphometric analyses that may impact the results found in this project. Sandner and Matthies (2017) found that fluctuations in asymmetry were a poor indicator of stress due to weak correlations in *Silene vulgaris* (Moench) as even after exposure to seven different stress treatments (including drought and metal toxicity) correlations were weak. The strongest correlations were only found at high stress intensities and so for chronic low-dose ionising radiation stress this may not have been the most suitable endpoint in terms of examining stresses of low intensity. That said, Sandner and Matthies did not measure asymmetry after radiation exposure so this cannot be completely dismissed as a useful endpoint.

Kozlov and Zvereva (2015) found that confirmation bias was a key driver of results where negative control birch leaves were measured by 31 scientists that were told either true or false information relating to a pollution event. The belief that the birch leaves were harvested in a polluted site influenced the results for fluctuating

asymmetry measurements. However, their test was carried out using manual measurements, whereas in the project reported here computer software was used to calculate the values, bypassing the risk of human error/perception during calculations.

Further work in the area of plant morphometrics in relation to chronic low dose exposure to IR might still be useful. Leaf size could be altered for many reasons, but in the case of IR, if leaf area is changed it may ultimately be because of reactive oxygen species (ROS). Cell expansion in leaves is partially controlled by apoplastic ROS homeostasis (Schmidt *et al*., 2016). An increase in antioxidant capacity has been documented in salinity and or drought-stressed *Zea mays* plants which restricts cell expansion. Increased ROS as a result of such abiotic stressors may too, restrict leaf cell proliferation. As a result of both factors, ROS is said to have a dual role in the regulation of such cell expansion (Schmidt, *et al*., 2016). It is more likely that changes in other subtler morphological characteristics would be suitable for further studies as ROS homeostasis does not operate alone and a plethora of other factors also affect cell expansion.

Lastly, Alves-Silvia *et al*. (2018) found that generally, a larger sample size (of around 800 leaves) provided a more normal distribution for results analysis for this sort but that the origins of the samples (i.e. many leaves from few plants or few leaves from many plants) had no bearing on the distribution. Data from the leaf morphometric analyses in this study followed an essentially normal distribution but could have been tighter, and so from this it would be logical to recommend a higher sample size for results with increased statistical robustness. If it is necessary to investigate other effects on leaf morphology to find significant differences due to IR or to use even larger sample sizes to show significant differences in symmetry/leaf area then any effects of IR at these dose rates are, by definition, subtle.

6.2.3 Physiological and epigenetic traits

Analysing plant physiological responses to IR stress from Cs-137 was carried out to support developmental and morphological endpoints. Although it is interesting to study development and morphology as standalone entities, having an understanding of what is 'happening on the inside as well as outside' should strengthen any findings overall, regardless of if they end up as complementary or conflicting results.

The initial idea for examining a physiological endpoint to support wider findings in morphology was to select a method that would allow for the gaining of an overview of DNA damage, one of the widest-studied endpoints in the literature concerning radiation effects in humans, plants and animals. The comet assay was the initial method of choice; however, a substantial amount of time was dedicated to protocol optimisation but failed to yield any useful results.

Results from samples sent to SCK-CEN in Mol, Belgium, and analysed by an expert team showed that radioactive treatment samples contained a significantly lower percentage of methylated DNA after exposure, which was an intriguing result given that previous evidence points to exposure as a cause for increased DNA methylation and in some cases, hypermethylation (Georgieva *et al*., 2017; Kovalchuk *et al*. 2003). While the results from this experiment showed the opposite phenomena, it can still be regarded as an effect. The same samples had no obvious morphological effects so these effects are considered subtle.

Later, it was decided that measuring total glutathione (GSH + GSSG) was another logical endpoint to measure and although the glutathione assay also required optimisation, results were successfully obtained.

No statistical difference in glutathione between treatment groups and generations of plants exposed to IR was discovered. Samples used in this experiment were extracted from the same plants tracked throughout the growth cycle (for developmental stages) and harvested for the morphometric analyses. The combination of findings – no systematic morphological trends coupled with no significant changes to antioxidant capacity observed in this experiment, are in good agreement with another closely-related study. Vandenhove *et al*. (2010) measured, in *A. thaliana*, physical growth alongside antioxidant enzymes involved in oxidative stress pathways at a range of doses (up to 2336 µGy/h) including doses not far in excess of those used in this project (60-80 µGy/h). No significant effects were detected with respect to antioxidant capacity for any of the enzymes involved in ROS defence. Vandenhove's study examined a comprehensive range of enzymes that included glutathione reductase. Further, there was no significant effect of dose rate on glutathione (and ascorbate) levels or concentrations in either reduced or oxidised forms and combined forms in both leaves and roots (Fig. 6.3).

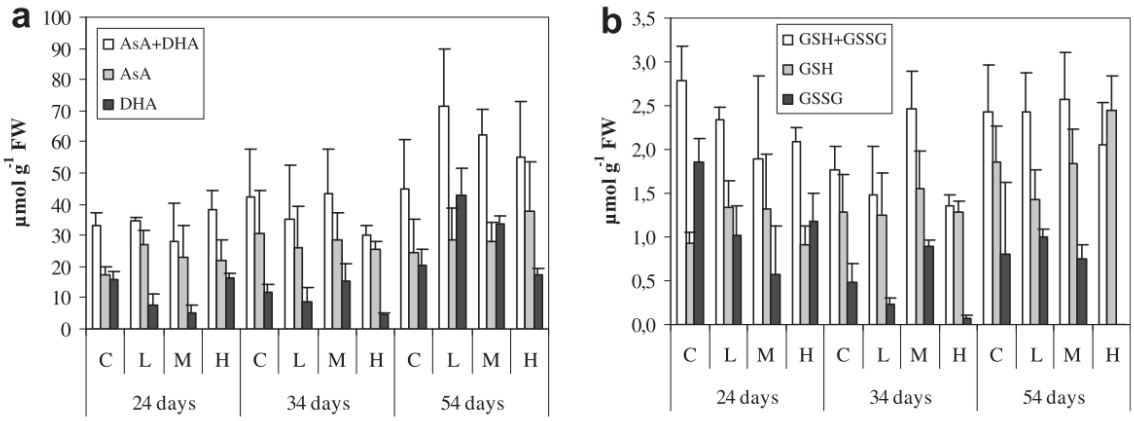

Fig. 6.3. Total ascorbate, AsA (reduced ascorbate) and DHA (dehydroascorbate) (µmol/g fresh weight) (A) and total glutathione, GSH (reduced glutathione) and GSSG (glutathione disulphide, expressed as glutathione equivalent) (µmol/g fresh weight) (B) in the leaves of A. thaliana exposed for 24, 34 and 54 days at 81 (L=low), 367

(M=medium) and 2336 (H=high) µGy/h along with controls (C). Each point represents mean ± SE of at least 3 biological replicates. Reproduced with permission from Vandenhove et al. (2010).

Comet assays were also performed and results showed that there was no effect of dose rate and DNA integrity.

Results of physiological experiments in the project reported here were, therefore, unsurprising given the outcomes of previous studies and overall current understanding of redox status in plants exposed to low doses of IR. Importantly, in contrast to previous studies they do, however, show that this lack of difference is maintained across generations. The model of Smith *et al*. (2012) shows that IR produces too few reactive oxygen species (ROS) to have a direct effect on the concentration of antioxidants in cells, and this includes glutathione. Even in the highest areas of contamination in the Chernobyl Exclusion Zone (412 µGy/h), both redox potential (the measure of a chemical species to gain electrons and undergo reduction) and the generation of ROS was not impacted via radiolysis (Smith *et al*. 2012). Therefore, results from this experiment also support the hypothesis that direct oxidative stress is not the damage-causing mechanism it is often claimed to be in the literature, but that other factors in the field, such as stress, pests and pathogens, are probably more closely linked to changes in antioxidant concentrations.

This understanding, that redox poise is only markedly changed under high levels of radiation exposure, is further exemplified in experiments with other stressors such as in Cheng *et al*. (2010) where glutathione concentration is only altered under severe drought in *A. thaliana.* Such a response may not even be described as a stress, but as a shock, depending on the circumstances. This topic of discussion is revisited in 6.4.

Scope for further research into this specific area exists. In this experiment, even the positive control of 10 µM cadmium showed no significant differences to both the negative control group and the Cs-137 treatment group. Elevated levels of cadmium in soils is of known toxicity to plants (Yadav, 2010), but at 10 µM no marked changes in morphology were detected in both morphological endpoints (development and leaf morphology). The concentration of cadmium was probably too low, and perhaps increasing the concentration to around 75 µM as described in an experiment by Qi *et al*. (2015) would serve as a better measure of metal toxicity for positive controls as marked differences may be more obvious at the higher concentration, while still not severely impacting plant growth and development. Cadmium at much higher concentrations would indeed, severely impact plant growth and development. This was confirmed in the preliminary phases of this experiment where 10 mM cadmium was erroneously mixed into soil. As a result, no seeds germinated (Fig. 6.4).

Fig. 6.4. Preliminary experiment with A. thaliana in c. 35 µGy/h Cs-137 (radioactive treatment), 10 mM CdCl2 (positive control) and negative control soils. Cadmium toxic effects are evident by the lack of growth in the positive control treatment, despite sowing a similar number of seeds to the radioactive treatment and negative control group.

6.2.4 Cosmic radiation

The effects of cosmic radiation on seeds of two crop plants, *E. sativa* (rocket) and *S. lycopersicum* (tomato) was a study developed alongside the transgenerational *A. thaliana* experiments (Chapters 2-3). Increasing interest in the habitability of other planets in the field of space exploration has provided a boon in the exobiology field. Exobiological research is focused on the origins of life, limits of life (survival in extreme environments) and the possibility of life elsewhere in the universe. Further, plant biology experiments are currently underway on the International Space Station (ISS) and the seeds used in this project arose from two of these experiments (as described in Chapter 5).

The decision to investigate Cs-137 uptake in leaves of cosmic-IR exposed rocket and tomato was unexpected. Initially, plants of both species were grown in a quick test to check if there were obvious visual differences between plants grown from seeds exposed to cosmic ionising radiation on board the ISS and then re-exposed to similar doses from Cs-137 compared to control plants that had remained on Earth. In addition, comparisons between plants grown from seeds exposed to IR on the ISS in clean soil was also sought alongside controls that remained on Earth. No morphological difference was detected but before the experiment was discarded, a Geiger-Muller gamma detector was placed over the leaves of the plants to check that they were not radioactive above background levels, in line with standard laboratory radioprotection protocol. The leaves registered above background and it was then discovered that the mature leaves of both species of crop plants had accumulated unexpectedly high Cs-137 in their leaves via transport from the soil.

To examine this in closer detail, leaf samples were oven-dried and processed for gamma counting. These opportunistic results exhibited uptake in leaves of tomato and

rocket that had been grown in soil spiked with Cs-137. Uptake results showed no statistically significant results between groups regardless of earlier exposure on board the ISS. This was unsurprising, given the (external) doses received in space were highly similar to the doses mixed into soil in the *A. thaliana* experiments. The data from the study of roots (ISS flown vs control) in non-active conditions also showed no significant differences. Due to only a small number of seeds provided for this project by the distributor (the Tomatosphere project via the Canadian Space Agency, and the Royal Horticultural School's Gardening project via the European Space Agency) robustness of results is questionable. However, the results serve as a clear demonstration that in contrast to *A. thaliana*, fast-growing leafy crop plants can readily accumulate Cs-137 if it is available. Six months on board the ISS may have induced subtle effects on rocket and tomato seeds that were not detectable in these experiments but profound effects on germination rate, morphology and root growth seem unlikely given the results of previous experiments in both this study and of the others that came before it.

6.3 Plant biology and radioecological studies – A multi-level approach

When studying effects of stressors in biology it is common to focus on one level of biological organisation (as reflected in much of the literature) but as a result the significance of effects within a hierarchy of organisation can be difficult to assess. To ensure this study did not neglect the biological hierarchy important for radiological protection, an effort was made to provide data at the precise biological levels where it was scarce. This was to complement existing data and provide an understanding of effects on plant systems as a whole.

The hierarchal model of effects in plants outlined in Chapter 1 explicitly sets out the different organisational levels (Fig. 6.5). This study primarily focused on effects at the organism level (labelled "Effects on individuals" in Fig. 6.5) and the transgenerational level, with some investigation into the reproductive and molecular level (denoted as "Genetic effects" in Fig. 6.5).

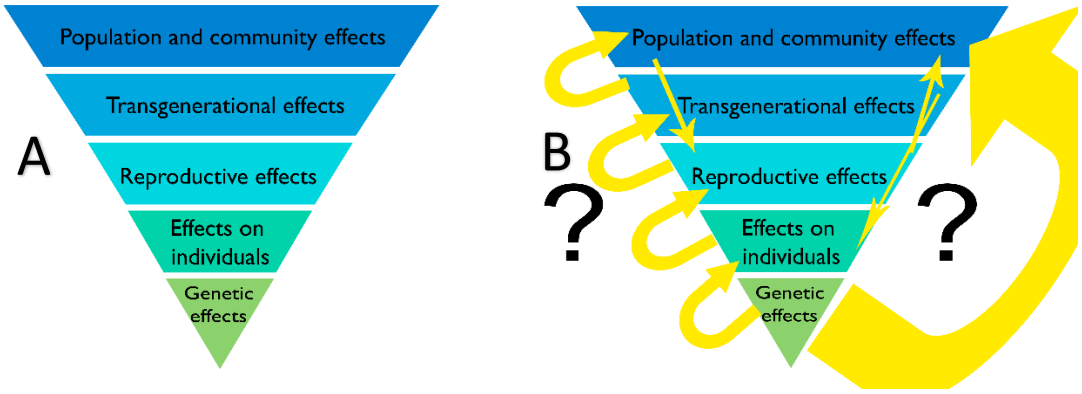

Fig. 6.5. Hierarchal model of effects in plants (A) from the broadest view of effects at the population and community level to genetic effects or effects at a molecular level. (B) Graphical representation of where questions remain surrounding effects at multiple levels, and if effects at one level are bridged with effects at another, or multiple levels simultaneously.

Relationships between effects at multiple biological levels are still unclear and not explicitly dealt with in the scientific literature. In the field of radioecology, the most popular endpoint for studies into the effects of IR on higher plants under controlled conditions is undoubtedly the molecular level. This is demonstrated by extensive literature searches on the subject (as detailed in Chapter 2). The multiple level methodology is beneficial to radioecological studies in particular as, ultimately, radioecologists are concerned with protecting populations, communities and whole-ecosystem responses to radioactivity in the environment.

Although this hierarchy is useful for pinpointing where effects might occur in response to radiation, it is important to recognise that at each level biological of organisation there is a great level of redundancy. At the molecular level, redundancy can be conceptualised in terms of genetic organisation. Estimates show that over 70% of all species of flowering plants have a ploidy levels that have increased at some point in their evolution (Meyers and Levin, 2006) so that if radiation is affecting a gene, for example through mutation, the plant may not show any functional or phenotypic changes as other copies could be acting as failsafe mechanisms. Much in the way that a car wheel usually has five bolts attaching it to the rest of the car, should one or two bolts become loose or fail, the wheel can still function properly. Further, even in each individual plant genome there are many genes with multiple copies. This notion of redundancy is applicable up the levels of the hierarchal model, right the way through to populations and communities. A forest exposed to low-dose chronic ionising radiation may indeed exhibit some subtle effects in terms of impacts on a small percentage of individuals (as demonstrated in Mousseau *et al*. 2013) but on a macro scale, the forest isn't being affected overall. The production of pollen, the production of seeds and the growth of seedlings are all subject to significant levels of redundancy. This repetitive pattern of redundancy through the biological effects levels enables us to question the radiological significance of effects reported at a single biological level.

Overall, the use of a hierarchal model for studying radiation effects in plants, through multiple endpoints, is a useful way of relating specific effects to the level at which they are examined. An emphasis on biological levels not only clarifies which effects may be observed, but also creates opportunities for questions regarding impacts at other levels. It also aids the visualisation of the redundancy of effects at one or multiple

levels. All this is helpful in providing a research approach where focus at one level is realised whilst the wider context of studies, including redundancy, acknowledged.

6.4 A new perspective on radiation effects on higher plants

Until Levitt first identified the absence of a hard definition for stress in plant biology equivalent to that in mechanics, biologists had long been using the term to describe a wide variety of environmental factors that have effects on higher plants. Levitt (1980) describes these factors as *potentially unfavourable to living organisms*, with the term 'resistance' given for mitigation mechanisms that enable plants to survive in these unfavourable conditions. Uniquely, Levitt then provided a perspective derived from mechanical understanding, referring to Newton's laws and the concepts of physical 'stress' and 'strain'. These definitions have proven useful in relation to biological effects and are not exclusive to plants, but to all biota, and are almost ubiquitous in their use. Schulze *et al*. (2005), however, analysed the stress concepts introduced by Levitt and highlighted the limitations of applying physical definitions to biological systems. They emphasised the lack of temporal parameters as being a key restriction in the application of Levitt's stress definition. This is because stress is a measured variable derived from both intensity and duration. This perspective of stress is particularly applicable to the radioecology field where a combination of intensity and duration are central to dose-effect relationships. The other factor absent in Levitt's definition was that of repair. In Levitt's physical stress concept there is mention of elastic and plastic conditions which pertain to certain states of damage. Elastic refers to reversible effects and plastic refers to irreversible change. Schulze *et al*. (2005) draw attention to the fact that organisms have the capacity to repair damage that is not too destructive. Another of Levitt's ideas is that of strain, which differs from stress

in a measured system. The magnitude of stress is measured as the force projected by the source (stressor) whereas strain is a measure of the change in the subject. Strain in this context relates to a transitional stage whereby an organism has been exposed to stress. Using this model, it is possible to describe a radiation source as a stress, and an effect as a strain. Further, irreversible effects would be called plastic strain whereas repairable effects would be elastic strain. It seems clear that at least some of the damage caused by IR, for example DNA damage, can potentially be reversed and is thus an elastic strain. While strain may be a suitable descriptor of effect type at the molecular level, it is suggested not to be relevant to radioecological studies that are concerned with whole-ecosystem responses and so for this project 'strain' is not an applicable term.

Despite a legacy of some discussion of plant stress concepts it appears that nomenclature, in the radioecological literature at least, is applied less by thought and more by instinct. This can complicate our understanding when assessing research outputs, particularly those with controversial findings.

I suggest that over time we have arrived at an impasse when describing responses to 'stress' factors affecting higher plants; stress, strain and shock are terms that are used interchangeably. For example, on the subject of heat stress in *N. tabacum,* Rizhsky *et al*. (2002) wrote:

In nature, plants encounter a combination of environmental conditions that may include stresses such as drought or heat shock…

And on the combined effects of salinity and heat stress in *S. salsa* Li *et al*. (2011) began:

Under natural conditions or in the field, plants are often subjected to a combination of different stresses such as salt stress and heat shock…

Further, explicit use of the terms 'osmotic or saline shocks' in Fernandez-Ballester *et al*. (1997) was used in combination with the description of sodium chloride application to *P. vulgaris* as "stressed". The situation is made more complex by the roles that shock proteins (e.g. heat shock proteins and cold shock proteins) have in plant 'stress' response. Nonetheless, it seems that clearly defining what is meant by shock and what constitutes stress may be of great use for not only the radioecology field, but also of wider plant biological research.

The Oxford English Dictionary defines shock as "*A sudden upsetting or surprising event or experience*" and stress as "*Physiological disturbance or damage caused to an organism by adverse circumstances*" (in biology) (Oxford University Press, 2018). It seems as though both terms are being used throughout literature when referring to one of the aforementioned scenarios.

In the context of plant responses to the environment, a simple question could be asked: Is it shock or is it stress? Or, is it neither one of these?

Then there is a deeper, more specialised focus: Is anything that deviates from optimal conditions of survival a stress? Is anything that causes a sudden biologically injurious (and irreversible) outcome a shock? Can shock be reversible? At what level of biological organisation should a shock or stress be defined?

To understand how and why biological organisms respond as they do to a range of environmental stressors, knowledge of their requirements for living is useful. Plants are sessile organisms and do not have the faunal advantage of physical relocation to avoid unsuitable conditions. Despite this, plants live in a wide variety of habitats on

Earth, many of which have challenging conditions for life. To do this they have evolved mechanisms to enable them to survive in their environments, so the conditions of an ideal environment for a plant are species-specific. Thus, plants do not have a 'one size fits all' recipe for survival.

All plants, just like all living things, do, however, need a suite of specific elements to support life, plus the conditions that make the environment suitable to take advantage of them. It is possible to imagine this as a list of requirements for plants - a essential list for survival would read: the essential elements, water (a solution for biochemical reactions, and to transport macro and micronutrients around the plant), CO_2 (to convert to glucose through photosynthesis), a suitable temperature range, a suitable pH, space to grow (above and below ground) and time. On top of this essential list could sit another list, a list of *desirable* conditions that would not just permit survival but also provide optimal conditions so that a plant could reach its full potential in terms of size, reproductive fitness and overall health. This list would typically be made up of optimal nutrient quantities and ratios, plus the absence of pests and other factors that if removed or reduced, would elicit a positive biological response. In an ideal scenario, a plant would have a complete list of essentials and desirables, which could enable a plant to live without stress.

When a plant is 'stressed' it can be assumed that one or more of the items on the lists are absent or sub-optimal, either permanently or temporarily. The severity of the stress depends on which factor is absent or sub-optimal, from which list it came, and the duration for which this occurs. It is important to remember that the desirable list for each species of plant is specific to that species' requirements (although many would possess similar lists). Thus, if one item on a list was lost then while one plant species could be severely impacted, another could continue to survive with (or without) a range

of impacts. Further, this picture is not always straightforward because there can be interactions. A change in a factor or a condition can have knock-on effects and cause reaction cascades. Roses thrive in acidic soils. If a rose was replanted in alkaline soil, it would be stressed and might eventually die, but if the rose was replanted in alkaline soil in extremely high temperature, then this process would be sped up and death be more certain because the severity of negative effects is amplified.

To add to the complexity of the status of stress, Borics *et al*. (2013) discussed the use of terms 'disturbance' and 'stress' in an ecological context and placed emphasis on the confusion in terminology in current research. Borics came up with a method of differentiating between stress and disturbance via frequency. Frequency is directly related to recovery time and is therefore species-specific. Using this model, when an event occurs that perturbs a biological system at a low frequency (that gives enough recovery time for a system to recover from change) then this is known as disturbance. Conversely, should the frequency be high enough that recovery time is hampered, resulting in irreversible change then this was deemed as stress. From this perspective, stress has medium and high frequencies, and disturbance has low frequency (Fig. 6.6).

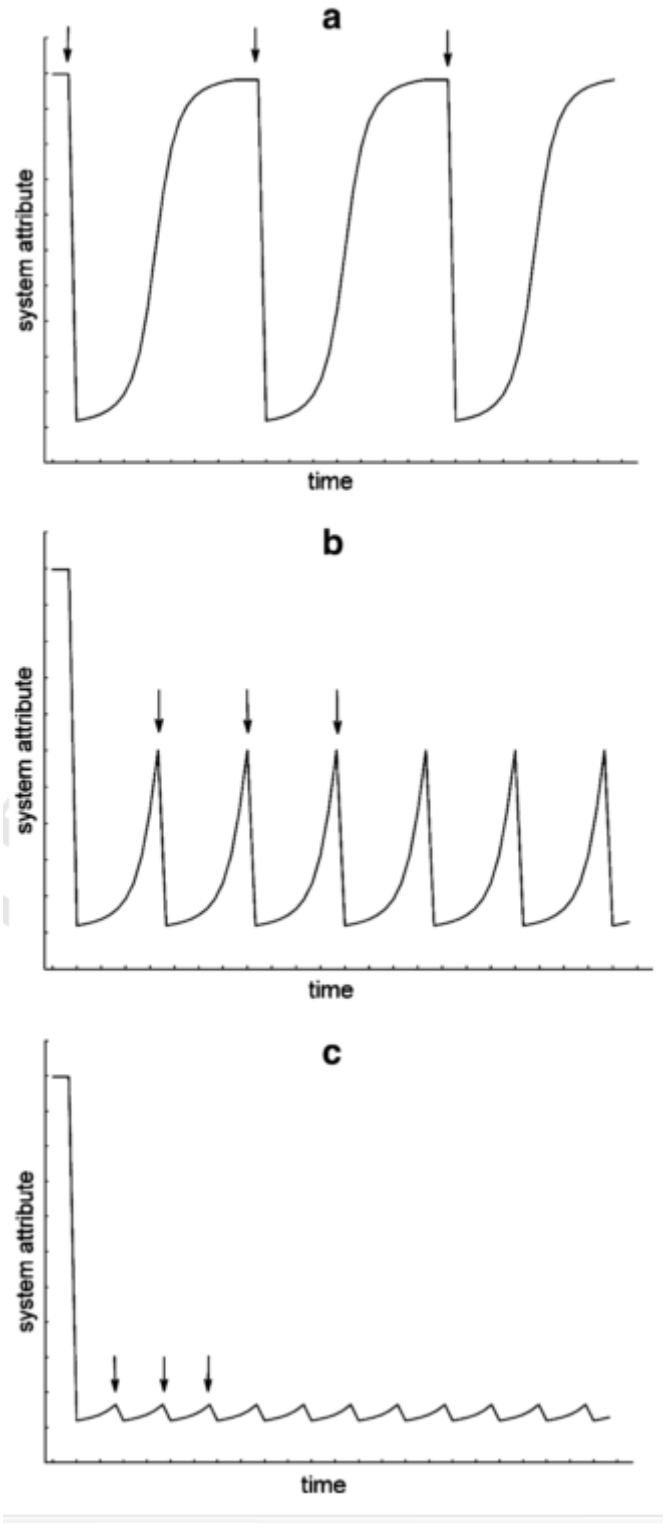

Fig. 6.6. Changes of a system variable (y) over time (x) during disturbance (a) medium frequency stress (b) and high frequency stress (c). Reproduced with permission from Borics et al. (2013).

In terms of radioecology of plant systems, using the Borics theory of disturbance and stress through frequency of events, it would mean that a dose of radiation that a plant could cope with and repair any damage that arose from it would be radiation disturbance. Further, irreversible damage would have the term stress apportioned to it regardless of dose, so long as the frequency/recovery time rule applies.

As for radiation effects on higher plants, increasing evidence has demonstrated that an acute exposure to a dose of IR above a certain threshold will severely hamper plant function and cause deleterious effects or death. Classification of these effects, traditionally in human biology results in what are known as deterministic effects (UNSCEAR, 2013), and in this argument, they would be described as shocked. I suggest that for plants, deterministic effects are acute shock effects arising from particular temporal occurrences.

Stochastic effects are slightly more problematic to define, as at present, there is no absolute method of testing if a specific effect that is sub-lethal is attributed entirely and unequivocally to radiation dose (UNSCEAR, 2013). This is particularly so for plants. Such effects are also closely related to the controversial linear no-threshold model for radiation effects, where incidence of effects increases proportionately with dose but there is no hard threshold for the initiation of effects. It is only risk that increases with dose, and not severity of effects. This description fits well with the notion of stress, and that stochastic effects (also known as probabilistic effects) are more in line with chronic stress effects. These are the ones that are governed by chance and common throughout the plant kingdom. Mutations that produce features such as fasciation (the morphological abnormality observed in the growing tip of plants) are a good example of stochastic effects as they are said to be randomly generated (RHS, 2018) so long as mechanical injury, viral or bacterial infection have not occurred.

Doses of IR used in experiments in this project resulted in no clear trend of effects in either the generations of *A. thaliana* exposed to IR from Cs-137 or the seeds that had been in space and exposed to radiation from cosmic sources (and further exposed to similar doses of it through Cs-137). In some generations from the experiment series that used *A. thaliana*, significant effects were observed but no distinct pattern emerged. This seemingly natural oscillation of effects perhaps best fits into the stochastic classification, should there be a classification at all. This could be a key driver for changing areas of focus in studies on low-dose radiation effects in plants. Just as in the literature that reflects field experiments, sometimes effects are observed and sometimes they are not. Researchers have long been attempting to link effects recorded in the field to effects in the laboratory (albeit despite a severe lack of controlled studies at lower doses). Further, they have been doing so and using terminology such as shock and stress interchangeably. Therefore, in the field of radioecology of plants (and wider plant biology), employing terms such as shock and stress may prove to be most useful when describing effects that fit into deterministic or stochastic categories. Further, referring to Levitt's elastic and plastic terminologies (1980), but with the addition of temporal and repair aspects by Schulze *et al*. (2005), might aid description of effects on a dynamic scale of damage. This dynamic scale is supported by the classification of environmental variables by Willey (2016) of which all three groups (resources, stressors and xenobiotics) are also subject to the same temporal and repair elements.

Employing this method of classification is extremely applicable to the study of effects at multiple biological levels as it is possible to define shock and stress from the molecular level right up to the population and community level. An example of this could be the Red Forest of Chernobyl, where in the immediate aftermath of the

explosion at the nuclear power plant widespread death of pine trees occurred in the vicinity. Using this methodology, one can say that the pine trees in the red forest at Chernobyl were not stressed by the nuclear fallout but that they were shocked by acute radiation. Conversely, exposing *A. thaliana* to chronic low-dose IR at doses that have affected DNA methylation rates can be described as chronic stress, regardless of whether effects are reported higher up the biological hierarchy so long as effects are defined as being present at the molecular level. The methodology used by Borics *et al*. (2013) should not go unmentioned due to its high relevance to arguments in this project. The frequency model shows a promising application for determination of dose-effect relationships owing to recovery time and would be interesting to explore, particularly when discussing the finer details in the stress category. It may be plausible that some short-lived damages reversed by repair mechanisms in plants as a result of exposure to IR could be deemed disturbances rather than stresses. Following this, irreversible effects that are non-lethal could be a result of stress and lethal effects, a result of shock. Lastly, if chronic low-dose IR in the field does not have any detrimental effect on populations of plants, but that the occasional individual may exhibit some form of negative or hormetic effect, does this matter? And, from an environmental protection perspective, in a world facing serious challenges due to climate change - should efforts not be focused elsewhere?

To summarise this section, a variety of terms have been used (sometimes interchangeably) when describing effects of IR on plants. This has led to a lack of clarity and fuelled confusion in the scientific and legislative communities. I suggest that for the purpose of radioecological studies, shock is the appropriate term for irrecoverable deleterious effects. Such effects might arise from significant high frequency or short timescale exposures. They are analogous to the deterministic

effects of human radiobiology. Stress, I suggest, should be restricted to effects of low frequency, which may cause the plant system to operate sub-optimally, and that appear over an extended period of time. Unlike shock, these effects may be recoverable or be withstood because of the redundancy in the biological hierarchy. They are analogous to the stochastic effects of human radiobiology. Using this distinction, effects of IR on plants that have a deterministic outcome of rapid occurrence should no longer be described as resulting from stress, but rather from shock. Effects that do not fall into this category can be considered stress and, depending on the aim of a radioprotection regime may, or may not have significant deleterious effects. A flow diagram was created to visualise the categorisation process (Fig. 6.7).

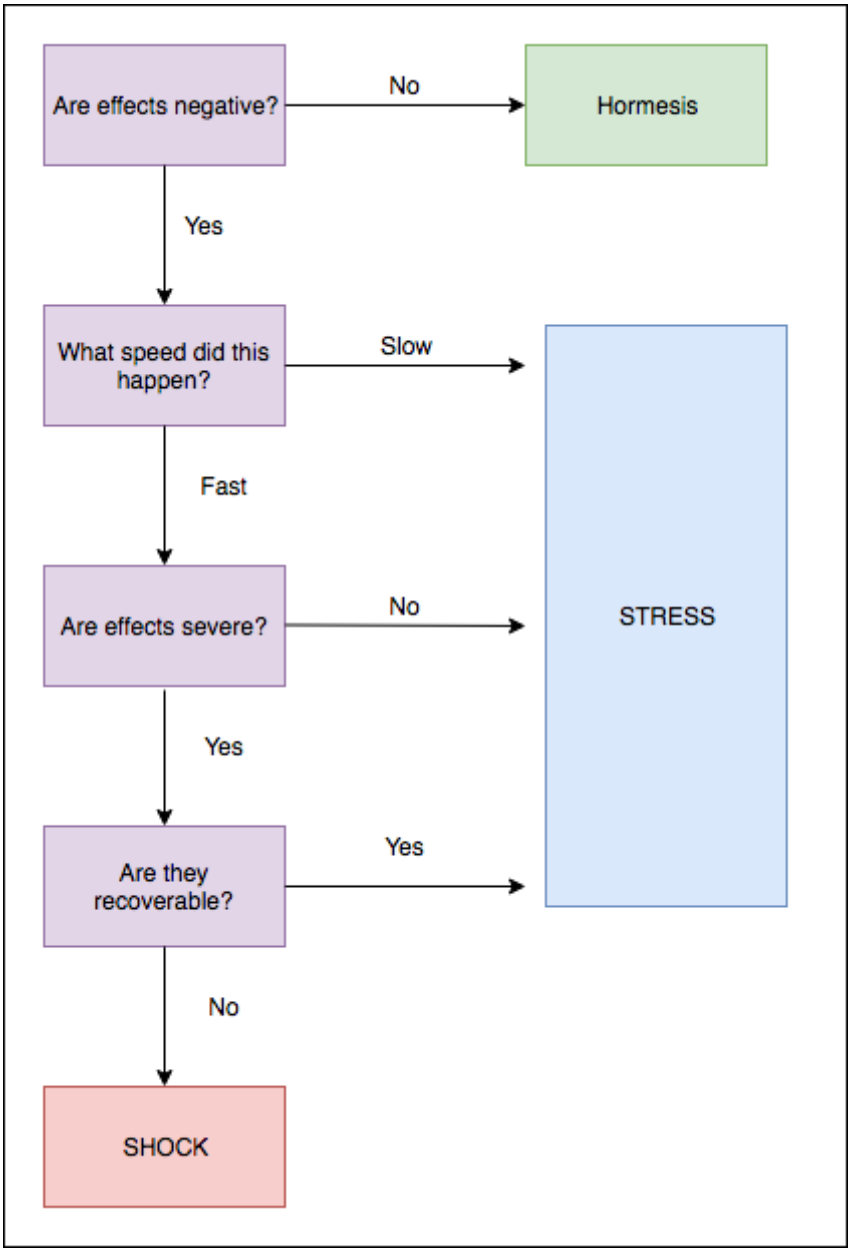

Fig. 6.7. Flow diagram to illustrate a simplistic way of examining the shock or stress classification for effects of IR on plants. Hormesis is displayed as to acknowledge positive effects.

6.5 Conclusion

The research reported here has generated data of a type vastly under-represented in studies into the effects of IR on plants. These data have no equivalents because of a marked shortage of research outputs that investigate chronic low-dose IR effects across generations under controlled conditions. Results of experiments on multiple species of plant of both agricultural and ecological significance, have demonstrated no clear morphological or physiological trend post-exposure to IR at chronic low doses but have exhibited some subtle effects concerning morphology and development. Plants exposed to IR at environmentally realistic dose rates may have to mitigate some potential damage physiologically, and this could be reflected in changes to growth timing but largely these effects appear to do no marked damage or hamper reproductive capabilities as plants in this experiment successfully produced good quality seed and other visible organs appeared normal. A novel protocol for the analysis of plant roots grown hydroponically *in situ* was developed but results indicated that further exploration of this protocol was needed to yield useful data. The addition of the investigation of plants grown from seeds that had been flown in space provided a wider-context for the research. A qualitative method of distinguishing effects observed at various levels of biological organisation via a hierarchical model was employed in this project and its merits as a tool for future research was discussed and recommended as a good option for providing a wider perspective for planned work. Further, questions were raised about the specific terminology used to describe environmental stressors to plants in various scenarios that have different biological outcomes and recommendations were made for the classification of effects of IR to plants to be clearly defined as a shock or a stress dependant on a combination of

temporal, repair and dose factors. Finally, an examination of studies of this type questions the necessity of examining the effects of lower doses of IR compared to the importance of examining other environmental stressors, which are potentially of greater urgency due to current and future challenges presented through climate change. Despite a variety of suggestions to the contrary, many in the scientific literature, the conclusions from the research reported here suggest that the DCRLs used to protect flora from the effects of IR are appropriate.

Glossary of terms

Allometry	The growth of body parts at different rates, resulting in a change of body proportions. The "body" in the context used in this thesis means the physical parts of a plant.
Antioxidant	A substance that inhibits oxidation, especially one used to counteract the deterioration of stored food products.
Apical	A plant grows new tissue from an apical meristem. The apical meristem is a group of cells that retain the ability to continue divisions, forming new cells continuously as the plant grows.
Apoptosis	The death of cells which occurs as a normal and controlled part of an organism's growth or development. Sometimes also referred to as "programmed cell death"
Chlorosis	Loss of the normal green coloration of leaves of plants, caused by iron deficiency in lime-rich soils, disease, or lack of light.
Chromosome	A threadlike structure of nucleic acids and protein found in the nucleus of most living cells, carrying genetic information in the form of genes.
Cytogenetic	The study of inheritance in relation to the structure and function of chromosomes.
Deterministic (effects)	describe a cause and effect relationship between radiation and certain side-effects. They are also called non-stochastic effects to contrast with chance-like stochastic effects (e.g. cancer induction). Deterministic effects have a threshold below which the effect does not occur. The threshold may be very low and may vary from person to person. However, once the threshold has been exceeded, the severity of an effect increases with dose.
Dose	An amount of ionising radiation received or absorbed at one time or over a specified period.
Dosimetry	The determination and measurement of the amount or dosage of radiation absorbed by a substance or living organism.
Dry matter	The part of a substance which would remain if all its water content was removed.
Ecotoxicology	The branch of science that deals with the nature, effects, and interactions of substances that are harmful to the environment.
epigenetic	Relating to or arising from non-genetic influences on gene expression.
Eukaryote	An organism consisting of a cell or cells in which the genetic material is DNA in the form of chromosomes contained within a distinct nucleus. Eukaryotes include all living organisms other than the eubacteria and archaea.
Fallout	Radioactive particles that are carried into the atmosphere after a nuclear explosion and gradually fall back as dust or in precipitation.
Fission	Division or splitting into two or more parts (chiefly of atoms).
Fluctuating asymmetry	The rising and falling irregularly in number or amount of lack of equality or equivalence between parts or aspects of something; lack of symmetry.
Freeware	Software that is available free of charge.
Genome	The complete set of genes or genetic material present in a cell or organism.

Geological	Relating to the study of the earth's physical structure and substance.
Germline	A series of germ cells each descended or developed from earlier cells in the series, regarded as continuing through successive generations of an organism.
Glutathione	A compound involved as a coenzyme in oxidation–reduction reactions in cells. It is a tripeptide derived from glutamic acid, cysteine, and glycine.
Half-life	The time taken for the radioactivity of a specified isotope to fall to half its original value.
Herbaceuous	From Latin herbaceus 'grassy' (from herba 'grass, herb') + -ous.
heterozygosity	The possession of two different alleles of a particular gene or genes by an individual.
Homeostasis	The tendency towards a relatively stable equilibrium between interdependent elements, especially as maintained by physiological processes.
Hormesis	The phenomenon or condition of a substance or other agent having a beneficial physiological effect at low levels of exposure even though toxic or otherwise harmful at higher levels.
Hydroponic	Relating to or involving hydroponics, the process of growing plants in sand, gravel, or liquid.
In situ	Latin: In the original place.
Ionising	Convert (an atom, molecule, or substance) into an ion or ions, typically by removing one or more electrons.
Meristem	A region of plant tissue, found chiefly at the growing tips of roots and shoots and in the cambium, consisting of actively dividing cells forming new tissue.
Methylation	Introduce a methyl group into (a molecule or compound).
Morphometrics	The process of measuring the external shape and dimensions of landforms, living organisms, or other objects.
Mutagnesis	The production of genetic mutations.
open-access	Availability to all.
Petiole	The stalk that joins a leaf to a stem.
Phenomics	The study of the phenotypic counterpart or expression of the genome; the complete set of phenotypic characteristics of an organism.
Phenotype	The set of observable characteristics of an individual resulting from the interaction of its genotype with the environment.
Photoinhibition	Inhibition of a physiological process (and hence sometimes the growth of an organism) by light, especially inhibition of photosynthesis at high levels of sunlight.
Photolysis	he decomposition or separation of molecules by the action of light.
Plastid	Double-membraned 'sac-like' organelles, generally involved in either the manufacture or storage of food. They include chloroplasts, chromoplasts and leucoplasts.
Ploidy	The number of sets of chromosomes in a cell, or in the cells of an organism.
Primordial	Existing at or from the beginning of time; primeval.
Prokaryote	A microscopic single-celled organism which has neither a distinct nucleus with a membrane nor other specialized organelles, including the bacteria and cyanobacteria.

Propagule	A vegetative structure that can become detached from a plant and give rise to a new plant, e.g. a bud, sucker, or spore.
Protocontinent	A landmass that existed at some point in the past. Protocontinents that are thought to have comprised some or all of the present-day continents in a single landmass are also known as supercontinents.
Quiescent	In a state or period of inactivity or dormancy.
Radiation	The emission of energy as electromagnetic waves or as moving subatomic particles, especially high-energy particles which cause ionisation.
Radioactive	Emitting or relating to the emission of ionizing radiation or particles.
Radioecology	The study of the ecological effects of radioactive materials and ionizing radiation.
Radiolysis	The molecular decomposition of a substance by ionising radiation.
Radionuclide	A radioactive nuclide.
Redox	A process in which one substance or molecule is reduced and another oxidised; oxidation and reduction considered together as complimentary processes.
Redundancy	The notion that loss can occur in populations without much effect (if any at all) on the structure/function of a community.
Senescence	The condition or process of deterioration with age. The last stage of life of a plant.
Sessile	Fixed in one place; immobile.
Silique	Latin, literally 'pod'.
Spectrophotometer	An apparatus for measuring the intensity of light in a part of the spectrum, especially as transmitted or emitted by particular substances.
Stochastic	Randomly determined; having a random probability distribution or pattern that may be analysed statistically but may not be predicted precisely.
Stressor	A chemical or biological agent, environmental condition, external stimulus or an event that causes stress to an organism.
supernatant	Denoting the liquid lying above a solid residue after crystallisation, precipitation, centrifugation, or other process.
Tectonic	Relating to the structure of the earth's crust and the large-scale processes which take place within it.
Thermoluminescence	The property of some materials which have accumulated energy over a long period of becoming luminescent when pre-treated and subjected to high temperatures. Specifically in this context: A thermoluminescent dosimeter (TLD) is a type of radiation dosimeter. It measures ionising radiation exposure by measuring the intensity of visible light emitted by a crystal inside the detector when the crystal is heated. The intensity of light emitted is dependent upon the radiation exposure.
Transgenerational	Acting across multiple generations.

References

Abramov, V.I., Fedorenko, O.M., and Shevchenko, V.A. (1992) Genetic consequences of radioactive contamination for populations of Arabidopsis. *Sci. Total Environ.* 112, 19-28.

Adu, M.O., Chatot, A., Wiesel, L., Bennett, M.J., Broadley, M.R., White, P.J. *et al*. (2014) A scanner system for high-resolution quantification of variation in root growth dynamics of Brassica rapa genotypes. *J. Exp. Bot*. 65, 2039–2048.

Ahuja, S., Kumar, M., Kumar, P., Gupta, V.K., Singhal, R.K., Yadav, A. *et al*. (2014). Metabolic and biochemical changes caused by gamma irradiation in plants. *J. Radioanal. Nucl. Chem.* 300, 199-212.

Alikamanoğlu, S., Yaycılı, O., Atak, Ç. and Rzakoulieva, A. (2007) Effect of magnetic field and gamma radiation on Paulowina tomentosa tissue culture. *Biotech. Biotechnol. Equip*. 21, 49-53.

Alves-Silva, E., Santos, J. C. and Cornelissen, T. G. (2018) How many leaves are enough? The influence of sample size on estimates of plant developmental instability and leaf asymmetry. *Ecological Indicators.* [Article in Press].

Anbar, A. D. (2008) Elements and Evolution. *Science*. 322(5907), 1481-1483.

Anjum, A., Umar, N. and Chan, M-T. (2010) *Acscorbate-Glutathione Pathway and Stress Tolerance in Plants*. Springer: Heidelberg.

Antonova, E.V., Karimullina, E.M., and Pozolotina, V.N. (2013) Intraspecific variation in Melandrium album along a radioactive contamination gradient at the Eastern Ural radioactive trace. *Russian J. Ecol*. 44, 18-27.

Archibald, J. M. (2015) Endosymbiosis and eukaryotic cell evolution. *Curr. Biol.* 25 (19), 911-921.

Arena, C., De Micco, V., and De Santo, A.V. (2012) Bioregenerative life support systems in space (BLSS): The effects of radiation on plants. *Annales Kinesiologiae*. 3(1).

Berger, T., Hajek, M., Bilski, P., Korner, C., Vanhavere, F. and Reitz, G. (2012) Cosmic radiation exposure of biological test systems during the EXPOSE-E mission. *Astrobiology*. 12(5), 387-92.

Berger, T., Przybyla, B., Matthiä, D., Reitz, G., Burmeister, S., Labrenz, J., Bilski, P., Horwacik, T., Twardak, A., Hajek, M., Fugger, M., Hofstätter, C., Sihver, L., Palfalvi, J.K., Szabo, J., Stradi, A., Ambrozova, I., Kubancak, J., Brabcova, K. P., Vanhavere, F., Cauwels, V., Van Hoey, O., Schoonjans, W., Parisi, A., Gaza, R., Semones, E., Yukihara, E.G., Benton, E.R., Doull, B. A, Uchihori, Y, Kodaira, S., Kitamura, H. and Boehme, M. (2016) DOSIS & DOSIS 3D: long-term dose monitoring onboard the Columbus Laboratory of the International Space Station (ISS). *J. Space Weather Space Clim*. 6, A39.

Berger, T. (2017) *DOSIS & DOSIS 3D on-board the ISS Current Status / Science Overview / Work in Progress* [Presentation at 22nd WRMISS meeting] Available from: *wrmiss.org/workshops/twentysecond/Berger.pdf [Accessed 21 July 2018].*

Biermans, G., Horemans, N., Vanhoudt, N., Vandenhove, H., Saenen, E., Van Hees, M., *et al*. (2015). *Arabidopsis thaliana* seedlings show an age-dependent response on

growth and DNA repair after exposure to chronic γ-radiation. *Environ. Exp. Bot.* 109, 122-130.

Björk, M. and Gilek, M. (eds) (2005) DELIVERABLE D4b: Overview of Ecological Risk Characterisation Methodologies ERICA Reports [online]. https://wiki.ceh.ac.uk/display/rpemain/ERICA+reports.

Blackith, R. E., and Reyment (1971) *R.A. Multivariate Morphometrics*. Academic Press. London-New York.

Blakeslee, A.F. (1936). *Twenty-five years of mutation research*. 1910-1935. Brooklyn Botanic Garden Memoirs 4, 29-40.

Boratyński, Z., Arias, J. M., Garcia, C., Mappes, T., Mousseau, T. A., Møller, A. P. *et al*. (2016) Ionising radiation from Chernobyl affects development of wild carrot plants. *Sci. Rep*. 6, 39282.

Bochicchio, R., Sofo, A., Terzano, R., Gattullo, C.E., Amato, M., and Scopa, A. (2015) Root architecture and morphometric analysis of *Arabidopsis thaliana* grown in Cd/Cu/Zn-gradient agar dishes: A new screening technique for studying plant response to metals. *Plant Physiol. Biochem.* 91, 20-7.

Borics, G., Varbio, G. and Padisak, J. (2013) Disturbance and stress: Different meanings in ecological dynamics? *Hydrobiologica* 711(1), 1-7.

Boubriak, I.I., Grodzinsky, D.M., Polischuk, V.P., Naumenko, V.D., Gushcha, N.P. *et al*. (2008) Adaptation and impairment of DNA repair function in pollen of Betula verrucosa and seeds of Oenothera biennis from differently radionuclide-contaminated sites of Chernobyl. *Ann. Bot.* 101, 267-276.

Boubriak, I., Akimkina, T., Polischuk, V. Long term effects of Chernobyl contamination on DNA repair function and plant resistance to different biotic and abiotic stress factors. (2016) *Cytol. Genet.* 50: 381.

Boyes, D.C., Zayed, A. M., Ascenzi, R., McCaskill, A. J., Hoffman, N. E. and Davis, K. R. (2001) Growth Stage–Based Phenotypic Analysis of Arabidopsis: A Model for High Throughput Functional Genomics in Plants. *The Plant Cell* 13, 1499-1510.

Boyko, A. and Kovalchuk, I (2008) Epigenetic control of plant stress response. *Environ Mol Mutagen.* 49(1), 61-72.

Bray, C.M. and West, C.E. (2005) DNA repair mechanisms in plants: crucial sensors and effectors for the maintenance of genome integrity. *New Phytol.* 168, 511-528.

Buisset-Goussen, A., Goussen, B., Della-Vedova, C., Galas, S., Adam-Guillermin, C., and Lecomte-Pradines, C. (2014) Effects of chronic gamma irradiation: a multigenerational study using Caenorhabditis elegans. *J. Environ. Radioact*. 137, 190-197.

Bylesjö, M., Segura, V., Soolanayakanahally, R. Y., Rae, A. M., Trygg, J., Gustafsson, P., Jansson, S. and Street, N. R. (2008) LAMINA: a tool for rapid quantification of leaf size and shape parameters. *BMC Plant Biology*. 8, 82.

Caplin, N. and Willey, N. J. (2018) Higher Plants and Radioprotection: From Acute High Doses to Chronic Low Doses. *Front. Plant Sci*. 9, 847.

Celik, O., Atak, C., and Suludere, Z. (2014) Response of soybean plants to gamma radiation: Biochemical analyses and expression patterns of trichome development. *Plant Omics* 7, 382-391.

Cheng, L., Yang, H., Lin, B., Wang, Y., Li, W., Wang, D. and Zhang, F. (2010) Effect of gamma-ray radiation on physiological, morphological characters and chromosome aberrations of minitubers in *Solanum tuberosum* L. *Int. J. Radiat. Biol.* 86(9), 791-799.

Cheng, Z.X., Lin, J.C., Lin, T.X., Xu, M., Huang, Z.W., Yang, Z.J. *et al*. (2014) Genome-wide analysis of radiation-induced mutations in rice (*Oryza sativa* L. ssp *indica*). *Molec. Biosys.* 10, 795-805.

Cheng, M. C., Ko, K., Chang, W. L., Kuo, W. C., Chen, G. H. and Lin, T. P.(2015) Increased glutathione contributes to stress tolerance and global translational changes in Arabidopsis *Plant J*. 83(5), 926-39.

Coe, J.P., Rahman, I., Sphyris, N., Clarke, A.R. and Harrison, D.J. (2002) Glutathione and p53 independently mediate responses against oxidative stress in ES cells. *Free Radical Biology and Medicine*. 15:32(2), 187-196.

Consolini, G. (2018) Emergence of Dynamical Complexity in the Earth's Magnetosphere. Pp 177-202 In *Machine Learning Techniques for Space Weather.* Eds Camporeale. E., Wing S.,Johnson, J.R., Elsevier.

Copplestone, D., Howard, B. J. and Brechignac, F. (2004). The ecological relevance of current approaches for environmental protection from exposure to ionising radiation. *J. Environ. Radioac*. 74(1-3), 31-41.

Couto, N., Wood, J., Barber, J. (2016) The role of glutathione reductase and related enzymes on cellular redox homoeostasis network. *Free Rad. Biol. & Med*. 95, 27-42.

Crown copyright (2017) *The Ionising Radiation Regulations.* Available from: https://www.legislation.gov.uk/uksi/2017/1075 [Accessed 13 April 2018].

Czarnocka, W. and Karpiński, S. (2018) Friend or foe? Reactive oxygen species production, scavenging and signaling in plant response to environmental stresses. *Free Rad. Biol. & Med.* (Article in Press).

Danchenko, M., Klubicova, K, Krivohizha, M. V., Berezhna, V. V., Sakada, V. I., Hajduch, M. *et al*. (2016) Systems biology is an efficient tool for investigation of low-dose chronic irradiation influence on plants in the Chernobyl zone. *Cytol. Genet.* 50, 400.

Dartnell, L. R. (2011) Ionizing radiation and life. *Astrobiol.* 11(6), 551-82.

De Micco, V., Paradiso, R., Aronne, G., De Pascale, S., Quarto, M., and Arena, C. (2014) Leaf anatomy and photochemical behaviour of *Solanum lycopersicum* L. plants from seeds irradiated with low-LET ionising radiation. *Sci. World J.* 428141.

DeLoughrey, E.M. (2013) The myth of isolates: ecosystem ecologies in the nuclear *Pacific. Cult. Geog.* 20, 167-184.

Demidchik, V. (2015) Mechanisms of oxidative stress in plants: From classical chemistry to cell biology. *Environ. Exp. Bot*. 109, 212-228.

Department for Business, Energy and Industrial Strategy (2018) *Geological Disposal Facility (GDF) for higher-activity radioactive waste* [online]. London: Department for Business, Energy and Industrial Strategy. Available from: https://www.gov.uk/government/collections/geological-disposal-facility-gdf-for-high-activity-radioactive-waste [Accessed 13 April 2018].

Department for Business, Energy and Industrial Strategy (2018) Special feature: Nuclear capacity in the UK [online] Available from: https://www.gov.uk/government/uploads/...data/.../Nuclear_Capacity_in_the_UK.pdf [Accessed 13 April 2018].

Doná M., Ventura L., Macovei A., Confaloneiri, M., Savio, M., Giovannini A. *et al*. (2013) Gamma irradiation with different dose rates induces different DNA damage responses in *Petunia x hybrida* cells. *J. Plant Physiol.* 170(8), 780-787.

Downie, H. F., Adu, M. O., Schmidt, S., Otten, W., Dupuy, L. X., White, P. J. *et al*. (2015) Challenges and opportunities for quantifying roots and rhizosphere interactions through imaging and image analysis. *Plant Cell Environ.* 38, 1213-1232.

Dyachenko, O. V., Zakharchenko, N. S., Shevchuk, T. V., Bohnert, H. J., Cushman, J. C. and Buryanov, Ya. I. (2006) Effect of hypermethylation of CCWGG Sequences in DNA of Mesembryanthemum crystallinum plants on their adaptation to salt stress. Biochem. 71(4), 570-575.

ERICA (2003) *Environmental risk from ionizing contaminants: assessment and management*. Developed under EU 6th Framework Program. Contract No, ERICA. FI6R-CT-2004-508847. www.erica-project.org.

European Union (2019) Holders of the copyright for this work carried out by: Cinelli, G, Gruber, V., De Felice, L., Bossew, P., Hernandez-Ceballos, M. A., Tollefsen, T., Mundigl, S. and De Cort, M. European annual cosmic-ray dose: estimation of population exposure*. Journal of Maps.* Vol. 13 , Iss. 2, 2017

Esnault, M.A., Legue, F., and Chena C. (2010) Ionizing radiation: Advances in plant response. *Environ. Exp. Bot.* 68, 231–237.

Evseeva, T., Majstrenko, T., Geras'kin, S, Brown, J. And Belykh, E. (2009) Estimation of ionizing radiation impact on natural *Vicia cracca* populations inhabiting areas contaminated with uranium mill tailings and radium production wastes. *Sci. Tot. Environ*. 407(20), 5335-43.

Fernandez-Ballester, G., Cerdá, A. and Martínez, V. (1997) Role of calcium in short-term responses of bean plants to osmotic or saline shocks. *J. Plant Physiol.* 151(6). 741-747.

Fiorani, F., & Schurr, U. (2013). Future Scenarios for Plant Phenotyping. *Ann. Rev. Plant Biol.*, 64(1), 267–291.

Foyer, C. H. and Noctor, G. (2011) Ascorbate and Glutathione: The Heart of the Redox Hub. *Plant Phys*. 155(1). 2-18.

Foyer, C. H. and Noctor, G. (2016) Stress-triggered redox signalling: what's in pROSpect? *Plant Cell Environ*. 39, 951–964.

Foyer, C. H., Ruban, A. V. and Noctor, G. (2017) Viewing oxidative stress through the lens of oxidative signalling rather than damage. *Biochem. J*. 474, 877-883.

Frei ER, Ghazoul J, Pluess AR (2014) Plastic Responses to Elevated Temperature in Low and High Elevation Populations of Three Grassland Species. *PLoS ONE* 9(6): e98677.

Freidberg, E.C. (1997) *Correcting the Blueprint of Life*. Cold Springharbor Laboratory Press.

Freidberg, E.C. (2003) DNA damage and repair. *Nature*. 421, 436-440.

Fulcher, N. and Sablowski, R. (2009) Hypersensitivity to DNA damage in plant stem cell niches. *Proc. Natl. Acad. Sci.* USA 106, 20984-20988.

Fuller, N., Smith, J. T., Nagorskaya, L. L., Gudkov, D. I. and Ford, A. T. (2017) Does Chernobyl-derived radiation impact the developmental stability of *Asellus aquaticus* 30 years on? *Sci Total Environ* 576, 242-250.

Gabrisova, D., Klubicova, K., Danchenko, M., Goemoery, D., Berezhna, V.V., Skultety, L.*et al*. (2016) Do cupins have a function beyond being seed storage proteins? *Front. Plant Sci.* 6,1215.

Garnier-Laplace, J., and Gilbin, R. (ed) (2006) *Derivation of predicted no effect dose rate values for ecosystems (and their sub-organisational levels) exposed to radioactive substances Deliverable D5*. European Commission, 6th Framework Contract No Fl6R-CT-2003-508847, Cadarache: IRSN.

Geras'kin, S. A., Kim, J. K., Oudalova, A. A., Vasiliyev, D. V., Dikareva, N. S., Zimin, V. L., & Dikarev, V. G. (2005). Bio-monitoring the genotoxicity of populations of Scots pine in the vicinity of a radioactive waste storage facility. *Mutation Research/Genetic Toxicology and Environmental Mutagenesis, 583(1), 55–66.*

Geras'kin, S.A., Fesenko, S.V., and Alexakhin, R.M. (2008). Effects of non-human species irradiation after the Chernobyl NPP accident. *Environ. Int.* 34, 880-897.

Geras'kin, S., Oudalova, A., Dikareva, N., Spiridonov, S., Hinton, T., Chernonog, E. *et al*. (2011) Effects of radioactive contamination on Scots pines in the remote period after the Chernobyl accident. *Ecotoxicology*. 20(6), 1195-208.

Geras'kin, S., Oudalova, A., Dikarev., V. G., Dikareva, N. S., Mozolin, E. M., Hinton, T., Spiridonov, S.I., Copplestone, D., and Garnier-Laplace, J. (2011) Effects of chronic exposure in populations of Koeleria gracilis Pers. From the Semipalatinsk nuclear test site, Kazakhstan. *J. Environ. Radioac.* 104: 55-63.

Geras'kin, S., Evseeva, T. and Oudalova, A. (2013) Effects of long-term chronic exposure to radionuclides in plant populations. *J. Environ. Radioac.* 121, 22-32.

Geras'kin, S *et al*. (2016) The Consequences of chronic radiation exposure of Scots Pine in the remote period after the Chernobyl accident. *Russian J. Ecol.* 47. 26-38.

Georgieva, M., Rashydov, N.M., and Hajduch, M. (2017) DNA damage, repair monitoring and epigenetic DNA methylation changes in seedlings of Chernobyl soybeans. *DNA Repair 50*, 14-21.

Ghiassi-Nejad, M., Beitollahi A., Asefi, M. and Reza-Najad, F. (2003) Exposure to 226Ra from consumption of vegetables in the high-level natural radiation area of Ramsar-Iran*. J. Environ. Radioac*. 66, 215-225.

Google Scholar (2018) No Title Available from: https://scholar.google.co.uk/scholar?oe=utf-8&client=firefox-b-ab&gfe_rd=cr&dcr=0&um=1&ie=UTF-8&lr&cites=8599984381812260062 [Accessed 04 April 2018].

Gray, L. H. and Scholes, M. E. (1951) The effect of ionizing radiations on the broad bean root. Vlll. *Brit. J. Radiol.* 24, 176-180.

Gudkov, I.N. and Grodzinsky, D. M. (1982) Cell radiosensitivity variation in synchronously-dividing root meristems of *Pisum sativum L.* and *Zea mays L.* during the mitotic cycle. *Int. J. Radiat. Biol. Relat. Stud. Phys. Chem. Med.* 41(4), 401-409.

Gunckel, J. E. (1956) IV. The Effects of ionizing radiation on plants: Morphological effects. *Quart. Rev. Biol*. 32(1), 46-56.

Hamideldin, N. and Hussin, O. S. (2014) Morphological, physiological and molecular changes in Solanum tuberosum L. in response to pre-sowing tuber irradiation by gamma rays. *Amer. J. Food Nutr*. 2(1), 1-6.

Hanson, F. B., & Heys, F. M. (1928) The effects of radium in producing lethal mutations in Drosophila melanogaster. *Science*. 68(1753), 115-116.

Harb, A., Krishnan, A., Ambavaram, M. and Pereira, A. (2010). Molecular and physiological analysis of drought stress in Arabidopsis reveals early responses leading to acclimation in plant growth. *Plant Physiology* 154(3), 1254-1271.

Hayashi, G., Moro, C. F., Rohila, J. S., Shibato, J., Kubo, A., Imanaka, T. *et al*. (2015) 2D-DIGE-based proteome expression changes in leaves of rice seedlings exposed to low-level gamma radiation at Iitate village, *Fukushima. Plant Signal. Behav.* 10(12), e1103406.

Hessen, D. (2008) Solar Radiation and Life. In *Solar Radiation and Human Health*, ed. Bjertness, E. The Norwegian Academy of Science and Letters, Oslo, Norway, pp 123-137.

Houle, D., Govindaraju, D.R., and Omholt, S (2010) Phenomics: the next challenge. *Nat. Rev. Genet*. 11, 855.

HPS (2015) Background radiation fact sheet. Available from: http://hps.org/documents/background_radiation_fact_sheet.pdf. [Accessed 19th January 2018].

IAEA (International Atomic Energy Agency) (1992) *Effects of ionizing radiation on plants and animals at levels implied by current radiation protection standards.* Technical Reports Series No. 332 (Vienna: IAEA).

IAEA (2003) Proceedings of the Third International Symposium on the Protection of the Environment from Ionising *Protection of the environment from ionising radiation: the development and application of a system of radiation protection for the environment*. IAEA. Vienna.

IAEA (2018) The Database on Nuclear Power Reactors. Available from: https://www.iaea.org/pris/. [Accessed 19th January 2018].

ICRP (International Commission on Radiological Protection) (2008) *Environmental Protection - the Concept and Use of Reference Animals and Plants*. ICRP Publication 108. Ann. ICRP 38 (4-6).

ICRP (2014) *Protection of the Environment under Different Exposure Situations*. ICRP Publication 124. Ann. ICRP 43(1).

Jackson, S.P. and Bartek, J. (2009) The DNA-damage response in human biology and disease. *Nature.* 461, 1071-8.

Jan, S., Parween, T., Siddiqi, T.O., and Mahmooduzzafar (2012) Enhancement in furanocoumarin content and phenylalanine ammonia lyase activity in developing seedlings of *Psoralea corylifolia L*. in response to gamma irradiation of seeds. *Radiat. Environ. Biophys.* 51, 341-347.

Jordan, C.F. (1986). The Ecological Effects of Ionising Radiation. In *Ecological Knowledge and Environmental Problem-Solving: Concepts and Case Studies* National Research Council, National Academies Press, Washington DC, pp 331-344.

Karam, P.A. and Leslie, S. A. (1999) Calculations of background beta-gamma radiation dose through geologic time. *Health Phys.* 77 (6), 662-7.

Karimullina, E., Antonova, E., Pozolotina, V., Tokarev, A., and Minko, S. (2015) The toxicity of engineered nanoparticles on seed plants chronically exposed to low-level environmental radiation. *Russ. J. Ecol.* 46, 236-245.

Kordium E.L., and Sidorenko, P.G. (1997) The results of the cytogenetic monitoring of the species of angiosperm plants growing in the area of the radionuclide contamination after the accident at the Chernobyl Atomic Electric Power Station. *Tsitol Genet* 31:39–46.

Kovalchuk, O., Kovalchuk, I., Arkhipov, A., Telyuk, P., Hohn, B., and Kovalchuk, L. (1998 a). The Allium cepa chromosome aberration test reliably measures genotoxicity of soils of inhabited areas in the Ukraine contaminated by the Chernobyl accident. Mut. Res. - *Genet. Toxicol. Environ. Mutag*. 415, 47-57.

Kovalchuk, I., Kovalchuk, O., Arkhipov, A., and Hohn, B. (1998 b). Transgenic plants are sensitive bioindicators of nuclear pollution caused by the Chernobyl accident. *Nat. Biotechnol.* 16, 1054-1059.

Kovalchuk, O., Burke, P., Arkhipov, A., Kuchma, N., James, S. J.,Kovalchuk, I. and Pogribny, I. (2003) Genome hypermethylation in *Pinus sylvestris* of Chernobyl—a mechanism for radiation adaptation? *Mutation Research/Fundamental and Molecular Mechanisms of Mutagenesis*. 529(1-2), 13-20.

Kovalchuk, I., Abramov, V., Pogribny, I., and Kovalchuk, O. (2004). Molecular aspects of plant adaptation to life in the Chernobyl zone. *Plant Physiol.* 135, 357-363.

Kozlov, M.V., and E.L. Zvereva (2015) Confirmation bias in studies of fluctuating asymmetry *Ecol. Indic.* 57, 293-297

Larson, C. M. (1988) An overview of the ERICA Integrated Approach to the assessment and management of environmental risks from ionising contaminants. *J. Environ. Radioac*. 99(9), 1364-1370.

Latowski, D., Surówka, E. and Strzałka, K. (2010) Regulatory Role of Components of Ascorbate–Glutathione Pathway. In *Ascorbate-Glutathione Pathway and Stress Tolerance in Plants*, Eds Anjum, A., Umar, S., Chain, M-T.. Springer, Science & Business Media, pp1-53.

Li, W., Zhang, C., Lu, Q., Wen, X. and Lu, C. (2011) The combined effect of salt stress and heat shock on proteome profiling in *Suaeda salsa. J. Plant Physiol* 168(15), 1743-1752.

Lin Z, Kong H., Nei, M., and Ma H. (2006) Origins and evolution of the recA/RAD51 gene family: evidence for ancient gene duplication and endosymbiotic gene transfer. *Proc. Natl Acad. Sci*. USA, 103, 10328-10333.

Lugo, A.E. (2004) H.T Odum and the Luquillo experimental forest. *Ecol. Model*. 178, 65-74.

Makarenko, E.S., Oudalova, A.A., and Geras'kin, S.A. (2016) Study of needle morphometric indices in Scots pine in the remote period after the Chernobyl accident. *Radioprot.* 51, 19-23.

Maity, J. P., Mishra, D. Chakraborty, A., Saha, A., Santra, S. C. and Chanda, S. (2005) Modulation of some quantitative and qualitative characteristics in rice (*Oryza sativa L*.) and mung (*Phaseolus mungo L*.) by ionizing radiation. *Radiat. Phys. Chem*. 74, 391-394.

Marcu, D. Damian, G. Cosma, C and Cristea, V. (2013a) Gamma radiation effects on seed germination, growth and pigment content, and ESR study of induced free radicals in maize (*Zea mays*). *J. Biol. Phys*. 39. 625-634.

Marcu, D., Cristea, V. and Daraban, L. (2013b) Dose-dependent effects of gamma radiation on lettuce (*Lactuca sativa* var. *capitala*) seedlings. *Int. J Radiat. Biol.* 89, 219-223.

Meyers, L. A. and Levin, D. A. (2006) On the abundance of polyploids in flowering plants. *Evol.* 60(6), 1198–1206.

Mittler, R. (2017) ROS Are Good. *Trends Plant Sc*i. 22(1), 11-19.

Mostafa, H.H.A., Wang, H.P., Shen, D., Qiu, Y., and Li, X.X. (2015) Sprout differentiation and mutation induction of garlic (*Allium sativum L.)* callus exposed to gamma radiation. *Plant Growth Reg.* 75, 465-471.

Møller, A.P. and Mousseau, T.A. (2015) Strong effects of ionizing radiation from Chernobyl on mutation rates. *Sci. Rep.* 5, 8363.

Møller, A.P., Shyu, J.G. and Mousseau, T.A. (2016). Ionizing radiation from Chernobyl and the fraction of viable pollen*. Int. J. Plant Sci.* 177, 727-735.

Morris, J. L. Puttick, M. N., Clark, J. W., Edwards, D., Kenrick, P., Pressel, S. Wellman, C. H., Yang, Z., Schneider, H. and Donoghue, C. J. (2018) Timescale of early land plant evolution. Proc Nat Acad. Sci. USA 115 (10), 2274-2283.

Mousseau, T.A., Welch, S.M., Chizhevsky, I., Bondarenko, O., Milinevsky, G., and Tedeschi, D.J. (2013) Tree rings reveal extent of exposure to ionizing radiation in Scots pine Pinus sylvestris. *Trees-Struc. Func*. 27, 1443-1453.

Muller, H. J. (1927) Artificial transmutation of the gene. *Science* 66(699), 84-87.

Nagata, T., Todoriki, S., Kikuchi, S. (2004) Radial expansion of root cells and elongation of root hairs of *Arabidopsis thaliana* induced by massive doses of gamma irradiation. *Plant Cell Physiol*. 45(11), 1557-1565.

National Aeronautics and Space Administration (2017*) Space Shuttle and International Space Station* Available from: https://www.nasa.gov/centers/kennedy/about/information/shuttle_faq.html [Accessed 05 April 2018].

National Aeronautics and Space Administration (2018) *Radiation Metadata for GLDS Studies* Available from: https://genelab-data.ndc.nasa.gov/genelab/environmental/radiation [Accessed 05 April 2018].

Navarrete, M. H., Carrera, P., deMiguel, M. and delaTorre, C. (1997) A fast comet assay variant for solid tissue cells. The assessment of DNA damage in higher plants. *Mutat. Res. Genet. Tox. Environ.* 389(2-3), 271-277.

Nelson-Beyer, W. and Meador, J. P. (2011) *Environmental Contaminants in Biota: Interpreting Tissue Concentrations*. 2nd Ed. Boca Raton: CRC Press.

Nishiguchi, M., Nanjo, T., and Yoshida, K. (2012) The effects of gamma irradiation on growth and expression of genes encoding DNA repair-related proteins in Lombardy poplar (*Populus nigra* var. *italica*). *J. Environ. Radioact*. 109, 19-28.

Niklas, K. J. (2004) Plant allometry: is there a grand unifying theory? *Biol. Rev*. 79, 871-889.

Noctor, G., Reichheld, J. P. and Foyer, C. H. (2017) ROS-related redox regulation and signalling in plants. *Sem. Cell & Dev. Biol.* (Article in Press).

Oladosu, Y. Rafii, M.Y., Abdullah, N., Hussin, G., Ramli, A., Rahim, H.A. *et al*. (2016) Principle and application of plant mutagenesis in crop improvement: a review. *Biotech. Biotechnol. Equip.* 30, 1-16.

Oxford University Press (2018) *Oxford English Dictionary* Available from: https://en.oxforddictionaries.com/ [Accessed 28 April 2018].

Pandey, P., Singh, J., Achary, V., Mohan., and Reddy, M. K. (2015) Redox homeostasis via gene families of ascorbate-glutathione pathway. *Front. Environ. Sci.* 3, 25.

Pattison, D.I., and Davies, M.J. (2006) Actions of ultraviolet light on cellular structures In *Cancer: Cell Structures, Carcinogens and Genomic Instability,* ed Bignold, L.P. Birkhäuser Verlag, Switzerland, pp 131-157.

Paul, A-L., Zupanska, A. K., Schultz, E. R. and Ferl, R.J. (2013) Organ-specific remodelling of the Arabidopsis transcriptome in response to spaceflight. *BMC Plant Biol*. 13,112.

Phillips, T. (2008) The role of methylation in gene expression. *Nature Education* 1(1),116.

Pozolotina, V.N., Antonova, E.V., and Bezel, V.S. (2012) Comparison of remote consequences in Taraxacum officinale seed progeny collected in radioactively or chemically contaminated areas. *Ecotoxicol.* 21, 1979-1988.

Qi, W. C., Zhang, L., Wang, L., Xu, H. B., Jin, Q. S. and Jiao, Z. (2015) Pretreatment with low-dose gamma irradiation enhances tolerance to the stress of cadmium and lead in Arabidopsis thaliana seedlings. *Ecotox. & Environ. Safety* 115, 243-249.

Rabbow, E., Rettberg, P., Barczyk, S., Bohmeier, M., Parpart, A., Panitz, C., Horneck, G., von Heise-Rotenburg, R., Hoppenbrouwers, T., Willnecker, R., Baglioni, P., Demets, R. and Dettmann, J. (2012) EXPOSE-E: an ESA astrobiology mission 1.5 years in space. *Astrobiology.* 12(5), 374-86.

Reitz, G. (2008) Characteristic of the radiation field in low earth orbit and in deep space. *Z. Med. Phys.* 18, 223-243.

Renault, H., Roussel, V., El Amrani, A., Arzel, M, Renault, D., Bouchereau, A and Deleu, C (2010). The Arabidopsis pop2-1 mutant reveals the involvement of GABA transaminase in salt stress tolerance. *BMC Plant Biology* 10, 20.

Remagnino, P., Mayo, S. Wilkin, P., Cope, J. and Kirkup, D. (2017). Morphometrics: A Brief Review. In *Computational Botany*, eds Remagnino, P., Mayo, S. Wilkin, P., Cope, J. and Kirkup, D., Springer, Berlin, pp 11-32.

Ricaud, L., Proux, C., Renou, J. P., Pichon, O., Fochesato, S., Ortet, P. and Montane, M. H (2007) ATM-mediated transcriptional and developmental responses to gamma-rays in Arabidopsis. *PLoS One.* 2(5), e430.

Rizhsky, L., Liang, H. and Mittler, R. (2002) The combined effect of drought stress and heat shock on gene expression in tobacco. *Plant Physiol* 130(3), 1143-1151.

RHS Royal Horticultural Society (2018) *Fasciation* Available from: https://www.rhs.org.uk/advice/profile?pid=525 [Accessed 30 April 2018].

Rohlf, F.J., Marcus, L.F. (1993) A revolution in morphometrics. TREE 8 (4), 129-132

Sahr, T., Voigt, G., Schimmack, W., Paretzke, H.G., and Ernst, D. (2005). Low-level radiocaesium exposure alters gene expression in roots of Arabidopsis. *New Phytol*. 168, 141-148.

Saghirzadeh, M., Gharaati, M. R., Mohammadi, S. and Ghiassi-Nejad, M. (2008) Evaluation of DNAS damage in the root cells of Allium cepa seeds growing in soil of high background radiation areas of Ramsar – Iran. *J. Environ. Radioac*. 99. 1698-1702.

Schmidt, R., Kunkowska, A. B. and Schippers, J. H. M. (2016) Role of reactive oxygen species during cell expansion in leaves. *Plant Physiology.* 172, 2098-2106/

Schulze, E. D., Beck, E. and Müller-Hohenstein, K. (2005) *Plant Ecology.* Berlin Heidelberg: Springer.

Sever-Mutlu, S., Djapo, H., Ozmen, S.F., Selim, C., and Tuncel, N. (2015). Gamma-ray irradiation induces useful morphological variation in Bermuda grass. *Not. Bot. Horti Agrobo*. 43, 515-520.

Simmons, D. (2008) Epigenetic influence and disease. *Nat. Educ.* 1(1), 6.

Shahbazi-Gahrouei, D., Gholami, M., & Setayandeh, S. (2013). A review on natural background radiation. *Advanced biomedical research*, *2*, 65.

Shapiguzov, A., Vainonen, J. P., Wrzaczek, M., and Kangasjarvi, J. (2012) ROS-talk - how the apoplast, the chloroplast, and the nucleus get the message through. Front. *Plant Sci* 3, 292-292.

Sidler, C., Li, D.P., Kovalchuk, O., and Kovalchuk, I. (2015). Development-dependent expression of DNA repair genes and epigenetic regulators in *Arabidopsis* plants exposed to ionizing radiation. *Radiat. Res*. 183, 219-232.

Siasou, E., Johnson, D., and Willey, N.J. (2017). An Extended dose–response model for microbial responses to ionizing radiation. *Front. Environ. Sci.* 5, 6.

Slesak, I, Slesak, H. and Kruk, J. (2012) Oxygen and Hydrogen Peroxide in the Early Evolution of Life on Earth: In silico Comparative Analysis of Biochemical Pathways. *Astrobiol.* 12, 8.

Smith, J.T., Willey, N.J., and Hancock, J.T. (2012). Low dose ionizing radiation produces too few reactive oxygen species to directly affect antioxidant concentrations in cells. *Biol. Lett.* 8, 594-597.

Stadler, L.J. (1928). Genetic effects of x-rays in maize. *Proc Natl. Acad. Sci.* USA 14, 69-75.

Stadler, J.L. (1928). Mutations in barley induced by X-Rays and radium. *Science* 68, 186-187.

Stadler, L.J. (1930). Some genetic effects of X-rays on plants. *J. Hered*. 21, 4-29.

Stalter, R., and Kincaid, D. (2009). Community Development Following Gamma Radiation at a Pine-Oak Forest, Brookhaven National Laboratory, Long Island, New York. *Am. J. Bot.* 96, 2206-2213.

Sugimoto, M., Oono, Y., Gusev, O., Matsumoto, T., Yazawa, T., Levinskik, M. A., Sychev, V. N., Bingham, G.E., Wheeler, R. and Hummerick, M. (2014) Genome-wide expression analysis of reactive oxygen species gene network in *Mizuna* plants grown in long-term spaceflight. *BMC Plant Bio.* 14,4.

Taheri, S., Abdullah, T.L., Ahmad, Z., and Abdullah, N.A.P. (2014). Effect of acute gamma irradiation on Curcuma alismatifolia varieties and detection of DNA polymorphism through SSR Marker. *Biomed Res. Internat.* 631813.

Takahashi, M. Shaw, G., and Coppin, F. (2016) Special issue: Radioactive contamination in forest ecosystems: From Chernobyl to Fukushima. *J. Environ. Radioac.* 161, 1-2.

Tepfer, D., Zalar, A. and Leach, S. (2012) Survival of plant seeds, their UV screens, and nptII DNA for 18 months outside the International Space Station. *Astrobiol.* 12(5), 512-28.

Tepfer, D. and Leach, S. (2017) Survival and DNA Damage in Plant Seeds Exposed for 558 and 682 Days outside the International Space Station. *Astrobiol*. 17:3. 205-215.

The Arabidopsis Information Resource (2002) *ABRC: Handling of Plants and Seeds*. Available from: https://www.arabidopsis.org/download_files/Protocols/abrc_plant_growth.pdf [Accessed 04 April 2018].

Tsukaya, H. (2017). Leaf shape diversity with an emphasis on leaf contour variation, developmental background, and adaptation. *Semin. Cell. Dev. Biol.* 79, 48-57.

UNSCEAR (United Nations Scientific Committee on the Effects of Atomic Radiation) (1996) *Sources and Effects of Ionizing Radiation*. United Nations, New York.

UNSCEAR (United Nations Scientific Committee on the Effects of Atomic Radiation) (2006) *Effects of Ionising Radiation.* United Nations, New York.

UNSCEAR (United Nations Scientific Committee on the Effects of Atomic Radiation) (2013) Sources, effects and risks of ionizing radiation. *Report to the General Assembly With Scientific Annexes. Volume I.* Available from: http://www.unscear.org/unscear/en/publications/2013_1_Attachments.html [Accessed 28 April 2018].

Van Hoeck, A., Horemans, N., Nauts, R., Van Hees, M., Vandenhove, H., and Blust, R. (2017). Lemna minor plants chronically exposed to ionising radiation: RNA-seq analysis indicates a dose rate dependent shift from acclimation to survival strategies. *Plant Sci*. 257, 84-95.

Vaizogullar, H.E., and Kara, Y. (2016) Effects of gamma radiation on crude oil yield and chemical composition of *Sesamum indicum*-Tan 99 seeds. *Bangl. J. Bot*. 45, 239-242.

Vandenhove, H., Vanhoudt, N., Cuypers, A., van Hees, M., Wannijn, J. and Horemans, N. (2010) Life-cycle chronic gamma exposure of Arabidopsis thaliana induces growth effects but no discernible effects on oxidative stress pathways. *Plant Physiol Biochem*. 48(9), 778-786.

Vanhoudt, N., Horemans, N., Wannijn, J., Robin, N. Van Hees, M. and Vandenhove, H. (2014) Primary stress responses in *Arabidopsis thaliana* exposed to gamma radiation. *J. Environ. Radioac*. 129, 1-6.

Vanyushin B.F. (2006) *DNA Methylation in Plants*. In: DNA Methylation: Basic Mechanisms. Eds Doerfler W., Böhm P., Springer, Berlin, Heidelberg, pp77-122.

Vanyushin, B. F. and V. V. Ashapkin (2011). DNA methylation in higher plants: past, present and future. *Biochim. Biophys. Acta* 1809(8), 360-368.

Volkova, P. Y., Geras'kin, S. A. and Kazakova, E. A. (2017) Radiation exposure in the remote period after the Chernobyl accident caused oxidative stress and genetic effects in Scots pine populations *Sci Rep.* 7, 43009.

Volkova P.Yu., Geras'kin, S.A., Horemans, N., Makarenko, E.S., Saenen, E., Duarte, G.T., Nauts, R., Bondarenko, V.S., Jacobs, G., Voorspoels, S. and Kudin, M. (2018) Chornic radiation exposure as an ecological factor: Hypermethylation and genetic differentiation in irradiated Scots pine populations. *Environ. Pollut*. 232, 105-112.

Wadhwa, S., Gallagher, F. J., Rodriguez-Saona, C. and Holzapfel, C. (2017) Exposure to heavy metal stress does not increase fluctuating asymmetry in populations of isopod and hardwood trees. *Ecol. Indic.* 76, 42-51.

Watanabe, Y., Ichikawa, S., Kubota, M., Hoshino, J., Kubota, Y., Maruyama, K., Fuma, S., Kawaguchi, I., Yoschenko, V.I. and Yoshida, S. (2015) Morphological defects in native Japanese fir trees around the Fukushima Daiichi Nuclear Power Plant. *Sci Rep* 5, 13232.

Willey, N.J. (2016) *Environmental Plant Physiology*. Garland Science. Oxford, UK.

Woodwell, G.M. (1962). Effects of ionizing radiation on terrestrial ecosystems. *Science*138, 572-577.

Xu, W., Ding, G., Yokawa, K., Baluška, F., Li, Q-F., Liu, Y., Shi, W., Liang, J. and Zhang, J. (2013) An improved agar-plate method for studying root growth and response of *Arabidopsis thaliana*. *Sci Rep.* 3, 1273.

Yadav, S. K. (2010) Heavy metals toxicity in plants: An overview on the role of glutathione and phytochelatins in heavy metal stress tolerance of plants. *S. Afr. J. Bot*. 76(2), 167-179.

Yadav, V. (2016) Effect of gamma radiation on various growth parameters and biomass of Canscora decurrens Dalz. *Int. J. Herb. Medic.* 4 (5), 109-115.

Yuan, P., Ding, G., Cai, H., Jin, K., Broadley, M., Xu, F and Shi, L. (2016) A novel Brassica-rhizotron system to unravel the dynamic changes in root system architecture of oilseed rape under phosphorus deficiency. Annals of Botany. 118:2. 173-84.

Zhang, L., Qi, W., Xu, H., Wang, L., and Jiao, Z. (2016). Effects of low-energy N^+-beam implantation on root growth in Arabidopsis seedlings. *Ecotoxicol. Environ. Saf*. 124, 111-119.

Annex A

Statistical Approach

The statistical tests used for each set of results presented in this work are detailed in the methods sections of individual chapters. In terms of data handling, for every set of data produced in each section the first goal was to ascertain whether or not data followed the normal distribution. This was established first via graphical representation, where histograms were used to examine the distribution of the data. The distribution of the data determined how well it accorded with normality, i.e. followed a "bell curve" of normal distribution. When necessary the Shapiro-Wilkes test of normality was applied to determine if parametric or non-parametric statistics were appropriate.

Experiments reported here either had two variables to compare for statistical significance, or no more than three groups. This applied to the statistics in every chapter, regardless of endpoint studied. If the data was normally distributed, then either Welch's two-sample t-tests were carried out (for data sets containing two groups) or, a oneway ANOVA (analysis of variance) was employed. A further development occurred post-ANOVA for normally distributed datasets, whereby if significance was detected, a deeper investigation was carried out by selecting two groups at a time from within the triple group datasets and a Welch's two sample t-test was carried out in order to pinpoint the source of the significance. On occasion, data did not follow a normal distribution. If this could not be mitigated by logging the data (as used in chapter 3) so that the aforementioned tests applicable to normal data could be used, then non-parametric tests were conducted instead. For any non-normal data

throughout this project, Kruskall-Wallis tests were used to test for differences between treatments. On occasion the data demanded a more thorough analysis before the statistical tests were performed. If applicable, Barlett's test for homogeneity of variance was conducted. This occurred when it was suspected that the data was normally distributed but not of equal variance for all samples across treatment groups. Bartlett's test checks the assumption of equal variance and was a suitable option to use before oneway ANOVA were performed. All statistical tests were performed using a 95% confidence level, meaning a 5% chance of incorrectly rejecting the null hypothesis was acceptable. If major significant findings were discovered, then this could have been further scrutinised to avoid Type I errors. However, any significant results were of low resolution when the data set was examined as a whole and it was deemed not necessary to delve further into these tests.

All statistical analyses were performed using R (https://www.r-project.org/) using the open source R Studio graphical user interface (https://www.rstudio.com). CRAN is a network of ftp and web servers around the world that store identical, up-to-date, versions of code and documentation for R. The version of R used in this project was obtained from the CRAN mirror site: https://www.stats.bris.ac.uk/R/.

Annex B

Supplementary information

7.1 Data outputs from R studio

7.1.1 Vertical symmetry

Generation 4 R output:

```
Normality test
shapiro.test(VertSymG4$CONTROL)

Shapiro-Wilk normality test

data:  VertSymG4$CONTROL

W = 0.99218, p-value = 0.7123

shapiro.test(VertSymG4$CADMIUM)

Shapiro-Wilk normality test

data:  VertSymG4$CADMIUM

W = 0.85269, p-value = 1.328e-07

shapiro.test(VertSymG4$`Cs-137`)

Shapiro-Wilk normality test

data:  VertSymG4$`Cs-137`

W = 0.96082, p-value = 0.04556



Data:  VertSymG4
Bartlett's K-squared = 21.764, df = 2, p-value = 1.88e-05

summary(anova_results)
            Df Sum Sq Mean Sq F value Pr(>F)
ind          2  0.226 0.11295   3.877 0.0219 *
Residuals   267  7.778 0.02913

> t.test(x$CONTROL, x$`Cs-137`)

    Welch Two Sample t-test

data:  x$CONTROL and x$`Cs-137`
```

```
t = -0.39385, df = 95.13, p-value = 0.6946
alternative hypothesis: true difference in means is not equal to 0
95 percent confidence interval:
 -0.06117051  0.04091735
sample estimates:
  mean of x   mean of y
-0.02388309 -0.01375650

> t.test (x$CONTROL, x$CADMIUM)

    Welch Two Sample t-test

data:  x$CONTROL and x$CADMIUM
t = -2.5217, df = 125.36, p-value = 0.01293
alternative hypothesis: true difference in means is not equal to 0
95 percent confidence interval:
 -0.11682118 -0.01408502
sample estimates:
  mean of x   mean of y
-0.02388309  0.04157002
> t.test (x$CADMIUM, x$`Cs-137`)

    Welch Two Sample t-test

data:  x$CADMIUM and x$`Cs-137`
t = 1.7052, df = 140.39, p-value = 0.09037
alternative hypothesis: true difference in means is not equal to 0
95 percent confidence interval:
 -0.008818965  0.119472005
sample estimates:
  mean of x   mean of y
 0.04157002 -0.01375650
```

Generation 5 R output:

```
shapiro.test(G5VertSym$CONTROL)

        Shapiro-Wilk normality test

data:  G5VertSym$CONTROL
W = 0.98318, p-value = 0.01289

> shapiro.test(G5VertSym$CADMIUM)

        Shapiro-Wilk normality test

data:  G5VertSym$CADMIUM
```

```
W = 0.97839, p-value = 0.005389

> shapiro.test(G5VertSym$Cs137)

        Shapiro-Wilk normality test

data:  G5VertSym$Cs137
W = 0.96063, p-value = 6.946e-06


 Bartlett test of homogeneity of variances

 Bartlett's K-squared = 10.856, df = 2, p-value = 0.004393

  Df Sum Sq  Mean Sq F value Pr(>F)
ind           2  0.005 0.002698    0.118  0.889
Residuals   621 14.219 0.022897

Welch Two Sample t-test

data:  G5VS$CONTROL and G5VS$Cs137
t = -0.043299, df = 424.91, p-value = 0.9655
alternative hypothesis: true difference in means is not equal to 0
95 percent confidence interval:
 -0.02880125  0.02755969
sample estimates:
 mean of x  mean of y
0.01468309 0.01530387
Welch Two Sample t-test

data:  G5VS$CONTROL and G5VS$CADMIUM
t = 0.42172, df = 371.52, p-value = 0.6735
alternative hypothesis: true difference in means is not equal to 0
95 percent confidence interval:
 -0.02224392  0.03438998
sample estimates:
  mean of x   mean of y
0.014683093 0.008610061

Welch Two Sample t-test

data:  G5VS$CADMIUM and G5VS$Cs137
t = -0.42668, df = 406.7, p-value = 0.6698
alternative hypothesis: true difference in means is not equal to 0
95 percent confidence interval:
 -0.03753372  0.02414609
sample estimates:
  mean of x   mean of y
0.008610061 0.015303872
```

Generation 6 R output:

```
shapiro.test(G6VertSym$CONTROL)

        Shapiro-Wilk normality test

data:  G6VertSym$CONTROL
W = 0.96112, p-value = 5.634e-05

> shapiro.test(G6VertSym$CADMIUM)

        Shapiro-Wilk normality test

data:  G6VertSym$CADMIUM
W = 0.98483, p-value = 0.04736

> shapiro.test(G6VertSym$`CS-137`)

        Shapiro-Wilk normality test

data:  G6VertSym$`CS-137`
W = 0.99007, p-value = 0.2121

 data:  Vertical symmetry G6
 Bartlett's K-squared = 3.7555, df = 2, p-value = 0.1529

 ANOVA

           Df Sum Sq  Mean  Sq F value Pr(>F)
 ind          2  0.007 0.003457   0.117  0.889
 Residuals   552 16.249 0.029436

 Welch Two Sample t-test

 data:  x$CONTROL and x$`CS-137`
 t = 0.29997, df = 370.16, p-value = 0.7644
 alternative hypothesis: true difference in means is not equal to 0
 95 percent confidence interval:
  -0.03069121  0.04174050
 sample estimates:
  mean of x  mean of y
 0.03003826 0.02451362

 data:  x$CONTROL and x$CADMIUM
```

```
t = 0.48249, df = 357.53, p-value = 0.6298
alternative hypothesis: true difference in means is not equal to 0
95 percent confidence interval:
 -0.02638112  0.04353427
sample estimates:
 mean of x  mean of y
0.03003826 0.02146169

data:  x$CADMIUM and x$`CS-137`
t = -0.17694, df = 367.94, p-value = 0.8597
alternative hypothesis: true difference in means is not equal to 0
95 percent confidence interval:
 -0.03697048  0.03086662
sample estimates:
 mean of x  mean of y
0.02146169 0.02451362
```

Generation 7 R output:

```
shapiro.test(G7VertSym$CONTROL)

        Shapiro-Wilk normality test

data:  G7VertSym$CONTROL
W = 0.9884, p-value = 0.09289

> shapiro.test(G7VertSym$CADMIUM)

        Shapiro-Wilk normality test

data:  G7VertSym$CADMIUM
W = 0.98645, p-value = 0.06114

> shapiro.test(G7VertSym$`Cs-137`)

        Shapiro-Wilk normality test

data:  G7VertSym$`Cs-137`
W = 0.96933, p-value = 0.0005357


        ANOVA
Df Sum Sq  Mean Sq F value Pr(>F)
ind          2   0.01 0.005043   0.208  0.812
Residuals   576  13.97 0.024263


        Welch Two Sample t-test

        data:  q$CONTROL and q$`Cs-137`
        t = -0.45907, df = 367.68, p-value = 0.6465
        alternative hypothesis: true difference in means is not equal to 0
        95 percent confidence interval:
         -0.04009389  0.02491693
        sample estimates:
          mean of x   mean of y
        0.004227665 0.011816144

        data:  q$CONTROL and q$CADMIUM
        t = 0.16068, df = 396.97, p-value = 0.8724
        alternative hypothesis: true difference in means is not equal to 0
        95 percent confidence interval:
         -0.02708297  0.03190406
        sample estimates:
          mean of x   mean of y
        0.004227665 0.001817118
```

```
data:  q$CADMIUM and q$`Cs-137`
t = -0.6154, df = 354.22, p-value = 0.5387
alternative hypothesis: true difference in means is not equal to 0
95 percent confidence interval:
 -0.04195371  0.02195566
sample estimates:
  mean of x   mean of y
0.001817118 0.011816144
```

7.1.2 Leaf area

Generation 4 R output:

shapiro.test(G4area$control)

Shapiro-Wilk normality test

data: G4area$control
W = 0.91715, p-value = 6.959e-08

> shapiro.test(G4area$cadmium)

Shapiro-Wilk normality test

data: G4area$cadmium
W = 0.97552, p-value = 0.006559

> shapiro.test(G4area$`cs-137`)

Shapiro-Wilk normality test

data: G4area$`cs-137`
W = 0.91046, p-value = 3.398e-06

Bartlett's K-squared = 1.0784, df = 2, p-value = 0.5832

There is no significant difference in the population variances- the variance within each of the populations is equal.

ANOVA

stacked_groups <- stack(y)

> anova_results <- aov(values~ind, data=stacked_groups)

> summary(anova_results)

	Df	Sum Sq	Mean Sq	F value	Pr(>F)	
ind	2	7.47	3.737	18.01	**3.13e-08**	***
Residuals	417	86.51	0.207			

Welch Two Sample t-test

```
data:  G4area$control and G4area$`cs-137`
t = 0.94539, df = 203.54, p-value = 0.3456
alternative hypothesis: true difference in means is not equal to 0
95 percent confidence interval:
 -0.06060363  0.17225620
sample estimates:
mean of x mean of y
 2.870335  2.814509

data:  G4area$control and G4area$cadmium
t = 5.8594, df = 314.71, p-value = 1.171e-08
alternative hypothesis: true difference in means is not equal to 0
95 percent confidence interval:
 0.1950898 0.3923457
sample estimates:
mean of x mean of y
 2.870335  2.576617

data:  G4area$`cs-137` and G4area$cadmium
t = 3.9898, df = 207.58, p-value = 9.168e-05
alternative hypothesis: true difference in means is not equal to 0
95 percent confidence interval:
 0.1203429 0.3554400
sample estimates:
mean of x mean of y
 2.814509  2.576617
```

Generation 5 R output:

```
shapiro.test(G5arealogged$CONTROL)

        Shapiro-Wilk normality test

data:  G5arealogged$CONTROL
W = 0.97095, p-value = 0.0002405

> shapiro.test(G5arealogged$CADMIUM)

        Shapiro-Wilk normality test

data:  G5arealogged$CADMIUM
W = 0.98112, p-value = 0.01251

> shapiro.test(G5arealogged$`CS-137`)

        Shapiro-Wilk normality test

data:  G5arealogged$`CS-137`
W = 0.96003, p-value = 6.782e-06
```

```
Bartlett test of homogeneity of variances

data:  G5arealogged
Bartlett's K-squared = 0.21197, df = 2, p-value = 0.8994

  summary(anova_results)
              Df Sum Sq Mean Sq F value Pr(>F)
  ind          2   0.08 0.03761   0.322  0.725
  Residuals  612  71.58 0.11696
```

Generation 6 R output:

```
shapiro.test(G6AreaLogged$CONTROL)

        Shapiro-Wilk normality test

data:  G6AreaLogged$CONTROL
W = 0.9803, p-value = 0.01062

> shapiro.test(G6AreaLogged$CADMIUM)

        Shapiro-Wilk normality test

data:  G6AreaLogged$CADMIUM
W = 0.97998, p-value = 0.01056

> shapiro.test(G6AreaLogged$`CS-137`)

        Shapiro-Wilk normality test

data:  G6AreaLogged$`CS-137`
W = 0.9783, p-value = 0.004749

  Bartlett's test of homogeneity of variances

  data:  z
  Bartlett's K-squared = 1.5892, df = 2, p-value = 0.4518

     Df Sum Sq Mean Sq F value Pr(>F)
ind          2   0.04 0.01763     0.2  0.819
Residuals  552  48.72 0.08825
```

Generation 7 R output:

```
shapiro.test(G7Arealogged$CONTROL)

        Shapiro-Wilk normality test

data:  G7Arealogged$CONTROL
W = 0.96249, p-value = 2.816e-05

> shapiro.test(G7Arealogged$CADMIUM)

        Shapiro-Wilk normality test

data:  G7Arealogged$CADMIUM
W = 0.95802, p-value = 1.635e-05

> shapiro.test(G7Arealogged$`CS-137`)

        Shapiro-Wilk normality test

data:  G7Arealogged$`CS-137`
W = 0.98056, p-value = 0.01297

Bartlett test of homogeneity of variances

data:  G7Arealogged
Bartlett's K-squared = 0.043153, df = 2, p-value = 0.9787

ANOVA
  Df Sum Sq Mean Sq F value    Pr(>F)
  ind          2   2.16   1.082   9.928 5.76e-05 ***
  Residuals   577  62.91   0.109
  ---
  Signif. codes:  0 '***' 0.001 '**' 0.01 '*' 0.05 '.' 0.1 ' ' 1
  38 observations deleted due to missingness

  Welch Two Sample t-test

  data:  e$CONTROL and e$`CS-137`
  t = 2.4311, df = 378.42, p-value = 0.01552
  alternative hypothesis: true difference in means is not equal to 0
  95 percent confidence interval:
   0.01561994 0.14776148
  sample estimates:
  mean of x mean of y
   2.051035  1.969344
  data:  e$CONTROL and e$CADMIUM
  t = 4.4241, df = 396.64, p-value = 1.253e-05
  alternative hypothesis: true difference in means is not equal to 0
  95 percent confidence interval:
```

0.08152784 0.21193375
sample estimates:
mean of x mean of y
2.051035 1.904304

data: e$CADMIUM and e$`CS-137`

t = -1.9094, df = 370.54, p-value = 0.05699

alternative hypothesis: true difference in means is not equal to 0
95 percent confidence interval:
-0.132021979 0.001941811
sample estimates:
mean of x mean of y
1.904304 1.969344

7.1.3 Root length

R output:

Kruskal-Wallis rank sum test

data: allgenroots

Kruskal-Wallis chi-squared = 5.0701, df = 2, p-value = 0.07926

7.1.4 Cosmic radiation morphometric data

Tomato leaf morphometric data

Output from R:

Welch Two Sample t-test

data: TomatoVSMP$Space and TomatoVSMP$Control

t = -0.036329, df = 80.39, p-value = 0.9711

alternative hypothesis: true difference in means is not equal to 0

95 percent confidence interval:

```
 -0.07598703   0.07326227
sample estimates:
  mean of x   mean of y
0.003325011  0.004687392
```

7.1.5 Rocket and tomato gamma count data

```
Output from R:
Welch Two Sample t-test

data:  RTGC2018$`Tomato ISS Cs-137` and RTGC2018$`Rocket Cs-137 ISS`
t = 1.2934, df = 4.4574, p-value = 0.2588
alternative hypothesis: true difference in means is not equal to 0
95 percent confidence interval:
 -24.00085  69.17641
sample estimates:
mean of x mean of y
 43.58245  20.99467
data:  RTGC2018$`Tomato Earth Cs-137` and RTGC2018$`Rocket Cs-137 Earth`
t = 0.58933, df = 5.5409, p-value = 0.5789
alternative hypothesis: true difference in means is not equal to 0
95 percent confidence interval:
 -27.25868  44.10136
sample estimates:
mean of x mean of y
 42.62118  34.19984

data:  RTGC2018$`Tomato Earth control` and RTGC2018$`Rocket Earth control`
t = -0.24254, df = 1.1245, p-value = 0.845
```

```
alternative hypothesis: true difference in means is not equal to 0
95 percent confidence interval:
 -2.246778  2.138465
sample estimates:
mean of x mean of y
 6.390468  6.444625


data:  RTGC2018$`Tomato ISS control` and RTGC2018$`Rocket ISS control`
t = 0, df = 1.0408, p-value = 1
alternative hypothesis: true difference in means is not equal to 0
95 percent confidence interval:
 -6.656087  6.656087
sample estimates:
mean of x mean of y
 6.634173  6.634173
```

7.1.6 Root data: rocket

```
    Normality test


shapiro.test(rocketrootslogged$Control)

        Shapiro-Wilk normality test

data:  rocketrootslogged$Control
W = 0.96657, p-value = 0.43

> shapiro.test(rocketrootslogged$ISS)

        Shapiro-Wilk normality test

data:  rocketrootslogged$ISS
W = 0.94266, p-value = 0.1869
```

```
        Welch Two Sample t-test

data:  rocketrootslogged$ISS and rocketrootslogged$Control
t = 1.3299, df = 51.215, p-value = 0.1894
alternative hypothesis: true difference in means is not equal to 0
95 percent confidence interval:
 -0.06435967  0.31704865
sample estimates:
mean of x mean of y
0.3438256 0.2174811
```

7.1.7 Root data: tomato

```
Shapiro-Wilk normality test

data:  tomatorootslogged$Control
W = 0.89314, p-value = 0.03073

> shapiro.test(tomatorootslogged$ISS)

        Shapiro-Wilk normality test

data:  tomatorootslogged$ISS
W = 0.94666, p-value = 0.2292

Kruskal-Wallis rank sum test

data:  tomatorootslogged
Kruskal-Wallis chi-squared = 0.035556, df = 1, p-value = 0.8504
```

7.1.8 DNA methylation

```
> View(DNA)
> stacked_groups <- stack(DNA)
> anova_results <- aov(values~ind,  data=stacked_groups)
> summary(anova_results)
            Df  Sum Sq Mean  Sq F value   Pr(>F)
ind          2 9846701  4923350    8.664 0.00469  **
Residuals   12 6818842   568237
---
Signif. codes:  0 ‘***’ 0.001 ‘**’ 0.01 ‘*’ 0.05 ‘.’ 0.1 ‘ ’ 1
```

7.2 Dose rate estimation calculations for beta-gamma

Area of disc	375 cm2		Radius (cm)	10.9	Squared	118.81
Depth of fill	43 mm					
Emission rate	1 photon/s/cm3					
Slice thickness	1 mm					
emission per cm3	1 per second	Total emission	1613	per second		
Target area	1 cm2 but assumed to be concentrated at a point					
Calculation is in cm						

Depth of slice	Height above soil	Flux from disc (s-1)
(mm)	(cm)	
0.5	1	0.11722955
1.5		0.112726785
2.5		0.1086076
3.5		0.104813489
4.5		0.101298501
5.5		0.098025884
6.5		0.094965779
7.5		0.092093596
8.5		0.089388842
9.5		0.086834256
10.5		0.08441516
11.5		0.082118969
12.5		0.079934809
13.5		0.077853219
14.5		0.075865914
15.5		0.073965597
16.5		0.072145809
17.5		0.070400802
18.5		0.068725437
19.5		0.067115101
20.5		0.06556564
21.5		0.064073293
22.5		0.062634646
23.5		0.061246593
24.5		0.059906295
25.5		0.058611151

26.5		0.057358772
27.5		0.056146959
28.5		0.05497368
29.5		0.053837057
30.5		0.052735346
31.5		0.051666929
32.5		0.050630297
33.5		0.049624043
34.5		0.048646852
35.5		0.047697493
36.5		0.046774813
37.5		0.045877725
38.5		0.045005211
39.5		0.04415631
40.5		0.043330115
41.5		0.04252577
42.5		0.041742465
	Total	2.963292553
Actual activity	100	kBq
Emission per second	85000	
So photons/s/cm2 at target	156.1561482	
Cs-137 pGy/photon/cm2	4.69	
So dose rate to air	63.27696973	
(µGy/h)		
Dose rate to water	70.2374364	
Height cm)	dose rate	attenuated
0.5	81	50.9
1	70	44.0
2	55	34.9
3	45	29.1
4	37	24.1
5	31	20.7
6	28	19.0
7	23	15.9
8	20	14.0
9	17.4	12.4
10	15.3	10.9
Internal beta dose rate	71	Assumed to be v small because not much in plants so not included

External, surface and at	36	
0.5	34	
1	33	
2	30	
3	26	
4	24	
5	21	
6	19	
7	17	
8	15	
9	13	
10	12	

7.3 Doses and dose rates used in lab and field studies of the effects of IR on plants

Species	F/L	Dose range	Length of exposure (hours)	Total Dose (Gy)	Lo	Hi	(plot)	Dose Rate (uGy/h)	Mean	Lo	Hi	(plot)	Author/Year
Winter rye, wheat, spring barley, oats	Field	28-4834 µGy/h	2 years (17520 hours)	42.59112	0.49056	84.6917	***42.10056***	28-4834 µGy/h	2431	28	##	***2403***	(Geras'kin et al., 2003a)
Scots pine, coach-grass	FIeld	2.5-27 µGy/h	2 years (17520 hours)	0.25842	0.0438	0.47304	***0.21462***	2.5-27 µGy/h	14.75	2.5	27	***12.25***	(Geras'kin et al., 2003b)
Wild vetch, Scots pine	FIeld	0.87-320 µGy/h	6 years (52560 hours)	8.4324636	0.045727	16.8192	***8.3867364***	0.87-320 µGy/h	160.435	0.87	##	***159.6***	(Evseeva et al., 2009, 2011)
Scots pine	Field	0.8-14.8 µGy/h	6 years (52560 hours)	0.409968	0.042048	0.77789	***0.36792***	0.8-14.8 µGy/h	7.8	0.8	15	***7***	(Geras'kin et al., 2010, 2011)
Crested hairgrass	Field	0.5-32 µGy/h	3 years (26280 hours)	0.42705	0.01314	0.84096	***0.41391***	0.5-32 µGy/h	16.25	0.5	32	***15.75***	(Geras'kin et al., 2012)
Cow vetch (*Vicia cracca*)	Field	0.2Gy	3650 hours	0.2	0.2	0.2	***0***		54.79452055	0	0	***0***	(Evseeva et al., 2009)
Soybean	Field	2 7.3 × 10^6 ± 2.4 × 10^6 Bq/m-2											Danchenko et al. (2009)
Flax	Field	2 7.3 × 10^6 ± 2.4 × 10^6 Bq/m-2											Klubicová et al. (2010)
Arabidopsis	Field	0.09565 -73.91 µGy/h		0.0888	0.000216	0.17738	0.088584	0.09565 - 73.91 µGy/h	37	0.09	74	36.91	Kovalchuk et al. (1998)

Arabidopsis, Tobacco	Lab	0.1-10.0 Gy	10 days (240 hours)	5.05	0.1	10	***4.95***		21041.66667	41 6.7	# #	***20 62 5***	(Kovalchuk et al., 2000)
Empress tree (tissue culture)	Lab	5 - 50 Gy	5 minutes (0.08 hours)	27.5	5	50	***22.5***		343750000	6E +07	# #	***3E +08***	(Alikamanoğlu et al., 2007)
Arabidopsis	Lab	10.9 - 18.4 Gy	168 hours	14.65	10.9	18.4	***3.75***		87202.38095	6488 1	# #	***22 32 1***	(Biermans et al., 2015)
Barrel clover (tissue culture)	Lab	6-50 Gy	170 minutes (2.83 hours)	28	6	50	***22***		9893992.933	2E +06	# #	***8E +06***	(Donà et al., 2014)
Petunia *(Petunia x hybrida)*	Lab	50-100 Gy	20 minutes (0.33 hours)	75	50	100	***25***		227272727.3	2E +08	# #	***8E +07***	(Donà et al., 2013)
Arabidopsis	Lab	100-2000 Gy	24 hours	1050	100	2000	***950***		43750000	4E +06	# #	***4E +07***	Kim et al. (2011)
Tobacco	Lab	30 or 50 Gy	Not given	40	30	50	***10***		555555.5556	4E +05	# #	***1E +05***	Cho et al. (2000)
Arabidopsis	Lab	1 Gy	40 seconds (0.01 hours)	1	1	1	***0***		100000000	0	0	***0***	Kovalchuk et al. (2007)
Arabidopsis	Lab	25-100 Gy	2.9 minutes (0.05 hours)	62.5	25	100	***37.5***		1250000000	5E +08	# #	***8E +08***	Berrin et al. (2005)
Arabidopsis	Lab	50 Gy	1.4 minutes (0.02 hours)	50	50	50	***0***		2500000000	3E +09	# #	***0***	Doucet-Chabeaud et al. (2001)

Arabidopsis	Lab	100 Gy	Not given	100	100	100	***0***		138888.889	1E+06	##	***0***	Culligan et al. (2006)
Arabidopsis	Lab	0.3–10 Gy	Not given	5.15	0.3	10	***4.85***		71527.77778	4167	##	***6736.1***	West et al. (2000)
Arabidopsis	Lab	100–400 Gy	Not given	250	100	400	***150***		3472222.222	1E+06	##	***2E+06***	Hefner et al. (2006)
Arabidopsis	Lab	100 Gy	11.76 minutes (0.20 hours)	100	100	100	***0***		500000000	5E+08	##	***0***	Hefner et al. (2003)
Arabidopsis	Lab	50–800 Gy	1 hour	825	50	800	***375***		825000000	5E+07	##	***4E+08***	Osakabe et al. (2006)
Arabidopsis	Lab	25–100 Gy	No access	62.5	25	100	***37.5***		868055.5556	3E+05	##	***5E+05***	Deveaux et al. (2000)
Arabidopsis	Lab	150–600 Gy	Not given	375	150	600	***225***		5208333.333	2E+06	##	***3E+06***	Doutriaux et al. (1998)
Arabidopsis	Lab	50–200 Gy	22 minutes (0.37 hours)	125	50	200	***75***		337837837.8	1E+08	##	***2E+08***	Bleuyard et al. (2005)
Arabidopsis	Lab	100 Gy	Not given	100	100	100	***0***		138888.889	1E+06	##	***0***	Preuss and Britt (2003)
Arabidopsis	Lab	20 Gy	Not given	20	20	20	***0***		277777.7778	3E+05	##	***0***	De Schutter et al. (2007)

Arabidopsis	Lab	200 Gy	4 hours	200	200	200	***0***		500000 00	5E +07	# #	0	Kim et al. (2009)
Arabidopsis	Lab	25-100 Gy	3 minutes (0.05 hours)	62.5	25	100	***37.5***		125000 0000	5E +08	# #	***8E +08***	Pierrugues et al. (2001)
Potato	Lab	10-30 Gy	30 seconds (0.008 hours)	20	10	30	***10***		250000 0000	1E +09	# #	***1E +09***	Hamideldin and Hussin (2014).
Maize and pea	Lab	3-32 Gy	89 minutes (1.48 hours)	17.5	3	32	***14.5***		118243 24.32	2E +06	# #	***1E +07***	Gudkov and Grodzinsky (1982)
Chickpea	Lab	50-750 Gy	4.2 seconds (0.001 hours)	400	50	750	***350***		4E+11	5E +10	# #	***4E +11***	Brahmi et al. (2014)
Red pepper	Lab	2-16 Gy	not given	11	2	16	***7***		152777 .7778	2777 8	# #	***9722 2***	Kim et al. (2004)
Rice, Mung bean	Lab	50-350 Gy	3 hours	200	50	350	***150***		666666 66.67	2E +07	# #	***5E +07***	Maity et al. (2005)
Potato, Sweet potato	Lab	100-900 Gy	20.5 krad/hr (4.39 hours)	500	100	900	***400***		113895 216.4	2E +07	# #	***9E +07***	Ogawa et al. (1969)
Lombardy poplar	Lab	10-300 Gy	20 hours	155	10	300	***145***		775000 0	5E +05	# #	***7E +06***	Nishiguchi et al. (2012)
Arabidopsis	Lab	25-150 Gy	17.6 minutes (0.29 hours)	87.5	25	150	***62.5***		301724 137.9	9E +07	# #	***2E +08***	Qi et al. (2015)

Arabidopsis	Lab	100 Gy	4.5 minutes (0.08 hours)	100	100	100	***0***		125000 0000	1E +09	# #	***0***	Ricaud et al. (2007)
Tobacco	Lab	0 - 10 Gy 30 Gy	63.8 minutes (1.06 hours)	20	10	30	***10***		188679 24.53	9E +06	# #	9E +06	Ptá˘cek et al. (2001)
Onion	Lab	0-50 Gy	121.6 seconds (0.03 hours)	50	50	50	***0***		166666 6667	2E +09	# #	***0***	Saghirzadeh et al. (2008)
Arabidopsis	Lab	0.1 µGy/h (external) , 50–100 µG/h (internal)					0	0.1 - 100 µGy/h	50.05	0.1	# #	***49.95***	Sahr et al. (2005)
Arabidopsis	Lab	3.9-58.8 Gy	167 hours	31.35	3.9	58.8	***27.45***		187724 .5509	2335 3	# #	***2E +05***	Vanhoudt et al. (2014)
Arabdopsis	Lab	3.5 Gy	72 hours	3.5	3.5	3.5	***0***		48611. 11111	6E +05	# #	***### #***	Vanhoudt et al. (2010)
Pea	Lab	0.4-10 Gy	20.4 minutes (0.34 hours)	60	0.4	10	***4.8***		176470 588.2	1E +06	# #	***1E +07***	Zaka et al. (2004)
Maize	Lab	0.1-1 kGy	not given	550	100	1000	450		763888 8.889	1E +06	# #	***6E +06***	Marcu et al. (2013)
Potato	Lab	0- 80 Gy	Not given	80	80	80	0		111111 1.111	1E +06	# #	***0***	Cheung et al. (2010)
Rice	Field	222.5 µGy/h	96 hours	0.02136	0.02136	0.02136	0	222.5 µGy/h	222.5	222.5	# #	***0***	Kimura et al. (2008)

Rice	Lab	4 µGy/h	72 hours	0.000288	0.000288	0.00029	0	4 µGy/h	4	4	4	4	
Carrot	Field	0.08 - 30.2 µGy/h	Not given, but assume 30 y from field at chernobyl (262800 h)	3.978792	0.021024	7.93656	3.957768	0.08 - 30.2 µGy/h	15.14	0.08	30	15.06	Boratyński et al. (2016)
Scot's pine	Field	0.08 - 34.5 µGy/h	Not given, but assume 30 y from field at chernobyl (262800 h)	4.543812	0.021024	9.0666	4.522788	0.08 - 34.5 µGy/h	17.29	0.08	35	17.21	Mousseau et al. (2013)
Broad Bean (V. Fabia)	Lab	70-291 rontgen (0.6 Gy- 2.6 Gy)	not given, assumed 1 hr	1.55	0.6	2.5	0.95		1550000	6E+05	##	1E+06	Gray and Scholes (1951)
Nicotiana Glauca	Lab	200-400 rontgen per day (43.2Gy - 84 Gy)	2 months (1460 hours) (1.8Gy/h - 3.5 Gy/hr)	3869	2628	5110	1241		2650000	2E+06	##	9E+05	Gunckel (1956)
Snapdragon	Lab	175- 285 rontgen per day (36 Gy - 60 Gy)	assume 2 months (1.5 Gy/hr- 2.5 Gy/hr)	2920	2190	3650	730	1500000 - 25000000 uGy/hr	2000000	2E+06	##	5E+05	Gunckel (1956)
Tradescantia Paludosa	Lab	37 r per day (0.3 Gy per day)	3 months (2190 hours) @ 0.0125	27.375	27.375	27.375	0	12500 µGy/h	12500	1250 0	##	0	Gunckel (1956)

			Gy/hr = 27.375Gy										
Nicotiana bigelovii xNicotiana Glauca	Lab	325 r per day (2.85 Gy per day)	assume 2 months (1460 hrs) @ 0.11875 Gy/hr	173.375	173.375	173.375	0	118750 µGy/h	118750	1E+05	# #	0	Gunckel (1956)
Nicotiana bigelovii xNicotiana Glauca	Lab	225 r per day (1.973 Gy per day)	Assume 2 months (1460 hrs) @ 0.08 Gy/hr	119.72	119.72	119.72	0	82000 µGy/h	82000	820000	# #	0	Gunckel (1956)
Rice	Field	5.34 µGy/day (0.2 µGy/h)	72-96 hours	18.69	16.02	21.36	2.67	0.2	0.2	0.2	0	0.2	Rakwal et al. (2009)